2017

Analysis and Design of Robust and High-Performance Complex Dynamical Networks

Milad Siami
Lehigh University

Analysis and Design of Robust and High-Performance Complex Dynamical Networks

by

Milad Siami

Presented to the Graduate and Research Committee

of Lehigh University

in Candidacy for the degree of

Doctor of Philosophy

in

Mechanical Engineering

Lehigh University

January 2017

Approved and recommended for acceptance as a dissertation in partial fulfillment of the requirements for the degree of Doctor of Philosophy.

Date

Accepted Date

Prof. Nader Motee
(Dissertation Advisor)

Committee Members:

Prof. Bassam Bamieh

Prof. Katya Scheinberg

Prof. Eugenio Schuster

To my lovely wife, Rozhin,

and my parents, Pari and Mahmoud.

Acknowledgements

I would like to express my sincere gratitude and appreciation to my advisor, Professor Nader Motee, who made the journey possible and provided me with invaluable guidance, unfailing encouragement, and endless support. I am thankful to Nader for providing me with a unique learning environment at Lehigh University. He always encouraged me to try and learn new stuff and expand my knowledge. Despite his extremely busy schedule, he was always available for meeting and discussion. Dear Nader, thanks for always being there for me and believing in me.

My gratitude also extends to the other members of my committee: Professors Bassam Bamieh, Katya Scheinberg, and Eugenio Schuster, for their help, advice, and constructive feedback. I am very grateful for the many people at Google that help me; Dr. Joëlle Skaf for the opportunity to work with her and learn from her intuition and knowledge, and also her contribution to a chapter of this dissertation; Dr. Hossin Azari for his help, friendship and advice; Dr. Sergei Vassilvitskii for his support and invaluable insight into machine learning.

My deepest gratitude goes to my collaborators, Nader Motee, Bassam Bamieh, Mostafa Khammash, John. C. Doyle, Genti Buzi, Sadegh Bolouki, and Joëlle Skaf. Also, I would like to thank Professors Anders Rantzer, Eduardo D. Sontag, Ali Jadbabaie, Munther Dahleh, Mihailo Jovanovic, Mehran Mesbahi, Farhad Jafari, Antonella Ferrara, Arjan

van der Schaft, Giacomo Como, and the rest of long-term visitors at IMA for our fruitful discussions during the Annual Thematic Program on “Control Theory and Its Applications”.

I would like to thank my wonderful lab-mates during last five years, Rozhin, Mirsaleh, Yaser, Chris, Hossein, Shima, and Daniel, for their friendship, encouragement, and creating a positive and productive atmosphere. JoAnn, Brie, Barbara, Jennifer, Ali and the rest of the administrative staff in Lehigh for making my time go smoothly. I am grateful to my wonderful friends, AliReza, Ebrahim, Forough, Siavash, Zharfa, Ramin, Maryam, Armin, Samira, Tayeb and Minoo for always being there for me during my graduate study at Lehigh.

I want to express my gratitude to my previous mentors and advisors, Professors Bijan Zangeneh, Saleh Tavazoei, Mohammad Haeri and Tomohisa Hayakawa, at Sharif University of Technology and Tokyo Institute of Technology, who got me so excited about Stochastic Analysis and Control theory that I had no choice but to pursue a Ph.D. program. Furthermore, I am in great debt to my friend, Javad Ebrahimi, who showed me the beauty of mathematics and introduced me to Mathematical Olympiad.

Much appreciation goes to my parents, Pari and Mahmoud, siblings, Bahar and Mehdi, sisters-in-law, Soma and Gelareh, and parents-in-law, Fereshteh and Hassan, for their love, support, and encouragement over the years.

Last but not least, I would like to express my sincere and deepest gratitude to my wonderful wife, Rozhin, for her unconditional love, understanding, patience, and unwavering support. This thesis would not have been possible without encouragement and endless love from her. To my wonderful wife and my parents, I love you and I dedicate this dissertation to you.

Contents

List of Tables

List of Figures

Abstract

In the first part of this dissertation, we develop some basic principles to investigate performance deterioration of dynamical networks subject to external disturbances. First, we propose a graph-theoretic methodology to relate structural specifications of the coupling graph of a linear consensus network to its performance measure. Moreover, for this class of linear consensus networks, we introduce new insights into the network centrality based not only on the network graph but also on a more structured model of network uncertainties. Then, for the class of generic linear networks, we show that the $\mathcal{H}_2$-norm, as a performance measure, can be tightly bounded from below and above by some spectral functions of state and output matrices of the system. Finally, we study nonlinear autocatalytic networks and exploit their structural properties to characterize their existing hard limits and essential tradeoffs.

In the second part, we consider problems of network synthesis for performance enhancement. First, we propose an axiomatic approach for the design and performance analysis of linear consensus networks by introducing a notion of systemic performance measure. We build upon this new notion and investigate a general form of combinatorial problem of growing a linear consensus network via minimizing a given systemic performance measure. Two efficient polynomial-time approximation algorithms are devised to tackle this network synthesis problem. Then, we investigate the optimal design problem of dis-

tributed system throttlers. A throttler is a mechanism that limits the flow rate of incoming metrics, *e.g.*, byte per second, network bandwidth usage, capacity, traffic, *etc*. Finally, a framework is developed to produce a sparse approximation of a given large-scale network with guaranteed performance bounds using a nearly-linear time algorithm.

Chapter 1

Introduction

In dynamical networks, improving the global performance and robustness to exogenous disturbances are critical for sustainability and energy efficiency in engineered infrastructures; examples include formation control of a group of autonomous vehicles, distributed emergency response systems, interconnected transportation networks, energy and power networks, metabolic pathways, cloud-based services, and sociotechnical networks [2–9]. One of the outstanding analysis problems in the context of dynamical networks is to investigate and characterize their intrinsic fundamental limits and tradeoffs on global performance. Providing solutions to this important challenge will enable us to develop underpinning principles to design efficient-by-design dynamical networks.

There are several related work in the literature that address performance and robustness issues in noisy linear consensus networks; for example see [2, 9–17] and the references therein. In [2], the authors investigate the deviation from the mean of states of a network on tori with additive noise inputs. The performance and robustness of networks on tori are analyzed in [10], in which the effect of imperfect communication links is considered. A rather comprehensive performance analysis of noisy linear consensus networks with arbitrary graph topologies has been recently reported in [12]. In [9, 17], the authors

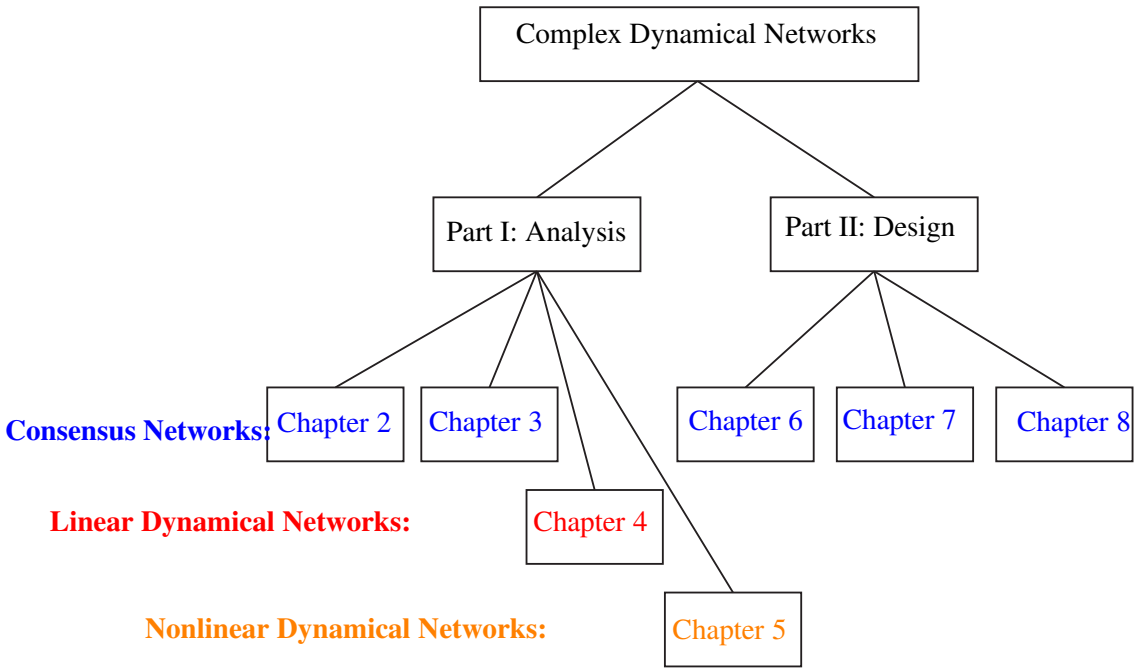

Figure 1.1: A representation of the dissertation structure.

consider the $\mathcal{H}_2$ performance measure for a class of consensus networks with exogenous inputs in the form of process and measurement noises. The proposed analysis method in [9, 17] applies the edge agreement protocol by considering a minimal realization of the edge interpretation system for simple unweighted coupling graphs.

This dissertation consists of two parts (see Figure 1.1). In Part I, we investigate performance deterioration of dynamical networks subject to external disturbances and related fundamental limits and tradeoffs. The issue of fundamental limits and their tradeoffs in large-scale interconnected dynamical systems lies at the very core of distributed feedback control systems theory as it reveals what is achievable, and conversely what is not achievable by distributed feedback control laws. In Part II, we consider problems of network synthesis for performance enhancement. Performance improvement in interconnected networks of coupled dynamical systems as well as reducing their design complexity by sparsifying their underlying coupling structures are two of the important design issues,

which have been subject of active research in past few years [4, 6, 18–23].

In Sections 1.1 and 1.2, we provide an overview of Parts I and II, respectively.

1.1 Performance Analysis and Tradeoffs (Part I)

The recent interest in understanding fundamental limitations of feedback in complex interconnected dynamical networks from biological systems and physics to engineering and economics has created a paradigm shift in the way systems are analyzed, designed, and built. Typical examples of such complex networks include metabolic pathways [24], vehicular platoons [25–29], arrays of micro-mirrors [30], micro-cantilevers [31], and smart power grids. These systems are diverse in their detailed physical behavior. However, they share an important common feature that all of them consist of an interconnection of a large number of systems. There have been some progress in characterization of fundamental limitations of feedback in this class of systems. For example, only to name a few, reference [32] gives conditions for string instability in an array of linear time-invariant autonomous vehicles with communication constraints, [33] provides a lower bound on the achievable quality of disturbance rejection using a decentralized controller for stable discrete time linear systems with time delays, [34] studies the performance of spatially invariant plants interconnected through a static network.

In what follows in this section, we describe our contribution in each chapter of Part I.

Chapter 2

In this chapter, we are particularly interested in the class of first-order linear consensus networks that are driven by exogenous stochastic disturbance inputs. We quantify inherent fundamental limits on the best achievable levels of performance in such networks and

show how the performance of a network in this class depends on the topology of the underlying coupling graph. The topology of the underlying coupling graph of a consensus network depends on the coupling structure among the subsystems, which are usually imposed by governing physical laws and/or global objectives. We consider linear consensus networks that are operating in closed-loop, *i.e.*, networks that have been already stabilized by a linear state feedback control law. In some applications such as formation control of autonomous vehicles, sparsity pattern of the underlying information structure in the controller array determines communication requirements among the vehicles, and as a result, it defines the sparsity pattern of the coupling graph topology of the closed-loop network.

In Section 2.4, the steady state variance of the output of a noisy consensus network is adopted as a performance measure to quantify performance deterioration of the network. This performance measure is equal to the square of the $\mathcal{H}_2$-norm of the network from the disturbance input to the output [5]. There have been several recent studies on the $\mathcal{H}_2$-based performance analysis of linear consensus networks [2, 5, 11, 17, 35–38] and references in there. The $\mathcal{H}_2$-norm of a system can be interpreted as a macroscopic performance measure, that captures the notion of coherence in dynamical networks [2].

Our first contribution shows that how the performance measure scales with the network size. For consensus networks with unweighted coupling graphs, it is shown that the performance measure is $\Omega(n)$ for networks with "fairly" sparse interconnection topologies such as tree and unicyclic graphs[1], where n is the network size. The performance measure scales in order of $\Omega(1)$ for networks with "fairly" dense graphs such as complete bipartite and complete graphs. In the worst case, the performance measure scales

[1]We employ the big omega notation in order to generalize the concept of asymptotic lower bound in the same way as $\mathcal{O}$ generalizes the concept of asymptotic upper bound. We adopt the following definition according to [39]:

$$f(n) = \Omega(g(n)) \;\Leftrightarrow\; g(n) = \mathcal{O}(f(n)), \tag{1.1}$$

where $\mathcal{O}$ represents the big O notation. In the left hand side of (4.1), the Ω notation implies that $f(n)$ grows at least of the order of $g(n)$.

in order of $\mathcal{O}(n^2)$, where networks with path-like graphs experience the worst levels of performance. Our second contribution is to reveal the importance of the graph topology in emergence of fundamental limits on the best achievable values for the performance measure. In Section 2.5, we prove that by subsuming more detailed graph specifications in our calculations, tighter lower bounds can be obtained for the best achievable values of the performance measure. In order to verify meaningfulness of our theoretical results, we performed extensive simulations and the results assert that our theoretical lower bounds are tighter for networks with rather dense coupling graphs. The impacts of the presented fundamental limits usually appear as intrinsic interplays between the performance measure and various sparsity measures in linear consensus networks. In our third contribution that is discussed in Section 2.6, we formulate several uncertainty-principle-like inequalities which assert that networks with more sparse coupling graphs incur higher levels of performance loss. The results presented in this chapter have been published in [12].

Chapter 3

In this chapter, we consider a class of noisy consensus networks that can be completely characterized by their coupling graphs and the structure of their noise inputs. The $\mathcal{H}_2$-norm square of the noisy network is used as the performance measure– we refer to [2, 4, 5, 10, 37, 38, 40] for related discussions. Motivated by realistic uncertain operational environment for a network with consensus dynamics (e.g., see [41]), six noise structures are investigated in this work. Uncertainties can arise from noisy dynamics, sensors, emitters, receivers, communication channels, and measurements. To the best of our knowledge, with an exception of the dynamics noise, the comprehensive analysis of performance measures with closed-form formulae for different types of noise for an arbitrary weighted graph has not been carried out previously in the literature. Our results

show that the impact of all these uncertainties can be encapsulated in the structure of the input matrix. Our main contribution is the introduction of a new class of agent and link centrality indices with respect to the adopted performance measure. The key idea is to measure the infinitesimal change in the value of the performance measure with respect to the variance of the noise input. For all of the six noise structures, we calculate explicit formulae for the centrality indices and show how they depend on the topology of the coupling graph of the network. In Section 3.7, we discuss that for each noise structure all agents or links can be ranked in ascending order according to the value of the corresponding centrality index. As a result, every node has four different rankings and each link has two different rankings. It is argued that modification of the underlying coupling graph of the network (for example by rewiring, weight adjustment, sparsification, and adding new links) may result in emergence of fundamental tradeoffs among these rankings. Several supporting numerical simulations are shown in Section 3.8 to illustrate the key point that centrality rank of an agent or link may significantly be different with respect to various noise structures. The results presented in this chapter have been published in [42].

Chapter 4

In this chapter, we derive explicit lower and upper bounds for this performance measure. Our proposed bounds are spectral functions of state and output matrices of the system. Furthermore, our proposed bounds are utilized to quantify bounds on the $\mathcal{H}_2$-norm squared of some network models with specific dynamical structures, e.g., systems with normal state matrices, linear consensus networks with directed graphs, and cyclic linear networks with negative feedback. As an important application, our results are applied to a general class of linear consensus networks over directed graphs. Most recent studies [2, 43] investigate the performance of noisy linear consensus networks over undi-

rected graphs. We prove that our performance bounds are tight if the underlying directed graph of the networks is strongly connected and balanced. Moreover, we apply our results to a class of cyclic networks with asymmetric structures. These networks has been used to model certain biochemical pathways [44]. We particularly show how the $\mathcal{H}_2$-norm of a cyclic linear dynamical network scales with the network size. It is shown that when all subsystems are identical, the network attains the best achievable performance among all cyclic networks with the same secant criterion. Finally, we compare our proposed bounds to all existing bounds in the literature and use some numerical simulations to show that our bounds are tighter than all previously reported bounds in [45–47]. The results presented in this chapter have been published in [48].

Chapter 5

In this chapter, our goal is to build upon our previous results [49,50] and develop methods to characterize hard limits on performance of autocatalytic pathways. First, we study the properties of such pathways through a two-state model, which obtained by lumping all the intermediate reactions into a single intermediate reaction (Figure 5.1). Then, we generalize our results to autocatalytic pathways, which are composed of a chain of enzymatically catalyzed intermediate reactions (Figure 5.2). We show that due to the existence of autocatalysis in the system (which is necessary for survival of the pathway), a fundamental tradeoff between fragility and net product of the pathway emerges. Also, we show that as the number of intermediate reactions grows, the price for performance increases.

The results presented in this chapter are based on [51].

1.2 Network Synthesis for Performance Enhancement (Part II)

Improving global performance as well as robustness to external disturbances in large-scale dynamical networks are crucial for sustainability, from engineering infrastructures to living cells; examples include a group of autonomous vehicles in a formation, distributed emergency response systems, interconnected transportation networks, energy and power networks, metabolic pathways and even financial networks. One of the fundamental problems in this area is to determine to what extent uncertain exogenous inputs can steer the trajectories of a dynamical network away from its working equilibrium point. To tackle this issue, the primary challenge is to introduce meaningful and viable performance and robustness measures that can capture essential characteristics of the network. A proper measure should be able to encapsulate transient, steady-state, macroscopic, and microscopic features of the perturbed large-scale dynamical network. To do so, in the first chapter of Part II, we introduce the notion of systemic performance measures. We briefly outline our contributions and the structure of each chapter in Part II as follow.

Chapter 6

In the first chapter of this part, we propose a new methodology to classify proper performance measures for a class of linear consensus networks subject to external stochastic disturbances. We take an axiomatic approach to quantify essential functional properties of a sensible measure by introducing the class of systemic performance measures and show that this class of measures should satisfy monotonicity, convexity, and orthogonal invariance properties. It is shown that several existing and widely used performance measures in the literature are in fact special cases of this class of systemic measures [9,11,19,38,52].

The first main contribution of this chapter is introduction of a class of systemic performance measures that are spectral functions of Laplacian eigenvalues of the coupling graph of a linear consensus network. Several gold-standard and widely used performance measures belong to this class, for example, to name only a few, spectral zeta function, Gamma entropy, expected transient output covariance, system Hankel norm, convergence rate to consensus state, logarithm of uncertainty volume of the output, Hardy-Schatten system norm or $\mathcal{H}_p$-norm, and many more. All these performance measures are monotone, convex, and orthogonally invariant. Our main goal is to investigate a canonical network synthesis problem: growing a linear consensus network by adding new interconnection links to the coupling graph of the network and minimizing a given systemic performance measure. In the context of graph theory, it is known that a simpler version of this combinatorial problem, when the cost function is the inverse of algebraic connectivity, is indeed NP-hard [53]. There have been some prior attempts to tackle this problem for some specific choices of cost functions (i.e., total effective resistance and the inverse of algebraic connectivity) based on semidefinite programing (SDP) relaxation methods [54, 55]. There is a similar version of this problem that is reported in [56], where the author studies convergence rate of circulant consensus networks by adding some long-range links. Moreover, a continuous (non-combinatorial) and relaxed version of our problem of interest has some connections to the sparse consensus network design problem [6, 57, 58], where they consider ℓ_1-regularized $\mathcal{H}_2$-optimal control problems. There are some related works [23, 59], it is shown that some metrics based on controllability and observability Gramians are modular or submodular set functions, where they show their proposed simple greedy heuristic algorithms have guarantees suboptimality bounds.

In our second main contribution, we propose two efficient polynomial-time approximation algorithms to solve the above mentioned combinatorial network synthesis prob-

lem: a linearization-based method and a simple greedy algorithm based on rank-one updates. Our complexity analysis asserts that computational complexity of our proposed algorithms are reasonable and make them particularly suitable for synthesis of large-scale consensus networks. To calculate sub-optimality gaps of our proposed approximation algorithms, we quantify the best achievable performance bounds for the network synthesis problem in Section 6.7. Our obtained fundamental limits are exceptionally useful as they only depend on the spectrum of the original network and they can be computed a priori. In Subsection 6.9.2, we classify a subclass of differentiable systemic performance measures that are indeed supermodular. For this subclass, we show that our proposed simple greedy algorithm can achieve a $(1 - 1/e)$-approximation of the optimal solution of the combinatorial network synthesis problem. Our extensive simulation results confirm effectiveness of our proposed methods.

The results presented in this chapter are based on [60].

Chapter 7

In this chapter, our goal is to develop a unified framework for analysis and design of discrete-time distributed rate-limiting systems with a local aggregated view of usage metrics. We investigate performance deterioration (*e.g.*, over-throttling, mismatch, convergence rate) of DSTs with respect to external uncertainties and the update cycle of servers. We develop a graph-theoretic framework to relate the underlying structure of the system to its overall performance measure. We then compare the performance/robustness of DSTs with different topologies. In this work, in addition to the overall performance measure for a network, each node has its own performance measure, which is one of the main differentiators between this work and some other related work [2, 12, 42, 61].

The rest of this chapter is organized as follows. In Section 7.3, we present some basic

mathematical concepts and notations employed in this chapter. In Section 7.4, we define and study a distributed system throttler (DST). In Section 7.5, we evaluate the overall performance of a DST with a given nodal performance measure. In Section 6.9, we focus on throttling algorithms which are used by servers. In Section 7.7, we study the impact of the server update cycle on performance. In Section 7.8, two synthesis problems are studied. In Section 7.9, some numerical results are demonstrated. In Section 7.10, we conclude our work and suggest directions for future research.

The results presented in this chapter are based on [62].

Chapter 8

In this chapter, we specifically address the following network design problem: given a linear consensus network with an undirected connected underlying graph, the *network sparsification* problem seeks to replace the coupling graph of the original network with a reasonably sparser subgraph so that the behavior of the original and the sparsified networks is similar in an appropriately defined sense. Such situations arise frequently when real-world large-scale dynamical networks need to be simulated, controlled or redesigned using efficient computational tools that are specifically tailored for optimization problems with sparse structures. We develop a general methodology that computes sparsifiers of a given consensus network using a nearly-linear time $\tilde{\mathcal{O}}(m)$[2] algorithm with guaranteed systemic performance bounds, where m is the number of links. Unlike other existing work on this topic in the literature, our proposed framework: (i) works for a broad class of systemic performance measures including $\mathcal{H}_2$-based performance measures, (ii) does not involve any sort of relaxations such as ℓ_0 to ℓ_1, (iii) provides guarantees for the ex-

[2]We use $\tilde{\mathcal{O}}(.)$ to hide poly $\log\log$ terms from the asymptotic bounds. Thus, $f(n) \in \tilde{\mathcal{O}}\left(g(n)\right)$ means that there exists $k > 0$ such that $f(n) \in \mathcal{O}\left(g(n)\log^k g(n)\right)$.

istence of a sparse solution, (iv) can partially sparsify predetermined portions of a given network; and most importantly, (v) gives guaranteed systemic performance certificates.

While our approach is relied on several existing works in algebraic graph theory [63, 64], our control theoretic contributions are threefold. First, we show that every given linear consensus network has a sparsifier network such that the two networks yield comparable performances with respect to any systemic performance measure. Second, we develop a framework to find a sparse approximation of large-scale consensus networks using a fast randomized algorithm. We note that while the coupling graph of the sparsified network is a subset of the coupling graph of the original network, the weights of links (the strength of each coupling) in the sparsified network are adjusted accordingly to reach predetermined levels of systemic performance. Third, we prove that our development can also be applied for partial sparsification of large-scale networks, which means that we can sparsify a prespecified subgraph of the original network to find an approximation of the network with fewer links. This is practically plausible as our algorithm can be spatially localized, if necessary, and it does not require to receive information of the entire coupling graph of the network.

The results presented in this chapter are based on [65].

Part I

Performance Analysis and Tradeoffs

Chapter 2

Fundamental Limits and Tradeoffs in Linear Consensus Networks

2.1 Abstract

We investigate performance deterioration in linear consensus networks subject to external stochastic disturbances. The expected value of the steady state dispersion of the states of the network is adopted as a performance measure. We develop a graph-theoretic methodology to relate structural specifications of the coupling graph of a linear consensus network to its performance measure. We explicitly quantify several inherent fundamental limits on the best achievable levels of performance and show that these limits of performance are emerged only due to the specific coupling topology of the coupling graphs. Furthermore, we discover some of the inherent fundamental tradeoffs between notions of sparsity and performance in linear consensus networks.

2.2 Introduction

In this chapter, we are particularly interested in the class of first-order linear consensus networks that are driven by exogenous stochastic disturbance inputs. We quantify inherent fundamental limits on the best achievable levels of performance in such networks and show how the performance of a network in this class depends on the topology of the coupling graph. The topology of the coupling graph of a consensus network depends on the coupling structure among the subsystems, which are usually imposed by governing physical laws and/or global objectives. We consider linear consensus networks that are operating in closed-loop, i.e., networks that have been already stabilized by a linear state feedback control law. In some applications such as formation control of autonomous vehicles, sparsity pattern of the information structure in the controller array determines communication requirements among the vehicles, and as a result, it defines the sparsity pattern of the topology of the coupling graph of the closed-loop network.

In Section 2.4, the steady state variance of the output of a noisy consensus network is adopted as a performance measure to quantify performance deterioration of the network. This performance measure is equal to the square of the $\mathcal{H}_2$-norm of the network from the disturbance input to the output [5]. Our first contribution shows that how the performance measure scales with the network size. For consensus networks with unweighted coupling graphs, it is shown in Section 2.5 that the performance measure is $\Omega(n)$ for networks with "fairly" sparse interconnection topologies such as tree and unicyclic graphs, where n is the network size. The performance measure scales in order of $\Omega(1)$ for networks with "fairly" dense graphs such as complete bipartite and complete graphs. In the worst case, the performance measure scales in order of $\mathcal{O}(n^2)$, where networks with path-like graphs experience the worst levels of performance. Our second contribution is to reveal the importance of the graph topology in emergence of fundamental limits on the best achievable

values for the performance measure. In Section 2.5, we prove that by subsuming more detailed graph specifications in our calculations one can obtain tighter lower bounds for the best achievable values of the performance measure. In order to verify meaningfulness of our theoretical results, we performed extensive simulations and the results assert that our theoretical lower bounds are tighter for networks with rather dense coupling graphs (see Figures 2.4-2.6 for more details). The impacts of the presented fundamental limits usually appear as intrinsic interplays between the performance measure and various sparsity measures in linear consensus networks. In our third contribution that is discussed in Section 2.6, we formulate several uncertainty-principle-like inequalities that assert that networks with more sparse coupling graphs incur higher levels of performance loss.

2.3 Mathematical Notations

Matrix Theory: The set of all nonnegative real numbers is denoted by $\mathbb{R}_+$. The $n \times 1$ vector of all ones is denoted by $\mathbb{1}_n$, the $n \times n$ identity matrix by I_n, the $m \times n$ zero matrix by $0_{m\times n}$, and the $n \times n$ matrix of all ones by J_n. We will eliminate subindices of these matrices whenever the corresponding dimensions are clear from the context. The centering matrix of size n is defined by $M_n := I_n - \frac{1}{n}J_n$. The transposition of matrix A is denoted by A^{T} and the Moore-Penrose pseudo-inverse of matrix A by $A^{\dagger}$. For a square matrix A, $\mathbf{Tr}(A)$ refers to the summation of on-diagonal elements of A. The following definitions are from [66].

Definition 2.3.1. *For every $x \in \mathbb{R}^n_+$, let us define $x^{\downarrow}$ to be a vector whose elements are a permuted version of elements of x in descending order. We say that x majorizes y, which is denoted by $x \trianglerighteq y$, if and only if $\mathbb{1}^T x = \mathbb{1}^T y$ and $\sum_{i=1}^{k} x_i^{\downarrow} \geq \sum_{i=1}^{k} y_i^{\downarrow}$ for all $k = 1, \ldots, n-1$.*

The vector majorization is not a partial ordering. This is because from relations $x \trianglerighteq y$ and $y \trianglerighteq x$ one can only conclude that the entries of these two vectors are equal, but possibly with different orders. Therefore, relations $x \trianglerighteq y$ and $y \trianglerighteq x$ do not imply $x = y$.

Definition 2.3.2. *The real-valued function $F : \mathbb{R}_+^n \to \mathbb{R}$ is called Schur–convex if $F(x) \geq F(y)$ for every two vectors x and y with property $x \trianglerighteq y$.*

Graph Theory: Throughout this chapter, we assume that all graphs are finite, simple, and undirected. A weighted graph $\mathcal{G}$ is represented by a triple $\mathcal{G} = (\mathcal{V}_\mathcal{G}, \mathcal{E}_\mathcal{G}, w_\mathcal{G})$, where $\mathcal{V}_\mathcal{G}$ is the set of nodes, $\mathcal{E}_\mathcal{G} \subseteq \big\{\{i,j\}\big|\, i,j \in \mathcal{V}_\mathcal{G},\ i \neq j\big\}$ is the set of edges, and $w_\mathcal{G} : \mathcal{E}_\mathcal{G} \to \mathbb{R}_+$ is the weight function. An unweighted graph $\mathcal{G}$ is a graph with constant weight function $w_\mathcal{G}(e) \equiv 1$ for all $e \in \mathcal{E}_\mathcal{G}$. For each $i \in \mathcal{V}_\mathcal{G}$, the degree of node i is defined by $d_i := \sum_{e=\{i,j\}\in\mathcal{E}_\mathcal{G}} w_\mathcal{G}(e)$. The sum of all edge weights in graph $\mathcal{G}$ is denoted by $W(\mathcal{G})$. The adjacency matrix $A_\mathcal{G} = [a_{ij}]$ of graph $\mathcal{G}$ is defined by setting $a_{ij} = w_\mathcal{G}(e)$ if $e = \{i,j\} \in \mathcal{E}_\mathcal{G}$, otherwise $a_{ij} = 0$. The Laplacian matrix of $\mathcal{G}$ is defined by $L_\mathcal{G} := D_\mathcal{G} - A_\mathcal{G}$, where $D_\mathcal{G} = \mathrm{diag}(d_1, \ldots, d_n)$ is a diagonal matrix. The eigenvalues of a Laplacian matrix $L_\mathcal{G}$ are indexed in ascending order $0 = \lambda_1 \leq \lambda_2 \leq \cdots \leq \lambda_n$. If $\mathcal{G}$ is connected, then $\lambda_2 > 0$. The class of all connected unweighted graphs with n nodes is denoted by $\mathbb{G}_n$ and $\mathbb{G}_n^{\mathrm{W}}$ represents the set of all connected weighted graphs with n nodes. The centering graph is a complete graph with Laplacian matrix M_n and is denoted by $\mathcal{M}_n$.

For comparison purposes throughout the chapter, we consider some of the standard graphs such as complete graph $\mathcal{K}_n$, star graph $\mathcal{S}_n$, cycle graph $\mathcal{C}_n$, path graph $\mathcal{P}_n$, bipartite graph $\mathcal{B}_{n_1,n_2}$, and complete bipartite graph $\mathcal{K}_{n_1,n_2}$. Every one of these graphs has its own comparable characteristics. For instance, among all graphs in $\mathbb{G}_n$ a complete graph has the maximum number of edges and a star graph has the maximum number of nodes with degree one. A path graph is a tree with minimum number of nodes of degree one. We refer to reference [67] for more details and discussions. A tree is a connected graph on n

nodes with exactly $n-1$ edges. A unicyclic graph is a connected graph with exactly one cycle. A d-regular graph is a graph where all nodes have identical degree d. A subgraph $\mathcal{F}$ of a graph $\mathcal{G}$ is a spanning subgraph if it has the same node set as $\mathcal{G}$. An edge is called a cut-edge whose deletion increases the number of connected components.

For a given Laplacian matrix $L_{\mathcal{G}}$, the corresponding resistance matrix $R_{\mathcal{G}} = [r_{ij}]$ is defined using the Moore-Penrose pseudo-inverse of $L_{\mathcal{G}}$ by setting $r_{ij} = l^{\dagger}_{ii} + l^{\dagger}_{jj} - l^{\dagger}_{ji} - l^{\dagger}_{ij}$, where $L^{\dagger}_{\mathcal{G}} = [l^{\dagger}_{ij}]$. The quantity r_{ij} is so called the effective resistance between nodes i and j. Finally, the total effective resistance $\mathbf{r}_{\text{total}}$ is defined as the sum of the effective resistances between all distinct pairs of nodes, i.e.,

$$\mathbf{r}_{\text{total}} \;=\; \frac{1}{2}\,\mathbb{1}_n^{\mathrm{T}} R_{\mathcal{G}}\,\mathbb{1}_n \;=\; \frac{1}{2}\sum_{i,j=1}^{n} r_{ij}. \tag{2.1}$$

2.4 Linear Consensus Networks and their Performance Measures

We consider a class of first-order consensus (FOC) networks whose dynamics are defined over coupling graphs $\mathcal{G} = (\mathcal{V}_{\mathcal{G}}, \mathcal{E}_{\mathcal{G}}, w_{\mathcal{G}})$ with n nodes. For this class of networks, each node corresponds to a subsystem with a scalar state variable and the interconnection topology between these subsystems is defined by the coupling graph $\mathcal{G}$. The state of the entire network is represented by $x = [x_1,\, x_2,\, \ldots, x_n]^{\mathrm{T}}$ where x_i is the state variable of subsystem i for all $i = 1, \ldots, n$. The dynamics of this class of FOC networks are governed by

$$\mathcal{N}(L_{\mathcal{G}}; L_{\mathcal{Q}}) : \begin{cases} \dot{x} \;=\; -L_{\mathcal{G}} x \;+\; \xi \\ y \;=\; C_{\mathcal{Q}} x \end{cases}, \tag{2.2}$$

where x is the vector of state variables, ξ is an exogenous white Gaussian noise with zero-mean and identity covariance matrix, y is the performance output of the network, $L_{\mathcal{G}}$ is the Laplacian matrix of $\mathcal{G}$, and $C_{\mathcal{Q}}$ is the output matrix of the network.

Definition 2.4.1. *A given graph $\mathcal{Q} = (\mathcal{V}_{\mathcal{Q}}, \mathcal{E}_{\mathcal{Q}}, w_{\mathcal{Q}})$ is the output graph of a linear consensus network $\mathcal{N}(L_{\mathcal{G}}; L_{\mathcal{Q}})$ if $\mathcal{Q}$ admits*

$$L_{\mathcal{Q}} \;:=\; C_{\mathcal{Q}}^T C_{\mathcal{Q}} \tag{2.3}$$

as its Laplacian matrix.

The output graph $\mathcal{Q}$ exists if the output matrix $C_{\mathcal{Q}}$ has zero row sums. In general, the output graph can be a disconnected graph with real-valued edge weights. The output graphs help us to better understand how the specific choice of performance output will affect a given performance measure. We adopt the following class of performance measures that are defined using the performance outputs.

Definition 2.4.2. *Suppose that $\mathcal{Q}$ is an output graph of $\mathcal{N}(L_{\mathcal{G}}; L_{\mathcal{Q}})$. The performance measure of $\mathcal{N}(L_{\mathcal{G}}; L_{\mathcal{Q}})$ is defined as the steady state variance of the performance output of the network, i.e.,*

$$\rho_{ss}(L_{\mathcal{G}}; L_{\mathcal{Q}}) \;:=\; \lim_{t\to\infty} \mathbb{E}\left[y(t)^T y(t)\right]. \tag{2.4}$$

In order to ensure that (2.4) is well-defined, marginally stable and unstable modes of $\mathcal{N}(L_{\mathcal{G}}; L_{\mathcal{Q}})$ must be unobservable from the performance output y. The following two assumptions are made for this reason.

Assumption 2.4.3. *For all networks $\mathcal{N}(L_{\mathcal{G}}; L_{\mathcal{Q}})$ in this chapter, it is assumed that $\mathcal{Q}$ is an output graph according to Definition 2.4.1.*

According to this assumption, $L_{\mathcal{Q}}$ is the Laplacian matrix of the output graph $\mathcal{Q}$. Examples of admissible output matrices include incidence and centering matrices. When the output matrix is the centering matrix, i.e., $C_{\mathcal{Q}} = M_n$, the corresponding output graph is a centering graph, i.e., $\mathcal{Q} = \mathcal{M}_n$.

Assumption 2.4.4. *For all $\mathcal{N}(L_{\mathcal{G}}; L_{\mathcal{Q}})$ networks in this chapter, the corresponding coupling graph $\mathcal{G}$ is assumed to be connected.*

Based on Assumption 6.3.5, one can verify that consensus network $\mathcal{N}(L_{\mathcal{G}}; L_{\mathcal{Q}})$ has only one marginally stable mode with eigenvector $\mathbb{1}$ and all other modes are stable. The marginally stable mode is unobservable from the performance output y, because the output matrix of the network satisfies $C_{\mathcal{Q}}\mathbb{1} = 0$. Therefore, the performance measure (2.4) is well-defined (cf. [2, Sec. III]).

The performance measure (2.4) quantifies the performance of the network in the average. This is because (2.4) is indeed equivalent to the square of the $\mathcal{H}_2$–norm of the system from the exogenous noise input to the performance output [2, 11, 17, 36]. When there is no exogenous noise input, the steady state of $\mathcal{N}(L_{\mathcal{G}}; L_{\mathcal{Q}})$ converges to the consensus state and the value of the performance measure becomes zero. In the following, we quantify performance measure (2.4) for the class of FOC networks.

Theorem 2.4.5. *For a given network $\mathcal{N}(L_{\mathcal{G}}; L_{\mathcal{Q}})$, the performance measure* (2.4) *can be quantified as*

$$\rho_{ss}(L_{\mathcal{G}}; L_{\mathcal{Q}}) \;=\; \frac{1}{2}\mathbf{Tr}(L_{\mathcal{Q}} L_{\mathcal{G}}^{\dagger}), \tag{2.5}$$

where $L_{\mathcal{G}}^{\dagger}$ is the Moore–Penrose pseudo inverse of $L_{\mathcal{G}}$.

Proof. Let us define the disagreement vector by [20]

$$x_d(t) \;:=\; M_n x(t) \;=\; x(t) - \frac{1}{n} J_n x(t). \tag{2.6}$$

By multiplying a vector by the centering matrix, we actually subtract the mean of all the entries of the vector from each entry. The dynamics of $\mathcal{N}(L_{\mathcal{G}}; L_{\mathcal{Q}})$ with respect to the new state transformation (8.16) is so called disagreement form of the network, which is given by

$$\mathcal{N}_d(L_{\mathcal{G}_d}; L_{\mathcal{Q}}) : \begin{cases} \dot{x}_d = -L_{\mathcal{G}_d} x_d + M_n \xi \\ y \;=\; C_{\mathcal{Q}}\, x_d \end{cases}$$

in which $L_{\mathcal{G}_d} = L_{\mathcal{G}} + \frac{1}{n} J_n$ and the new state matrix is indeed stable. One can easily verify that the transfer functions from ξ to y in both networks $\mathcal{N}(L_{\mathcal{G}}; L_{\mathcal{Q}})$ and $\mathcal{N}_d(L_{\mathcal{G}_d}; L_{\mathcal{Q}})$ are identical. Therefore, the $\mathcal{H}_2$–norm of the system from ξ to y in both representations are well-defined and equivalent. Let us consider the integral form of the output of network $\mathcal{N}_d(L_{\mathcal{G}_d}; L_{\mathcal{Q}})$ as follows

$$y(t) \;=\; C_{\mathcal{Q}} \int_0^t e^{-L_{\mathcal{G}_d}(t-\tau)} M_n \xi(\tau)\, d\tau. \tag{2.7}$$

By substituting $y(t)$ from (2.7) in (2.4), calculating the expected value, and finally taking the limit, the value of the performance measure can be calculated using the trace formula $\mathbf{Tr}(P_c L_{\mathcal{Q}})$, where matrix P_c is the controllability Gramian of the disagreement network $\mathcal{N}_d(L_{\mathcal{G}_d}; L_{\mathcal{Q}})$ and it is the solution of the Lyapunov equation

$$L_{\mathcal{G}_d} P_c + P_c L_{\mathcal{G}_d} - M_n = 0.$$

Since $-L_{\mathcal{G}_d}$ is stable, the above Lyapunov equation has a unique positive definite solution [68, Th. 7.11]. Using the fact that $L_{\mathcal{G}}^{\dagger} L_{\mathcal{G}_d} = L_{\mathcal{G}_d} L_{\mathcal{G}}^{\dagger} = M_n$, we get $P_c = \frac{1}{2} L_{\mathcal{G}}^{\dagger}$ and the desired result follows. □

If the output graph is a centering graph, then the performance measure (2.5) reduces

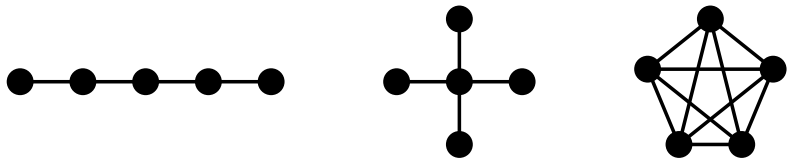

(a) (b) (c)

Figure 2.1: This figure illustrates the results of Theorems 2.5.1 and 2.5.2 for the following extreme cases. The performance measure (2.10) is (a) maximal for $\mathcal{P}_5$ among all graphs as well as among all trees in $\mathbb{G}_5$, (b) minimal for $\mathcal{S}_5$ among all trees in $\mathbb{G}_5$, and (c) minimal for $\mathcal{K}_5$ among all graphs in $\mathbb{G}_5$.

to

$$\rho_{\mathbf{ss}}(L_{\mathcal{G}}; M_n) \;=\; \frac{1}{2}\mathbf{Tr}(L_{\mathcal{G}}^{\dagger}) \;=\; \frac{1}{2}\sum_{i=2}^{n}\lambda_i^{-1}, \tag{2.8}$$

where λ_i for $i = 2, \ldots, n$ are nonzero eigenvalues of $L_{\mathcal{G}}$ and $\lambda_1 = 0$ according to Assumption 6.3.5.

Remark 2.4.6. *The performance measure* (2.5) *relates to the concept of coherence in consensus networks and the expected dispersion of the state of the system in steady state [2,11]. It also has close connections to the total effective resistance of graph $\mathcal{G}$ as follows*

$$\rho_{\boldsymbol{ss}}(L_{\mathcal{G}}; M_n) \;=\; \frac{1}{2n}\mathbf{r}_{\textit{total}}, \tag{2.9}$$

where the total effective resistance of $\mathcal{G}$ is given by $\mathbf{r}_{\textit{total}} \;=\; n\sum_{i=2}^{n}\lambda_i^{-1}$; we refer to [2,69] for more details.

2.5 Fundamental Limits on the Performance Measure

We evaluate the performance of the class of FOC networks (2.2) with respect to the centering output graph with the following corresponding performance measure

$$\rho_{\mathbf{ss}}(L_{\mathcal{G}}; M_n) \;=\; \frac{1}{2}\sum_{i=2}^{n} \lambda_i^{-1}. \tag{2.10}$$

In this section, several scenarios are investigated in order to reveal the important role of the coupling graphs of FOC networks on emergence of fundamental limits on (2.10).

2.5.1 Universal Bounds and Scaling Laws

The following result presents universal lower and upper bounds for the best and worst achievable values for (2.10) among all FOC networks with arbitrary unweighted coupling graphs.

Theorem 2.5.1. *For a given FOC network with an unweighted coupling graph $\mathcal{G} \in \mathbb{G}_n$, the performance measure* (2.10) *is bounded by*

$$\frac{1}{2} - \frac{1}{2n} \;\leq\; \rho_{\mathbf{ss}}(L_{\mathcal{G}}; M_n) \;\leq\; \frac{n^2-1}{12}. \tag{2.11}$$

Furthermore, the lower bound is achieved if and only if $\mathcal{G} = \mathcal{K}_n$, and the upper bound is reached if and only if $\mathcal{G} = \mathcal{P}_n$.

Proof. We use the result of Theorem 2.6.1 that implies that for any graph $\mathcal{G}$ with n nodes, we have $\rho_{\mathbf{ss}}(L_{\mathcal{G}}; M_n) \;\geq\; \rho_{\mathbf{ss}}(L_{\mathcal{K}_n}; M_n)$, because graph $\mathcal{G}$ is always a subgraph of $\mathcal{K}_n$. A straightforward computation shows that $\rho_{\mathbf{ss}}(L_{\mathcal{K}_n}; M_n) \;=\; \frac{n-1}{2n}$. On the other hand, every connected graph $\mathcal{G}$ contains a spanning tree $\mathcal{T}$. Using Theorem 2.6.1 and the fact that $\mathcal{T}$ is a subgraph of $\mathcal{G}$, we get $\rho_{\mathbf{ss}}(L_{\mathcal{G}}; M_n) \;\leq\; \rho_{\mathbf{ss}}(L_{\mathcal{T}}; M_n)$. Moreover, Theorem 2.5.2 provides

an upper bound for $\rho_{\mathbf{ss}}(L_{\mathcal{T}}; M_n)$, which is valid for all trees $\mathcal{T}$. Hence, this upper bound provides the desired upper bound. □

The bounds in inequalities (2.11) only depend on the network size and it is assumed that nothing specific is known about the interconnection topology of the network. These bounds can be tightened if we consider more specific subclasses of graphs. In the following three theorems, we improve upon the bounds in Theorem 2.5.1 for three important classes of graphs.

Theorem 2.5.2. *For a given FOC network with an unweighted tree coupling graph $\mathcal{T} \in \mathbb{G}_n$ and $n \geq 5$, the performance measure* (2.10) *is bounded by*

$$\frac{(n-1)^2}{2n} \leq \rho_{\boldsymbol{ss}}(L_{\mathcal{T}}; M_n) \leq \frac{n^2-1}{12}. \tag{2.12}$$

Moreover, the lower bound is achieved if and only if $\mathcal{T} = \mathcal{S}_n$ and the upper bound is achieved if and only if $\mathcal{T} = \mathcal{P}_n$.

Proof. We consider the characteristic polynomial of the Laplacian matrix of the coupling graph $\mathcal{T}$

$$\Phi_{\mathcal{T}}(\lambda) \;=\; \sum_{k=0}^{n} (-1)^{n-k}\, c_k(\mathcal{T})\, \lambda^k. \tag{2.13}$$

From (6.52) and Vieta's formulas for (2.13), it follows that

$$\rho_{\mathbf{ss}}\left(L_{\mathcal{T}}; M_n\right) \;=\; \frac{c_2(\mathcal{T})}{2c_1(\mathcal{T})}. \tag{2.14}$$

We also know that $c_1(\mathcal{T}) = \prod_{i=2}^{n} \lambda_i$ and it is equal to n for trees. Therefore, one can rewrite (2.14) as follows

$$\rho_{\mathbf{ss}}\left(L_{\mathcal{T}}; M_n\right) \;=\; \frac{c_2(\mathcal{T})}{2n}. \tag{2.15}$$

One of the invariant characteristics of a graph is its Wiener number that is denoted by $W(\mathcal{T})$ [70]. This quantity is equal to the sum of distances between all pairs of nodes of $\mathcal{T}$. It is well known that the second coefficient of the Laplacian characteristic polynomial of a tree coincides with the Wiener number, *i.e.*$c_2(\mathcal{T}) = W(\mathcal{T})$. According to this fact and (2.15), it follows that

$$\rho_{\mathbf{ss}}(\mathcal{T}) = \frac{W(\mathcal{T})}{2n}. \tag{2.16}$$

According to [71], if $\mathcal{T}$ is a tree with n nodes that is neither $\mathcal{P}_n$ nor $\mathcal{S}_n$, then

$$W(\mathcal{S}_n) < W(\mathcal{T}) < W(\mathcal{P}_n). \tag{2.17}$$

Furthermore, it is shown that [71]

$$W(\mathcal{P}_n) = \binom{n+1}{3} \text{ and } W(\mathcal{S}_n) = (n-1)^2. \tag{2.18}$$

From (2.16), (2.17) and (2.18), we have

$$\frac{(n-1)^2}{2n} < \rho_{\mathbf{ss}}(L_{\mathcal{T}}; M_n) < \frac{n^2-1}{12}.$$

On the other hand, it follows from (2.18) and (2.16) that

$$\rho_{\mathbf{ss}}(L_{\mathcal{P}_n}; M_n) = \frac{n^2-1}{12} \text{ and } \rho_{\mathbf{ss}}(L_{\mathcal{S}_n}; M_n) = \frac{(n-1)^2}{2n}.$$

Therefore, the lower bound in (2.12) is achieved if and only if $\mathcal{T} = \mathcal{S}_n$, and the upper bound is achieved if and only if $\mathcal{T} = \mathcal{P}_n$. □

The lower bound in (2.12) implies that if the value of the performance measure for some FOC network is strictly less than $\frac{(n-1)^2}{2n}$, then the unweighted coupling graph of the network must contain at least one cycle. The next result quantifies tight bounds for FOC

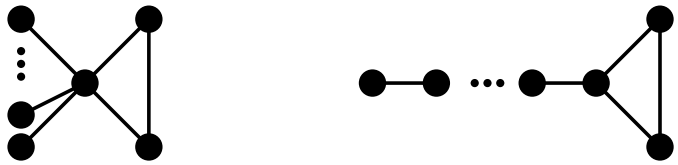

(a) (b)

Figure 2.2: The unicyclic graphs that achieve the lower and upper bounds in Theorem 2.5.3: (a) $\mathcal{G} = \mathcal{S}(\mathcal{K}_3; \mathcal{K}_1, \ldots, \mathcal{K}_1)$, and (b) $\mathcal{P}(\mathcal{K}_3; \mathcal{K}_1, \ldots, \mathcal{K}_1)$.

networks with exactly one cycle in their coupling graphs.

Theorem 2.5.3. *For a given FOC network with an unweighted unicyclic coupling graph in $\mathbb{G}_n$ and $n \geq 13$, the performance measure* (2.10) *is bounded by*

$$\frac{(n-1)^2}{2n} - \frac{1}{3} \leq \rho_{ss}(L_{\mathcal{G}}; M_n) \leq \frac{n^2-1}{12} + \frac{3}{2n} - 1. \tag{2.19}$$

Moreover, the lower bound is achieved if and only if $\mathcal{G} = \mathcal{S}(\mathcal{K}_3; \mathcal{K}_1, \ldots, \mathcal{K}_1)$, which is a star-like graph that is formed by replacing the center of $\mathcal{S}_n$ by a clique $\mathcal{K}_3$, and the upper bound is achieved if and only if $\mathcal{G} = \mathcal{P}(\mathcal{K}_3; \mathcal{K}_1, \ldots, \mathcal{K}_1)$, which is a path-like graph that is formed by replacing one of the end nodes of $\mathcal{P}_n$ by a clique $\mathcal{K}_3$.

Proof. According to (2.9), the performance measure (2.10) can be expressed based on the total effective resistance of the coupling graph $\mathcal{G}$. Moreover, the total effective resistance of a graph is the same as its Kirchhoff index. The rest of the proof is a revised version of proof of [72, Th. 4.4]. We omit the details due to space limitations. □

The lower and upper bounds in (2.19) are tight, in the sense that if the value of the performance measure for a FOC network does not satisfy (2.19), then the coupling graph of this network is either a tree (with no cycle) or has at least two cycles. The following result investigates the performance of a FOC network with a bipartite coupling graph. In this case, the network consists of two disjoint sets of nodes and the states of one set depend

on the states of the other set and vice versa. Bipartite graphs appear in several applications such as networks of electricity sellers and buyers [73, Ch.12], power networks [74, Sec. 2], and networks of leaders and followers agents where leaders are only influenced by their followers and vice versa.

Theorem 2.5.4. *For a given FOC network with an unweighted bipartite graph $\mathcal{G} \in \mathbb{G}_n$, the performance measure* (2.10) *is bounded by*

$$1 - \frac{\lfloor \frac{n}{2} \rfloor}{n \lceil \frac{n}{2} \rceil} \leq \rho_{ss}(L_{\mathcal{G}}; M_n) \leq \frac{n^2 - 1}{12}.$$

Furthermore, the lower bound is achieved if and only if $\mathcal{G} = \mathcal{K}_{\lfloor \frac{n}{2} \rfloor, \lceil \frac{n}{2} \rceil}$, and the upper bound is achieved if and only if $\mathcal{G} = \mathcal{P}_n$, where $\lfloor . \rfloor$ and $\lceil . \rceil$ are the floor and ceiling operators, respectively.

Proof. According to Theorem 2.5.1, a path graph $\mathcal{P}_n$ has the maximal level of performance measure among all graphs with n nodes. Moreover, $\mathcal{P}_n$ is in fact a bipartite graph. Therefore, we get

$$\rho_{\mathbf{ss}}(L_{\mathcal{G}}; M_n) \leq \frac{n^2 - 1}{12}.$$

The best achievable lower bound can be obtained by some calculations from (2.9) and the result of [75, Th. 3.1], which provides bounds on Kirchhoff index of a bipartite graph. □

The lower bound in Theorem 2.5.4 is tight. This is because if the value of the performance measure is strictly less than $1 - \frac{\lfloor \frac{n}{2} \rfloor}{n \lceil \frac{n}{2} \rceil}$ for a given FOC network with an unweighted coupling graph, then the coupling graph of the network cannot be a bipartite graph.

2.5.2 Bound Calculations via Exploiting Structure of Coupling Graphs

In the previous subsection, we derived lower and upper bounds for the performance measure of networks with unweighted graphs. These bounds are only functions of the network size. In this subsection, we incorporate additional knowledge of graph specifications in calculating lower and upper bounds for the performance measure. We consider five important graph specifications and extend our analysis for FOC networks with weighted and unweighted coupling graphs.

Graph diameter and number of edges

The diameter of a graph is the largest distance between every pair of nodes in that graph.

Theorem 2.5.5. *For a given FOC network with an arbitrary unweighted graph $\mathcal{G} \in \mathbb{G}_n$, the performance measure* (2.10) *is bounded by*

$$\mathfrak{L}_{\mathcal{G}} \leq \rho_{\boldsymbol{ss}}(L_{\mathcal{G}}; M_n) \leq \mathfrak{U}_{\mathcal{G}}, \tag{2.20}$$

where $\mathfrak{L}_{\mathcal{G}} = \frac{(n-1)^2}{4m}$ *and*

$$\mathfrak{U}_{\mathcal{G}} = \frac{1}{2n}\left(n-1+\left[\binom{n}{2}-m\right]\operatorname{diam}(\mathcal{G})\right),$$

where $\operatorname{diam}(\mathcal{G})$ *is the diameter and* m *is the number of edges of* $\mathcal{G}$.

Proof. For the lower bound, we apply the inequality of arithmetic and harmonic means and (6.52)

$$\rho_{\mathbf{ss}}\left(L_{\mathcal{G}}; M_n\right) = \frac{1}{2}\sum_{i=2}^{n}\lambda_i^{-1} \geq \frac{(n-1)^2}{2\sum_{i=2}^{n}\lambda_i} = \frac{(n-1)^2}{4m}.$$

On the other hand, using (2.9) and (2.1) for the upper bound, we get

$$\rho_{\mathbf{ss}}\left(L_{\mathcal{G}}; M_n\right) \;=\; \frac{1}{2n}\sum_{i\neq j} r_{ij} \;=\; \frac{1}{2n}\left(\sum_{e\in\mathcal{E}_{\mathcal{G}}} r_e + \sum_{e\notin\mathcal{E}_{\mathcal{G}}} r_e\right). \tag{2.21}$$

Moreover, based on [76, Lemma 2] for unweighted graph we have $\sum_{e\in\mathcal{E}_{\mathcal{G}}} r_e \;=\; n-1$. From this fact and (2.21), it follows that

$$\rho_{\mathbf{ss}}\left(L_{\mathcal{G}}; M_n\right) \;=\; \frac{n-1}{2n} \;+\; \frac{1}{2n}\sum_{e\notin\mathcal{E}_{\mathcal{G}}} r_e. \tag{2.22}$$

We note that the distance between two nodes of graph $\mathcal{G}$ is less than or equal to $\mathrm{diam}(\mathcal{G})$. Therefore, we have $r_{ij} = r_{\{i,j\}} \leq \mathrm{diam}(\mathcal{G})$. Using this fact and (2.22), we get the desired upper bound

$$\rho_{\mathbf{ss}}\left(L_{\mathcal{G}}; M_n\right) \;\leq\; \frac{1}{2n}\left(n-1 \;+\; \left[\binom{n}{2} - m\right]\mathrm{diam}(\mathcal{G})\right).$$

□

Remark 2.5.6. *We note that a star graph $\mathcal{S}_n$ achieves the upper bound in* (2.20)*, which means that among all unweighted connected graphs with* $\mathrm{diam}(\mathcal{G}) = 2$ *and* $n-1$ *links graph $\mathcal{S}_n$ has the maximal performance measure. Also If $\mathcal{G} = \mathcal{K}_n$, then the lower and upper bounds in* (2.20) *coincide and* $\rho_{\mathbf{ss}}(L_{\mathcal{K}_n}; M_n) \;=\; \frac{n-1}{2n}$.

Total weight sum

The sum of all edge weights in a weighted graph $\mathcal{G}$ is defined by $W(\mathcal{G}) := \sum_{e\in\mathcal{E}_{\mathcal{G}}} w_{\mathcal{G}}(e)$.

Proposition 1. *For a given FOC network with an arbitrary weighted coupling graph*

$\mathcal{G} \in \mathbb{G}_n^W$, *the performance measure* (2.10) *is bounded from below by*

$$\rho_{\boldsymbol{ss}}(L_{\mathcal{G}}; M_n) \geq \frac{(n-1)^2}{4W(\mathcal{G})}. \tag{2.23}$$

Proof. It can be shown that $\rho_{\mathbf{ss}}(L_{\mathcal{G}}; M_n)$ is a Schur–convex function with respect to $[\lambda_2, \ \ldots \ , \lambda_n]^{\mathrm{T}} \in \mathbb{R}_{++}^{n-1}$, where λ_i for $i = 2, \ldots, n$ are eigenvalues of $L_{\mathcal{G}}$. On the other hand, we have

$$\frac{\mathbf{Tr}(L_{\mathcal{G}})}{n-1} \mathbb{1}_{n-1}^{\mathrm{T}} \trianglelefteq [\lambda_2, \ \ldots \ , \lambda_n]^{\mathrm{T}}.$$

Therefore, according to the definition of Schur–convex functions, we can conclude inequality (2.23). □

Number of spanning trees

A spanning subgraph of $\mathcal{G}$ is called a spanning tree if it is also a tree. The weighted number of spanning trees of a connected graph $\mathcal{G} = (\mathcal{V}_{\mathcal{G}}, \mathcal{E}_{\mathcal{G}}, w_{\mathcal{G}})$ is defined by

$$\mathfrak{T}(\mathcal{G}) := \sum_{\mathcal{T}} \prod_{e \in \mathcal{E}_{\mathcal{T}}} w_{\mathcal{G}}(e), \tag{2.24}$$

where the summation runs over all spanning trees $\mathcal{T}$ of $\mathcal{G}$. For unweighted graphs, the total number of spanning trees of a connected graph is an invariant graph specification.

Proposition 2. *For a given FOC network with an arbitrary weighted coupling graph* $\mathcal{G} \in \mathbb{G}_n^W$, *the performance measure* (2.10) *is bounded from below by*

$$\rho_{\boldsymbol{ss}}(L_{\mathcal{G}}; M_n) \geq \frac{n-1}{2\sqrt[n-1]{n\mathfrak{T}(\mathcal{G})}}, \tag{2.25}$$

where $\mathfrak{T}(\mathcal{G})$ *is the number of spanning trees of* $\mathcal{G}$ *defined by* (2.24).

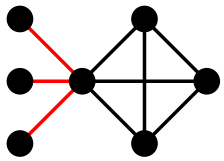

Figure 2.3: A schematic graph of $\mathcal{S}(\mathcal{K}_4; \mathcal{K}_1, \mathcal{K}_1, \mathcal{K}_1)$ that has the minimal value of performance measure among all graphs in $\mathbb{G}_7$ with exactly 3 cut edges (highlighted by red color).

Proof. By applying the inequality of arithmetic and geometric means to (6.52), we get

$$\rho_{\mathbf{ss}}(L_{\mathcal{G}}; M_n) \;=\; \frac{1}{2}\sum_{i=2}^{n} \lambda_i^{-1} \;\geq\; \frac{n-1}{2}\sqrt[n-1]{\prod_{i=2}^{n} \lambda_i^{-1}}. \tag{2.26}$$

Using Kirchhoff's matrix tree theorem the number of spanning trees of graph can be expressed as $\mathfrak{T}(\mathcal{G}) \;=\; \frac{1}{n}\prod_{i=2}^{n} \lambda_i$. Then, using this fact and (2.26), we get the desired lower bound. □

The result of this proposition holds for general weighted connected graphs. However, for some particular classes of unweighted connected graphs, the total number of spanning trees can be calculated explicitly as a function of n. For example, for an unweighted complete graph $\mathcal{K}_n$ the total number of spanning trees is $\mathfrak{T}(\mathcal{G}) = n^{n-2}$. In fact, the lower bound in (2.25) is tight for weighted and unweighted graphs and it can be achieved by complete graphs. Nonetheless, our analysis shows that the proposed lower bound in (2.25) is not tight for the class of unweighted tree, cycle, and complete bipartite graphs. As we discussed earlier, our results in Subsection 2.5.1 are tight for these classes of graphs.

Number of cut edges

An edge e is called a cut edge of $\mathcal{G}$ if removing e from $\mathcal{G}$ results in more than one connected component. The total number of cut edges in $\mathcal{G}$ is denoted by $\kappa(\mathcal{G})$.

Theorem 2.5.7. *For a given FOC network with an arbitrary unweighted coupling graph $\mathcal{G} \in \mathbb{G}_n$ that has $\kappa(\mathcal{G})$ cut edges, the performance measure* (2.10) *is bounded from below by*

$$\rho_{ss}(L_{\mathcal{G}}; M_n) \geq \frac{1}{2n} + \frac{\kappa(\mathcal{G}) + 1}{2} - \frac{1}{n - \kappa(\mathcal{G})}. \tag{2.27}$$

The equality holds if and only if $\mathcal{G} = \mathcal{S}(\mathcal{K}_{n-\kappa(\mathcal{G})}; \mathcal{K}_1, \ldots, \mathcal{K}_1)$, i.e.$\mathcal{G}$ is a star graph that is formed by replacing the center of the star with a clique $\mathcal{K}_{n-\kappa(\mathcal{G})}$.

Proof. It is shown that the performance measure of (2.2) can be calculated by

$$\rho_{\mathbf{ss}}(L_{\mathcal{G}}; M_n) = \frac{\mathbf{r}_{\text{total}}}{2n}.$$

Moreover, in reference [77] it is shown that the $\mathbf{r}_{\text{total}}$ can be bounded from below as

$$\mathbf{r}_{\text{total}} \geq n\left(\kappa(\mathcal{G}) + 1\right) + 1 - \frac{2n}{n - \kappa(\mathcal{G})}$$

for all connected graphs with n nodes and $\kappa(\mathcal{G})$ cut edges. The lower bound can be achieved if and only if $\mathcal{G} = \mathcal{S}(\mathcal{K}_{n-\kappa(\mathcal{G})}; \mathcal{K}_1, \ldots, \mathcal{K}_1)$. □

For a given graph in $\mathbb{G}_n$, the number of cut edges satisfies $0 \leq \kappa(\mathcal{G}) \leq n - 1$, where a tree with $n - 1$ cut edges has the maximum and a complete graph with zero cut edge has the minimum number of cut edges among all graphs in $\mathbb{G}_n$. A simple calculation reveals that the lower bound in (2.27) gains its maximum value for tree and its minimum value for complete graphs. This asserts that the lower bound in (2.27) is tight according to the results of theorems 2.5.1 and 2.5.2.

Degree sequence

A degree sequence is a monotonic nonincreasing sequence of the node degrees of the coupling graph.

Theorem 2.5.8. *For a given FOC network with an arbitrary weighted coupling graph* $\mathcal{G} \in \mathbb{G}_n^W$ *and degree sequence* $\left\{d_i\right\}_{i=1}^n$*, the performance measure* (2.10) *is bounded from below by*

$$\rho_{\boldsymbol{ss}}(L_{\mathcal{G}}; M_n) \geq \Delta(\mathcal{G}), \tag{2.28}$$

where

$$\Delta(\mathcal{G}) := \max_{\alpha>0} \left\{ -\frac{1}{n\alpha} + \sum_{i=1}^{n} \frac{1}{2d_i + \alpha} \right\}. \tag{2.29}$$

For an arbitrary unweighted coupling graph $\mathcal{G} \in \mathbb{G}_n$*, the quantity* (2.29) *reduces to* $\Delta(\mathcal{G}) = -\frac{1}{2n} + \frac{n-1}{2n} \sum_{i=1}^{n} \frac{1}{d_i}$*, where the equality holds if* $\mathcal{G}$ *is a complete graph or complete bipartite graph.*

Proof. The proof is done for two different cases as follows.

Weighted graph: Let us assume that $\tilde{L}_{\mathcal{G}} = L_{\mathcal{G}} + \alpha J_n$ and $\alpha > 0$. The eigenvalues of $\tilde{L}_{\mathcal{G}}$ are $n\alpha, \lambda_2, \cdots, \lambda_n$, where λ_i's are eigenvalues of $L_{\mathcal{G}}$. Based on Schur–Horn theorem the diagonal elements of $\tilde{L}_{\mathcal{G}}$ are majorized by its eigenvalues. Therefore, we have

$$\sum_{i=1}^{n} \frac{1}{d_i + \alpha} \leq \frac{1}{n\alpha} + \sum_{i=2}^{n} \lambda_i^{-1}. \tag{2.30}$$

From the definition of $\rho_{\mathbf{ss}}(L_{\mathcal{G}}; M_n)$ and (2.30), it follows that

$$\frac{-1}{n\alpha} + \sum_{i=1}^{n} \frac{1}{2d_i + \alpha} \leq \rho_{\mathbf{ss}}\left(L_{\mathcal{G}}; M_n\right). \tag{2.31}$$

Unweighted graph: Using the same idea in the proof of Theorem 2.5.5, we can rewrite

the performance measure of (2.2) as follows

$$\rho_{\mathbf{ss}}(L_{\mathcal{G}}; M_n) \;=\; \frac{n-1}{2n} \;+\; \frac{1}{2n} \sum_{e \notin \mathcal{E}_{\mathcal{G}}} r_e.$$

Note that $r_{ij} = r_{\{i,j\}} \geq \frac{1}{d_i} + \frac{1}{d_j}$. This implies that

$$\begin{aligned} \rho_{\mathbf{ss}}(L_{\mathcal{G}}; M_n) \;&\geq\; \frac{n-1}{2n} \;+\; \frac{1}{2n} \sum_{\{i,j\} \notin \mathcal{E}_{\mathcal{G}}} \left(\frac{1}{d_i} + \frac{1}{d_j} \right) \\ &=\; \frac{-1}{2n} \;+\; \frac{n-1}{2n} \sum_{i=1}^{n} \frac{1}{d_i}. \end{aligned}$$

The interested reader is referred to [78] for similar arguments. □

For unweighted coupling graphs, the lower bound given by Theorem 2.5.8 is tighter than the lower bound given by Theorem 2.5.5. For d-regular weighted coupling graphs, the lower bound is $\Delta(\mathcal{G}) = \frac{(n-1)^2}{2nd}$. This lower bound is tight for FOC networks with weighted coupling graphs, in the sense that the performance measure of a FOC network with the weighted coupling graph $\mathcal{K}_n$ with identical edge weights $d/(n-1)$ meets the lower bound.

Remark 2.5.9. *In Theorem 2.5.1, it is shown that the performance measure of a FOC network with an arbitrary unweighted coupling graph in $\mathbb{G}_n$ is always less than or equal to $(n^2-1)/12$. In the following, we show by means of three simple examples that the performance measure of a FOC network with a weighted coupling graph can be made arbitrarily large. We consider a FOC network with three nodes and path coupling graph. The edge weights are given by $w(\{1,2\}) = a$ and $w(\{2,3\}) = 1-a$, where $a > 0$. For different values of parameter a, the total sum of edge weights is equal to 1. However, we have $\rho_{ss}(L_{\mathcal{G}}; M_n) \to \infty$ as $a \to 0$. Which implies that the performance measure cannot be uniformly bounded from above. Now for this graph, let us change the edge weights to*

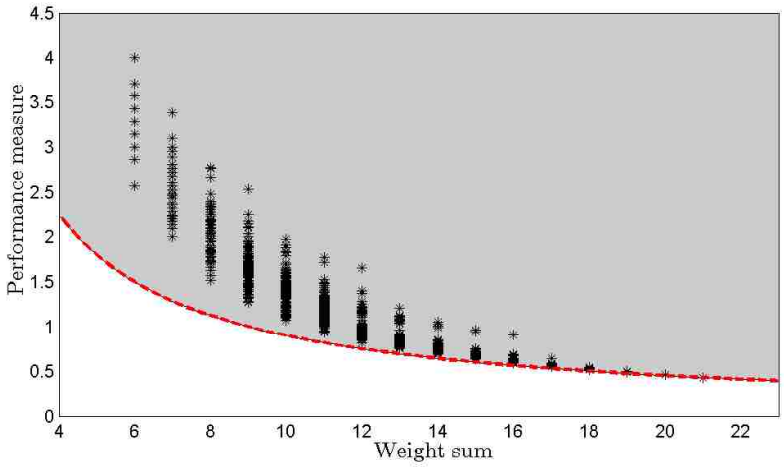

Figure 2.4: The gray shaded area depicts the value of the performance measure for all FOC networks with coupling graphs in $\mathbb{G}_7^{\mathrm{W}}$ and star markers correspond to performance measures of all FOC networks with unweighted graphs in $\mathbb{G}_7$. The red dashed curve portrays the lower bound in (2.23).

$w(\{1,2\}) = a$ *and* $w(\{2,3\}) = a^{-1}$. *According to* (2.24)*, the total number of spanning trees of this graph is equal to* 1. *It is straightforward to verify that* $\rho_{ss}(L_{\mathcal{G}}; M_n) \to \infty$ *as* $a \to 0$. *In the third scenario, let us consider a cyclic graph with four nodes and edge weights* $w(\{1,2\}) = w(\{3,4\}) = a$ *and* $w(\{2,3\}) = w(\{1,4\}) = 1 - a$. *In this case, the weighted degree sequence is* $d_1 = d_2 = d_3 = d_4 = 1$. *A simple calculation shows that* $\rho_{ss}(L_{\mathcal{G}}; M_n) \to \infty$ *as* $a \to 0$. *These examples explain why the performance measure of a FOC network with a weighted coupling graph can be arbitrarily large.*

2.5.3 Interpretation of Bounds as Fundamental Limits

The value of the performance measure (2.4) for linear consensus network (2.2) is equal to the average output energy of the network when $\xi(t) = 0$ for all $t \geq 0$ and with a white Gaussian random initial condition $x(0)$ that satisfies $\mathbb{E}\left[x(0)x(0)^{\mathrm{T}}\right] = I_n$. In fact, it can be shown that

$$\rho_{\mathbf{ss}}(A; L_{\mathcal{Q}}) = \mathbb{E}\left[\int_0^\infty y(t; x(0))^{\mathrm{T}} y(t; x(0))\, dt\right], \tag{2.32}$$

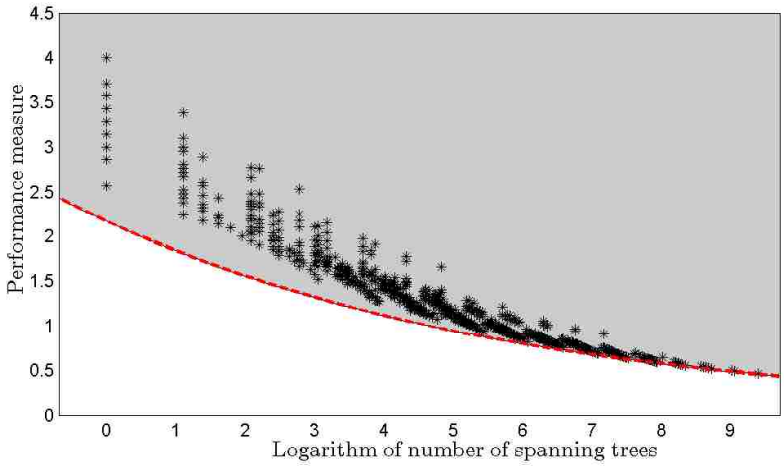

Figure 2.5: The gray shaded area depicts the value of the performance measure for all FOC networks with coupling graphs in $\mathbb{G}_7^{\mathrm{W}}$ and star markers correspond to performance measures of all FOC networks with unweighted graphs in $\mathbb{G}_7$. The red dashed curve depicts the lower bound in (2.25).

where $y(t; x(0))$ is the output of the linear dynamical network with respect to initial condition $x(0)$. This relationship enables us to equivalently interpret the performance measure (2.4) as the average energy needed to be consumed throughout the network in order to render the state of the randomly perturbed linear dynamical network to its equilibrium (i.e., consensus) state. Therefore, our theoretical bounds in Subsections 2.5.1 and 2.5.2 can be viewed as quantification of inherent fundamental limits on the minimum average energy required to be dissipated in the network in order to reach the consensus state again in steady state. The use of term *fundamental* (or equivalently *hard*) limits for lower and upper bounds in Subsections 2.5.1 and 2.5.2 is appropriate and meaningful. The reason is that according to our results, the performance measure of a linear consensus network whose coupling graph has some known graph specification (e.g., number of nodes, number of spanning trees, total sum of edge weights, degree sequence, etc.) cannot be better and worse than our theoretical lower bounds and upper bounds, respectively. The philosophy behind our several results presented in Subsection 2.5.2 can be explained by

portraying the value of performance measure for FOC networks versus various known graph specifications. In order to conceptualize the idea, we only focus on three graph specifications in our analysis. Figures 2.4, 2.5, and 2.6 depict the value of the performance measures for FOC networks with coupling graphs in $\mathbb{G}_7^{\mathrm{W}}$. In these figures, the points with star markers correspond to performance measures of all FOC networks with unweighted graphs in $\mathbb{G}_7$. The total number of such networks are $1,866,256$. In all three figures, the gray shaded area above the red dashed curve corresponds to performance measures of FOC networks with weighted coupling graphs. In Figure 2.4, the performance measure (2.10) is drawn for different values of weight sum $W(\mathcal{G})$. The lower bound in (2.23) is highlighted by a red dashed curve and it draws a fundamental limit on the best achievable performance measures. One observes that the lower bound in (2.23) is tight for a given value of weight sum. In fact, for a given $W(\mathcal{G})$ there exists a weighted graph with total weight sum $W(\mathcal{G})$ whose performance measure reaches the exact value of the fundamental limit $\frac{(n-1)^2}{4W(\mathcal{G})}$, where in this simulation $n = 7$. However, this lower bound is loose for unweighted graphs. For unweighted graphs, the weight sum is equal to the total number of edges in the coupling graph and it only assumes integer values. By exhausting all possible choices for unweighted graphs with identical number of edges in Figure 2.4, we show that there is a gap between the actual best achievable lower bound and our theoretical fundamental limit in (2.23). It can be perceived that this gap is smaller for denser coupling graphs. This observation suggests that our theoretical fundamental limit in (2.23) is looser for sparse coupling graphs and have tighter gaps for dense coupling graphs. Nevertheless, having more detailed knowledge about graph specifications helps to close the gap. For example, the weight sums for FOC networks with tree and unicyclic coupling graphs are equal to 6 and 7, respectively. In these cases, the actual minimum and maximum achievable values of performance measure exactly matches with our theoretical

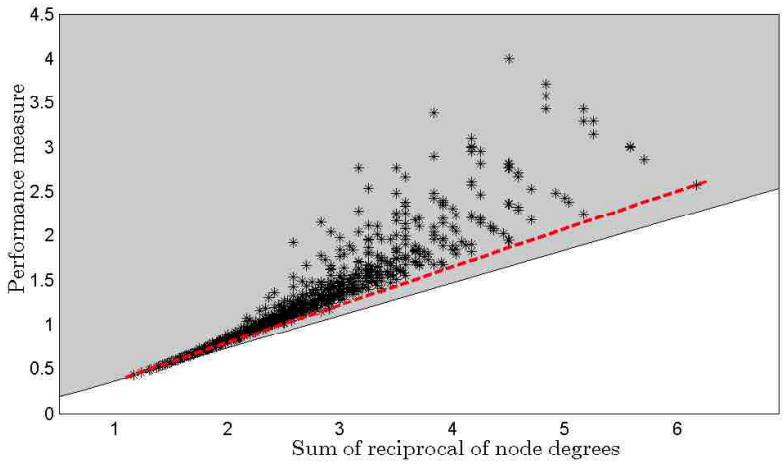

Figure 2.6: The gray shaded area depicts the value of the performance measure for all FOC networks with coupling graphs in $\mathbb{G}_7^{\mathrm{W}}$ and star markers correspond to performance measures of all FOC networks with unweighted graphs in $\mathbb{G}_7$. The red dashed curve outlines the lower bound in (2.28) for unweighted graphs.

fundamental limits in (2.19) and (2.12).

To summarize our discussion in this part, one can also set out similar arguments for Figures 2.5 and 2.6 to infer that our theoretical fundamental limits in Subsection 2.5.2 are looser for "fairly" sparse coupling graphs and have tighter gaps for dense coupling graphs. As we discussed in Subsection 2.5.1, one can exploit the structural properties of networks with sparse coupling graphs (e.g., trees and unicyclics) to quantify tight fundamental limits.

2.6 Fundamental Tradeoffs Between Notions of Sparsity and the Performance Measure

One of the design objectives for large-scale linear consensus networks is to optimize network coherence by designing a coupling graph that has the best possible sparsity and locality features. A fundamental property of performance measures (2.10) is that they

are monotonically decreasing functions of the coupling graphs in the cone of positive semidefinite matrices. This property implies that the value of the performance measure increases by sparsifying the coupling graph, which is consistent with our results in Subsection 2.5.1. In this section, we quantify fundamental tradeoffs between the performance measure (2.10) and sparsity measures of FOC networks. The results of the following theorem assert that the performance of a spanning subnetwork of a given FOC network never outperforms the performance of the parent network.

Theorem 2.6.1. *Suppose that $\mathcal{G} \in \mathbb{G}_n^W$ is the coupling graph of a given FOC network. If $\mathcal{F}$ is a connected spanning subgraph of $\mathcal{G}$, then*

$$\rho_{\boldsymbol{ss}}(L_{\mathcal{G}}; M_n) \leq \rho_{\boldsymbol{ss}}(L_{\mathcal{F}}; M_n), \tag{2.33}$$

and the equality holds if and only if $\mathcal{G} = \mathcal{F}$.

Proof. Since graph $\mathcal{F}$ is a subgraph of graph $\mathcal{G}$, we have the following inequality for every $x \in \mathbb{R}^n$:

$$\begin{aligned} x^{\mathrm{T}} L_{\mathcal{G}} x &= \sum_{e=\{i,j\}\in\mathcal{E}_{\mathcal{G}}} w(e)\,(x_i - x_j)^2 \\ &\geq \sum_{e=\{i,j\}\in\mathcal{E}_{\mathcal{F}}} w(e)\,(x_i - x_j)^2 = x^{\mathrm{T}} L_{\mathcal{F}} x. \end{aligned} \tag{2.34}$$

This inequality implies that $L_{\mathcal{F}} \leq L_{\mathcal{G}}$, or equivalently we have $L_{\mathcal{G}}^{\dagger} \leq L_{\mathcal{F}}^{\dagger}$. From the linearity property of the trace operator and the fact that $L_{\mathcal{F}}^{\dagger} - L_{\mathcal{G}}^{\dagger}$ is a positive semi-definite matrix, we get

$$\begin{aligned} \frac{1}{2}\mathbf{Tr}(L_{\mathcal{F}}^{\dagger} - L_{\mathcal{G}}^{\dagger}) &= \frac{1}{2}\mathbf{Tr}(L_{\mathcal{F}}^{\dagger}) - \frac{1}{2}\mathbf{Tr}(L_{\mathcal{G}}^{\dagger}) \\ &= \rho_{\mathbf{ss}}(L_{\mathcal{F}}; M_n) - \rho_{\mathbf{ss}}(L_{\mathcal{G}}; M_n) \geq 0. \end{aligned}$$

This completes the proof. □

The result of this theorem implicitly asserts that adding new edges to the coupling graph of a consensus network may improve the global performance of the network. In the following, we identify several Heisenberg-like inequalities that quantify inherent fundamental tradeoffs between global performance and sparsity in FOC networks. First, we consider the following sparsity measure

$$\|A_{\mathcal{G}}\|_0 := \operatorname{card}\big\{a_{ij} \neq 0 \mid \ A_{\mathcal{G}} = [a_{ij}]\big\}, \tag{2.35}$$

where $A_{\mathcal{G}}$ is the adjacency matrix of the coupling graph $\mathcal{G}$. For a given graph, the value of this sparsity measure is equal to twice the number of the edges.

Theorem 2.6.2. *For a given FOC network with an arbitrary unweighted coupling graph $\mathcal{G} \in \mathbb{G}_n$, there is a fundamental tradeoff between the performance measure* (2.10) *and the sparsity measure* (2.35) *that is characterized in the multiplicative form by the following inequality*

$$\rho_{ss}(L_{\mathcal{G}}; M_n)\, \|A_{\mathcal{G}}\|_0 \geq \frac{(n-1)^2}{2} \tag{2.36}$$

and in the additive form by

$$\frac{\rho_{ss}(L_{\mathcal{G}}; M_n) - \frac{1}{2} + \frac{1}{2n}}{\operatorname{diam}(\mathcal{G})} + \frac{\|A_{\mathcal{G}}\|_0}{4(n-1)} \leq \frac{n}{4}. \tag{2.37}$$

Let us consider the class of networks with identical number of nodes and compare several scenarios. The inequality (2.36) asserts that the best achievable values of performance measure (2.10) for sparse FOC networks are comparably larger (worse) with respect to less sparse FOC networks. For all FOC networks with identical diameters,

inequality (2.37) implies that networks with more edges have smaller (better) values of performance measures. Among all FOC networks with identical number of edges, the ones with larger diameters can assume larger (worse) values of performance measures.

Theorem 2.6.3. *Let us consider the class of FOC networks with arbitrary unweighted coupling graphs in $\mathbb{G}_n$ and a given desired performance level ρ^*_{ss}. Then, the sparsity measure* (2.35) *for this class of networks satisfies*

$$\frac{(n-1)^2}{2\rho^*_{ss}} \;\leq\; \|A_{\mathcal{G}}\|_0 \;\leq\; (n-1)\left[n - 4\left(\frac{\rho^*_{ss} - \frac{1}{2} + \frac{1}{2n}}{\mathrm{diam}(\mathcal{G})}\right)\right]. \tag{2.38}$$

The result of this Theorem states that the graph diameter can be employed as a design parameter to achieve a desirable level of performance and sparsity.

The second sparsity measure that we consider in this section is so called $\mathcal{S}_{0,1}$–measure and defined by

$$\|A_{\mathcal{G}}\|_{\mathcal{S}_{0,1}} := \max\Big\{\max_{1\leq i\leq n}\|A_{\mathcal{G}}(i,.)\|_0, \max_{1\leq j\leq n}\|A_{\mathcal{G}}(.,j)\|_0\Big\},$$

where $A_{\mathcal{G}}(i,.)$ represents the i'th row and $A_{\mathcal{G}}(.,j)$ the j'th column of adjacency matrix $A_{\mathcal{G}}$. The value of the $\mathcal{S}_{0,1}$–measure of a matrix is the maximum number of nonzero elements among all rows and columns of that matrix [79]. The $\mathcal{S}_{0,1}$–measure of adjacency matrix of an unweighted graph is equal to the maximum node degree. The following result quantifies an inherent tradeoff between the performance measure and this sparsity measure.

Theorem 2.6.4. *For a given FOC network with an arbitrary unweighted coupling graph $\mathcal{G} \in \mathbb{G}_n$ and $n \geq 3$, there is a fundamental tradeoff between the performance measure*

(2.10) *and the $\mathcal{S}_{0,1}$–measure that is characterized by*

$$\left(\rho_{ss}(L_{\mathcal{G}}; M_n) + \frac{1}{2n}\right) \|A_{\mathcal{G}}\|_{\mathcal{S}_{0,1}} \geq \frac{n-1}{2}. \tag{2.39}$$

The value of the $\mathcal{S}_{0,1}$–measure reveals some valuable information about sparsity as well as the spatial locality features of a given adjacency matrix, while sparsity measure (2.35) only provides information about sparsity. The inequality (2.39) asserts that the best achievable levels of performance measure (2.10) decreases by improving local connectivity in the coupling graph of a FOC network.

The third sparsity measure of our interest for the class of FOC networks with unweighted coupling graphs is defined by

$$\sigma(\mathcal{G}) := \max_{i,j \in \mathcal{V}_{\mathcal{G}}} \Big\{ \mathrm{card}\big\{\mathfrak{N}(i) \cup \mathfrak{N}(j)\big\} \Big\}, \tag{2.40}$$

where $\mathfrak{N}(i)$ is the set of all nodes that are connected to node i by an edge. The value of the sparsity measure $\sigma(\mathcal{G})$ is equal to the maximum number of nodes that are connected to any pair of nodes among all pairs of nodes in the graph. It is easy to verify that $\sigma(\mathcal{G}) \leq n$. The following result quantifies an inherent tradeoff between the performance measure and this sparsity measure.

Theorem 2.6.5. *For a given FOC network with an arbitrary unweighted coupling graph $\mathcal{G} \in \mathbb{G}_n$ and $n \geq 3$, there is a fundamental tradeoff between the performance measure* (2.10) *and sparsity measure* (2.40) *that is quantified by*

$$\rho_{ss}(L_{\mathcal{G}}; M_n)\, \sigma(\mathcal{G}) \geq \frac{n-1}{2}. \tag{2.41}$$

Moreover, the equality holds if $\mathcal{G} = \mathcal{K}_n$.

Proof. Based on the inclusion-exclusion principle, we have

$$\text{card}\{\mathfrak{N}(i) \cup \mathfrak{N}(j)\} \;=\; d_i + d_j - \text{card}\{\mathfrak{N}(i) \cap \mathfrak{N}(j)\}, \tag{2.42}$$

where d_i and d_j are degrees of node i and node j, respectively. Using (2.40) and (2.42), it follows that

$$\sigma(\mathcal{G}) \;=\; \max_{\substack{i,j \in \mathcal{V}_\mathcal{G} \\ i \neq j}} \Big\{ d_i + d_j - |\mathfrak{N}(i) \cap \mathfrak{N}(j)| \Big\}.$$

Then, according to [80] for the maximum eigenvalue of $L_\mathcal{G}$ we have $\lambda_n \;\leq\; \sigma(\mathcal{G})$. By combining this inequality and (6.52), we get the desired lower bound. □

To summarize our results in this section, we conclude that there are intrinsic fundamental tradeoffs between the two favorable design objectives in linear consensus networks: minimizing the performance measure and sparsifying the coupling graph.

2.7 Discussion

Several relevant network synthesis problems can be formulated in order to optimize the performance measure of a linear consensus network. There has been some recent work in this area, such as [6, 18, 43]. Some of these design problems are inherently combinatorial and intractable. For instance, problems of minimizing the performance measure by rewiring a given network with fixed number of edges or by adding a few new edges to the network are generally NP-hard problems (see Chapter 6). Therefore, having some meaningful estimates for the best achievable values of the performance measure is helpful in evaluating the efficiency of a proposed approximate algorithm to solve such non-convex and generally intractable design problems. Our lower and upper bounds in this chapter provide sensible estimates for the best achievable values of the performance measure as

a function of graph specifications. Moreover, if we consider the network size as design parameter, our results in Section 2.5.1 show how rapidly the performance of a linear consensus network deteriorates as the size of network grows larger.

One observes that the performance measure (2.10) has several interesting functional properties. This measure is a convex function of Laplacian eigenvalues and monotonically decreasing with respect to adding new edges to the coupling graph. The results of Section 2.6 highlight the importance of monotonicity property by quantifying inherent fundamental tradeoffs between sparsity and performance. A promising research direction is to investigate whether these functional properties can be used to categorize larger classes of admissible performance measures for linear consensus networks [18] (see Chapter 6).

Chapter 3

Centrality Measures in Linear Consensus Networks

3.1 Abstract

We propose new insights into the network centrality based not only on the network graph, but also on a more structured model of network uncertainties. The focus of this chapter is on the class of uncertain linear consensus networks in continuous time, where the network uncertainty is modeled by structured additive Gaussian white noise input on the update dynamics of each agent. The performance of the network is measured by the expected dispersion of its states in steady-state. This measure is equal to the square of the $\mathcal{H}_2$-norm of the network and it quantifies the extent by which its state deviates away from the consensus state in steady-state. We show that this performance measure can be explicitly expressed as a function of the Laplacian matrix of the network and the covariance matrix of the noise input. We investigate several structures for noise input and provide engineering insights on how each uncertainty structure can be relevant in real-world set-

tings. Then, a new centrality index is defined in order to assess the influence of each agent or link on the network performance. For each noise structure, the value of the centrality index is calculated explicitly and it is shown that how it depends on the network topology as well as the noise structure. Our results assert that agents or links can be ranked according to this centrality index and their rank can drastically change from the lowest to the highest, or vice versa, depending on the noise structure. This fact hints at emergence of fundamental tradeoffs on network centrality in presence of multiple concurrent network uncertainties with different structures.

3.2 Introduction

The notion of centrality in the context of complex networks determines the importance of each element within a network [81–90]. There are numerous ways to characterize the notion of importance in a dynamical network. One possible way is first to adopt a suitable performance index for the entire network and then quantify influence of each individual element in the network on the performance index. This view naturally leads to definition of a centrality index and an ordered ranking of elements (e.g., agents and links) by their importance. Depending on the choice of performance index, one can end up with different centrality indices [81, 82].

There are several studies in the literature that aim at defining network centrality measures based on network graphs. The node degree centrality measure is one of the popular centrality measures in the context of social networks [91,92], where nodes with higher degrees in the network graph are of greater importance. Another context in which the degree centrality has found applications is scientific research indexing, where articles with higher citations are respected to be the more influential ones. There are several other widely used centrality indices, including eigenvector centrality [83], Katz centrality [84], close-

ness centrality [85], PageRank (used by Google) [86], betweenness centrality [87, 88], percolation centrality [93], cross-clique centrality [94], Freeman centralization [91], and topological centrality [95]. A comprehensive review of centrality measures can be found in [82]. Despite the presence of a large body of work on the concept of centrality in the literature, an extension of the concept to noisy dynamical networks is sorely missing.

There are several related works in the literature that address performance and robustness issues in noisy linear consensus networks; for example see [2, 9–17] and the references therein. In [2], the authors investigate the deviation from the mean of states of a network on tori with additive noise inputs. The performance and robustness of networks on tori are analyzed in [10], where the effect of imperfect communication links is considered. A rather comprehensive performance analysis of noisy linear consensus networks with arbitrary graph topologies has been recently reported in [12]. In [9, 17], the authors consider the $\mathcal{H}_2$ performance measure for a class of consensus networks with exogenous inputs in the form of process and measurement noises. The proposed analysis method in [9, 17] applies the edge agreement protocol by considering a minimal realization of the edge interpretation system for simple unweighted coupling graphs.

In this chapter, networks with linear consensus dynamics in the presence of structured additive noise inputs (as uncertainties) are considered. We consider a class of noisy consensus networks that can be completely characterized by their coupling graphs and the structure of their noise inputs. The $\mathcal{H}_2$-norm square of the noisy network is used as the performance measure– we refer to [2, 4, 5, 10, 37, 38, 40] for related discussions. Motivated by realistic uncertain operational environment for a network with consensus dynamics (e.g., see [41]), six noise structures are investigated in this work. Uncertainties can arise from noisy dynamics, sensors, emitters, receivers, communication channels, and measurements. To the best of our knowledge, with an exception of the dynamics noise,

the comprehensive analysis of performance measures with closed-form formulae for different types of noise for an arbitrary weighted graph has not been carried out previously in the literature. Our results show that the impact of all these uncertainties can be encapsulated in the structure of the input matrix. Our main contribution is the introduction of a new class of agent and link centrality indices with respect to the adopted performance measure. The key idea is to measure the infinitesimal change in the value of the performance measure with respect to the variance of the noise input. For all of the six noise structures, we calculate explicit formulae for the centrality indices and show how they depend on the topology of the coupling graph of the network. In Section 3.7, we discuss that for each noise structure all agents or links can be ranked in ascending order according to the value of the corresponding centrality index. As a result, every node has four different rankings and each link has two different rankings. It is argued that modification of the underlying coupling graph of the network (for example by rewiring, weight adjustment, sparsification, and adding new links) may result in emergence of fundamental tradeoffs among these rankings. Several supporting numerical simulations are shown in Section 3.8 to illustrate the key point that centrality rank of an agent or link may significantly be different with respect to various noise structures.

3.3 Preliminaries

Throughout the chapter, n is the number of agents and $\mathcal{V} = \{1, \ldots, n\}$ is the set of agents. The continuous time index is denoted by t. Capital letters, such as A and B refer to real-valued matrices. The transposition, Moore-Penrose pseudo-inverse, and trace of a matrix A are denoted by A^{T}, $A^{\dagger}$, and $\mathbf{Tr}(A)$, respectively. Matrices $I_n \in \mathbb{R}^{n\times n}$ and $J_n \in \mathbb{R}^{n\times n}$ are the identity matrix and the matrix of all ones, respectively. The centering matrix of

size n is defined by

$$M_n \ := \ I_n - \frac{1}{n} J_n.$$

A graph can be represented by a triplet $\mathcal{G} = (\mathcal{V}, \mathcal{E}, w)$, where each agent is represented by a node, $\mathcal{E} \subseteq \{\{i, j\} \mid i, j \in \mathcal{V},\ i \neq j\}$ is the set of edges, and $w : \mathcal{E} \to (0, +\infty)$ is the weight function. The degree of each node $i \in \mathcal{V}$ is defined by

$$d_i \ := \sum_{e=\{i,j\} \in \mathcal{E}} w(e). \tag{3.1}$$

The adjacency matrix $A = [a_{ij}]$ of graph $\mathcal{G}$ is defined by setting $a_{ij} = w(e)$ if $e = \{i, j\} \in \mathcal{E}$, and $a_{ij} = 0$ otherwise. The Laplacian matrix of $\mathcal{G}$ is defined by

$$L := \Delta - A,$$

where $\Delta = \text{diag}([d_1 \ \cdots \ d_n])$ is the degree matrix of $\mathcal{G}$. Assuming that $\{e_1, \ldots, e_m\}$ is the link set of the graph $\mathcal{G}$, we denote by E an n-by-m oriented incidence matrix of $\mathcal{G}$ defined as the following: given an arbitrary direction for all the links of $\mathcal{G}$, $E_{ik} = 1$ if the node i is the head end of the link e_k, $E_{ik} = -1$ if the node i is the tail end of the link e_k, and $E_{ik} = 0$ if the link e_k is not attached to the node i (for any orientation of links of the graph). Moreover, W is the m-by-m diagonal matrix with diagonal elements $W_{kk} = w(e_k)$ for every k, $1 \leq k \leq m$. We note that

$$L \ = \ EWE^{\mathrm{T}}.$$

Assumption 3.3.1. *All graphs considered in this chapter are assumed to be undirected, simple, and connected. The set of Laplacian matrices of all such graphs on n nodes are denoted by $\mathfrak{L}_n$.*

The Moore-Penrose pseudo-inverse of L, denoted by $L^{\dagger}$, is a square, symmetric, doubly-centered, positive semidefinite matrix [96]. The *effective resistance* between nodes i and j is defined by:

$$r_{ij} \;:=\; l^{\dagger}_{ii} + l^{\dagger}_{jj} - l^{\dagger}_{ji} - l^{\dagger}_{ij}. \tag{3.2}$$

A sensible interpretation of this notion is to think of effective resistance r_{ij} as the electrical resistance measured between the nodes i and j when the graph represents an electrical circuit with branch conductances given by the corresponding link weights. The white Gaussian noise with zero mean and variance σ^2 is represented by $\xi \sim N(0, \sigma^2)$.

3.4 Noisy Linear Consensus Networks

Consider a network of n agents with set of agents $\mathcal{V}$. Assume that each agent $i \in \mathcal{V}$ has scalar state variable $x_i(t)$ at time $t \geq 0$. The governing dynamics of linear time-invariant averaging algorithm in continuous-time is given by

$$\dot{x}_i(t) \;=\; \sum_{j \neq i} a_{ij} \left(x_j(t) - x_i(t) \right), \tag{3.3}$$

where all coefficient a_{ij}'s are assumed to be nonnegative. Assuming symmetric communications, i.e, $a_{ij} = a_{ji}$ for every $i, j \in \mathcal{V}$, we refer to a_{ij} as the coupling weight between agents i and j.

By imposing $a_{ii} = 0$ for all $i \in \mathcal{V}$, matrix $A = [a_{ij}]$ can be viewed as the adjacency matrix of a weighted undirected and simple graph herein called the network coupling graph and denoted by $\mathcal{G}$. The system (3.3) can be rewritten in the following compact form

$$\dot{x}(t) \;=\; -Lx(t), \tag{3.4}$$

where $x = [x_1 \ \cdots \ x_n]^{\mathrm{T}}$ is the state vector. Consensus is said to occur if for some fixed $c \in \mathbb{R}$ we have

$$\lim_{t\to\infty} x(t) \ = \ c\mathbb{1}_n,$$

where $\mathbb{1}_n \in \mathbb{R}^n$ is the vector of all ones. According to Assumption 3.3.1, the dynamics (3.4) achieves consensus [97, 98]. We now consider network dynamics (3.4) in presence of structured noise

$$\dot{x}(t) \ = \ -Lx(t) \ + \ B\xi(t), \tag{3.5}$$

where $L \in \mathfrak{L}_n$, and $\xi(t)$ is the vector of stochastic disturbance inputs.

Assumption 3.4.1. *All components of the vector of noise input $\xi(t)$ are assumed to be independent of each other for all $t \geq 0$.*

Each component of $\xi(t)$ for all $t \geq 0$ is assumed to be a white Gaussian noise with zero mean and a known variance. The input matrix B captures the noise structure in the network. The dimension and structure of matrix B may vary depending on the location of noise sources in the network. In the rest of this chapter, we will refer to this matrix as the noise structure matrix. Keeping in mind that reaching consensus is what is sought in a consensus network, deviation from consensus in steady-state can be viewed as a viable performance measure for (3.4) that can be quantified as follows

$$\rho_{\text{ss}} \ := \ \lim_{t\to\infty} \mathbb{E}\Big[\big(x(t) - \bar{x}(t)\big)^{\mathrm{T}}\big(x(t) - \bar{x}(t)\big)\Big], \tag{3.6}$$

where

$$\bar{x}(t) \ := \ \left(\frac{1}{n}\sum_{i=1}^{n} x_i(t)\right)\mathbb{1}_n$$

is the vector with all elements equal to the empirical mean of states. The larger values of ρ_{ss} indicate inferior performance levels. In an ideal situation where noise input is absent,

ρ_{ss} is equal to zero.

Definition 3.4.2. *For a noisy linear consensus network* (3.5)*, suppose that* $\xi_i(t) \sim N(0, \sigma_i^2)$ *for all* $t \geq 0$ *is the noise associated with agent* i *with a known noise structure matrix* $B \in \mathbb{R}^{n\times n}$*. The centrality index of agent* $i \in \mathcal{V}$ *is defined by*

$$\eta_i := \frac{\partial \rho_{ss}}{\partial(\sigma_i^2)}. \tag{3.7}$$

This quantity is equal to the rate at which ρ_{ss} changes with respect to the change of the variance of the white noise associated with agent i. Thus, the centrality index of an agent quantifies the effect of agent noise on the performance of the network.

Definition 3.4.3. *For a noisy linear consensus network* (3.5)*, suppose that* $\xi_e(t) \sim N(0, \sigma_e^2)$ *for all* $t \geq 0$ *is the noise associated with link* e *with variance* σ_e^2 *and a known noise structure matrix* $B \in \mathbb{R}^{n\times m}$*, where* m *is the total number of links in the underlying graph of the network. The centrality index* ν_e *of link* $e \in \mathcal{E}$ *is defined by*

$$\nu_e := \frac{\partial \rho_{ss}}{\partial(\sigma_e^2)}. \tag{3.8}$$

This quantity is equal to the rate at which ρ_{ss} changes with respect to the change of the variance of the white noise associated with link e. Thus, the centrality index of a link measures impact of a link noise on the overall network performance.

In the rest of the chapter, we calculate explicit values for the agent and link centrality indices for the class of networks (3.5) subject to several realistic noise structures.

Theorem 3.4.4. *For a noisy linear consensus network* (3.5)*, the value of the centrality indices* (3.7) *and* (3.8) *solely depend on the Laplacian matrix* L *and the noise structure matrix* B*. Moreover, the value of the performance measure* ρ_{ss} *is a linear function of*

the variance of the components of the vector of noise input. More specifically, for the centrality index (3.7)*, we have*

$$\rho_{ss} \ = \sum_{i \in \mathcal{V}} \sigma_i^2 \, \eta_i, \tag{3.9}$$

where

$$\eta_i \ = \ \frac{\partial \rho_{ss}}{\partial(\sigma_i^2)} \ = \ \frac{1}{2} \left[B^{\mathrm{T}} L^{\dagger} B \right]_{ii} \quad \textit{for all} \ \ i \in \mathcal{V},$$

and for the centrality index (3.8)*, the following equation holds*

$$\rho_{ss} \ = \sum_{e \in \mathcal{E}} \sigma_e^2 \nu_e, \tag{3.10}$$

where

$$\nu_e \ = \ \frac{\partial \rho_{ss}}{\partial(\sigma_e^2)} \ = \ \frac{1}{2} \left[B^{\mathrm{T}} L^{\dagger} B \right]_{ee} \quad \textit{for all} \ e \in \mathcal{E}.$$

Proof. Let us first consider dynamics (3.5) with a general noise structure $B \in \mathbb{R}^{n \times p}$ and obtain its performance. Define $\xi_i(t) = \sigma_i \psi_i(t)$ for every $1 \leq i \leq p$ and rewrite dynamics (3.5) as:

$$\dot{x}(t) \ = \ -Lx(t) \ + \ B' \psi(t), \tag{3.11}$$

where $B' \ = \ B \ \mathrm{diag}\big([\sigma_1, \ \cdots \ , \sigma_p]\big)$. Notice that ψ_i's are i.i.d Gaussian processes with variance 1. To simplify our analysis, we define an output y for the network with dynamics (3.11) as the following:

$$y(t) \ = \ x(t) - \bar{x}(t) \ = \ M_n x(t). \tag{3.12}$$

Performance ρ_{ss} of the network with dynamics (3.11-3.12) is now equal to its squared $\mathcal{H}_2$-norm from input ψ to output y. It is note worthy that the unique marginally stable mode of dynamics (3.11-3.12) is not observable from the output, which results in the

boundedness of the $\mathcal{H}_2$-norm. From the results of [99] on the $\mathcal{H}_2$-norm, we now conclude:

$$\rho_{\text{ss}} \;=\; \frac{1}{2\pi}\int_{-\infty}^{\infty} \mathbf{Tr}\left(G^*(j\omega)G(j\omega)\right)d\omega, \tag{3.13}$$

where $G(s)$ is the transfer function of system (3.11-3.12):

$$G(s) \;=\; M_n\big(sI+L\big)^{-1}B'. \tag{3.14}$$

Let Λ be a diagonal matrix with eigenvalues $0=\lambda_1\leq\ldots\leq\lambda_n$ of L on its diameter and U be the corresponding orthonormal matrix of eigenvectors. Thus, we have $L=U\Lambda U^{\mathrm{T}}$. To calculate $G(s)$, we shall replace L and M_n in (3.14) using the following equations:

$$\begin{aligned} M_n &= U\text{diag}\big([0\;1\;\cdots\;1]\big)U^{\mathrm{T}},\\ L &= U\text{diag}\big([0\;\lambda_2\;\cdots\;\lambda_n]\big)U^{\mathrm{T}}. \end{aligned}$$

Doing so, one concludes:

$$G(s) \;=\; U\text{diag}\left(\left[0\;\frac{1}{s+\lambda_2}\;\cdots\;\frac{1}{s+\lambda_n}\right]\right)U^{\mathrm{T}}B'.$$

Thus, since $UU^{\mathrm{T}}=I_n$, one can write:

$$\begin{aligned} &\mathbf{Tr}\left(G^*(j\omega)G(j\omega)\right) \\ &\quad= \mathbf{Tr}\left(U\text{diag}\left(\left[0\;\frac{1}{w^2+\lambda_2^2}\;\cdots\;\frac{1}{w^2+\lambda_n^2}\right]\right)U^{\mathrm{T}}B'B'^{\mathrm{T}}\right) \end{aligned} \tag{3.15}$$

On the other hand, we have that

$$\int_{-\infty}^{\infty}\frac{1}{w^2+\lambda_i^2}\,d\omega \;=\; \frac{\pi}{\lambda_i}. \tag{3.16}$$

From (3.13), (3.15), and (3.16), one obtains:

$$\begin{aligned} \rho_{\text{ss}} &= \tfrac{1}{2\pi}\,\mathbf{Tr}\left(B'B'^{\mathrm{T}}U\text{diag}\left(\left[0\ \tfrac{\pi}{\lambda_2}\ \cdots\ \tfrac{\pi}{\lambda_n}\right]\right)U^{\mathrm{T}}\right) \\ &= \tfrac{1}{2}\,\mathbf{Tr}\left(B'B'^{\mathrm{T}}L^{\dagger}\right). \end{aligned} \tag{3.17}$$

When $B \in \mathbb{R}^{n\times n}$, from relation (3.17) we have

$$\begin{aligned} \rho_{\text{ss}} &= \tfrac{1}{2}\,\mathbf{Tr}\left(B'B'^{\mathrm{T}}L^{\dagger}\right) \\ &= \tfrac{1}{2}\,\mathbf{Tr}\left(B\text{diag}[\sigma_1^2\ \cdots\ \sigma_n^2]B^{\mathrm{T}}L^{\dagger}\right) \\ &= \tfrac{1}{2}\,\mathbf{Tr}\left(\text{diag}[\sigma_1^2\ \cdots\ \sigma_n^2]B^{\mathrm{T}}L^{\dagger}B\right). \end{aligned} \tag{3.18}$$

According to (3.18), it follows that

$$\eta_i \;=\; \partial\rho_{\text{ss}}/\partial(\sigma_i^2) \;=\; \frac{1}{2}\left[B^{\mathrm{T}}L^{\dagger}B\right]_{ii}, \tag{3.19}$$

where the subscript $[.]_{ii}$ indicates the (i,i)th element and $i \in \mathcal{V}$. According to (3.19), we can rewrite (3.18) as follows

$$\rho_{\text{ss}} \;=\; \sum_{i\in\mathcal{V}} \sigma_i^2\,\eta_i.$$

When $B \in \mathbb{R}^{n\times m}$, in which m is the number of links, from relation (3.17) we have

$$\begin{aligned} \rho_{\text{ss}} &= \tfrac{1}{2}\,\mathbf{Tr}\left(B'B'^{\mathrm{T}}L^{\dagger}\right) \\ &= \tfrac{1}{2}\,\mathbf{Tr}\left(\text{diag}[\sigma_1^2\ \cdots\ \sigma_m^2]B^{\mathrm{T}}L^{\dagger}B\right). \end{aligned} \tag{3.20}$$

According to (3.20):

$$\nu_i \;=\; \partial\rho_{\text{ss}}/\partial(\sigma_i^2) \;=\; \frac{1}{2}\left[B^{\mathrm{T}}L^{\dagger}B\right]_{ii}, \tag{3.21}$$

where the subscript $[.]_{ii}$ indicates the (i,i)th element and $i \in \mathcal{E}$. According to (3.21), we

can rewrite (3.18) in the form of (3.10). □

Our focus in this chapter is on consensus networks with undirected underlying graphs. It is straightforward to generalize our results for strongly connected, balanced directed graphs. For the general case, however, when the state matrix is not normal, *i.e.* $LL^{\mathrm{T}} \neq L^{\mathrm{T}}L$, obtaining a succinct formula for the centrality measure seems to be more challenging. In [4], the authors proposed bounds that the $\mathcal{H}_2$-norm, as a performance measure, can be tightly bounded from below and above by some spectral functions of state and output matrices. Thus, one can obtain explicit bounds on the centrality measures. In addition, [100] shows how one can approximate a strongly connected digraph by some weighted undirected graph that inherits some specific properties of the original digraph. These results may be utilized to approximate centrality measures for directed networks.

3.5 Agent Centrality Index

In this section, we consider four types of noise structures for network (3.5) and calculate the agent centrality index (3.7) for each case. These noise structures usually appear when one implements a consensus algorithm based on model (3.3) in noisy environments using uncertain communication channels and noisy sensors. In order to execute each update equation (3.3), each agent needs to operate in a noisy environment, sense its own state, transmit its own state information to its neighboring agents, and receive state information from its neighboring agents. In practical situations, all these steps involve uncertainties, where in this chapter we model them by structured additive noise inputs.

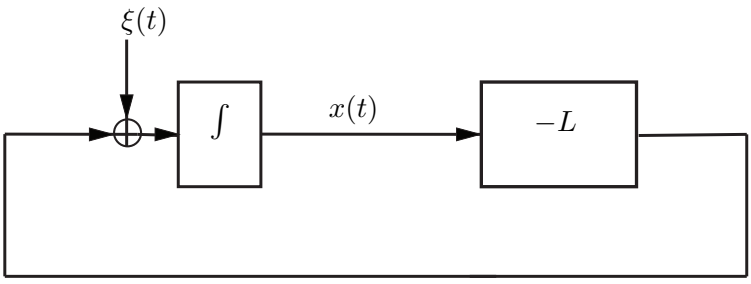

Figure 3.1: A representation of linear consensus network (3.22) with dynamics noises.

3.5.1 Dynamics Noise

This noise structure captures the effect of environment noise on dynamics of each agent. In this case, the dynamics of agent i is described by

$$\dot{x}_i(t) \;=\; \sum_{j\neq i} a_{ij}\big(x_j(t) - x_i(t)\big) \;+\; \xi_i(t), \tag{3.22}$$

where $\xi_i(t) \sim N(0, \sigma_i^2)$ for all $i \in \mathcal{V}$. This class of noisy linear consensus networks has been studied before in the literature (see [2, 4, 5, 38] and references in there). The network dynamics (3.22) can be rewritten as a special case of (3.5) where $B = I_n$. Figure 3.1 depicts a block diagram representation of linear consensus network (3.22) with dynamics noise. This representation is meant to illustrate the underlying mechanism of the dynamics and show how noise may affect the consensus process.

Theorem 3.5.1. *For the consensus network (3.22) with dynamics noise, the value of the centrality index* (3.7) *can be expressed by*

$$\eta_i \;=\; \frac{1}{2}\, l^{\dagger}_{ii}, \tag{3.23}$$

where $l^{\dagger}_{ii}$ for $i \in \mathcal{V}$ are the diagonal elements of $L^{\dagger}$.

Proof. From our arguments in Part 3.5.1, in case of the dynamics noise structure, one has to deal with dynamics (3.11)-(3.12) where

$$B' \;=\; \text{diag}\big([\sigma_1 \;\cdots\; \sigma_n]\big).$$

We now have:

$$B'B'^{\mathrm{T}} \;=\; \text{diag}\big([\sigma_1^2 \;\cdots\; \sigma_n^2]\big). \tag{3.24}$$

Relation (3.23) now immediately follows from (3.17) and (3.24). □

3.5.2 Receiver Noise

The communication receiver noise is the second type of noise source that can be considered in updating law (3.3). If agents i and j are neighbors, agent i receives $x_j(t) + \xi_i(t)$ as opposed to the clean state information $x_j(t)$, as a result of its noisy communication receiver. According to this noise model, the update equation of agent i takes the following form

$$\dot{x}_i(t) \;=\; \sum_{j\neq i} a_{ij}\big(x_j(t) - x_i(t) + \xi_i(t)\big), \tag{3.25}$$

where $\xi_i(t) \sim N(0, \sigma_i^2)$ for all $i \in \mathcal{V}$. The network dynamics (3.25) can be written as a special case of (3.5) where B is equal to the degree matrix $\Delta = \text{diag}([d_1 \;\cdots\; d_n])$ of the underlying coupling graph of the network.

Theorem 3.5.2. *For the consensus network (3.25) with communication receiver noise, the value of the centrality index* (3.7) *can be calculated as*

$$\eta_i \;=\; \frac{1}{2}\, d_i^2 l_{ii}^{\dagger}. \tag{3.26}$$

where d_i and $l_{ii}^{\dagger}$ for $i \in \mathcal{V}$ are the node degrees and the diagonal elements of $L^{\dagger}$, respec-

tively.

Proof. Based on the description of receiver noises in Part 3.5.2, one has to now consider dynamics (3.11-3.12) with

$$B' \;=\; \Delta\,\mathrm{diag}\big([\sigma_1 \;\cdots\; \sigma_n]\big), \tag{3.27}$$

and calculate ρ_{ss} using (3.17). From (3.27):

$$B'B'^{\mathrm{T}} \;=\; \mathrm{diag}\big([\sigma_1^2 d_1^2 \;\cdots\; \sigma_n^2 d_n^2]\big),$$

which together with (3.17) result in (3.26). □

3.5.3 Emitter Noise

The third type of noise source in updating law (3.3) can be due to the communication emitters of the neighboring agents. If agents i and j are neighbors, agent i now receives $x_j(t) + \xi_j(t)$ rather than pure state information $x_j(t)$, due to the noisy communication emitter of neighboring agent j. This noise model amounts to the following update equation for agent i:

$$\dot{x}_i(t) \;=\; \sum_{j\neq i} a_{ij}\big(x_j(t) - x_i(t) + \xi_j(t)\big), \tag{3.28}$$

where $\xi_i(t) \sim N(0, \sigma_i^2)$ for all $i \in \mathcal{V}$. One can reformulate the overall dynamics of the network with individual dynamics (3.28) and show that it is a special case of (3.5) with $B = A$, where A is the adjacency matrix of the underlying coupling graph of the network.

Theorem 3.5.3. *For the consensus network (3.28) with communication emitter noise, the*

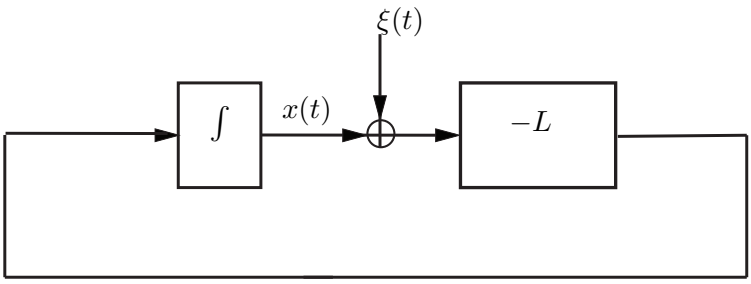

Figure 3.2: A representation of linear consensus network (3.31) with sensor noises.

value of the centrality index (3.7) *can be computed as*

$$\eta_i \;=\; \frac{1}{2}\left(d_i^2 l_{ii}^\dagger + \left(\frac{2}{n}-1\right) d_i\right), \tag{3.29}$$

where d_i *and* $l_{ii}^\dagger$ *for* $i \in \mathcal{V}$ *are, respectively, the node degrees and the diagonal elements of* $L^\dagger$.

Proof. From our discussion in Part 3.5.3, the case of emitter noises corresponds to dynamics (3.11-3.12) with

$$B' \;=\; A\ \mathrm{diag}\big([\sigma_1\ \cdots\ \sigma_n]\big).$$

We now have:

$$\begin{aligned} B'^{\mathrm{T}} L^\dagger B' \;&=\; (\Delta - L)L^\dagger(\Delta - L) \\ &=\; \Delta L^\dagger \Delta - M_n\Delta - \Delta M_n + L. \end{aligned} \tag{3.30}$$

Finally, using the result of Theorem 3.4.4 and (3.30), we obtain the desired result (3.29).

□

3.5.4 Sensor Noise

The fourth type considered here is the case of noisy sensors, where each agent obtains a noisy measurement of its own current state and transmit it to the neighboring agents. The

update equation of agent i can now be described by

$$\dot{x}_i(t) \;=\; \sum_{j\neq i} a_{ij}\Big[\big(x_j(t)+\xi_j(t)\big)-\big(x_i(t)+\xi_i(t)\big)\Big], \tag{3.31}$$

where $\xi_i(t) \sim N(0,\sigma_i^2)$ for all $i \in \mathcal{V}$. In this scenario, agent i receives $x_j(t)+\xi_j(t)$ instead of $x_j(t)$, due to the noisy sensors of its neighboring agents. On the other hand, agent i also measures a contaminated version of its own current state. The overall dynamics of the network with individual dynamics (3.31) can be rewritten as a special case of (3.5) with $B = -L$. Figure 3.2 shows a representation of this linear consensus network with sensor noises.

Theorem 3.5.4. *For the consensus network (3.31) with sensor noise, the value of the centrality index* (3.7) *can be computed as*

$$\eta_i \;=\; \frac{1}{2}\, d_i, \tag{3.32}$$

where d_i for $i \in \mathcal{V}$ are the node degrees.

Proof. In case of sensor noises, one again deals with dynamics (3.11-3.12), but this time:

$$B' \;=\; -\,L\,\mathrm{diag}\big([\sigma_1 \;\cdots\; \sigma_n]\big).$$

Thus,

$$B'B'^{\mathrm{T}} \;=\; L\mathrm{diag}\big([\sigma_1^2 \;\cdots\; \sigma_n^2]\big)L. \tag{3.33}$$

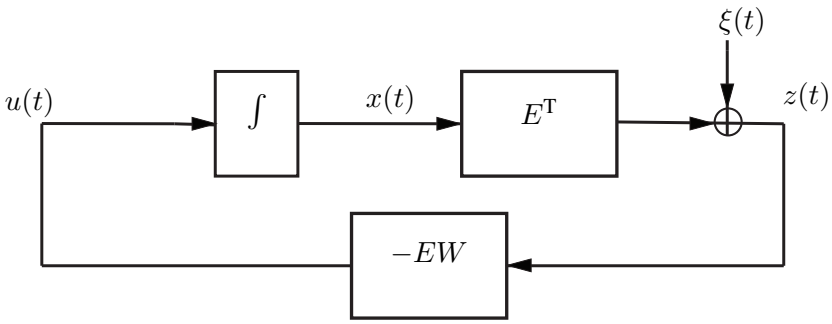

Figure 3.3: A representation of linear consensus network (3.36-3.38) with communication channel noises.

From (3.17) and (3.33), we conclude:

$$\begin{aligned} \rho_{\text{ss}} &= \tfrac{1}{2}\,\mathbf{Tr}\left(L\text{diag}\left([\sigma_1^2\ \cdots\ \sigma_n^2]\right)M_n\right) \\ &= \tfrac{1}{2}\,\mathbf{Tr}\left(\text{diag}\left([\sigma_1^2\ \cdots\ \sigma_n^2]\right)L\right) \\ &= \tfrac{1}{2}\sum_{i=1}^{n}\sigma_i^2 d_i^2. \end{aligned} \tag{3.34}$$

Finally, using the centrality index of an agent (3.7) and (3.34), we get the desired result.

□

Remark 3.5.5. *For a connected, undirected graph with the damping factor* $\alpha = 1$*, PageRank is proportional to the centrality measure* (3.32)*; see [101] for more details.*

3.6 Link Centrality Index

Besides the above mentioned agent based noise inputs, there are two possible scenarios for link noises that we will consider in the following.

3.6.1 Communication Channel Noise

The first type of link noise is the communication channel noise that captures a passing signal's distortion through a communication channel between two agents in the network. This type of uncertainty can be modeled as a white Gaussian noise $\xi_e(t) \sim N(0, \sigma_e^2)$ for each $e \in \mathcal{E}$. More specifically, for an arbitrary link $e = \{i, j\} \in \mathcal{E}$, one of the endpoints of e, say i, receives $x_j(t) + \xi_e(t)$ instead of $x_j(t)$ at each time t, while the other endpoint, i.e., j, receives $x_i(t) - \xi_e(t)$ as opposed to the clean state information $x_i(t)$. Attributing a virtual orientation for e, that considers i as its head end, we derive an oriented incidence matrix E and conclude that the update algorithm of agent i can be described by

$$\dot{x}_i(t) \;=\; \sum_{e=\{i,j\}\in\mathcal{E}} a_{ij}\big(x_j(t) - x_i(t) + \xi_e(t)\big). \tag{3.35}$$

According to Assumption 3.4.1, all noises associated with distinct communication channels are independent. The overall dynamics of the network can be rewritten as a special case of (3.5) with $B = EW$, notice that $L = EWE^{\mathrm{T}}$.Also, in this case, we can recall the two-port representation of linear consensus network (3.5) as described in [17, 102] that can be cast in the following compact form

$$\dot{x}(t) \;=\; u(t), \tag{3.36}$$

$$z(t) \;=\; E^{\mathrm{T}}x(t) + \xi(t), \tag{3.37}$$

where $\xi(t) = [\,\xi_{e_1},\ \ldots\ ,\ \xi_{e_m}\,]^{\mathrm{T}}$ is the vector of noise input, $\xi_e(t) \sim N(0, \sigma_e^2)$ for all $e \in \mathcal{E}$, and the internal feedback control law is given by

$$u(t) \;= -EWz(t), \tag{3.38}$$

as depicted in Figure 3.3.

Theorem 3.6.1. *For the consensus network (3.36-3.37) with communication channel noise, the value of the link centrality index* (3.8) *can be calculated as*

$$\nu_e \;=\; \frac{1}{2} a_e^2 r_e, \tag{3.39}$$

where $r_e := l^\dagger_{ii} + l^\dagger_{jj} - 2l^\dagger_{ij}$ *is the effective resistance of edge* $e = \{i, j\}$ *and* $a_e = a_{ij}$.

Proof. Using the same approach presented in the proof of Theorem 3.5.1, we can describe the dynamics of network by (3.11-3.12) in which

$$B' \;=\; EW\,\mathrm{diag}([\sigma_1 \;\cdots\; \sigma_m]) \tag{3.40}$$

where E denotes the incidence matrix of underlying graph $\mathcal{G}$ and W is the diagonal matrix whose diagonal elements are respectively $w(e) = a_{ij}$ for all $e = \{i, j\} \in \mathcal{E}$. The ordering of diagonal elements in W complies with row ordering in the corresponding incident matrix E. Then, calculating the squared $\mathcal{H}_2$–norm of the network reduces to

$$\rho_{\text{ss}} \;=\; \frac{1}{2}\,\mathbf{Tr}\left(B'B'^{\mathrm{T}}L^\dagger\right). \tag{3.41}$$

Using (3.40), we get

$$B'B'^{\mathrm{T}} \;=\; E\,\mathrm{diag}([\sigma_1^2 a_{e_1}^2 \;\cdots\; \sigma_m^2 a_{e_m}^2])E^{\mathrm{T}}. \tag{3.42}$$

Substituting (3.42) into (3.41), we get

$$\rho_{\text{ss}} \;=\; \frac{1}{2}\,\mathbf{Tr}\left(E\,\mathrm{diag}([\sigma_1^2 a_{e_1}^2 \;\cdots\; \sigma_m^2 a_{e_m}^2])E^{\mathrm{T}}L^\dagger\right)$$

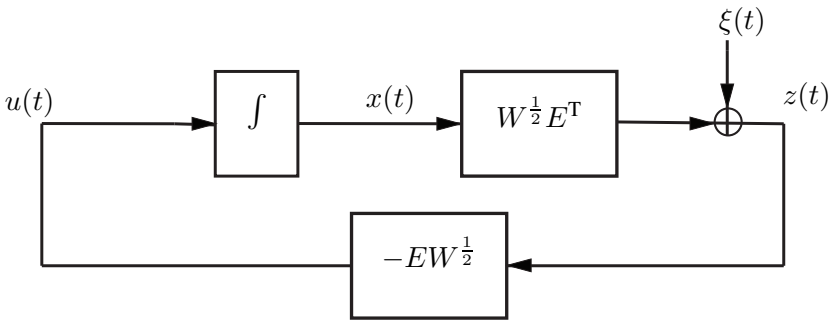

Figure 3.4: A representation of linear consensus network (3.43-3.45) with measurement noises.

$$\begin{aligned} &= \frac{1}{2}\,\mathbf{Tr}\left(\,\mathrm{diag}([\sigma_1^2 a_{e_1}^2\ \cdots\ \sigma_m^2 a_{e_m}^2])E^{\mathrm{T}}L^{\dagger}E\right) \\ &= \frac{1}{2}\sum_{e\in\mathcal{E}}\sigma_e^2 a_e^2 r_e. \end{aligned}$$

The last equality holds as the diagonal elements of $E^{\mathrm{T}}L^{\dagger}E$ are r_e's for $e \in \mathcal{E}$. □

3.6.2 Measurement Noise

The second type of link noise model is used to mimic the effect of measurement noise that occurs in practice. For this case, similar to the pervious case, we can use the two-port representation of linear consensus network (3.5) as follows:

$$\dot{x}(t) = u(t), \tag{3.43}$$

$$z(t) = W^{1/2}E^{\mathrm{T}}x(t) + \xi(t), \tag{3.44}$$

where $\xi(t) = [\,\xi_{e_1},\ \ldots\ ,\ \xi_{e_m}\,]^{\mathrm{T}}$ is the vector of noise input, $\xi_e(t) \sim N(0, \sigma_e^2)$ for all $e \in \mathcal{E}$, and the internal feedback control law is given by

$$u(t) = -EW^{1/2}z(t), \tag{3.45}$$

as presented in Figure 3.4.

Theorem 3.6.2. *For the consensus network (3.43-3.44) with measurement noise, the value of the link centrality index* (3.8) *is given by*

$$\nu_e \;=\; \frac{1}{2} r_e, \tag{3.46}$$

where r_e is the effective resistance of edge e in the underlying graph of the network.

Proof. Using the same approach presented in the proof of Theorem 3.6.1, we can describe the dynamics of network by (3.11-3.12) in which

$$B' \;=\; E \operatorname{diag}\left([\sigma_1 \;\cdots\; \sigma_m]\right), \tag{3.47}$$

where E denotes the incidence matrix of underlying graph $\mathcal{G}$. We denote the row of E corresponds with link e by E_e, then according to the definition of effective resistance, we have

$$r_e \;=\; E_e L^\dagger E_e^{\mathrm{T}} \;=\; l^\dagger_{ii} + l^\dagger_{jj} - 2l^\dagger_{ij}, \tag{3.48}$$

where, $e = \{i, j\} \in \mathcal{E}$. Then, calculating the squared $\mathcal{H}_2$–norm of the network reduces to

$$\begin{aligned}
\rho_{\text{ss}} \;&=\; \frac{1}{2}\,\mathbf{Tr}\left(B' B'^{\mathrm{T}} L^\dagger\right) \\
&=\; \frac{1}{2}\,\mathbf{Tr}\left(E \operatorname{diag}([\sigma_1^2 \;\cdots\; \sigma_m^2]) E^{\mathrm{T}} L^\dagger\right) \\
&=\; \frac{1}{2}\,\mathbf{Tr}\left(\operatorname{diag}([\sigma_1^2 \;\cdots\; \sigma_m^2]) E^{\mathrm{T}} L^\dagger E\right) \\
&=\; \frac{1}{2}\sum_{e\in\mathcal{E}} \sigma_e^2 r_e.
\end{aligned}$$

where in the last equality we use (3.48). □

Noise structure	Centrality index η_i
Dynamics noises	$\frac{1}{2}l_{ii}^{\dagger}$
Receiver noises	$\frac{1}{2}d_i^2 l_{ii}^{\dagger}$
Emitter noises	$\frac{1}{2}\big(d_i^2 l_{ii}^{\dagger} + (\frac{2}{n}-1)d_i\big)$
Sensor noises	$\frac{1}{2}d_i$

Table 3.1: The centrality index of an agent in a noisy linear consensus network for various noise structures.

Noise structure	Centrality index ν_i
Communication noises	$\frac{1}{2}a_e^2 r_e$
Measurement noises	$\frac{1}{2}r_e$

Table 3.2: The centrality index of a link for two noise structures.

Remark 3.6.3. *In [95], the authors refer to quantity $1/l_{ii}^{\dagger}$ as topological centrality of node i that indicates its overall position as well as its overall connectedness in the network. This measure is closely related to the centrality index of agent i in a linear consensus network with dynamics noise (see Table 3.1). Moreover, [95] presents three alternative interpretations for this measure in terms of: (i) detour overheads in random walks, (ii) voltage distributions and the phenomenon of recurrence when the network is treated as an electrical circuit, and (iii) the average connectedness of nodes when the network breaks into two.*

3.7 Centrality Rank and Inherent Tradeoffs

The results of Sections 3.5 and 3.6 are summarized in Tables 3.1 and 3.2. For a given noise structure, agents and links in a consensus network with dynamics (3.5) can be ranked according to the values of their corresponding centrality indices.

Definition 3.7.1. *For a given noise structure, agent $j \in \mathcal{V}$ precedes $i \in \mathcal{V}$ in rank if*

$\eta_i \leq \eta_j$. *Similarly, link* $e_2 \in \mathcal{E}$ *precedes link* $e_1 \in \mathcal{E}$ *in rank if* $\nu_{e_1} \leq \nu_{e_2}$.

Fundamental tradeoffs on centrality rank of agents and links may emerge depending on the noise structure. In the following result, we show that enhancing couplings (e.g., by strengthening link weight or establishing new links) can improve centrality of an agent or a link with respect to some noise structures and worsen it with respect to some other types.

Theorem 3.7.2. *For a given agent* $i \in \mathcal{V}$ *and link* $e \in \mathcal{E}$*, suppose that functions* $\phi_i, \psi_e, \delta_i : \mathfrak{L}_n \to \mathbb{R}$ *are defined by* $\phi_i(L) = l^{\dagger}_{ii}$*,* $\psi_e(L) = r_e$*, and* $\delta_i(L) = d_i$*. Then, functions* ϕ_i *and* ψ_e *are monotonically decreasing and function* δ_i *is monotonically increasing as a function of* L*, i.e., for all* $L_1 \preceq L_2$ *it follows that*

$$\phi_i(L_2) \leq \phi_i(L_1), \tag{3.49}$$

$$\psi_e(L_2) \leq \psi_e(L_1), \tag{3.50}$$

$$\delta_i(L_1) \leq \delta_i(L_2). \tag{3.51}$$

Proof. Let us consider the real-valued function $f(L, Q) = \mathbf{Tr}(QL)$. From matrix calculus, one gets

$$\frac{\partial f(L,Q)}{\partial L} = Q. \tag{3.52}$$

When $Q_i = \mathrm{diag}[0, \cdots, 1, \cdots, 0]$, i.e., a diagonal matrix with only one nonzero element on its i-th diagonal element, function f reduces to $f(L, Q_i) = \delta_i(L) = d_i$. According to (3.52) and the fact that $Q_i \succeq 0$, one can conclude that function $f(L, Q_i) = \delta_i(L)$ is monotonically increasing.

In the next step, let us consider the real-valued function $g(L, Q) = \mathbf{Tr}(QL^{\dagger})$. A direct matrix calculation gives us

$$\frac{\partial g(L,Q)}{\partial L} = -L^{\dagger}QL^{\dagger}. \tag{3.53}$$

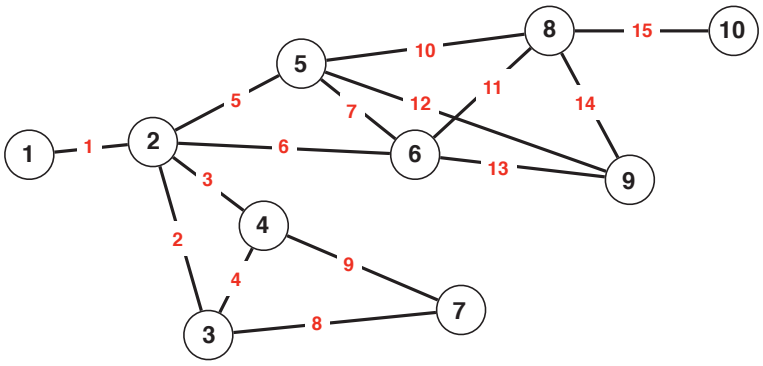

Figure 3.5: The network topology for Example 3.8.1. The red labels on the links represent link numbers.

The function $g(L, Q_i)$ is equal to $l^\dagger_{ii}$. Therefore, $\phi_i(L) = l^\dagger_{ii}$ is monotonically decreasing, because $-L^\dagger Q_i L^\dagger \preceq 0$ for all $i = 1, \ldots, n$. Furthermore, if Q_e is the Laplacian matrix of a graph with only one link $e = \{i, j\}$, then the function $g(L, Q_e)$ is equal to r_e. Using (3.53) and the fact that $-L^\dagger Q_e L^\dagger \preceq 0$, we can conclude that $\psi_e(L) = r_e$ is monotonically decreasing. □

According to this theorem, by enhancing couplings one may expect to observe drastic changes in each agent's and link's ranking with respect to various noise structures. For instance, suppose that for a given consensus network agent i is ranked s_1 w.r.t. sensor noise and t_1 w.r.t. dynamics noise, where $s_1 > t_1$. It is likely that after adding new links or increasing weight links, the same agent i gets ranked s_2 w.r.t. sensor noise and t_2 w.r.t. dynamics noise, but this time $t_2 > s_2$. This key point is explained in details using several numerical simulations in the following section.

The result of Theorem 3.7.2 can be leveraged further to identify inherent performance tradeoffs due to direction of monotonicity for different types of uncertainties. From the

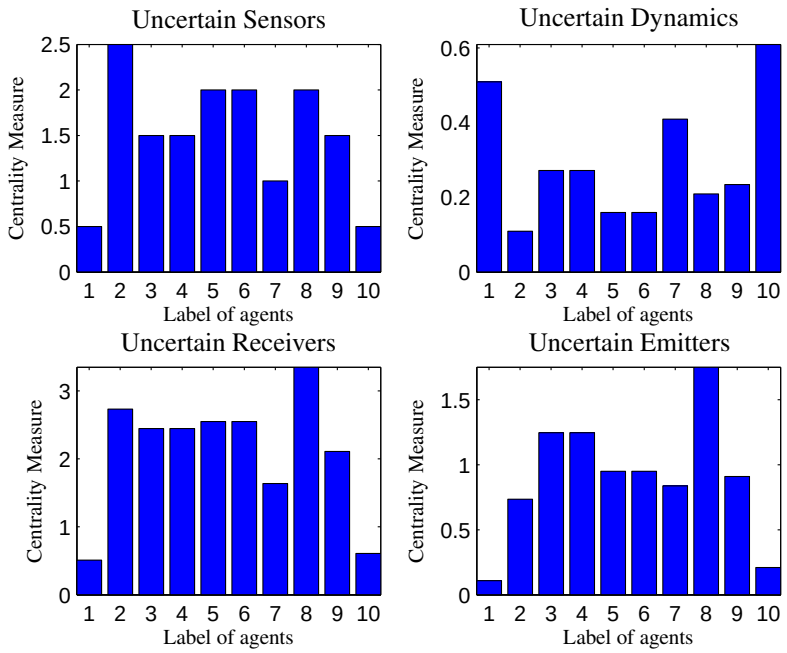

Figure 3.6: The agent centrality indices for different noise structures and the coupling graph of Figure 3.5.

result of Theorem 3.4.4, the value of performance measure can be equivalently characterized with respect to various centrality measures as follows

$$\begin{aligned} \rho_{ss} &= \frac{1}{2}\sum_{i\in\mathcal{V}}\sigma_i^2\phi_i(L) \\ &= \frac{1}{2}\sum_{i\in\mathcal{V}}\sigma_i^2\delta_i(L) \\ &= \frac{1}{2}\sum_{e\in\mathcal{E}}\sigma_e^2\psi_e(L), \end{aligned}$$

Therefore, according to Theorem 3.7.2, if $L_1 \preceq L_2$, we can conclude that in presence of dynamics and sensor noises the performance of network 2 is not worse than the performance of network 1, whereas in presence of measurement noise the performance of network 2 is not better than the performance of network 1. For a given network with Laplacian matrix L_1, inequality $L_1 \preceq L_2$ can be realized via several possible scenar-

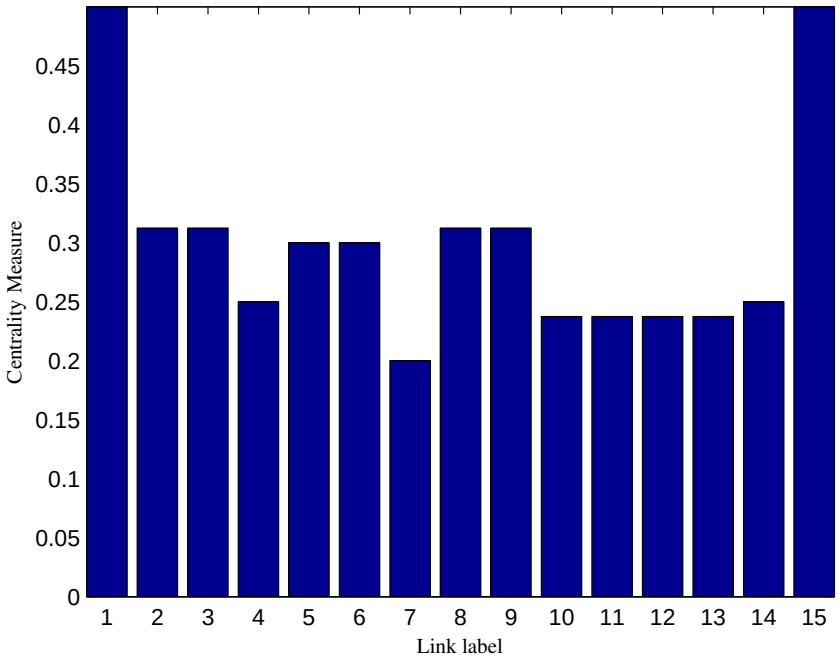

Figure 3.7: The link centrality indices for the coupling graph of Figure 3.5. Since the coupling graph is unweighted, both proposed link centrality indices in Table 3.2 are identical.

ios; for example, network 2 can be constructed by (i) adding new weighted edges to the graph of network 1, (ii) increasing weights of some of the existing links in network 1, (iii) rewiring topology of network 1 while ensuring $L_1 \preceq L_2$. The final conclusion is that strengthening couplings among the agents may improve or deteriorate the performance depending on the noise structure.

3.8 Illustrative Numerical Examples

In this section, we support our theoretical results by illustrating several examples to provide better insight about agent and link centrality measures in noisy linear consensus networks.

Example 3.8.1. *Let us consider a noisy linear consensus network with coupling graph shown in Figure 3.5. It is assumed that every link has weight* 1*. For this network, the centrality index of all* 10 *agents are calculated for different noise structures according to Table 3.1 and are depicted in Figure 3.6. One observes that while agents 1 and 10 are the most central agents w.r.t. dynamics noise, they are the least central w.r.t. the other remaining three noise structures. According to Figure 3.6 for uncertain sensors, one can rank all agents based on their corresponding node degrees, which can be easily deduced from the graph topology. However, we observe that in presence of dynamics, receiver, and emitter noises there is no trivial way to relate topology of the underlying coupling graph of the network to agents' centrality rank. For the same network, the links are ranked according to Table 3.2 and the result is depicted in Figure 3.7. Since the underlying graph is unweighted, both centrality measures in Table 3.2 are the same. One observes that links number* 1 *and* 15 *are the most central links. This is compatible with the fact that by eliminating any of these two links the underlying graph becomes disconnected.*

Example 3.8.2. *We simulate a noisy linear consensus network with coupling graph shown in Figure 3.8, where it is assumed that all link weights are equal to* 1*. This graph is indeed a rewired form of the graph in Figure 3.5 – both graphs share the same number of nodes and links. The agent centrality indices are drawn according to Table 3.1 in Figure 3.9. It can be seen that all agents have equal ranks (i.e., importance) in the network for all four noise structures. The link centrality indices are depicted in Figure 3.10, where it is shown that all links have equal ranks. These observations are consistent with our results and can be explained as follows: since the coupling graph in Figure 3.8 is symmetric (i.e.link-transitive and node-transitive) and unweighted, all nodes and links contribute equally to the performance of the network.*

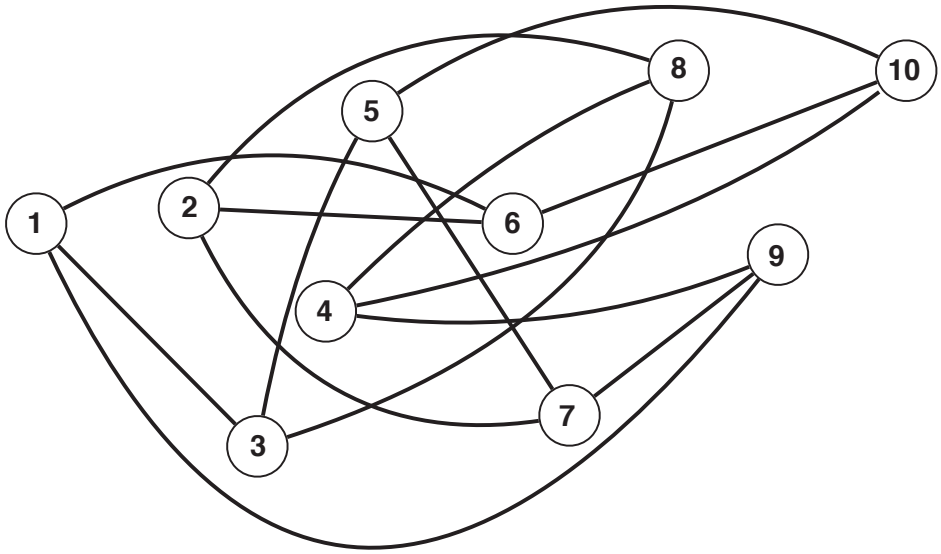

Figure 3.8: The network topology for Example 3.8.2.

Example 3.8.3. *In our last simulation, we study link centrality rank for a noisy linear consensus network with coupling graph in Figure 3.11, where this graph consists of* 108 *links and three groups of* 10 *agents that each group is shown by red, green, and blue colors. We calculate link centrality indices according to Table 3.2 for several scenarios. In Figure 3.12, the link centrality indices are depicted when it is assumed that all links in the graph have weights equal to* 1*, except for* $w(\mathrm{A}) = w(\mathrm{B}) = w(\mathrm{C}) = w(\mathrm{D}) = 0.2$*. One observes that the intergroup links* $\mathrm{A}, \mathrm{B}, \mathrm{C}$*, and* D *are significantly more important than the intragroup links. Both links* A *and* B *are the most central ones as without them the network graph will be disconnected.*

The link centrality index of an edge with respect to measurement noise is proportional to the effective resistance of that link from our results in Table 3.2. The result of Theorem 3.7.2 asserts that by increasing weights of links A*,* B*,* C*, and* D*, their centrality rank will drop accordingly. This can be clearly seen in our simulations in Figures 3.12, 3.13, 3.14, and 3.15, where the weights of these four links are increased from* 0.2 *to* 1*, then to* 3*,*

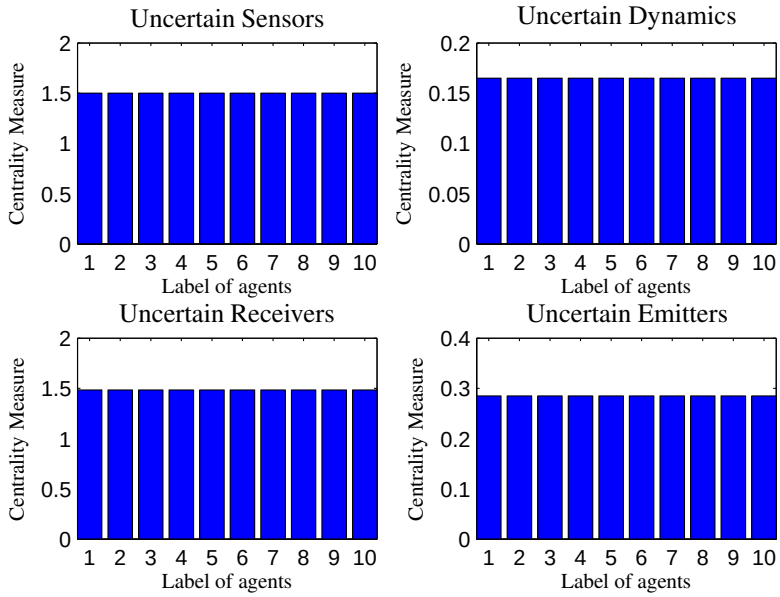

Figure 3.9: The centrality indices of all agents for a noisy linear consensus network defined by the coupling graph in Figure 3.8.

and finally to 10. *These four links, however, remain the most central links with respect to communication noises and their roles do not change by changing their weights.*

3.9 Conclusion

A new definition of centrality, with respect to the $\mathcal{H}_2$-norm square, is introduced for networks with consensus dynamics subject to structured additive noise inputs. In such networks, the centrality of each agent or link depends on the underlying coupling graph of the network as well as the structure of noise input. We model several noise structures based on realistic operational situations. It is shown that the centrality index of agents and links solely depends on the characteristics of the underlying coupling graph. We discuss that the centrality rank of agents or links may vary substantially when comparing various noise structures. More importantly, it is argued that when one modifies the cou-

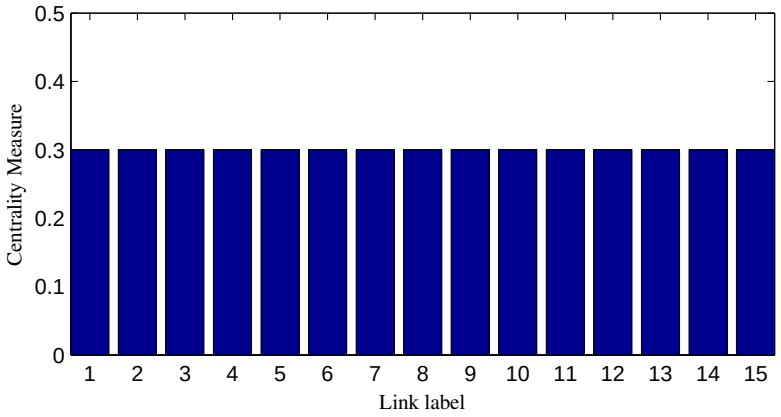

Figure 3.10: Links' centrality for the coupling graph of Figure 3.8. Since, the coupling graph is unweighted both link centrality measures in Table 3.2 are the same.

pling graph of the network (for instance by rewiring, weight adjustment, sparsification, and adding new links), the agent and link centrality ranks may drastically shift up or down in the list. Since in real-world situations there are several possible sources of uncertainties that can affect the dynamics of a consensus network simultaneously, it would be a challenging task to determine the most central agents or links without taking into account the existing fundamental tradeoffs among various centrality ranks. This inherent phenomenon in uncertain consensus networks suggests revisiting and reformulating several existing canonical network optimization problems in the literature by taking into account the agent and link centrality ranks in the design process in order to synthesize more robust consensus networks.

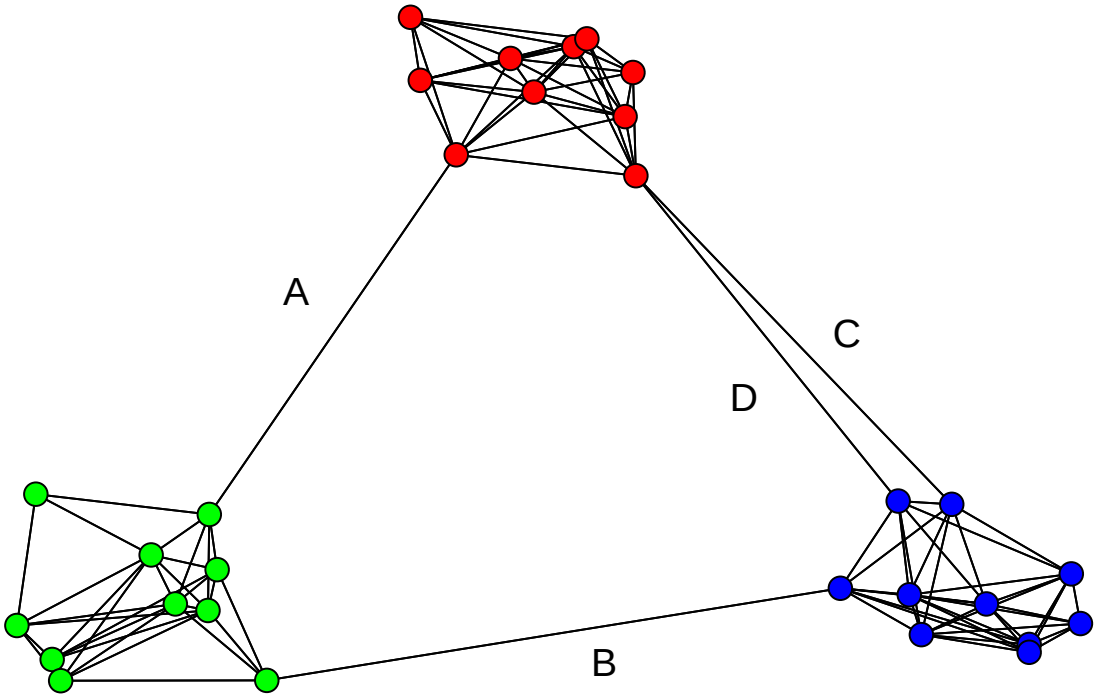

Figure 3.11: The network topology for Example 3.8.3.

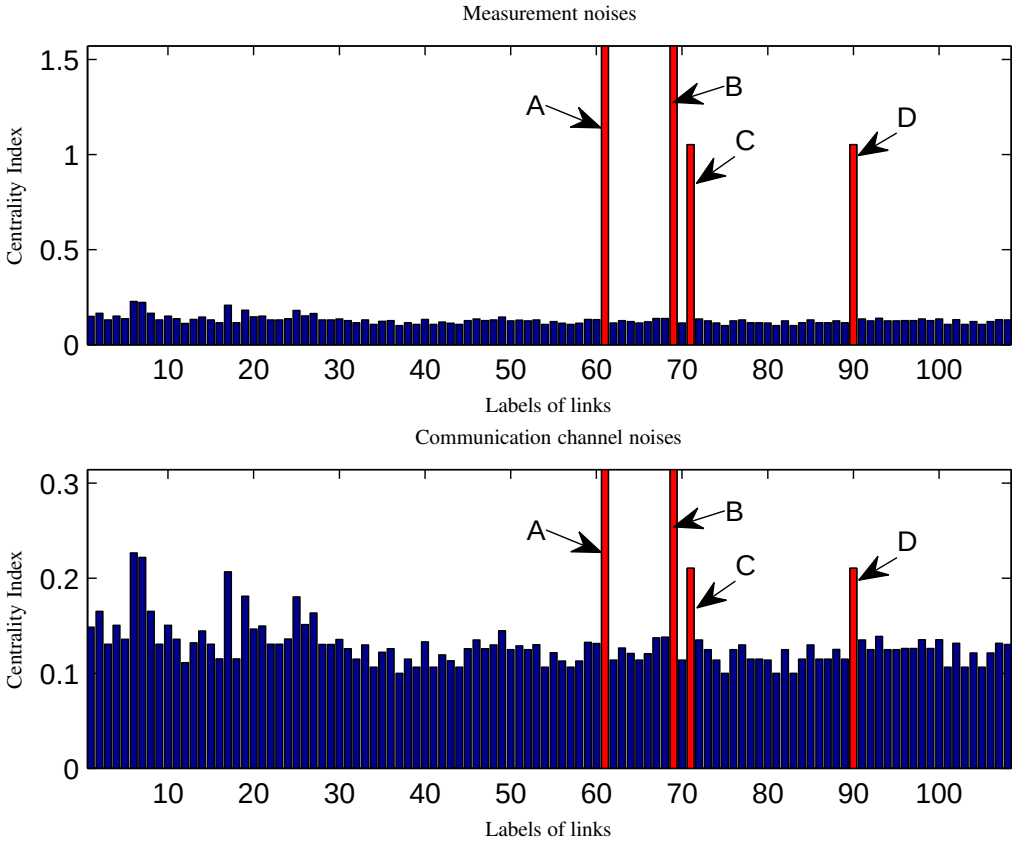

Figure 3.12: The link centrality indices for the consensus network with graph topology Figure 3.11. It is assumed that all link weights are equal to 1, except for $w(\mathrm{A}) = w(\mathrm{B}) = w(\mathrm{C}) = w(\mathrm{D}) = 0.2$. The centrality indices of links $\mathrm{A}, \mathrm{B}, \mathrm{C}$, and D are shown by red bars.

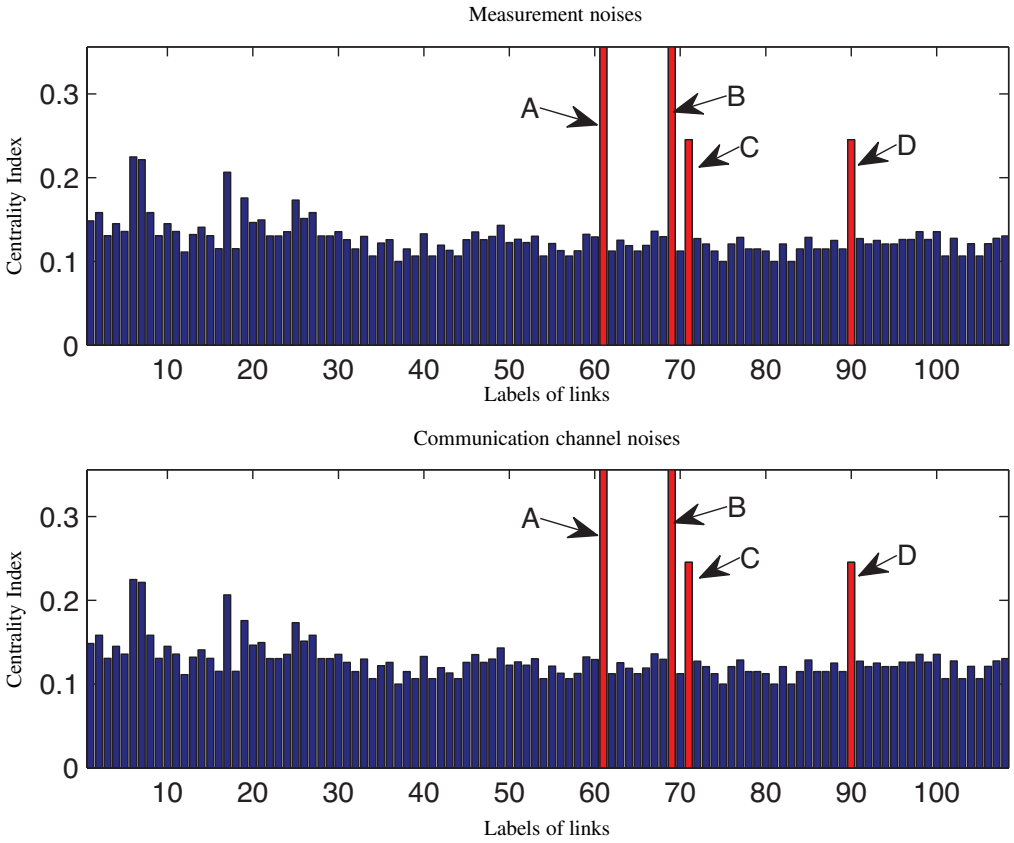

Figure 3.13: The link centrality indices for the consensus network with graph topology Figure 3.11, where all link weights are equal to 1. In this plot A, B, C, and D are labels of links between three clusters. The centrality indices of links $\mathrm{A}, \mathrm{B}, \mathrm{C}$, and D are shown by red bars.

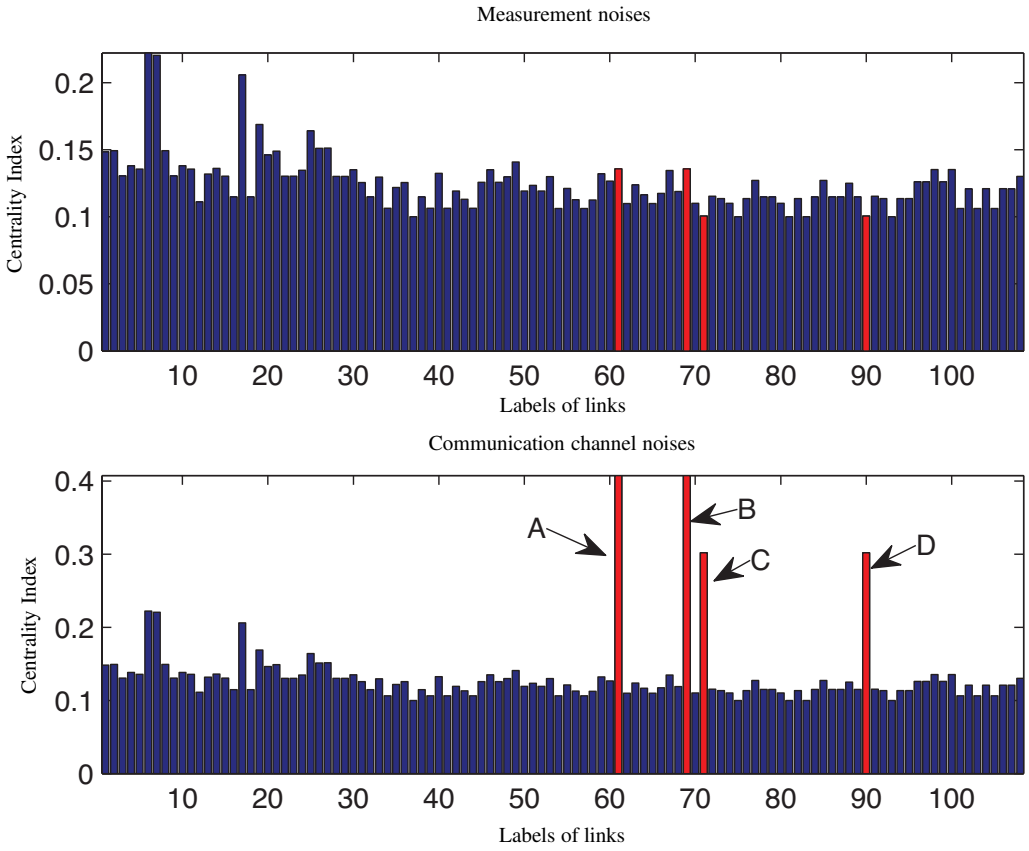

Figure 3.14: The link centrality indices for the consensus network with graph topology Figure 3.11. It is assumed that all link weights are equal to 1, except for $w(\mathrm{A}) = w(\mathrm{B}) = w(\mathrm{C}) = w(\mathrm{D}) = 3$. The centrality indices of these links $\mathrm{A}, \mathrm{B}, \mathrm{C}$, and D are shown by red bars.

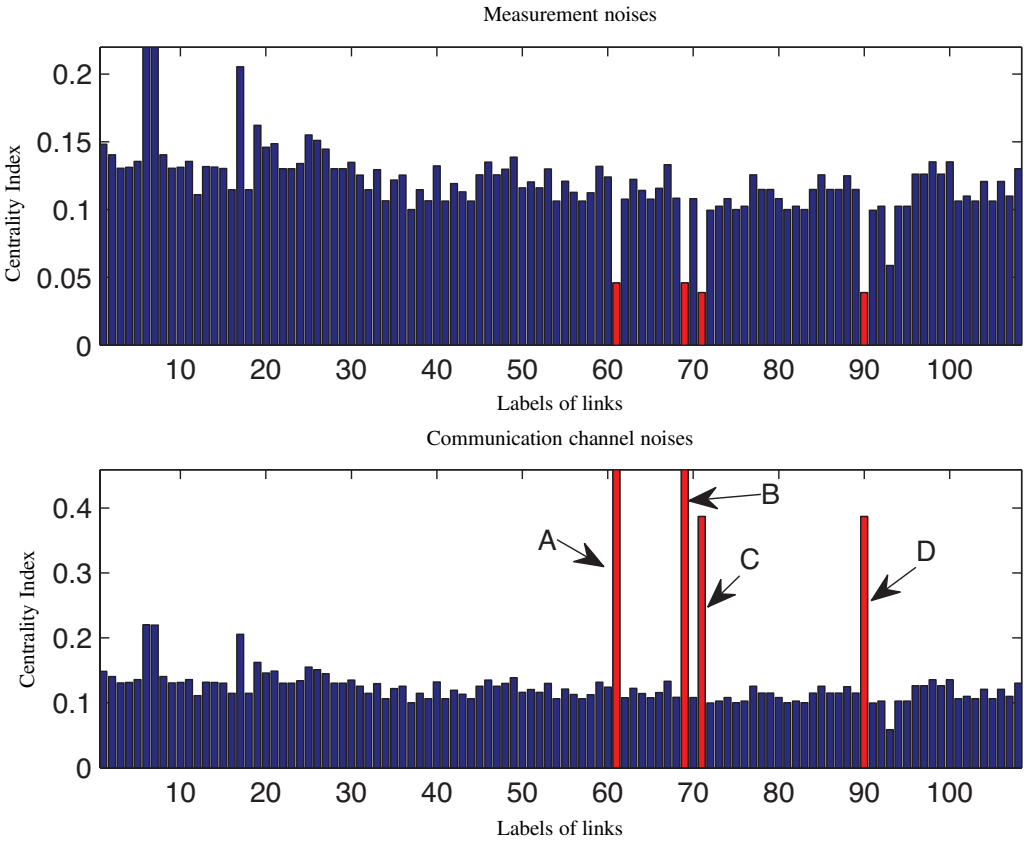

Figure 3.15: The link centrality indices for the consensus network with graph topology Figure 3.11. It is assumed that all link weights are equal to 1, except for $w(\mathrm{A}) = w(\mathrm{B}) = w(\mathrm{C}) = w(\mathrm{D}) = 10$. The indices of links $\mathrm{A}, \mathrm{B}, \mathrm{C}$, and D are shown by red bars.

Chapter 4

New Bounds on the $\mathcal{H}_2$-Norm of Linear Dynamical Networks

4.1 Abstract

In this chapter, we obtain new lower and upper bounds for the $\mathcal{H}_2$-norm of a class of linear time-invariant systems subject to exogenous noise inputs. We show that the $\mathcal{H}_2$-norm, as a performance measure, can be tightly bounded from below and above by some spectral functions of state and output matrices of the system. In order to show the usefulness of our results, we calculate bounds for the $\mathcal{H}_2$-norm of some network models with specific coupling or graph structures, e.g., systems with normal state matrices, linear consensus networks with directed graphs, and cyclic linear networks. As a specific example, the $\mathcal{H}_2$-norm of a linear consensus network over a directed cycle graph is computed and shown how its performance scales with the network size. Our proposed spectral bounds reveal the important role and contribution of fast and slow dynamic modes of a system in the best and worst achievable performance bounds under white noise excitation. Finally, we

use several numerical simulations to show the superiority of our bounds over the existing bounds in the literature.

4.2 Introduction

The performance analysis of noisy linear systems has been the focus of numerous studies over the past few decades [2, 5, 99, 103, 104] and the references therein. In a majority of these works, quantifying the corresponding performance measures reduces to solving some Algebraic Lyapunov Equations (ALEs). Although there are several efficient methods to compute the exact solutions of ALEs, their computational complexity increase rapidly when dealing with linear systems with large dimensions. Thus, such algorithms are only applicable to systems of moderate size [105]. There are some methods to estimate bounds on the solutions of ALEs [47, 106–109]. Bounds on the solution of an ALE can be used as an approximations of its exact solution, especially for large-scale linear networks as these bounds can usually be calculated through inexpensive computations. In [45], authors summarize some of the previous results up to that date.

The $\mathcal{H}_2$-norm of a noisy linear time-invariant system, from its noise input to the output, has been considered as a viable performance measure in the literature [5, 99, 104]. This performance measure can be calculated using the solution of an ALE. In this chapter, we derive explicit lower and upper bounds for this performance measure. Our proposed bounds are spectral functions of state and output matrices of the system. Furthermore, our proposed bounds are utilized to quantify bounds on the $\mathcal{H}_2$-norm squared of some network models with specific dynamical structures, e.g., systems with normal state matrices, linear consensus networks with directed graphs, and cyclic linear networks with negative feedback. As an important application, our results are applied to a general class of linear consensus networks over directed graphs. Most recent works [2, 43] investigate

the performance of noisy linear consensus networks over undirected graphs. We prove that our performance bounds are tight if the underlying directed graph of the networks is strongly connected and balanced. Moreover, we apply our results to a class of cyclic networks with asymmetric structures. These networks has been used to model certain biochemical pathways [44]. We particularly show how the $\mathcal{H}_2$-norm of a cyclic linear dynamical network scales with the network size. It is shown that when all subsystems are identical, the network attains the best achievable performance among all cyclic networks with the same secant criterion. Finally, we compare our proposed bounds to all existing bounds in the literature and use some numerical simulations to show that our bounds are tighter than all previously reported bounds in [45–47].

4.3 Mathematical Notations

$\mathbb{R}$ denotes the set of real numbers, $\mathbb{C}$ denotes the set of complex numbers, $\mathbf{Re}\{.\}$ denotes the real part of a complex number, $(.)^{\mathrm{T}}$ denotes transpose and $(.)^{\mathrm{H}}$ denotes Hermitian transpose. Matrix $I_n \in \mathbb{R}^{n\times n}$ is the identity matrix and matrix $\mathbf{0}$ is the matrix of all zeros. The $n \times 1$ vector of all ones is denoted by $\mathbb{1}_n$ and the centering matrix is defined by $M_n := I_n - \frac{\mathbb{1}_n \mathbb{1}_n^{\mathrm{T}}}{n}$. For a square matrix A, $\mathbf{Tr}(A)$ refers to the summation of on-diagonal elements of A. We write $\lambda_{\max}(M)$ (resp., $\lambda_{\min}(M)$) for the maximum (resp., minimum) eigenvalue of M, $\mathbf{diag}[v]$ for a square diagonal matrix with the elements of vector v on its diagonal and zero everywhere else, and $\|.\|_2$ for the 2-norm of a vector. The eigenvalues of a matrix $X \in \mathbb{R}^{n\times n}$ are indexed according to their real-parts in ascending order, *i.e.*$\mathbf{Re}\{\lambda_1(X)\} \leq \mathbf{Re}\{\lambda_2(X)\} \leq \cdots \leq \mathbf{Re}\{\lambda_n(X)\}$. $\mathbb{E}[v]$ stands for the expected value of random variable v. We employ the big omega notation in order to generalize the concept of asymptotic lower bound in the same way as $\mathcal{O}$ generalizes the concept of

asymptotic upper bound. We adopt the following definition according to [39]:

$$f(n) = \Omega(g(n)) \quad \Leftrightarrow \quad g(n) = \mathcal{O}(f(n)), \tag{4.1}$$

where $\mathcal{O}$ represents the big O notation. In the left hand side of (4.1), the Ω notation implies that $f(n)$ grows at least of the order of $g(n)$.

4.4 $\mathcal{H}_2$-Norm of Noisy Linear Systems

The steady-state variance of outputs of linear systems driven by external stochastic disturbances can be regarded as a measure of performance. We consider a linear time-invariant system

$$\dot{x}(t) = Ax(t) + \xi(t), \tag{4.2}$$

$$y(t) = Cx(t), \tag{4.3}$$

with $x(0) = \mathbf{0}$, where $x \in \mathbb{R}^n$ is the state and $y \in \mathbb{R}^m$ is the output of the system. For all linear systems in this chapter, it is assumed that the input signal $\xi \in \mathbb{R}^n$ is a white noise process with zero mean and identity covariance, i.e.,

$$\mathbb{E}\left[\xi(t)\xi^{\mathrm{T}}(\tau)\right] = I_n \delta(t-\tau), \tag{4.4}$$

where $\delta(.)$ is the delta function. It is assumed that the state matrix A is Hurwitz.

Definition 4.4.1. *The $\mathcal{H}_2$–norm of linear system* (4.2)-(4.3) *from ξ to y is defined as the*

square root of the following quantity

$$\rho_{ss}\left(A;Q\right) \quad := \quad \lim_{t\to\infty}\mathbb{E}\left[x^{\mathrm{T}}(t)Qx(t)\right], \tag{4.5}$$

where $Q = C^TC$.

For unstable linear systems, the outputs of the system have finite steady-state variance as along as the unstable modes of the system are not observable from the output of the system. The value of performance measure (4.5) for (4.2)-(4.3) can be quantified as

$$\rho_{\mathbf{ss}}\left(A;Q\right) \quad = \quad \mathbf{Tr}(P), \tag{4.6}$$

where P is the unique solution of the following ALE

$$PA \,+\, A^{\mathrm{T}}P \,+\, Q \quad = \quad \mathbf{0}. \tag{4.7}$$

4.5 New Spectral Bounds on the $\mathcal{H}_2$-Norm

For simplicity of our representations, we present our results for the performance measure (4.5), instead of the $\mathcal{H}_2$-norm. According to Definition 4.4.1 by taking a simple square root, all results can be converted to bounds for the $\mathcal{H}_2$-norm.

Theorem 4.5.1. *Suppose that linear system* (4.2)-(4.3) *is stable with input noise covariance* (4.4) *and* $Q = I_n$. *Then, we have*

$$\sum_{i=1}^{n}\frac{-1}{2\mathbf{Re}\{\lambda_i(A)\}} \quad \leq \quad \rho_{ss}\left(A;Q\right). \tag{4.8}$$

The lower bound in (4.8) *is achieved if and only if* A *is normal, i.e.*$A^TA = AA^T$. *In*

addition, if the symmetric part of the state matrix A, defined by $A_s := (A^T + A)/2$, is Hurwitz, then we get

$$\rho_{ss}\,(A;Q) \;\leq\; \sum_{i=1}^{n} \frac{-1}{2\lambda_i(A_s)}. \tag{4.9}$$

Proof. Since A is Hurwitz, all its eigenvalues have strictly negative real parts. Therefore, the unique solution of $A^{\mathrm{T}}P + PA + I_n = 0$, can be expressed in the following closed form

$$P \;=\; \int_0^\infty e^{A^{\mathrm{T}}t} e^{At} dt. \tag{4.10}$$

According to Schur decomposition theorem [110], there exists a unitary matrix $V \in \mathbb{C}^{n\times n}$ such that $A = V(\Gamma + N)V^{\mathrm{H}}$ where $\Gamma = \mathbf{diag}\,[\lambda_1(A), \cdots, \lambda_n(A)]$, N is strictly upper triangular, and V^{H} is the conjugate transpose of V. Let us consider the integrand of (4.10)

$$\begin{aligned}
\mathbf{Tr}(e^{A^{\mathrm{T}}t} e^{At}) &= \mathbf{Tr}(e^{(\Gamma^{\mathrm{H}}+N^{\mathrm{H}})t} V^{\mathrm{H}} V e^{(\Gamma+N)t} V^{\mathrm{H}} V) \\
&= \mathbf{Tr}(V^{\mathrm{H}} V e^{(\Gamma^{\mathrm{H}}+N^{\mathrm{H}})t} e^{(\Gamma+N)t}) \\
&= \mathbf{Tr}(V e^{(\Gamma^{\mathrm{H}}+N^{\mathrm{H}})t} e^{(\Gamma+N)t} V^{\mathrm{H}}).
\end{aligned} \tag{4.11}$$

Furthermore, we have

$$e^{(\Gamma+N)t} \;=\; e^{\Gamma t} + M_t \;\text{ and }\; e^{(\Gamma^{\mathrm{H}}+N^{\mathrm{H}})t} = e^{\Gamma^{\mathrm{H}} t} + M_t^{\mathrm{H}}, \tag{4.12}$$

where M_t is an upper-triangular Nilpotent matrix. From (4.12), we have

$$\begin{aligned}
\mathbf{Tr}(e^{(\Gamma^{\mathrm{H}}+N^{\mathrm{H}})t} e^{(\Gamma+N)t}) &= \mathbf{Tr}(e^{\Gamma t} e^{\Gamma^{\mathrm{H}} t} + M_t M_t^{\mathrm{H}}) \\
&\geq \mathbf{Tr}(e^{(\Gamma^{\mathrm{H}}+\Gamma)t}).
\end{aligned} \tag{4.13}$$

From (4.11) and (4.13), it follows that

$$\begin{aligned} \mathbf{Tr}(e^{A^{\mathrm{T}}t}e^{At}) &= \mathbf{Tr}(Ve^{(\Gamma^{\mathrm{H}}+N^{\mathrm{H}})t}e^{(\Gamma+N)t}V^{\mathrm{H}}) \\ &\geq \mathbf{Tr}(e^{(\Gamma^{\mathrm{H}}+\Gamma)t}) = \mathbf{Tr}(e^{2\mathbf{Re}\{\Gamma\}t}). \end{aligned} \tag{4.14}$$

Since $\mathbf{Re}\{\lambda_i(A)\} < 0$ for all $i = 1, \ldots, n$, we can conclude from (4.10) and (4.14) that

$$\mathbf{Tr}(P) = \int_0^\infty \mathbf{Tr}(e^{\bar{A}^{\mathrm{T}}t}e^{\bar{A}t})dt \geq \sum_{i=1}^{n} \frac{-1}{2\mathbf{Re}\{\lambda_i(A)\}}. \tag{4.15}$$

In the last inequality, we apply the fact that the trace and sum operators are linear and they can commute with the integral. The lower bound is achieved if and only if equalities in (4.14) and (4.13) hold, or equivalently, A is a normal matrix, *i.e.*$A^{\mathrm{T}}A = AA^{\mathrm{T}}$. In order to prove inequality (4.9), we first use Bernstein inequality [111]

$$\mathbf{Tr}(e^{A^{\mathrm{T}}t}e^{At}) \leq \mathbf{Tr}(e^{(A^{\mathrm{T}}+A)t}). \tag{4.16}$$

Then, by taking an integral from both sides of (4.16) we get

$$\mathbf{Tr}(P) = \int_0^\infty \mathbf{Tr}(e^{A^{\mathrm{T}}t}e^{At})dt \leq \int_0^\infty \mathbf{Tr}(e^{(A^{\mathrm{T}}+A)t})dt. \tag{4.17}$$

According to our assumptions $A + A^{\mathrm{T}}$ is Hurwitz. Therefore, using this fact and (4.17) we conclude that

$$\mathbf{Tr}(P) \leq \int_0^\infty \mathbf{Tr}(e^{(A^{\mathrm{T}}+A)t})dt = \sum_{i=1}^{n} \frac{-1}{2\lambda_i(A_s)}.$$

□

The following theorem shows that the lower and upper bounds in Theorem 4.5.1 can

be tightened further by assuming more structure on the state matrix.

Theorem 4.5.2. *Suppose that linear system* (4.2)-(4.3) *is stable with input noise covariance* (4.4) *and normal state matrix* A*. Then,*

$$\sum_{i=1}^{n} \frac{-\lambda_{n-i+1}(Q)}{2\mathbf{Re}\{\lambda_i(A)\}} \leq \rho_{ss}\left(A; Q\right) \leq \sum_{i=1}^{n} \frac{-\lambda_i(Q)}{2\mathbf{Re}\{\lambda_i(A)\}}. \tag{4.18}$$

Moreover, both bounds in (4.18) are achieved if Q *has* n *identical eigenvalues.*

Proof. Every symmetric matrix Q can be decomposed as $Q = UDU^{\mathrm{T}}$, where $UU^{\mathrm{T}} = U^{\mathrm{T}}U = I$ and $D = \mathbf{diag}\left[\lambda_1(Q), \cdots \lambda_n(Q)\right]$. Thus, we can rewrite (4.7) as

$$\bar{A}^{\mathrm{T}}\bar{P} \ + \ \bar{P}\bar{A} \ + \ D \quad = \quad 0, \tag{4.19}$$

where $\bar{A} = U^{\mathrm{T}}AU$ and $\bar{P} = U^{\mathrm{T}}PU$. Since A is Hurwitz, the unique solution of (4.19) can be expressed by

$$\bar{P} \quad = \quad \int_0^{\infty} e^{\bar{A}^{\mathrm{T}}t} D e^{\bar{A}t} dt. \tag{4.20}$$

Since $\bar{A}$ is normal, there exists a unitary matrix $\bar{V} \in \mathbb{C}^{n\times n}$ such that $\bar{A} = \bar{V}\Gamma\bar{V}^{\mathrm{H}}$, where $\Gamma \ = \ \mathbf{diag}\left[\lambda_1(A), \cdots, \lambda_n(A)\right]$ and $\bar{V}^{\mathrm{H}}$ is the conjugate transpose of $\bar{V}$. Next, let us consider the integrand of (4.20)

$$\begin{aligned} \mathbf{Tr}(e^{\bar{A}^{\mathrm{T}}t} D e^{\bar{A}t}) \quad &= \quad \mathbf{Tr}(e^{\bar{A}^{\mathrm{H}}t} D e^{\bar{A}t}) \\ &= \quad \mathbf{Tr}(e^{\Gamma^{\mathrm{H}}t}\bar{V}^{\mathrm{H}} D \bar{V} e^{\Gamma t}\bar{V}^{\mathrm{H}}\bar{V}) \\ &= \quad \mathbf{Tr}(\bar{V}^{\mathrm{H}} D \bar{V} e^{(\Gamma^{\mathrm{H}}+\Gamma)t}). \end{aligned} \tag{4.21}$$

We observe that $\bar{V}^{\mathrm{H}} D \bar{V}$ and $e^{(\Gamma^{\mathrm{H}}+\Gamma)t}$ are Hermitian. Thus, according to [112, Theorem.

II. 2], we get

$$\mathbf{Tr}(\bar{V}^{\mathrm{H}} D \bar{V} e^{(\Gamma^{\mathrm{H}}+\Gamma)t}) \;\geq\; \sum_{i=1}^{n} \lambda_{n-i+1}(Q) e^{2\mathbf{Re}\{\lambda_i(A)\}t}. \tag{4.22}$$

Since $\mathbf{Re}\{\lambda_i(A)\} \neq 0$ for all $i = 1, \ldots, n$, from (4.20) and (4.22) we have

$$\begin{aligned} \mathbf{Tr}(P) \quad &\geq \quad \int_0^{\infty} \sum_{i=1}^{n} \lambda_{n-i+1}(Q) e^{2\mathbf{Re}\{\lambda_i(A)\}t} dt \\ &= \quad -\sum_{i=1}^{n} \frac{\lambda_{n-i+1}(Q)}{2\mathbf{Re}\{\lambda_i(A)\}}. \end{aligned} \tag{4.23}$$

In the last inequality, we apply the fact that the trace and sum operators are linear and they can be interchanged by the integral. When A is normal, then $\lambda_i(A + A^{\mathrm{T}}) = 2\mathbf{Re}\{\lambda_i(A)\}$. This is because according to the Schur decomposition for normal matrices, there exists a unitary $V \in \mathbb{C}^{n\times n}$ such that $A = V\Gamma V^{\mathrm{H}}$, where $\Gamma = \mathbf{diag}\{\lambda_1(A), \ldots (A), \lambda_n(A)\}$ and V^{H} denotes the conjugate transpose of matrix V. Using this fact, it follows that

$$\begin{aligned} A_s \quad &= \quad \frac{A + A^{\mathrm{H}}}{2} \;=\; V\left(\frac{\Gamma + \Gamma^{\mathrm{H}}}{2}\right) V^{\mathrm{H}} \\ &= \quad V\mathbf{diag}\big(\mathbf{Re}\{\lambda_1(A)\}, \ldots, \mathbf{Re}\{\lambda_n(A)\}\big) V^{\mathrm{H}}. \end{aligned} \tag{4.24}$$

This implies that $\lambda_i(A_s) = \mathbf{Re}\{\lambda_i(A)\}$ for all $i = 1, \ldots, n$. In order to prove the RHS inequality in (4.18), we use [113, Corollary 2.1.1], which gives us the upper bound in (4.18). When Q has identical eigenvalues, then the upper and lower bounds have equal values; therefore, both bounds in (4.8) are achieved. □

All symmetric and orthogonal matrices are examples of normal matrices. One of the outcomes of the Theorem 4.5.2 is that when A is normal and Q has n identical eigenvalues, the value of the performance measure (4.5) is exactly equal to the upper and lower

bounds in (4.18) and can be calculated as a function of eigenvalues of the symmetric part of A or equivalently the real parts of eigenvalues of A.

4.6 Applications to Some Network Models

In this section, we apply the results of the previous section to some systems with specific interconnection topologies. One of the challenging problems in the area of linear dynamical networks is to discover relationships between the $\mathcal{H}_2$-norm of a linear network and the structure of its underlying interconnection topology. In general, carrying out such network analysis problems are difficult, if not impossible. In the following, we show that because of the particular functional form of bounds in Theorems 4.5.1 and 4.5.2, one can exploit structural properties of some classes of linear time-invariant networks in order to calculate their $\mathcal{H}_2$-norm bounds in more explicit forms and relate them to their graph topologies.

4.6.1 Linear Consensus Networks over Directed Graphs

We consider a class of linear consensus networks where the interconnection topology between subsystems is defined using a directed graph [12, 114]. This class of networks can be modeled by (4.2)-(4.3) with $A = -L$, in which L is the Laplacian matrix of the underlying directed graph. We assume that all directed graphs in this section are weighted and strongly connected [115]. As a result, we have $\lambda_1(L) = 0$ and $\mathbf{Re}\{\lambda_i(L)\} > 0$ for all $n = 2, \ldots, n$. In order to guarantee a well-defined and bounded $\mathcal{H}_2$-norm for this class of networks, it is further assumed that only stable modes of the network are observable from the output.We stress that in both Theorems 4.5.1 and 4.5.2, it is assumed that matrix A is Hurwitz. Next result extends Theorem 4.5.1 to marginally stable linear consensus

networks over directed graphs.

Theorem 4.6.1. *Consider a linear system* (4.2)-(4.3) *with* $A = -L$ *and input noise covariance* (4.4)*, where* L *corresponds to Laplacian matrix of a directed weighted graph that is strongly connected and balanced. Then, it follows that*

$$\sum_{i=2}^{n} \frac{1}{2\mathbf{Re}\{\lambda_i(L)\}} \;\leq\; \rho_{ss}\left(-L; Q\right) \;\leq\; \sum_{i=2}^{n} \frac{1}{\lambda_i(L+L^T)}, \tag{4.25}$$

where $Q = M_n$ *is the centering matrix. Moreover, the lower bound in* (4.25) *is achieved if and only if* L *is normal.*

Proof. First, we show that if the underlying graph is balanced and strongly connected, then $L + L^{\mathrm{T}}$ has only one zero eigenvalue and the rest of them are strictly positive. Since the underlying graph is balanced, the row sum and column sum of Laplacian matrix L is zero. Therefore, $L + L^{\mathrm{T}}$ has zero row and column sums and it can be considered as Laplacian matrix of an undirected graph. However, this undirected graph is connected because L is the Laplacian matrix of a strongly connected graph. As a result, $L + L^{\mathrm{T}}$ has only one zero eigenvalue, i.e., $\lambda_1(L + L^{\mathrm{T}}) = 0$ and $\lambda_2(L + L^{\mathrm{T}}) > 0$. Now, let us define the disagreement vector by

$$x_d(t) \;:=\; M_n x(t) \;=\; x(t) - \tfrac{1}{n}\mathbb{1}_n\mathbb{1}_n^{\mathrm{T}} x(t). \tag{4.26}$$

By multiplying a vector by the centering matrix, we actually subtract the mean of all the entries of the vector from each entry. The dynamics of linear network (4.2)-(4.3) with respect to the new state transformation (4.26) is so-called disagreement form of the network that is given by

$$\dot{x}_d(t) \quad = \quad -\left(L + \tfrac{1}{n}\mathbb{1}_n\mathbb{1}_n^{\mathrm{T}}\right) x_d(t) + M_n\xi(t), \tag{4.27}$$

$$y(t) \quad = \quad x_d(t). \tag{4.28}$$

It can be shown that the transfer function of the network from ξ to y stays invariant under state transformation (4.26) [12]. We show that (4.27)-(4.28) and the following system have identical performance measure (4.5):

$$\dot{x}_d(t) \quad = \quad -\left(L + \tfrac{1}{n}\mathbb{1}_n\mathbb{1}_n^{\mathrm{T}}\right)^{\mathrm{T}} x_d(t) + \xi(t), \tag{4.29}$$

$$y(t) \quad = \quad M_n x_d(t). \tag{4.30}$$

Both state matrices in (4.27) and (4.29) are Hurwitz. Therefore, the $\mathcal{H}_2$-norm of both systems from ξ to y are well-defined. The squared $\mathcal{H}_2$-norm of (4.27)-(4.28) is given by $\rho_{\mathbf{ss}}(A, Q) \; = \; \frac{1}{2}\mathbf{Tr}(P)$, where P is the unique solution of

$$P\left(L + \tfrac{1}{n}\mathbb{1}_n\mathbb{1}_n^{\mathrm{T}}\right) \; + \; \left(L + \tfrac{1}{n}\mathbb{1}_n\mathbb{1}_n^{\mathrm{T}}\right)^{\mathrm{T}} P \quad = \quad M_n. \tag{4.31}$$

The squared $\mathcal{H}_2$-norm of (4.29)-(4.30) is given by

$$\lim_{t\to\infty} \mathbb{E}\left[y^{\mathrm{T}}(t)y(t)\right] \; = \; \frac{1}{2}\mathbf{Tr}(P_o), \tag{4.32}$$

where P_o is the unique solution of

$$\left(L + \tfrac{1}{n}\mathbb{1}_n\mathbb{1}_n^{\mathrm{T}}\right)^{\mathrm{T}} P_o + P_o\left(L + \tfrac{1}{n}\mathbb{1}_n\mathbb{1}_n^{\mathrm{T}}\right) \; = \; M_n. \tag{4.33}$$

It is evident that both equations (4.31) and (4.33) return identical unique solutions, i.e., $P_o = P$. Hence, by applying Theorem 4.5.1 to system (4.29)-(4.30), we get the desired result. □

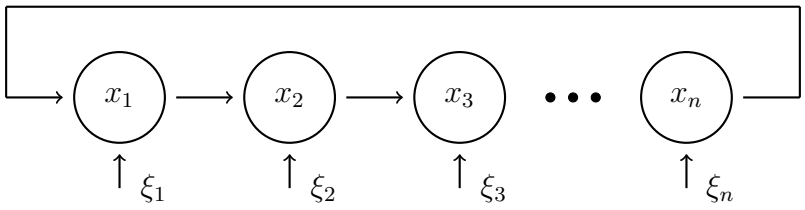

Figure 4.1: Schematic diagram of a linear consensus network with a directed cycle graph with n agents. Each agent i is subject to stochastic disturbance ξ_i.

The class of directed graphs with normal Laplacian matrices are balanced, but vice versa is not true in general.

Theorem 4.6.2. *Let us consider a linear consensus network over a strongly connected graph with Laplacian matrix L. If we assume that L is normal and $Q = C^TC$ with $C\mathbb{1} = \mathbf{0}$, then it follows that*

$$\sum_{i=2}^{n} \frac{\lambda_i(Q)}{2\mathbf{Re}\{\lambda_i(L)\}} \leq \rho_{ss}\left(-L; Q\right) \leq \sum_{i=2}^{n} \frac{\lambda_{n-i+2}(Q)}{2\mathbf{Re}\{\lambda_i(L)\}}. \tag{4.34}$$

Moreover, the lower and upper bounds in (4.34) *are achieved if and only if $Q = q\left(I_n - \frac{1}{n}\mathbb{1}_n\mathbb{1}_n^{\mathrm{T}}\right)$ for all $q \geq 0$.*

The proof of Theorem 4.6.2 can be derived with some modifications from the proofs of Theorems 4.5.2 and 4.6.1. Similar to the proof of Theorem 4.6.1, first we need to form the disagreement network, and then, utilize Theorem 4.5.2 to conclude the proof.

Example 4.6.3. *Let us consider a consensus network with a directed cycle graph given by Figure 4.1, i.e.all the edges being oriented in the same direction with positive weight w. Without loss of generality, we may assume that $w = 1$. The Laplacian matrix of this graph is denoted by L_{c} which is a circulant matrix. According to results of [116], the corresponding Laplacian eigenvalues are given by*

$$\lambda_k(L_{\mathrm{c}}) \;=\; 1 + \mathrm{e}^{\mathbf{i}\pi\left(1-\frac{(-1)^k 2\lfloor\frac{k}{2}\rfloor}{n}\right)}, \tag{4.35}$$

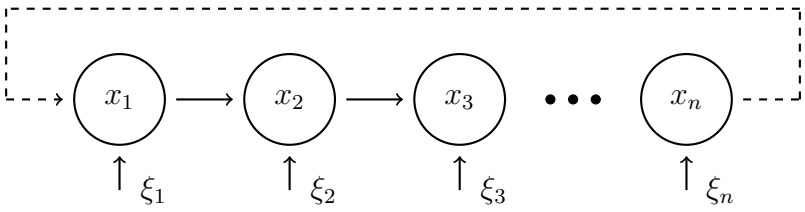

Figure 4.2: Schematic diagram of a noisy cyclic network. The dashed link indicates a negative (inhibitory) feedback.

where $k = 1, \cdots n$. As a result, their real parts can be calculated as

$$\mathbf{Re}\{\lambda_k(L_{\mathrm{c}})\} = 1 + \cos\left(\pi - \tfrac{(-1)^k 2\lfloor \frac{k}{2} \rfloor \pi}{n}\right) = 2\sin\left(\tfrac{2\pi \lfloor \frac{k}{2} \rfloor}{n}\right).$$

Since the corresponding underlying graph is strongly connected and its Laplacian matrix is normal, we can apply Theorem 4.6.2 to get

$$\sum_{k=2}^{n} \frac{\lambda_k(Q)}{2\sin\left(\frac{2\pi \lfloor \frac{k}{2} \rfloor}{n}\right)} \leq \rho_{\boldsymbol{ss}}\left(-L_{\mathrm{c}}; Q\right) \leq \sum_{k=2}^{n} \frac{\lambda_{n-k+2}(Q)}{2\sin\left(\frac{2\pi \lfloor \frac{k}{2} \rfloor}{n}\right)}.$$

When $Q = I_n - \frac{1}{n}\mathbb{1}_n\mathbb{1}_n^{\mathrm{T}}$, the performance measure can be calculated explicitly as a function of network size as $\rho_{\boldsymbol{ss}}\left(-L_{\mathrm{c}}; Q\right) = \frac{n^2-1}{12}$. According to Definition 4.4.1, we conclude that the $\mathcal{H}_2$-norm of a linear consensus network with directed cycle graph deteriorates by $\mathcal{O}(n)$ as network size gets larger.

4.6.2 Linear Networks with Cyclic Interconnection Topology

The class of cyclic networks has been studied in the context of systems biology, e.g., in autocatalytic pathway with ring topology [4, 117–119]. In order to obtain analytical bounds using our results from Section 4.5, we limit our attention to the class of linear cyclic networks shown in Figure 4.2.

We can represent the dynamics of the overall cyclic network in the compact canonical

form (4.2)-(4.3) with the following state matrix

$$A = \begin{bmatrix} -a & 0 & \dots & 0 & -c_n \\ c_1 & -a & \dots & 0 & 0 \\ \vdots & \vdots & \ddots & \vdots & \vdots \\ 0 & 0 & \dots & -a & 0 \\ 0 & 0 & \dots & c_{n-1} & -a \end{bmatrix}, \tag{4.36}$$

and output matrix $C = I_n$. In the next theorem, we use our results in Section 4.5 to exploit structural properties of this class of linear dynamical networks in order to compute their $\mathcal{H}_2$-norm bounds.

Theorem 4.6.4. *For the cyclic linear dynamical network with state matrix (4.36) and output matrix $C = I_n$, let us define $\mathfrak{c} := \sqrt[n]{c_1 c_2 \cdots c_n}$ and assume that the stability condition $\gamma := a/\mathfrak{c} > \cos(\pi/n)$ holds. Then the corresponding performance measure is lower bounded by*

$$\rho_{ss}\,(A; Q) \;\geq\; \mathfrak{L}(n, \beta, \mathfrak{c}), \tag{4.37}$$

where

$$\mathfrak{L}(n, \beta, \mathfrak{c}) \;=\; \begin{cases} \frac{n \tan \frac{\beta}{2}}{2\mathfrak{c} \sin \frac{\beta}{n}} & \textit{if} \quad \gamma < 1 \\ \frac{n^2}{4\mathfrak{c}} & \textit{if} \quad \gamma = 1 \\ \frac{n \tanh \frac{\beta}{2}}{2\mathfrak{c} \sinh \frac{\beta}{n}} & \textit{if} \quad \gamma > 1 \end{cases} \tag{4.38}$$

and

$$\beta := \begin{cases} \arccos(\gamma) n & \textit{if} \quad \gamma \leq 1 \\ \operatorname{arcosh}(\gamma) n & \textit{if} \quad \gamma > 1 \end{cases}. \tag{4.39}$$

The equality in (4.37) is achieved if and only if $c_1 = \ldots = c_n$, which means that all subsystems of the network are identical.

Proof. The stability condition $\gamma > \cos(\pi/n)$ implies that A is Hurwitz [118, 119]. Therefore, the $\mathcal{H}_2$–norm squared is well-defined and finite. The characteristic polynomial of A is given by

$$(\lambda + a)^n \; + \; c_1 c_2 \cdots c_n \; = \; 0. \tag{4.40}$$

Therefore, the eigenvalues of the matrix are

$$\lambda_k \; = \; \; - a \; + \; \mathfrak{c}\, \mathrm{e}^{\mathbf{i}(\frac{\pi}{n} + \frac{2\pi k}{n})} \tag{4.41}$$

for $k = 0, 1, \cdots, n-1$. By substituting these eigenvalues into the lower bound (4.9), we get

$$\begin{aligned} -\sum_{i=1}^{n} \frac{1}{2\mathbf{Re}\{\lambda_i(A)\}} &= \sum_{k=0}^{n-1} \frac{1}{2\mathbf{Re}\left\{-a + \mathfrak{c}\, \mathrm{e}^{\mathbf{i}(\frac{\pi}{n} + \frac{2\pi k}{n})}\right\}} \\ &= \sum_{k=0}^{n-1} \frac{1}{2\mathfrak{c}\left(\gamma - \cos(\frac{\pi}{n} + \frac{2\pi k}{n})\right)}. \end{aligned} \tag{4.42}$$

First, let us assume that $\gamma < 1$ and substitute $\gamma = \cos(\beta/n)$ in (4.42). It follows that

$$\begin{aligned} -\sum_{i=1}^{n} \frac{1}{2\mathbf{Re}\{\lambda_i(A)\}} \; &= \; \frac{1}{2\mathfrak{c}} \sum_{k=0}^{n-1} \frac{1}{\cos(\frac{\beta}{n}) - \cos(\frac{\pi}{n} + \frac{2\pi k}{n})} \\ &= \; \frac{1}{4\mathfrak{c}} \sum_{k=0}^{n-1} \csc(\tfrac{(2k+1)\pi}{2n} + \tfrac{\beta}{2n}) \csc(\tfrac{(2k+1)\pi}{2n} - \tfrac{\beta}{2n}) \\ &= \; \frac{n \tan\frac{\beta}{2}}{2\mathfrak{c} \sin\frac{\beta}{n}}, \end{aligned}$$

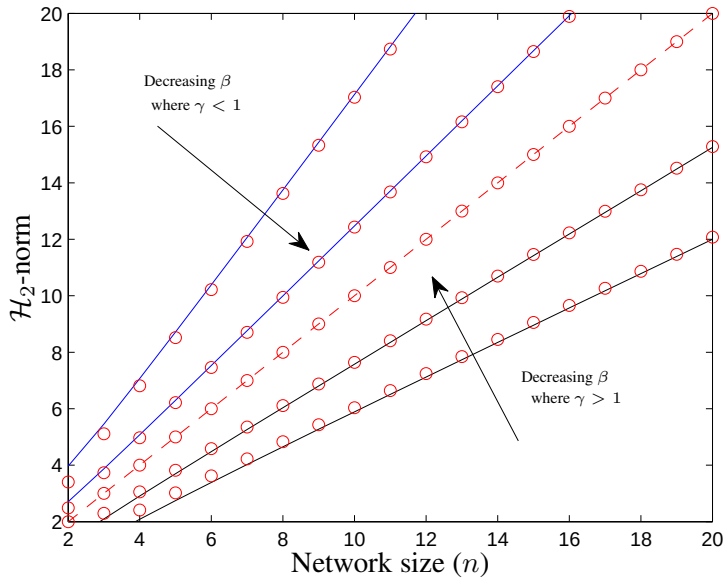

Figure 4.3: The lower bound (4.38), which is depicted by small red circles (○), is compared asymptotically to its approximation in (4.43). It can be observed that (4.43) tightly approximates (4.38).

where the Birkhoff Ergodic theorem is used to conclude the last equation. Similar steps can be taken when $\gamma > 1$. In each case by substituting γ from (4.39) in (4.42), one can obtain the desired result (4.37). According to Theorem 4.5.1, the equality in (4.37) is achieved if and only if A is a normal matrix. On the other hand, based on the cyclic structure of matrix (4.36), we conclude that A is normal if and only if $c_1 = \ldots = c_n$. □

The secant criterion reported in [118] and [119] for cyclic linear networks provides a stability condition. This condition implies that the unperturbed system with $\xi = 0$ is stable if and only if $\gamma > \cos(\pi/n)$. For a fixed parameter β, the stability condition of the cyclic network is not affected when the number of intermediate subsystems changes. However, the result of Theorem 4.6.4 asserts that the lower bound of the performance measure (4.5) increases (i.e., the network performance deteriorates) when the network size increases. More explicitly, we have the following approximation for the lower bound

(4.38)

$$\mathfrak{L}(n,\beta,\mathfrak{c}) \approx \begin{cases} \frac{\tan\frac{\beta}{2}}{2\mathfrak{c}\beta}n^2 & \text{if} \quad \gamma<1 \\ \frac{1}{4\mathfrak{c}}n^2 & \text{if} \quad \gamma=1 \\ \frac{\tanh\frac{\beta}{2}}{2\mathfrak{c}\beta}n^2 & \text{if} \quad \gamma>1 \end{cases}. \tag{4.43}$$

According to Definition 4.4.1, we conclude that when parameter β is fixed, the $\mathcal{H}_2$-norm of the cyclic network deteriorates in the order of $\Omega(n)$ as the network size becomes larger. We should mention that the $\mathcal{H}_2$-norm of n-identical coupled subsystems may scale in different orders depending on their underlying graph topology, for more details please see [12].

Example 4.6.5. *In order to support our theoretical results, we consider a cyclic network* (4.2)-(4.3) *with state matrix* (4.36)*,* $\mathfrak{c} := c_1 = \ldots = c_n$*, and* $C = I_n$*. The asymptotic scaling of the* $\mathcal{H}_2$*-norm for this class of networks is depicted in terms of network size and parameter* β *in Figure 4.3. In this case, the* $\mathcal{H}_2$*-norm of the cyclic network can be calculated by the square root of* (4.38)*. These values are depicted by small red circles (*$\circ$*) versus the number of subsystems* n*. Moreover, these values are compared asymptotically to their approximation given by the square root of (4.43). It can be observed that the square root of (4.43) tightly approximates the* $\mathcal{H}_2$*-norm of the cyclic network.*

4.7 Tightness of Our New Bounds

In this section, we compare our results with the existing results in the literature. In Table 4.1, we summarize several lower bounds on the $\mathcal{H}_2$-norm squared of system (4.2)-(4.3) based on all existing works in the literature to the best of our knowledge. When $Q = I_n$, the lower bound in Theorem 4.5.1 is tighter than all existing lower bounds reported in

Table 4.1: Comparison of existing lower bounds on $\rho_{\mathbf{ss}}$ in the literature.

Methods	Lower Bounds
Theorem 4.5.1	$\sum_{i=1}^{n} \frac{-1}{2\mathbf{Re}\{\lambda_i(A)\}}$
Theorem 4.5.2	$\sum_{i=1}^{n} \frac{-\lambda_{n-i+1}(Q)}{2\mathbf{Re}\{\lambda_i(A)\}}$
[109]	$-\frac{\mathbf{Tr}(Q)}{2\lambda_{\min}(A_s)}$
[108]	$-\frac{n^2\lambda_{\min}(Q)}{2\mathbf{Tr}(A)}$
[107]	$-\frac{\mathbf{Tr}(Q)}{2\mathbf{Tr}(A)}$
[106]	$-\frac{\left(\sum_i \lambda_i(Q)^{\frac{1}{2}}\right)^2}{2\mathbf{Tr}(A)}$
[47]	$\sum_{i=1}^{n} \lambda_i \left(\frac{Q}{a} - \frac{AA^{\mathrm{T}}}{a^2}\right)^{\frac{1}{2}}$ for $Q \succ \frac{AA^{\mathrm{T}}}{a}$

reference papers [106–108]. In the following, we provide analytical proofs for our claim. It is true that

$$-\mathbf{Tr}(A) \quad = \quad -\sum_{i=1}^{n} \mathbf{Re}\{\lambda_i(A)\}, \tag{4.44}$$

and $-\mathbf{Re}\{\lambda_i(A)$ are positive for all $i = 1, \ldots, n$. From the arithmetic and harmonic mean inequalities, it follows that

$$\frac{-n^2}{2\mathbf{Tr}(A)} \leq \sum_{i=1}^{n} \frac{-1}{2\mathbf{Re}\{\lambda_i(A)\}}. \tag{4.45}$$

Moreover, we have that $\frac{-n}{2\mathbf{Tr}(A)} \leq \frac{-n^2}{2\mathbf{Tr}(A)}$. As a result, when $Q = I_n$ the following ordering on bounds holds

$$\underbrace{\frac{-n}{2\mathbf{Tr}(A)}}_{[107]} \leq \underbrace{\frac{-n^2}{2\mathbf{Tr}(A)}}_{[106,108]} \leq \underbrace{\sum_{i=1}^{n} \frac{-1}{2\mathbf{Re}\{\lambda_i(A)\}}}_{\text{Theorem 4.5.1}}.$$

On the other hand, if A is normal, then the lower bound in Theorem 4.5.2 is tighter than the lower bounds presented in [106–108]. In the next few lines, we will prove this claim.

We know that

$$\frac{\mathbf{Tr}(Q)}{-2\mathbf{Tr}(A)} = \frac{\sum_{i=1}^{n}\lambda_i(Q)}{-2\mathbf{Tr}(A)} \leq \frac{\left(\sum_{i=1}^{n}\lambda_i(Q)^{\frac{1}{2}}\right)^2}{-2\mathbf{Tr}(A)} \tag{4.46}$$

and

$$\frac{\mathbf{Tr}(Q)}{-2\mathbf{Tr}(A)} \leq \frac{\left(\sum_{i=1}^{n}\lambda_i(Q)^{\frac{1}{2}}\right)^2}{-2\mathbf{Tr}(A)}. \tag{4.47}$$

From the Cauchy–Schwarz inequality, we get

$$\left(\sum_{i=1}^{n}\lambda_i(Q)^{\frac{1}{2}}\right)^2 \leq \sum_{i=1}^{n}\frac{\lambda_{n-i+1}(Q)}{-\mathbf{Re}\{\lambda_i(A)\}}\left(-\sum_{i=1}^{n}\mathbf{Re}\{\lambda_i(A)\}\right). \tag{4.48}$$

Then, equation (4.44) and inequality (4.48) give us

$$-\frac{\left(\sum_{i=1}^{n}\lambda_i(Q)^{\frac{1}{2}}\right)^2}{2\mathbf{Tr}(A)} \leq -\sum_{i=1}^{n}\frac{\lambda_{n-i+1}(Q)}{2\mathbf{Re}\{\lambda_i(A)\}}. \tag{4.49}$$

According to (4.46), (4.47) and (4.49), we conclude that our proposed lower bound is tighter than the lower bounds reported in [106–108]. In summary, we have

$$\underbrace{\frac{\mathbf{Tr}(Q)}{-2\mathbf{Tr}(A)}}_{[107]} \leq \underbrace{\frac{\left(\sum_{i=1}^{n}\lambda_i(Q)^{\frac{1}{2}}\right)^2}{-2\mathbf{Tr}(A)}}_{[106]} \leq \underbrace{\sum_{i=1}^{n}\frac{-\lambda_{n-i+1}(Q)}{2\mathbf{Re}\{\lambda_i(A)\}}}_{\text{Theorem 4.5.2}}$$

and

$$\underbrace{\frac{n^2\lambda_{\min}(Q)}{-2\mathbf{Tr}(A)}}_{[108]} \leq \underbrace{\frac{\left(\sum_{i=1}^{n}\lambda_i(Q)^{\frac{1}{2}}\right)^2}{-2\mathbf{Tr}(A)}}_{[106]} \leq \underbrace{\sum_{i=1}^{n}\frac{-\lambda_{n-i+1}(Q)}{2\mathbf{Re}\{\lambda_i(A)\}}}_{\text{Theorem 4.5.2}}.$$

To support our results, we illustrate by means of two simulation examples that our lower bounds for the performance measure (4.5) are the tightest among the other known bounds given in Table 4.1.

Example 4.7.1. *Let us define the parametrized family of matrices A_α as follows*

$$A_\alpha \;=\; (1-\alpha)A_0 + \alpha A_1 \tag{4.50}$$

for all $0 \leq \alpha \leq 1$, where A_0 and A_1 are given by

$$A_0 = \begin{bmatrix} -5 & 3 & 3 & 3 \\ 0 & -5 & 2 & 2 \\ 0 & 0 & -6 & 1 \\ 0 & 0 & 0 & -6 \end{bmatrix} \text{ and } A_1 = \begin{bmatrix} -8 & 3 & 2 & 1 \\ 1 & -8 & 3 & 2 \\ 2 & 1 & -8 & 3 \\ 3 & 2 & 1 & -8 \end{bmatrix}.$$

We evaluate the performance of the parametrized family of linear system (4.2)-(4.3) *with state matrix A_α and output matrix $C = I_4$ for all $0 \leq \alpha \leq 1$. In Figure 4.4, our lower bound based on Theorem 4.5.1 is compared with other known bounds summarized in Table 4.1. One observes from this figure that our lower bound outperforms all existing lower bounds for all $0 \leq \alpha \leq 1$. For all $0 \leq \alpha < 1$, the parametrized matrix A_α is not normal. However, this matrix becomes normal for $\alpha = 1$. Therefore, as it is seen in the figure our lower bounds reach the exact value of the performance measure for $\alpha = 1$.*

Example 4.7.2. *We illustrate tightness of our bounds on the performance measure of the parametrized family of linear consensus networks over directed graph that are defined using the following parametrized family of Laplacian matrices*

$$L_\alpha \;=\; (1-\alpha)L_0 + \alpha L_1 \tag{4.51}$$

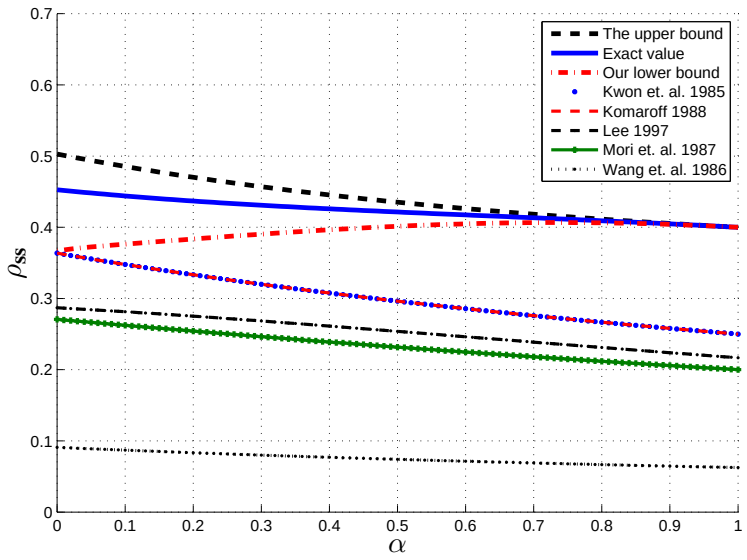

Figure 4.4: A numerical comparison of the results presented in Table 4.1 for the family of linear systems given in Example 4.7.1.

for all $0 \leq \alpha \leq 1$*, where* L_0 *and* L_1 *are given by*

$$L_0 = \begin{bmatrix} 2 & -1 & -1 & 0 \\ -1 & 3 & -1 & -1 \\ -1 & -1 & 4 & -2 \\ 0 & -1 & -2 & 3 \end{bmatrix}, \; L_1 = \begin{bmatrix} 4 & -2 & 0 & -2 \\ -2 & 2 & 0 & 0 \\ 0 & 0 & 1 & -1 \\ -2 & 0 & -1 & 3 \end{bmatrix}$$

and the following output matrix

$$C = \begin{bmatrix} 1 & -1 & 0 & 0 \\ 0 & 1 & -1 & 0 \\ 0 & 0 & 1 & -1 \\ -1 & 0 & 0 & 1 \end{bmatrix}.$$

In Figure 4.5, our lower bound is compared with other known bounds presented in Table

4.1. The simulation results confirm that our proposed lower bound is tighter than all the previously existing results in the literature. It should be noted that since $Q = C^{\mathrm{T}}C$ is not full-rank (i.e., singular) the result of [47] is not applicable to this family of systems.

4.8 Discussion and Conclusion

The proposed lower and upper bounds in Theorem 4.5.1 are functions of the real parts of eigenvalues of the state matrix of the system and the eigenvalues of its symmetric part, respectively. We have shown that the spectral lower bound in Theorem 4.5.1 is tighter than all existing lower bounds reported in Table 4.1. Our proposed lower bound requires computation of all eigenvalues of a $n \times n$ state matrix that in general has higher computational complexity than those lower bounds in Table 4.1. This extra complexity is the price of having comparably tighter estimates for the performance measure. Calculation of eigenvalues (modes) of some classes of linear dynamical networks with normal or symmetric state matrices are inexpensive and may lead to closed-form expressions for all eigenvalues, e.g., spatially invariant systems with lattice or ring topologies and linear consensus networks with path, star, cycle, complete, and complete bipartite graph topologies; see Chapter 2, [2, 12] and references in there. For networks with generic $n \times n$ state matrices, the best currently known bounds for arithmetic complexity of computing all eigenvalues and their associated eigenspaces is given by $\mathcal{O}\big(n^3 + (n \log^2 n) \log b\big)$ for an approximation within 2^{-b}; see [120] for more details. This bound is reported to be optimal up to a logarithmic factor, where it is shown that a much better randomized arithmetic complexity of order $\mathcal{O}\big(n^2 \log n + (n \log^2 n) \log b\big)$ can be achieved for some important special classes of matrices such as Toeplitz, Hankel, Toeplitz-like, Hankel-like, and Toeplitz-like-plus-Hankel-like matrices.

The value of having a spectral lower bound like (4.8) is beyond its computational

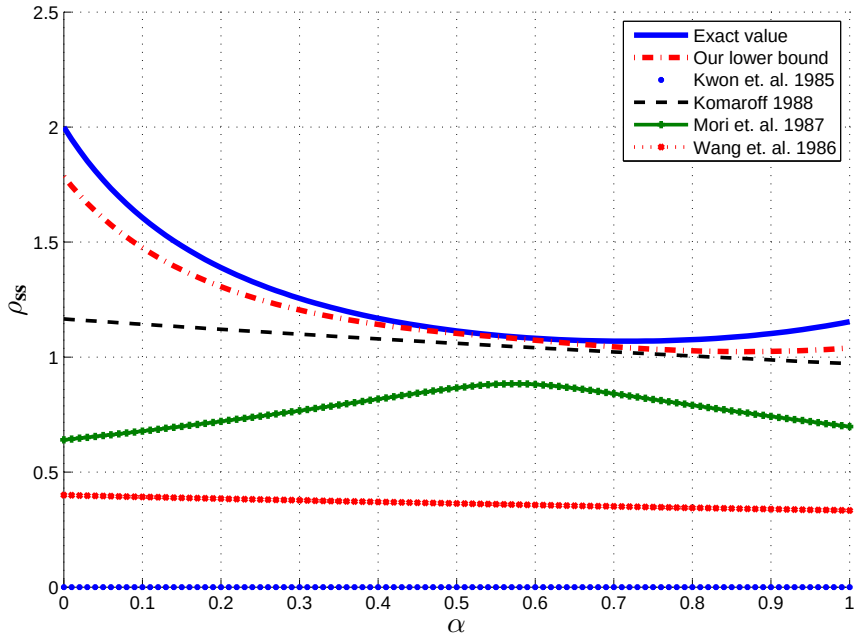

Figure 4.5: A numerical comparison of the results presented in Table 4.1 for the family of consensus networks given in Example 4.7.2.

complexity as it provides valuable insight on how the expected output energy under white noise excitation depends on the dynamic modes of the system, which is given by the lower bound $\frac{-1}{2}\sum_{i=1}^{n}\mathbf{Re}\{\lambda_i\}^{-1}$. We may think of term $\frac{-1}{2}\mathbf{Re}\{\lambda_i\}^{-1}$ as a quantity that can be associated with the energy of the i'th mode of the system, which is inversely proportional to its distance from the imaginary axis in the complex domain. The first key point is that for networks with a few slow modes, we can still obtain rather tight lower bounds by only identifying those slow modes; for example see [121] for some efficient identification algorithms. The second key point about the spectral lower bound is that it helps to unravel the fundamental role of slow modes in performance deterioration: slower modes are more energetic and dominant after transient phase in time, i.e., the high energy components of the output signal are the ones that are temporally slow. This suggests some useful insights on how to design inter-network feedback control laws by replacing slow

modes of the network in order to achieve better performance bounds. This is one of our future research directions.

Chapter 5

Performance Limitations in Nonlinear Autocatalytic Networks

5.1 Abstract

In this chapter, we develop some basic principles to study autocatalytic networks and exploit their structural properties in order to characterize their existing hard limits and essential tradeoffs. In a dynamical system with autocatalytic structure, the system's output is necessary to catalyze its own production. We consider a simplified model of glycolysis as our motivating example. First, we consider the properties of such pathways through a two-state model, which obtained by lumping all the intermediate reactions into a single intermediate reaction. Then, we generalize our results to autocatalytic pathways, which are composed of a chain of enzymatically catalyzed intermediate reactions. We explicitly derive the hard limit on the minimum $\mathcal{L}_2$-gain disturbance attenuation and the hard limit of its minimum output energy. Finally, we show how these resulting hard limits lead to some fundamental tradeoffs between transient and steady-state behavior of the network

and its net production.

5.2 Introduction

The class of dynamical networks with autocatalytic structures can be found in most of the planet's cells from bacteria to human, engineered, and economic systems [103]. In an interconnected control system with autocatalytic structure, the system's product (output) is necessary to power and catalyze its own production. The destabilizing effects of such "positive" autocatalytic feedback can be countered by negative regulatory feedback. There have been some recent interest to study models of glycolysis pathway which is an example of an autocatalytic dynamical network in biology that generates adenosine triphospate (ATP) which is the cell's energy currency and is consumed by different mechanisms in the cell [49, 103]. Other examples of autocatalytic networks include engineered power grids whose machinery are maintained using their own energy product as well as financial systems which operate based on generating monetary profits by investing money in the market. Recent results show that there can be severe theoretical hard limits on the resulting performance and robustness in autocatalytic dynamical networks. It is shown that the consequence of such tradeoffs stems from the autocatalytic structure of the system [49, 103, 122].

The recent interest in understanding fundamental limitations of feedback in complex interconnected dynamical networks from biological systems and physics to engineering and economics has created a paradigm shift in the way systems are analyzed, designed, and built. Typical examples of such complex networks include metabolic pathways [24], vehicular platoons [25–29], arrays of micro-mirrors [30], micro-cantilevers [31], and smart power grids. These systems are diverse in their detailed physical behavior, however, they share an important common feature that all of them consist of an interconnec-

tion of a large number of systems. There have been some progress in characterization of fundamental limitations of feedback in this class of systems [32–34].

Most of the above cited research on fundamental limitations of feedback in interconnected dynamical systems have been focused on networks with linear time-invariant dynamics. The main motivation of this chapter stems from a recent work presented in [103] which shows that glycolysis oscillation can be an indirect effect of fundamental tradeoffs in this system. The results of this work is based on a linearized model of a two-state model of glycolysis pathway and tradeoffs are stated using Bode's results. In this chapter, our approach to characterize hard limits is essentially different in the sense that it uses higher dimensional nonlinear models of the pathway. We interpret fundamental limitations of feedback by using hard limits (lower bounds) on $\mathcal{L}_2$-gain disturbance attenuation of the system [123–125], and $\mathcal{L}_2$-norm squared of the output of the system [49, 126].

In this chapter, our goal is to build upon our previous results [49,50] and develop methods to characterize hard limits on performance of autocatalytic pathways. First, we study the properties of such pathways through a two-state model, which obtained by lumping all the intermediate reactions into a single intermediate reaction (Figure 5.1). Then, we generalize our results to autocatalytic pathways, which are composed of a chain of enzymatically catalyzed intermediate reactions (Figure 5.2). We show that due to the existence of autocatalysis in the system (which is necessary for survival of the pathway), a fundamental tradeoff between fragility and net product of the pathway emerges. Also, we show that as the number of intermediate reactions grows, the price for performance increases.

5.3 Minimal Autocatalytic Pathway Model

5.3.1 Two-State Model

We consider autocatalysis mechanism in a glycolysis pathway. The central role of glycolysis is to consume glucose and produce adenosine triphosphate (ATP), the cell's energy currency. Similar to many other engineered systems whose machinery runs on its own energy product, the glycolysis reaction is autocatalytic. The ATP molecule contains three phosphate groups and energy is stored in the bonds between these phosphate groups. Two molecules of ATP are consumed in the early steps (hexokinase, phosphofructokinase/PFK) and four ATPs are generated as pyruvate is produced. PFK is also regulated such that it is activated when the adenosine monophosphate (AMP)/ATP ratio is low; hence it is inhibited by high cellular ATP concentration [24, 127]. This pattern of product inhibition is common in metabolic pathways. We refer to [103] for a detailed discussion.

Experimental observations in Saccharomyces cerevisiae suggest that there are two synchronized pools of oscillating metabolites [128]. Metabolites upstream and downstream of phosphofructokinase (PFK) have 180 degrees phase difference, suggesting that a two-dimensional model incorporating PFK dynamics might capture some aspects of system dynamics [129], and indeed, such simplified models qualitatively reproduce the experimental behavior [24, 127].

We will first assume that a lumped variable, x, can capture the essence of all intermediate metabolites. We consider a minimal model with three biochemical reactions as

follows

$$\begin{cases} \text{PFK Reaction:} & s \ + \ \alpha y \xrightarrow{R_{\text{PFK}}} \ x, \\ \text{PK Reaction:} & x \xrightarrow{R_{\text{PK}}} (\alpha+1)y \ + \ x', \\ \text{Consumption:} & y \xrightarrow{R_{\text{CONS}}} \varnothing. \end{cases} \tag{5.1}$$

In the PFK reaction, s is some precursor and source of energy for the pathway with no dynamics associated, y denotes the product of the pathway (ATP), x is intermediate metabolites, x' is one of the by-products of the second biochemical reaction (pyruvate kinase/PK). $\varnothing$ is a null state, $\alpha > 0$ is the number of y molecules that are invested in the pathway, and $\alpha + 1$ is the number of y molecules produced. $A \xrightarrow{k} B$ denotes a chemical reaction that converts the chemical species A to the chemical species B at rate k.

The PFK reaction consumes $\alpha + 1$ molecules of ATP with allosteric inhabitation by ATP. In the second reaction, pyruvate kinase (PK) produces $\alpha + 1$ molecules of ATP for a net production of one unit; Finally the third reaction models the cell's consumption of ATP. We refer to Figure 5.1 for a schematic diagram of biochemical reactions in the minimal model.

A set of ordinary differential equations that govern the changes in concentrations x and y can be written as

$$\begin{cases} \dot{x} \ = \ R_{\text{PFK}}(y) \ - \ R_{\text{PK}}(x,y), \\ \dot{y} \ = \ -\alpha \, R_{\text{PFK}}(y) \ + \ (\alpha+1) \, R_{\text{PK}}(x,y) \ - \ R_{\text{CONS}}(y). \end{cases} \tag{5.2}$$

We choose the reaction rates as follows; for the PFK reaction we have

$$R_{\text{PFK}}(y) \ = \ \frac{2y^a}{1+y^{2h}}, \tag{5.3}$$

where a is the cooperativity of ATP binding to PFK and h is the feedback strength of ATP on PFK. For the PK reaction we choose

$$R_{\text{PK}}(x, y) \;=\; \frac{2kx}{1 + y^{2g}}, \tag{5.4}$$

where k is intermediate reaction rate and g is the feedback strength of ATP on PK. The coefficients 2 in the numerator and feedback coefficient of the reactions' rates come from the normalization. Finally, the product y is consumed by basal consumption rate of $1 + \delta$, *i.e.*

$$R_{\text{CONS}} \;=\; 1 \;+\; \delta, \tag{5.5}$$

where δ is the perturbation in ATP consumption. These reaction rates are consistent with biological intuition and experimental data in the case of the glycolysis pathway [103]. In the final reaction, the effect of an external time–varying disturbance δ on ATP demand is considered. The product of the pathway, ATP, inhibits the enzyme that catalyzes the first and second reactions, and the exponents h and g capture the strength of these inhibitions, respectively.

We now rewrite (5.2)–(5.5) in the following nonlinear dynamics

$$\begin{cases} \dot{x}_1 \;=\; \frac{2x_2^a}{1+x_2^{2h}} \;-\; \frac{2kx_1}{1+x_2^{2g}}, \\ \dot{x}_2 \;=\; -\,\alpha\frac{2x_2^a}{1+x_2^{2h}} \;+\; (\alpha+1)\frac{2kx_1}{1+x_2^{2g}} \;-\; (1+\delta)\,, \end{cases} \tag{5.6}$$

with output variable

$$y = x_2 \tag{5.7}$$

for $x_1, x_2 \geq 0$.

In order to make several comparisons possible, we normalize all concentrations such

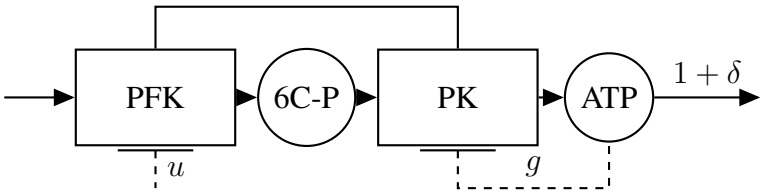

Figure 5.1: A schematic diagram of the minimal glycolysis model. The constant glucose input along with α ATP molecules produce a pool of intermediate metabolites, which then produces $\alpha + 1$ ATP molecules.

that the equilibrium point of the unperturbed system (i.e., when $\delta = 0$) becomes

$$\begin{bmatrix} x_1^* \\ x_2^* \end{bmatrix} = \begin{bmatrix} \frac{1}{k} \\ 1 \end{bmatrix}. \tag{5.8}$$

In the minimal glycolysis model (5.6) expression $\frac{2}{1+x_2^{2h}}$ can be interpreted as the effect of the regulatory feedback control mechanism employed by nature, which captures inhibition of the catalyzing enzyme. This observation suggests the following control system model for the minimal model of the glycolysis pathway

$$\begin{bmatrix} \dot{x}_1 \\ \dot{x}_2 \end{bmatrix} = \begin{bmatrix} 1 \\ -\alpha \end{bmatrix} x_2^a u + \begin{bmatrix} -1 \\ \alpha + 1 \end{bmatrix} \frac{2kx_1}{1 + x_2^{2g}} - \begin{bmatrix} 0 \\ 1 + \delta \end{bmatrix}, \tag{5.9}$$

where u is the control input and captures the effect of a general feedback control mechanism. Our primary motivation behind development and analysis of such control system models for this metabolic pathways is to rigorously show that existing fundamental tradeoffs in such models are truly unavoidable and independent of control mechanisms used to regulate such pathways. For glycolysis autocatalytic pathways, the results of the following sections assert that the existing fundamental limits on performance of the pathway depend only on the autocatalytic structure of the underlying network.

Stability properties of this model: According to [103], the equilibrium point (5.8) of two-state glycolysis model (5.6) is stable if

$$0 \ < \ h - a \ < \ \frac{k + g(1+\alpha)}{\alpha}.$$

Our aim is to show that for any stabilizing control input there is a hard limit on the performance measure of the pathway.

5.3.2 Performance Measures

We use two different methods to quantify hard limits for the glycolysis pathway models. We quantify hard limits (in the form of lower bounds) on measures of robustness and performance by considering $\mathcal{L}_2$-gain disturbance attenuation and $\mathcal{L}_2$-norm squared of the output of the system.

$\mathcal{L}_2$-Gain from Disturbance Input to Output

In order to quantify lower bounds on the best achievable robustness measure for two-state model (5.9), we need to solve the corresponding regional state feedback $\mathcal{L}_2$-gain disturbance attenuation problem with guaranteed stability. This problem consists of determining a control law, u, such that the closed-loop system has the following properties. First, the zero equilibrium of the system (5.9) with $\delta(t) = 0$, for all $t \geq 0$, is asymptotically stable with region of attraction containing Ω (an open set containing the equilibrium point). Second, for every $\delta \in L_2(0, T)$ such that the trajectories of the system remain in Ω , the $\mathcal{L}_2$-gain of the system from δ to y, is less than or equal to γ, *i.e.*

$$\int_0^T (y(t) - y^*)^2 dt \ \leq \ \gamma^2 \int_0^T \delta^2(t) dt, \tag{5.10}$$

for all $T \geq 0$ and zero initial state.

It is well-known that there exists a solution to the static state feedback $\mathcal{L}_2$-gain disturbance attenuation problem with stability, in some neighborhood of the equilibrium point, if there exists a smooth positive definite solution of the corresponding Hamilton-Jacobi inequality (see [123, 125] for more details).

The simplest robust performance requirement for model (5.9) is that the concentration of y (ATP) remains nearly constant when there is a small constant disturbance in ATP consumption δ (see [49, 103]). But even temporary ATP depletion can result in cell death. Therefore, we are interested in a more complete picture of the transient response to external disturbances.

We show that there exists a hard limit on the best achievable disturbance attenuation, γ^*, for system (5.9) such that the problem of disturbance attenuation (5.10) with internal stability is solvable for all $\gamma > \gamma^*$ and not for $\gamma < \gamma^*$. The interesting observation is that the optimal disturbance attenuation γ^* is indeed a hard limit function on robustness of system (5.9). It is known that for linear systems, optimal disturbance attenuations can be calculated based on the zero-dynamics subsystem of the system [126]. The hard limit function is zero if and only if the disturbance δ does not influence the unstable part of the zero-dynamics of the system (as defined in [124] for nonlinear systems).

Total Output Energy

We characterize fundamental limitations of feedback for system (5.9) with initial condition $x(0) = x_0$ and zero external disturbances (i.e., $\delta(t) = 0$) by considering the corresponding cheap optimal control problem. This case consists of finding a stabilizing state

feedback control which minimizes the functional

$$J_\epsilon(x_0;u) \;=\; \frac{1}{2}\int_0^\infty \;\left[\; (y(t)-y^*)^2 \;+\; \epsilon^2\,(u(t)-u^*)^2 \;\right]\,dt, \tag{5.11}$$

when ϵ is a small positive number. As $\epsilon \to 0$, the optimal value $J^*_\epsilon(x_0)$ tends to $J^*_0(x_0)$, the ideal performance of the system. It is well-known (e.g., see [130], page 91) that this problem has a solution if there exists a positive semidefinite optimal value function which satisfies the corresponding Hamilton–Jacobi-Bellman equation (HJBE). The interesting fact is that the ideal performance is indeed a hard limit on performance of system (5.9). It is known that the ideal performance is the optimal value of the minimum energy problem for the zero-dynamics of the system (see [126] for more details). The ideal performance (hard limit function) is zero if and only if the system has an asymptotically stable zero-dynamics subsystem.

5.3.3 Fundamental limits on the Performance Measures

$\mathcal{L}_2$-Gain Disturbance Attenuation

Theorem 5.3.1. *Consider the optimal $\mathcal{L}_2$-gain disturbance attenuation problem for the minimal glycolysis model (5.9). Then, the best achievable disturbance attenuation gain γ^* for system (5.9) satisfies the following inequality*

$$\gamma^* \;\geq\; \mathbf{\Gamma}(\alpha,k,g), \tag{5.12}$$

and the hard limit function is given by

$$\mathbf{\Gamma}(\alpha,k,g) \;=\; \frac{\alpha}{k+g\alpha}. \tag{5.13}$$

Proof. We recall that the optimal value of the achievable disturbance attenuation level γ^* is a number with the property that the problem of disturbance attenuation with internal stability is locally solvable for each prescribed level of attenuation $\gamma > \gamma^*$ and not for $\gamma < \gamma^*$. In the first step, we introduce a new auxiliary variable $z = x_1 + \frac{1}{\alpha}x_2$. By transforming the dynamics of the system using the following change of coordinates

$$\begin{bmatrix} y \\ z \end{bmatrix} = \begin{bmatrix} 0 & 1 \\ 1 & \frac{1}{\alpha} \end{bmatrix} \begin{bmatrix} x_1 \\ x_2 \end{bmatrix}, \tag{5.14}$$

we obtain the following form

$$\begin{cases} \dot{y} &= -\frac{\alpha+1}{\alpha}\frac{2ky}{1+y^{2g}} + (\alpha+1)\frac{2kz}{1+y^{2g}} - \alpha y^a u - (1+\delta) \\ \dot{z} &= \frac{1}{\alpha}\frac{2kz}{1+y^{2g}} - \frac{1}{\alpha^2}\frac{2ky}{1+y^{2g}} - \frac{1}{\alpha}(1+\delta). \end{cases} \tag{5.15}$$

Note that the optimal $\mathcal{L}_2$-gain disturbance attenuation of transformed system (5.15) and the original system are the same. Based on [131, Section 8.4] the optimal disturbance level for the linearized problem will provide a lower bound for the optimal disturbance of the nonlinear system. Furthermore, for the linear system this problem reduces to a disturbance attenuation problem for the zero dynamics with cost on the control input. Thus we consider the linearized zero dynamics of (5.15) as follows

$$\dot{\bar{z}} = \frac{k}{\alpha}\bar{z} - \frac{g\alpha + k}{\alpha^2}\bar{y} - \frac{1}{\alpha}\delta, \tag{5.16}$$

where

$$\begin{cases} \bar{z} &= z - z^* = z - (x^* + \frac{1}{\alpha}y^*) \\ \bar{y} &= y - y^* \end{cases} \tag{5.17}$$

We now calculate optimal disturbance attenuation problem (from δ to y) for the zero dynamics with cost on its control input y. For system (5.16), the optimal value of γ is given by (see [124, 132] for more details)

$$\gamma_L^* \;=\; \frac{\alpha}{k+g\alpha}. \tag{5.18}$$

Thus, we can conclude that

$$\gamma^* \;\geq\; \gamma_L^* \;=\; \mathbf{H}(\alpha,k,g) \;=\; \frac{\alpha}{k+g\alpha}.$$

This completes the proof.

□

Remark 5.3.2. *Theorem 5.3.1 illustrates a tradeoff between robustness and efficiency (as measured by complexity and metabolic overhead). From (5.12) the glycolysis mechanism is more robust efficient if k and g are large. On the other hand, large k requires either a more efficient or a higher level of enzymes, and large g requires a more complex allosterically controlled PK enzyme; both would increase the cell's metabolic load. The obtained hard limit in Theorem 5.3.1 is increasing function with respect to α. It means that increasing α (more energy investment for the same return) can result in worse performance. It is important to note that these results are consistent with results in [103], where a linearized model with a different performance measure is used.*

Total Output Energy

In this subsection, we show that there exists a hard limit on the best achievable ideal performance (output energy) of system (5.9). One can see that some minimum output energy (*i.e.*ATP) is required to stabilize the unstable zero-dynamics (5.15). This output

energy represents the energetic cost of the cell to stabilize it to its steady-state. In the following theorem, we show that the minimum output energy is lower bounded by a constant which is only a function of the parameters and initial conditions of the glycolysis model. This hard limit is independent of the feedback control strategy used to stabilize the system.

Theorem 5.3.3. *Suppose that the equilibrium of interest is given by (5.8) and* $u^* = 1$. *Then, there is a hard limit on the performance measure of the unperturbed (*$\delta = 0$*) system (5.9) in the following sense*

$$\int_0^\infty (y(t;u_0) - \bar{y})^2 \, dt \;\geq\; \frac{\alpha^3 k}{(g\alpha + k)^2} \, z_0^2 + J(z_0; \alpha, k, g), \tag{5.19}$$

where $z_0 = (x(0) - x^*) + \frac{1}{\alpha}(y(0) - y^*)$, u_0 *is an arbitrary stabilizing feedback control law for system (5.9),* $J(0;\alpha,k,g) = J(z;\alpha,k,0) = 0$ *and* $|J(z;\alpha,k,g)| \leq c|z|^3$ *on an open set* Ω *around the origin in* $\mathbb{R}$.

Proof. By introduction of a new variable $z = x_1 + \frac{1}{\alpha}y$, we rewrite (5.9) in the canonical form (5.15). We denote by $\pi(y, z; \epsilon)$ the solution of the HJB PDE corresponding to the cheap optimal control problem to (5.9). We apply the power series method [133, 134] by first expanding $\pi(y, z; \epsilon)$ in series as follows

$$\pi(y, z; \epsilon) \;=\; \pi^{[2]}(y, z; \epsilon) \;+\; \pi^{[3]}(y, z; \epsilon) \;+\; \ldots \tag{5.20}$$

in which kth order term in the Taylor series expansion of $\pi(y, z; \epsilon)$ is denoted by $\pi^{[k]}(y, z; \epsilon)$. Then (5.20) is plug into the corresponding HJB equation of the optimal cheap control

problem. The first term in the series is

$$\pi^{[2]}(y,z;\epsilon) \;=\; \begin{bmatrix} y-y^* & z-z^* \end{bmatrix} P(\epsilon) \begin{bmatrix} y-y^* \\ z-z^* \end{bmatrix},$$

where $P(\epsilon)$ is the solution of algebraic Riccati equation to the cheap control problem for the linearized model (A_0, B_0). It can be shown that $P(\epsilon)$ can be decomposed in the form of a series in ϵ (see [135] for more details)

$$P(\epsilon) \;=\; \begin{bmatrix} \epsilon P_1 & \epsilon P_2 \\ \epsilon P_2 & P_0 + \epsilon P_3 \end{bmatrix} + \mathcal{O}(\epsilon^2).$$

Since the pole of the zero-dynamics of the linearized model is located at the $\frac{k}{\alpha}$, we can verify that $P_0 = \frac{\alpha^3 k}{(g\alpha+k)^2}$. Therefore, it follows that $\pi^{[2]}(y,z;\epsilon) = \frac{\alpha^3 k}{(g\alpha+k)^2} z_0^2 + \mathcal{O}(\epsilon)$.

We only explain the key steps. One can obtain governing partial differential equations for the higher-order terms $\pi^{[k]}(y,z;\epsilon)$ for $k \geq 3$ by equating the coefficients of terms with the same order. It can be shown that $\pi^{[k]}(y,z) = \pi_0^{[k]}(z) + \epsilon\pi_1^{[k]}(y,z) + \mathcal{O}(\epsilon)$ for all $k \geq 3$. Then, by constructing approximation of the optimal control feedback by using computed Taylor series terms, one can prove that $\pi(y,z;\epsilon) \to \frac{\alpha^3}{k} z_0^2 +$ (higher order terms in z_0) as $\epsilon \to 0$. Thus, the ideal performance cost value is $\frac{\alpha^3}{k} z_0^2 + J(z_0)$.

□

Remark 5.3.4. *Based on Theorems 5.3.1 and 5.3.3, a fundamental tradeoff between fragility and net production of the pathway emerges as follows: increasing α (number of ATP molecules invested in the pathway), increases fragility of the network to small disturbances (based on Theorem 5.3.1) and it can result in undesirable transient behavior (based on Theorem 5.3.3). For instance, if the level of ATP drops below some threshold,*

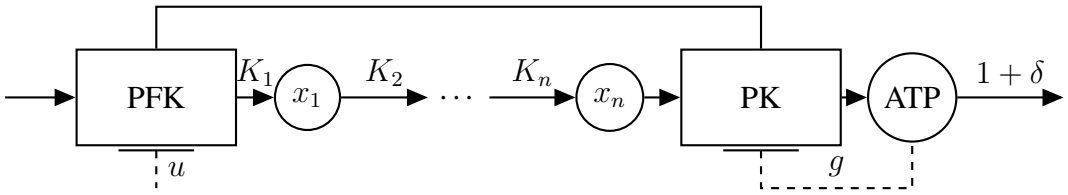

Figure 5.2: A schematic diagram of a glycolysis pathway model with intermediate reactions. The constant glucose input along with α ATP molecules produce a pool of intermediate metabolites, which then produces $\alpha + 1$ ATP molecules.

there will not be sufficient supply of ATP for different pathways in the cell and that can result to cell death.

5.4 Autocatalytic Pathways With Multiple Intermediate Metabolite Reactions

In this section, we consider autocatalytic pathways with multiple intermediate metabolite reactions as shown in Figure 5.2. In Subsection 5.3.1, we studied the property of such pathways with a two-state model (5.9), which is obtained by lumping all the intermediate reactions into a single intermediate reaction (see Figure 5.2).

$$\begin{cases} \text{PFK Reaction:} & s + \alpha y \xrightarrow{R_{\text{PFK}}} x_1, \\ \text{Intermediates:} & x_1 \xrightarrow{R_{\text{IR}}} x_2 \cdots \xrightarrow{R_{\text{IR}}} x_n, \\ \text{PK Reaction:} & x_n \xrightarrow{R_{\text{PK}}} (\alpha+1)y + x', \\ \text{Consumption:} & y \xrightarrow{R_{\text{CONS}}} \varnothing. \end{cases} \tag{5.21}$$

A set of ordinary differential equations that govern the changes in concentrations of

x_i for $i = 1, \ldots, n$ and y can be cast as follows

$$\begin{cases} \dot{x}_1 \;=\; R_{\text{PFK}}(y) \;-\; R_{\text{IR}}(x_1), \\ \dot{x}_2 \;=\; R_{\text{IR}}(x_1) \;-\; R_{\text{IR}}(x_2), \\ \quad \ldots \\ \dot{x}_n \;=\; R_{\text{IR}}(x_{n-1}) \;-\; R_{\text{PK}}(x_n, y), \\ \dot{y} \;=\; (\alpha+1)R_{\text{PK}}(x_n, y) \;-\; \alpha R_{\text{PFK}}(y) \;-\; R_{\text{CONS}}, \end{cases} \tag{5.22}$$

for $x_i \geq 0$ and $y \geq 0$.

Our notations are similar to those of the two-state pathway model (5.1). We choose the reaction rates as follows

$$\begin{cases} R_{\text{PFK}}(y) \;=\; \frac{2y^a}{1+y^{2h}}, \\ R_{\text{PK}}(x_n, y) \;=\; \frac{2K_n x_n}{1+y^{2g}}, \\ R_{\text{IR}}(x_i) \;=\; K_i x_i \;\text{ for }\; n = 1, 2, \ldots, n, \\ R_{\text{CONS}} \;=\; 1 + \delta \end{cases} \tag{5.23}$$

Furthermore, In the glycolysis model (5.22), similar to the minimal model (5.9), expression $\frac{2}{1+x^{2h}}$ can be interpreted as the effect of the regulatory feedback control mechanism employed by nature, which captures inhibition of the catalyzing enzyme. Hence, we can derive a control system model for the autocatalytic pathway with multiple intermediate metabolite reactions as follows

$$
\begin{cases}
\dot{x}_1 \;=\; y^a u \;-\; K_1 x_1, \\
\dot{x}_2 \;=\; K_1 x_1 \;-\; K_2 x_2, \\
\quad \cdots \\
\dot{x}_n \;=\; K_{n-1} x_{n-1} \;-\; \frac{2K_n x_n}{1+y^{2g}}, \\
\dot{x}_{n+1} \;=\; (\alpha+1)\frac{2K_n x_n}{1+x_{n+1}^{2g}} \;-\; \alpha x_{n+1}^a u \;-\; (1+\delta), \\
y \;=\; x_{n+1},
\end{cases}
\tag{5.24}
$$

for $x_i \geq 0$ and $y \geq 0$. In order to simplify our analysis, we assume that $K := K_1 = \cdots = K_n > 0$. We normalize all concentrations such that unperturbed steady states are

$$
y^* = x_{n+1}^* = 1, \quad x_i = \frac{1}{K}, \quad 1 \leq i \leq n. \tag{5.25}
$$

5.4.1 $\mathcal{L}_2$-Gain Disturbance Attenuation

We extend our results in Theorem 5.3.1 to higher dimensional model of autocatalytic pathways. In the following theorem, we show that there exists a hard limit on the best achievable disturbance attenuation of system (5.24).

Theorem 5.4.1. *Consider the optimal $\mathcal{L}_2$-gain disturbance attenuation problem for the minimal glycolysis model (5.24). Then, the best achievable disturbance attenuation gain γ^* for system (5.24) satisfies the following inequality*

$$
\gamma^* \;\geq\; \mathbf{\Gamma}(\alpha, K, g, n), \tag{5.26}
$$

and the hard limit function is given by

$$\mathbf{\Gamma}(\alpha, K, g, n) \;=\; \frac{1}{\big(K + g\alpha(\frac{\alpha+1}{\alpha})^{\frac{n-1}{n}}\big)\big((\frac{\alpha+1}{\alpha})^{\frac{1}{n}} - 1\big)}.$$

Proof. First, by introducing a new variable $z_1 = x_1 + \frac{1}{\alpha}y$, we can cast the zero-dynamics of (5.24) in the following form

$$\begin{cases} \dot{z}_1 \;=\; -\,Kz_1 \;+\; \frac{\alpha+1}{\alpha}\frac{2Kx_n}{1+y^{2g}} \;+\; \frac{K}{\alpha}y - \frac{1}{\alpha}(\delta+1), \\ \dot{x}_2 \;=\; Kz_1 \;-\; \frac{K}{\alpha}y \;-\; Kx_2, \\ \quad \cdots \\ \dot{x}_n \;=\; Kx_{n-1} \;-\; \frac{2Kx_n}{1+y^{2g}}. \end{cases} \tag{5.27}$$

Let us define

$$z := \begin{bmatrix} z_1 & x_2 & \dots & x_n \end{bmatrix}^{\mathrm{T}},$$

and

$$z^* := \begin{bmatrix} \frac{1}{K} + \frac{1}{\alpha} & \frac{1}{K} & \cdots & \frac{1}{K} \end{bmatrix}^{\mathrm{T}}.$$

Then, we rewrite (5.27) in the following form

$$\dot{\bar{z}} \;=\; A\bar{z} \;+\; B\bar{y} \;+\; C\delta \;+\; \bar{f}(\bar{z}, \bar{y}), \tag{5.28}$$

where

$$A \;=\; \begin{bmatrix} -K & 0 & 0 & \dots & (1+\frac{1}{\alpha})K \\ K & -K & 0 & \dots & 0 \\ 0 & K & -K & \dots & 0 \\ & \vdots & & \ddots & \vdots \\ 0 & 0 & 0 & \dots & -K \end{bmatrix},$$

$$B \;=\; \begin{bmatrix} -\frac{\alpha+1}{\alpha}g+\frac{K}{\alpha} \\ -\frac{K}{\alpha} \\ \vdots \\ g \end{bmatrix},\; C \;=\; \begin{bmatrix} -\frac{1}{\alpha} \\ 0 \\ \vdots \\ 0 \end{bmatrix}, \tag{5.29}$$

$\bar{z} = z - z^*$, $\bar{y} = y - y^*$, $\bar{f}(0,0) = 0$ and

$$\|\frac{\partial \bar{f}(\bar{z},\bar{y})}{\partial(\bar{z},\bar{y})}\| \;\leq\; c|(\bar{z},\bar{y})|, \tag{5.30}$$

near the origin in $\mathbb{R}^n$ for $c > 0$. Now, according to [125] we know that if the system (5.28) has $\mathcal{L}_2$-gain $\leq \gamma$, then the linearized system has $\mathcal{L}_2$-gain $\leq \gamma$. Hence, we only consider the linearized system, *i.e.*

$$\dot{\bar{z}} \;=\; A\bar{z} \;+\; B\bar{y} \;+\; C\delta. \tag{5.31}$$

Note that $\lambda = K\left[(\frac{\alpha+1}{\alpha})^{\frac{1}{n}} - 1\right]$ is the eigenvalue of A with the greatest real part. And the corresponding left eigenvector of λ, is $v = \begin{bmatrix} 1 & (\frac{\alpha+1}{\alpha})^{\frac{1}{n}} & \dots & (\frac{\alpha+1}{\alpha})^{\frac{n-1}{n}} \end{bmatrix}^{\mathrm{T}}$. Now, we consider the following subsystem of (5.31)

$$\dot{\tilde{z}} = \lambda\tilde{z} + \Big[\big((1+\frac{1}{\alpha})^{\frac{n-1}{n}} - (1+\frac{1}{\alpha})\big)g - \frac{K}{\alpha}\big((1+\frac{1}{\alpha})^{\frac{1}{n}} - 1\big)\Big]\tilde{y} - \frac{1}{\alpha}\delta.$$

Based on the result of [132] and [124], the formula to compute the optimal value of γ reduces to

$$\gamma_L^* \;\geq\; \frac{1}{\big(K + g\alpha(1+\frac{1}{\alpha})^{\frac{n-1}{n}}\big)\big((1+\frac{1}{\alpha})^{\frac{1}{n}} - 1\big)}.$$

Note that according to Proposition 6 of [125], γ_L^* is a lower bound for the optimal γ^* of the nonlinear system (5.24). □

Remark 5.4.2. *It can be easily shown that* $\mathbf{\Gamma}(\alpha, K, g, n) \in \mathcal{O}(n)$*, and it can be approxi-*

mated for large n by

$$\mathbf{\Gamma}(\alpha, K, g, n) \approx \frac{n}{\big(g(\alpha+1)+K\big)\ln(1+\frac{1}{\alpha})}. \tag{5.32}$$

This means that as the number of intermediate reactions n grows, the price paid for robustness, $\mathbf{\Gamma}(\alpha, K, g, n)$, increases linearly with n.

5.4.2 Total Output Energy

We now show that there exists a hard limit on the best achievable ideal performance (output energy) of system (5.24).

Theorem 5.4.3. *Suppose that the equilibrium of interest is given by (5.25) and $u^* = 1$. Then, there is a hard limit on the performance measure of the unperturbed (i.e., $\delta = 0$) system (5.24) in the following sense*

$$\begin{aligned}\int_0^\infty (y(t;u_0)-y^*)^2\,dt \\ \geq \mathbf{H}(z_0;\alpha,K,g,n) + J(z_0;\alpha,K,g,n),\end{aligned} \tag{5.33}$$

where

$$\mathbf{H}(z_0;\alpha,K,g,n) = \frac{\alpha^2 K\big(\frac{1}{\alpha}(y(0)-y^*)+\sum_{i=1}^n(\frac{\alpha+1}{\alpha})^{\frac{i-1}{n}}(x_i(0)-x_i^*)\big)^2}{\big((\frac{\alpha+1}{\alpha})^{\frac{1}{n}}-1\big)\big(K+g\alpha(\frac{\alpha+1}{\alpha})^{\frac{n-1}{n}}\big)^2},$$

and u_0 is an arbitrary stabilizing feedback control law for system (5.24), $J(0;\alpha,K,g,n) = J(z;\alpha,K,0,n) = 0$ and $|J(z;\alpha,K,g,n)| \leq c|z-z^*|^3$, where z is close enough to z^*.

Proof. The proof of this theorem is adjusted from [125, 126] and Theorem 5.3.3.

□

Remark 5.4.4. *In the case that $n = 1$, i.e.with only one intermediate reaction, the results of Theorems 5.4.1 and 5.4.3 reduce to the results of Theorems 5.3.1 and 5.3.3, respectively.*

Remark 5.4.5. *It can be easily shown that $\mathbf{H}(z_0; \alpha, K, g, n) \in \mathcal{O}(n)$, and it is approximated by*

$$\mathbf{H}(z_0; \alpha, K, g, n) \approx \frac{\alpha^2 K\big(\frac{1}{\alpha}(y(0) - y^*) + \sum_{i=1}^{n}(\frac{\alpha+1}{\alpha})^{\frac{i-1}{n}}(x_i(0) - x_i^*)\big)^2}{\big(K + g(\alpha+1)\big)^2 \ln(\frac{\alpha+1}{\alpha})} n.$$

This means that as the number of intermediate reactions n grows, the price paid for robustness, $\mathbf{H}(z_0; \alpha, K, g, n)$, increases linearly with n.

5.5 General Autocatalytic Pathways

In this section, we consider networks with autocatalytic structures as shown in Figure 5.3. We focus on a class of nonlinear dynamical networks with cyclic feedback structures driven by disturbance. We consider a group of nonlinear systems with state-space models

$$\begin{cases} \dot{x}_i &= -f_i(x_i) + u_i, \\ y_i &= g_i(x_i), \end{cases} \tag{5.34}$$

for $1 \leq i \leq n$, and

$$\begin{cases} \dot{x}_{n+1} &= -f_{n+1}(x_{n+1}) + u_{n+1} - \alpha u, \\ y_{n+1} &= u, \end{cases} \tag{5.35}$$

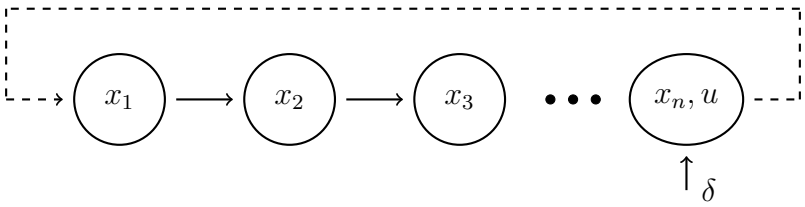

Figure 5.3: The schematic diagram of the nonlinear network (5.36) with a cyclic feedback structure with an output disturbance δ and control input u.

where $f_i(\cdot)$ and $g_i(\cdot)$ for $i = 1, \ldots, n$ are increasing functions. Moreover, $u_i(t)$, $y_i(t)$ and $x_i(t)$ are input, output and state variables of each subsystem, respectively. The state-space representation of the nonlinear cyclic interconnected network shown in Figure 5.3 is given by

$$\begin{cases} \dot{x}_1 &= -f_1(x_1) + y_{n+1}, \\ \dot{x}_2 &= -f_2(x_2) + y_1, \\ &\cdots \\ \dot{x}_{n+1} &= -f_{n+1}(x_{n+1}) + y_n - \alpha u + \delta, \\ y &= x_{n+1}. \end{cases} \tag{5.36}$$

Assumption 5.5.1. *We assume that x_i^*'s and y^* are equilibrium points of the unperturbed system (5.36), i.e., when $\delta = 0$. Moreover, it is assumed that*

$$a := f_1'(x_1^*) = f_2'(x_2^*) = \cdots = f_n'(x_n^*), \tag{5.37}$$

where $f_i'(x_i^*) := \left.\frac{\mathrm{d}f_i}{\mathrm{d}x_i}\right|_{x_i = x_i^*}$.

Theorem 5.5.2. *For cyclic networks (5.36), if*

$$r := \left(\frac{g_1'(x_1^*) g_2'(x_2^*) \cdots g_n'(x_n^*)}{\alpha} \right)^{\frac{1}{n}} > a, \tag{5.38}$$

then there exists a hard limit on the best achievable disturbance attenuation (i.e., $\gamma^* > 0$) for system (5.36) such that the regional state feedback L_2–gain disturbance attenuation problem with stability constraint is solvable for all $\gamma > \gamma^*$ and is not solvable for all $\gamma < \gamma^*$. Furthermore, the hard limit function is given by

$$\gamma^* \geq \mathbf{\Gamma}(f_{n+1}'(y^*), r, a) = \frac{1}{f_{n+1}'(y^*) + r - a}. \tag{5.39}$$

Proof. In the first step, we introduce a new auxiliary variable $z_1 = x_1 + \frac{1}{\alpha} x_{n+1}$. We can cast the linearized zero-dynamics of (5.36) in the following form

$$\dot{z} \;=\; A_0 z \;+\; B_0 y \;+\; C_0 \delta, \tag{5.40}$$

where $z = [z_1, x_2, \cdots, x_n]^{\mathrm{T}}$,

$$A_0 = \begin{bmatrix} -a & 0 & \dots & 0 & \alpha^{-1} g_n'(x_n^*) \\ g_1'(x_1^*) & -a & \dots & 0 & 0 \\ \vdots & \vdots & \ddots & \vdots & \vdots \\ 0 & 0 & \dots & -a & 0 \\ 0 & 0 & \dots & g_{n-1}'(x_{n-1}^*) & -a \end{bmatrix},$$

$$B_0 = \begin{bmatrix} \frac{a - f'_{n+1}(y^*)}{\alpha} \\ -\frac{g'_1(x_1^*)}{\alpha} \\ \vdots \\ 0 \\ 0 \end{bmatrix}, \text{ and } C_0 = \begin{bmatrix} \alpha^{-1} \\ 0 \\ \vdots \\ 0 \\ 0 \end{bmatrix}. \tag{5.41}$$

Then, we consider the characteristic equation of matrix A_0 which is given by

$$(\lambda + a)^n - r^n \;=\; 0. \tag{5.42}$$

From (5.38) and (5.42), it follows that $\lambda_1 = r - a$ is the eigenvalue of A_0 with the largest real-part value with left eigenvector

$$v_1 = \Big[\, 1 \,,\; \frac{r}{g'_1(x_1^*)} \,,\; \cdots \,,\; \frac{r^{n-1}}{g'_1(x_1^*)g'_2(x_2^*)\cdots g'_{n-1}(x_{n-1}^*)} \,\Big]^{\mathrm{T}}.$$

The unstable subsystem of (5.40) is characterized by

$$\dot{z} \;=\; \lambda_1 z \,+\, \alpha^{-1}\big(a - f'_{n+1}(y^*) \,-\, r\big)\, y \,+\, \alpha^{-1}\delta. \tag{5.43}$$

From the results of [132] and [124], the formula to compute the optimal value of γ reduces to

$$\gamma_L^* = \frac{1}{f'_{n+1}(y^*) + r - a}. \tag{5.44}$$

We emphasize that according to [125, Proposition 6], γ_L^* is a lower bound for the optimal γ^* for the nonlinear system (5.36). □

In following example, we apply our results to metabolic pathway (5.1) and quantify

its existing hard limits. We assume that the second reaction in (5.1) has no ATP feedback ATP on PK (*i.e.*$g = 0$). Also, in the following example, we consider two scenarios for the consumption rate R_{CONS}; First, we assume the product y is consumed by basal consumption rate $1 + \delta$ and then we consider the consumption rate depends on y.

Example 5.5.3. *Consider the minimal representation of autocatalytic glycolysis pathway given by* (5.1)*. First, we assume that the second reaction in* (5.1) *has no ATP feedback ATP on PK (i.e.*$g = 0$*). Then, we can rewrite* (5.6) *as follows*

$$\dot{x}_1 = \frac{2y^a}{1+y^{2h}} - kx_1, \tag{5.45}$$

$$\dot{y} = -\alpha\frac{2y^a}{1+y^{2h}} + (\alpha+1)kx_1 - (1+\delta), \tag{5.46}$$

for $x1 \geq 0$*,* $y \geq 0$*. By considering expression* $\frac{2y^a}{1+y^{2h}}$ *as the regulatory feedback control employed by nature which captures inhibition of the catalyzing enzyme, a control system model for glycolysis is derived as follows*

$$\dot{x}_1 = -k\,x_1 + u, \tag{5.47}$$

$$\dot{y} = (\alpha+1)k\,x_1 - \alpha\,u - 1 - \delta, \tag{5.48}$$

where u *is the control input. Using* (5.47)-(5.48) *and Theorem 5.5.2, it follows that*

$$\gamma > \frac{\alpha}{k}, \tag{5.49}$$

where the equilibrium point of the unperturbed system is given by $x_1 = 1/k$ *and* $y = 1$*. As we expected* (5.49) *is consistent with the result of Theorem 5.3.1. Next, we consider*

the consumption rate depends on y, and given by

$$R_{\text{CONS}} \;=\; k_y y + \delta,$$

(see [122] for more details). Then, a set of ordinary differential equations that govern the changes in concentrations x_1 and y can be written as

$$\begin{aligned} \dot{x}_1 &= -k\, x_1 \;+\; \frac{2y^a}{1+y^{2h}}, \\ \dot{y} &= -\alpha \frac{2y^a}{1+y^{2h}} \;+\; (\alpha+1) k\, x_1 \;-\; \left(k_y y + \delta\right), \end{aligned}$$

for $x_1 \geq 0$, $y \geq 0$. The exogenous disturbance disturbance input is assumed to be $\delta \in L_2([0,\infty))$. To highlight fundamental tradeoffs due to autocatalytic structure of the system, we normalize the concentration such that steady-states are

$$y^* = 1 \;\; \textit{and} \;\; {x_1}^* = \frac{k_y}{k}. \tag{5.50}$$

Similar to the first case, we can consider expression $\frac{2y^a}{1+y^{2h}}$ as the regulatory feedback control employed by nature which captures inhibition of the catalyzing enzyme. Hence, we can derive a control system model for glycolysis as follows

$$\dot{x}_1 \;=\; -k\, x_1 + u, \tag{5.51}$$

$$\dot{y} \;=\; (\alpha+1) k\, x_1 - \alpha\, u - k_y\, y - \delta, \tag{5.52}$$

where u is the control input. Now, applying Theorem 5.5.2 to this model, it follows that

$$\gamma \;>\; \frac{\alpha}{k + \alpha k_y}. \tag{5.53}$$

Equation (5.53) illustrates a tradeoff between robustness and efficiency (as measured by complexity and metabolic overhead). From (5.53) the glycolysis mechanism is more robust efficient if k and k_y are large. On the other hand, large k requires either a more efficient or a higher level of enzymes, and large k_y requires a more complex allosterically controlled PK enzyme; both would increase the cell's metabolic load. We note that the existing hard limit is an increasing function of α. This implies that increasing α (more energy investment for the same return) can result in worse performance. It is important to note that these results are consistent with results in [122], where a linearized model with a different performance measure is used.

5.6 Conclusion

By using blending ideas from biology and nonlinear control theory, our objective is to develop a methodology to characterize fundamental limits on robustness and performance measures in dynamical networks with autocatalytic structures. We study the hard limits of the ideal performance of a glycolysis model. It is shown that glycolysis model can be used as a basis for such study. Then, we explicitly derive hard limits on the performance of the autocatalytic pathways with intermediate reactions which are characterize as $\mathcal{L}_2$-norm squared of the output and $\mathcal{L}_2$-gain of disturbance attenuation.

Part II

Network Synthesis for Performance Enhancement

Chapter 6

Growing Linear Consensus Networks

6.1 Abstract

We propose an axiomatic approach for design and performance analysis of noisy linear consensus networks by introducing a notion of systemic performance measure. This class of measures are spectral functions of Laplacian eigenvalues of the network that are monotone, convex, and orthogonally invariant with respect to the Laplacian matrix of the network. It is shown that several existing gold-standard and widely used performance measures in the literature belong to this new class of measures. We build upon this new notion and investigate a general form of combinatorial problem of growing a linear consensus network via minimizing a given systemic performance measure. Two efficient polynomial-time approximation algorithms are devised to tackle this network synthesis problem: a linearization-based method and a simple greedy algorithm based on rank-one updates. Several theoretical fundamental limits on the best achievable performance for the combinatorial problem is derived that assist us to evaluate optimality gaps of our proposed algorithms. A detailed complexity analysis confirms the effectiveness and viability of our algorithms to handle large-scale consensus networks.

6.2 Introduction

The interest in control systems society for performance and robustness analysis of large-scale dynamical network is rapidly growing [2, 5, 9–11, 25, 35, 36, 136, 137]. Improving global performance as well as robustness to external disturbances in large-scale dynamical networks are crucial for sustainability, from engineering infrastructures to living cells; examples include a group of autonomous vehicles in a formation, distributed emergency response systems, interconnected transportation networks, energy and power networks, metabolic pathways and even financial networks. One of the fundamental problems in this area is to determine to what extent uncertain exogenous inputs can steer the trajectories of a dynamical network away from its working equilibrium point. To tackle this issue, the primary challenge is to introduce meaningful and viable performance and robustness measures that can capture essential characteristics of the network. A proper measure should be able to encapsulate transient, steady-state, macroscopic, and microscopic features of the perturbed large-scale dynamical network.

In this chapter, we propose a new methodology to classify proper performance measures for a class of linear consensus networks subject to external stochastic disturbances. We take an axiomatic approach to quantify essential functional properties of a sensible measure by introducing the class of systemic performance measures and show that this class of measures should satisfy monotonicity, convexity, and orthogonal invariance properties. It is shown that several existing and widely used performance measures in the literature are in fact special cases of this class of systemic measures [9, 11, 19, 38, 52].

The performance analysis of linear consensus networks subject to external stochastic disturbances has been studied in [2, 5, 8, 38, 50, 52], where the $\mathcal{H}_2$-norm of the network was employed as a scalar performance measure. In [2], the authors interpret the $\mathcal{H}_2$-norm of the system as a macroscopic performance measure capturing the notion of coherence.

It has been shown that if the Laplacian matrix of the coupling graph of the network is normal, the $\mathcal{H}_2$-norm is a function of the eigenvalues of the Laplacian matrix [2, 50, 52]. In [5], the authors consider general linear dynamical networks and show that tight lower, and upper bounds can be obtained for the $\mathcal{H}_2$-norm of the network from the exogenous disturbance input to a performance output, which are functions of the eigenvalues of the state matrix of the network. Besides the commonly used $\mathcal{H}_2$-norm, there are several other performance measures that have been proposed in [2, 9, 114].

The first main contribution of this chapter is introduction of a class of systemic performance measures that are spectral functions of Laplacian eigenvalues of the coupling graph of a linear consensus network. Several gold-standard and widely used performance measures belong to this class, for example, to name only a few, spectral zeta function, Gamma entropy, expected transient output covariance, system Hankel norm, convergence rate to consensus state, logarithm of uncertainty volume of the output, Hardy-Schatten system norm or $\mathcal{H}_p$-norm, and many more. All these performance measures are monotone, convex, and orthogonally invariant. Our main goal is to investigate a canonical network synthesis problem: growing a linear consensus network by adding new interconnection links to the coupling graph of the network and minimizing a given systemic performance measure. In the context of graph theory, it is known that a simpler version of this combinatorial problem, when the cost function is the inverse of algebraic connectivity, is indeed NP-hard [53]. There have been some prior attempts to tackle this problem for some specific choices of cost functions (i.e., total effective resistance and the inverse of algebraic connectivity) based on semidefinite programing (SDP) relaxation methods [54, 55]. There is a similar version of this problem that is reported in [56], where the author studies convergence rate of circulant consensus networks by adding some long-range links. Moreover, a continuous (non-combinatorial) and relaxed version of our problem of in-

terest has some connections to the sparse consensus network design problem [6, 57, 58], where they consider ℓ_1-regularized $\mathcal{H}_2$-optimal control problems. There are some related works [23, 59], it is shown that some metrics based on controllability and observability Gramians are modular or submodular set functions, where they show their proposed simple greedy heuristic algorithms have guarantees suboptimality bounds.

In our second main contribution, we propose two efficient polynomial-time approximation algorithms to solve the above mentioned combinatorial network synthesis problem: a linearization-based method and a simple greedy algorithm based on rank-one updates. Our complexity analysis asserts that computational complexity of our proposed algorithms are reasonable and make them particularly suitable for synthesis of large-scale consensus networks. To calculate sub-optimality gaps of our proposed approximation algorithms, we quantify the best achievable performance bounds for the network synthesis problem in Section 6.7. Our obtained fundamental limits are exceptionally useful as they only depend on the spectrum of the original network and they can be computed a priori. In Subsection 6.9.2, we classify a subclass of differentiable systemic performance measures that are indeed supermodular. For this subclass, we show that our proposed simple greedy algorithm can achieve a $(1 - 1/e)$-approximation of the optimal solution of the combinatorial network synthesis problem. Our extensive simulation results confirm effectiveness of our proposed methods.

6.3 Preliminaries and Definitions

6.3.1 Mathematical Background

The set of real numbers is denoted by $\mathbb{R}$, the set of non–negative by $\mathbb{R}_+$, and the set of positive real numbers by $\mathbb{R}_{++}$. The cardinality of set $\mathcal{E}$ is shown by $|\mathcal{E}|$. We assume that

$\mathbb{1}_n$, I_n, and J_n denote the $n \times 1$ vector of all ones, the $n \times n$ identity matrix, and the $n \times n$ matrix of all ones, respectively. For a vector $v = [v_i] \in \mathbb{R}^n$, $\mathrm{diag}(v) \in \mathbb{R}^{n \times n}$ is the diagonal matrix with elements of v orderly sitting on its diameter, and for $A = [a_{ij}] \in \mathbb{R}^{n \times n}$, $\mathrm{diag}(A) \in \mathbb{R}^n$ is diagonal elements of square matrix A. We denote the generalized matrix inequality with respect to the positive semidefinite cone $\mathbb{S}^n_+$ by " $\preceq$ " .

Throughout this chapter, it is assumed that all graphs are finite, simple, undirected, and connected. A graph herein is defined by a triple $\mathcal{G} = (\mathcal{V}, \mathcal{E}, w)$, where $\mathcal{V}$ is the set of nodes, $\mathcal{E} \subseteq \big\{\{i,j\} \;\big|\; i,j \in \mathcal{V},\ i \neq j\big\}$ is the set of links, and $w : \mathcal{E} \to \mathbb{R}_{++}$ is the weight function. The adjacency matrix $A = [a_{ij}]$ of graph $\mathcal{G}$ is defined in such a way that $a_{ij} = w(e)$ if $e = \{i,j\} \in \mathcal{E}$, and $a_{ij} = 0$ otherwise. The Laplacian matrix of $\mathcal{G}$ is defined by $L := \Delta - A$, where $\Delta = \mathrm{diag}[d_1, \ldots, d_n]$ and d_i is degree of node i. We denote the set of Laplacian matrices of all connected weighted graphs with n nodes by $\mathfrak{L}_n$. Since $\mathcal{G}$ is both undirected and connected, the Laplacian matrix L has $n-1$ strictly positive eigenvalues and one zero eigenvalue. Assuming that $0 = \lambda_1 < \lambda_2 \leq \ldots \leq \lambda_n$ are eigenvalues of Laplacian matrix L, we define operator $\Lambda : \mathbb{S}^n_+ \to \mathbb{R}^{n-1}_{++}$ by

$$\Lambda(L) \;=\; \begin{bmatrix} \lambda_2 & \ldots & \lambda_n \end{bmatrix}^{\mathrm{T}}. \tag{6.1}$$

The Moore-Penrose pseudo-inverse of L is denoted by $L^\dagger = [l^\dagger_{ji}]$, which is a square, symmetric, doubly-centered and positive semi–definite matrix. For a given link $e = \{i,j\}$, $r_e(L)$ denotes the effective resistance between nodes i and j in a graph with the Laplacian matrix L, where its value can be calculated as follows

$$r_e(L) \;=\; l^\dagger_{ii} + l^\dagger_{jj} - 2l^\dagger_{ij}, \tag{6.2}$$

where $L^\dagger = [l^\dagger_{ji}]$. For every real q, powers of pseudo inverse of L is represented by $L^{\dagger,q} := \left(L^\dagger\right)^q$.

Definition 6.3.1. *The derivative of a scalar function $\rho(.)$, with respect to the n-by-n matrix X, is defined by*

$$\nabla\rho(X) := \begin{bmatrix} \frac{\partial\rho}{\partial x_{11}} & \frac{\partial\rho}{\partial x_{12}} & \cdots & \frac{\partial\rho}{\partial x_{1n}} \\ \frac{\partial\rho}{\partial x_{21}} & \frac{\partial\rho}{\partial x_{22}} & \cdots & \frac{\partial\rho}{\partial x_{2n}} \\ \vdots & \vdots & \ddots & \vdots \\ \frac{\partial\rho}{\partial x_{n1}} & \frac{\partial\rho}{\partial x_{n2}} & \cdots & \frac{\partial\rho}{\partial x_{nn}} \end{bmatrix},$$

where $X = [x_{ij}]$. The directional derivative of function $\rho(X)$ in the direction of matrix Y is given by

$$\nabla_Y\rho(X) = \left\langle \nabla\rho(X), Y \right\rangle = \mathbf{Tr}\left(\nabla\rho(X)Y\right),$$

where $\langle ., . \rangle$ denotes the inner product operator.

The following Majorization definition is from [66].

Definition 6.3.2. *For every $x \in \mathbb{R}^n_+$, let us define $x^\downarrow$ to be a vector whose elements are a permuted version of elements of x in descending order. We say that x majorizes y, which is denoted by $x \trianglerighteq y$, if and only if $\mathbf{1}^T x = \mathbf{1}^T y$ and $\sum_{i=1}^k x_i^\downarrow \geq \sum_{i=1}^k y_i^\downarrow$ for all $k = 1, \ldots, n-1$.*

The vector majorization is not a partial ordering. This is because from relations $x \trianglerighteq y$ and $y \trianglerighteq x$ one can only conclude that the entries of these two vectors are equal, but possibly with different orders. Therefore, relations $x \trianglerighteq y$ and $y \trianglerighteq x$ do not imply $x = y$.

Definition 6.3.3 ([66])**.** *The real-valued function $F : \mathbb{R}^n_+ \to \mathbb{R}$ is called Schur–convex if $F(x) \geq F(y)$ for every two vectors x and y with property $x \trianglerighteq y$.*

6.3.2 Noisy linear consensus networks

We consider the class of linear dynamical networks that consist of multiple agents with scalar state variables x_i and control inputs u_i whose dynamics evolve in time according to

$$\dot{x}_i(t) = u_i(t) + \xi_i(t) \tag{6.3}$$

$$y_i(t) = x_i(t) - \bar{x}(t) \tag{6.4}$$

for all $i = 1, \ldots, n$, where $x_i(0) = 0$ is the initial condition and

$$\bar{x}(t) = \frac{1}{n}\big(x_1(t) + \ldots + x_n(t)\big)$$

is the average of all states at time instant t. The impact of the uncertain environment on each agent's dynamics is modeled by the exogenous noise input $\xi_i(t)$. By applying the following feedback control law to the agents of this network

$$u_i(t) = \sum_{j=1}^{n} k_{ij}\big(x_j(t) - x_i(t)\big), \tag{6.5}$$

the resulting closed-loop system will be a first-order linear consensus network. The closed-loop dynamics of network (6.3)-(6.4) with feedback control law (6.5) can be written in the following compact form

$$\dot{x}(t) = -L\,x(t) + \xi(t) \tag{6.6}$$

$$y(t) = M_n\,x(t), \tag{6.7}$$

with initial condition $x(0) = 0$, where $x = [x_1, \ldots, x_n]^{\mathrm{T}}$ is the state, $y = [y_1, \ldots, y_n]^{\mathrm{T}}$ is the output, and $\xi = [\xi_1, \ldots, \xi_n]^{\mathrm{T}}$ is the exogenous noise input of the network. The state matrix of the network is a graph Laplacian matrix that is defined by $L = [l_{ij}]$, where

$$l_{ij} := \begin{cases} -k_{ij} & \text{if} \quad i \neq j \\ \\ k_{i1} + \ldots + k_{in} & \text{if} \quad i = j \end{cases} \tag{6.8}$$

and the output matrix is a centering matrix that is defined by

$$M_n \ := \ I_n - \frac{1}{n} J_n. \tag{6.9}$$

The underlying coupling graph of the consensus network (6.6)-(6.7) is a graph $\mathcal{G} = (\mathcal{V}, \mathcal{E}, w)$ with node set $\mathcal{V} = \{1, \ldots, n\}$, edge set

$$\mathcal{E} = \Big\{ \{i, j\} \ \Big| \ \forall \, i, j \in \mathcal{V}, \ k_{ij} \neq 0 \Big\}, \tag{6.10}$$

and weight function

$$w(e) = k_{ij} \tag{6.11}$$

for all $e = \{i, j\} \in \mathcal{E}$, and $w(e) = 0$ if $e \notin \mathcal{E}$. The Laplacian matrix of graph $\mathcal{G}$ is equal to L.

Assumption 6.3.4. *All feedback gains (weights) satisfy the following properties for all* $i, j \in \mathcal{V}$*:*

(a) non-negativity: $k_{ij} \geq 0$,

(b) symmetry: $k_{ij} = k_{ji}$,

(c) simpleness: $k_{ii} = 0$.

Property (b) implies that feedback gains are symmetric and (c) means that there is no self-feedback loop in the network.

Assumption 6.3.5. *The coupling graph $\mathcal{G}$ of the consensus network* (6.6)-(6.7) *is connected and time-invariant.*

According to Assumption 6.3.4, the underlying coupling graph is undirected and simple. Assumption 6.3.5 implies that only one of the modes of network (6.6) is marginally stable with eigenvector $\mathbb{1}_n$ and all other ones are stable. The marginally stable mode, which corresponds to the only zero Laplacian eigenvalue of L, is unobservable from the output (6.7). The reason is that the output matrix of the network satisfies $M_n\mathbb{1}_n = 0$. When there is no exogenous noise input, i.e., $\xi(t) \equiv 0$ for all time, the state of all agents converges to the consensus state of the network [114, 138], which for our case the consensus state is zero, i.e.,

$$\lim_{t\to\infty} x(t) = 0. \tag{6.12}$$

When the network is fed with a nonzero exogenous noise input, the limit behavior (6.12) is not expected anymore and the state of all agents will be fluctuating around the consensus state without converging to it. Before providing a formal statement of the problem of growing a linear consensus network, we need to introduce a new class of performance measures for networks (6.6)-(6.7) that can capture the effect of noise propagation throughout the network and quantify degrees to which the state of all agents are dispersed from the consensus state.

6.4 Systemic Performance Measures

The notion of systemic performance measure refers to a real-valued operator over the set of all linear consensus networks governed by (6.6)-(6.7) with the purpose of quantify-

ing the quality of noise propagation in these networks. We have adopted an axiomatic approach to introduce and categorize a class of performance measures that captures the quintessence of a meaningful measure of performance in networks. Our approach has been mainly motivated by our examination of functional properties of several existing gold standard measures of performance in engineering and science literature. In order to state our findings in a formal setting, we observe that every network with dynamics (6.6)-(6.7) is uniquely determined by its Laplacian matrix. Therefore, it is reasonable to define a systemic performance measure as an operator on the set of Laplacian matrices $\mathfrak{L}_n$.

Definition 6.4.1. *An operator $\rho : \mathfrak{L}_n \to \mathbb{R}$ is called a systemic performance measure if it satisfies the following properties for all Laplacian matrices in $\mathfrak{L}_n$:*
1. Monotonicity: If $L_2 \preceq L_1$, then

$$\rho(L_1) \ \leq \ \rho(L_2);$$

2. Convexity: For all $0 \leq \alpha \leq 1$,

$$\rho(\alpha L_1 + (1-\alpha)L_2) \ \leq \ \alpha\rho(L_1) + (1-\alpha)\rho(L_2);$$

3. Orthogonal invariance: For all orthogonal matrices $U \in \mathbb{R}^{n\times n}$,

$$\rho(L) \ = \ \rho(ULU^T).$$

Property 1 guarantees that strengthening couplings in a consensus network never worsens the network performance with respect to a given systemic performance measure. The coupling strength among the agents can be enhanced by several means, for

example, by adding new feedback interconnections and/or increasing weight of an individual feedback interconnection. The monotonicity property induces a partial ordering[1] on all linear consensus networks governed by (6.6)-(6.7). Property 2 requires that a viable performance measure should be amenable to convex optimization algorithms for network synthesis purposes. Property 3 implies that a systemic performance measure depends only on the Laplacian eigenvalues.

Theorem 6.4.2. *Every operator $\rho : \mathfrak{L}_n \to \mathbb{R}$ that satisfies Properties 2 and 3 in Definition 6.4.1 is indeed a Schur-convex function of Laplacian eigenvalues, i.e., there exists a Schur-convex spectral function $\Phi : \mathbb{R}^{n-1} \to \mathbb{R}$ such that*

$$\rho(L) \;=\; \Phi(\lambda_2, \ldots, \lambda_n). \tag{6.13}$$

Proof. For every $L \in \mathfrak{L}_n$, the value of the systemic performance measure can be written as a composition of two functions as follows

$$\rho(L) \;=\; (\phi \circ \Lambda)(L), \tag{6.14}$$

where function $\Lambda : \mathbb{S}^n_+ \to \mathbb{R}^{n-1}_{++}$ is defined by (6.1) and function $\phi : \mathbb{R}^{n-1}_{++} \to \mathbb{R}$ is characterized by

$$\phi(v) \;=\; \rho(W^{\mathrm{T}}\mathrm{diag}(v)W), \tag{6.15}$$

for any matrix $W = EU$ with $U \in \mathbb{R}^{n\times n}$ being an orthogonal matrix satisfying

$$L \;=\; U^{\mathrm{T}}\mathrm{diag}([0, \Lambda(L)^{\mathrm{T}}])U$$

[1]This implies that the family of networks (6.6)-(6.7) can be ordered using a relation that has reflexivity, antisymmetry, and transitivity properties.

Systemic Performance Measure	Matrix Operator Form
Spectral zeta function $\zeta_q(L)$	$\big(\mathrm{Tr}\big(L^{\dagger,q}\big)\big)^{\frac{1}{q}}$
Gamma entropy $I_\gamma(L)$	$\gamma^2 \mathrm{Tr}\Big(L - \big(L^2 - \gamma^{-2} M_n\big)^{\frac{1}{2}}\Big)$
Expected transient output covariance $\tau_t(L)$	$\frac{1}{2}\mathrm{Tr}\big(L^\dagger (I - e^{-Lt})\big)$
System Hankel norm $\eta(L)$	$\frac{1}{2}\max\big\{\mathrm{Tr}(L^\dagger X) \;\big|\; X = X^{\mathrm{T}},\ \mathrm{rank}(X) = 1,\ \mathrm{Tr}(X) = 1\big\}$
Uncertainty volume of the output $\upsilon(L)$	$(1-n)\log 2 - \mathrm{Tr}\left(\log\left(L + \frac{1}{n} J_n\right)\right)$
Hardy-Schatten system norm or $\mathcal{H}_p$-norm $\theta_p(L)$	$\alpha_0 \left(\mathbf{Tr}\left(L^{\dagger,p-1}\right)\right)^{\frac{1}{p}}$

Table 6.1: Some important examples of spectral systemic performance measures and their corresponding matrix operator forms.

and $E \in \mathbb{R}^{(n-1)\times n}$ given by the following projection matrix

$$E \;=\; \left[\; 0_{(n-1)\times 1} \;\;\big|\;\; I_{n-1} \;\right]. \tag{6.16}$$

Thus, we can conclude that (6.13) holds with $\Phi(\lambda_2, \ldots, \lambda_n) = \phi(\Lambda(L))$. In the next step, we need to show that operator ρ is convex and symmetric with respect to Laplacian eigenvalues $\lambda_2, \ldots, \lambda_n$. Property 2 indicates that ρ is convex on Laplacian matrices and any convex function on Laplacian matrices is also convex function with respect to Laplacian eigenvalues [139]. Property 3 implies that operator ρ is symmetric with respect to $\lambda_2, \ldots, \lambda_n$ as ρ is invariant under any permutation of eigenvalues. It is known that every function that is convex and symmetric is also Schur-convex [139]. □

The Laplacian eigenvalues of network (6.6)-(6.7) depend on global features of the underlying coupling graph. This is the reason why every performance measure that satisfies Definition 6.4.1 is tagged with adjective *systemic*. Table 6.1 shows some important ex-

amples of systemic performance measure and their corresponding matrix operator forms. In Section 6.6, we prove functional properties and discuss applications of these measures in details.

6.5 Growing a Linear Consensus Network

The network synthesis problem of interest is to improve the systemic performance of network (6.6)-(6.7) by establishing $k \geq 1$ new feedback interconnections among the agents. Suppose that the underlying graph of the network $\mathcal{G} = (\mathcal{V}, \mathcal{E}, w)$ is defined according to (6.10)-(6.11) and a set of candidate feedback interconnection links $\mathcal{E}_c = \{\varepsilon_1, \ldots, \varepsilon_p\} \subseteq \mathcal{V} \times \mathcal{V}$, which is endowed with a weight function $\varpi : \mathcal{E}_c \to \mathbb{R}_{++}$, is also given. The weight of a link $\varepsilon_i \in \mathcal{E}_c$ is represented by $\varpi(\varepsilon_i)$ and we assume that it is pre-specified and fixed. The network growing problem is to select exactly k feedback interconnection links from $\mathcal{E}_c$ and append them to $\mathcal{G}$ such that the systemic performance measure of the resulting network is minimized over all possible choices.

Let us represent the set of all possible appended subgraphs by

$$\hat{\mathfrak{G}}_k := \Big\{ \hat{\mathcal{G}} = (\mathcal{V}, \hat{\mathcal{E}}, \hat{w}) \,\Big|\, \hat{\mathcal{E}} \in \Pi_k(\mathcal{E}_c),\ \forall \varepsilon_i \in \hat{\mathcal{E}} :\ \hat{w}(\varepsilon_i) = \varpi(\varepsilon_i) \Big\},$$

where the set of all possible choices to select k links is denoted by

$$\Pi_k(\mathcal{E}_c) := \big\{ \hat{\mathcal{E}} \subseteq \mathcal{E}_c \,\big|\, |\hat{\mathcal{E}}| = k \big\}.$$

Then, the network synthesis problem can be cast as the following combinatorial optimization problem

$$\underset{\hat{\mathcal{G}} \in \hat{\mathfrak{G}}_k}{\text{minimize}} \quad \rho(L + \hat{L}), \tag{6.17}$$

where $\hat{L}$ is the Laplacian matrix of an appended candidate subgraph $\hat{\mathcal{G}}$ and the resulting network with Laplacian matrix $L + \hat{L}$ is referred to as the augmented network. The role of the candidate set $\mathcal{E}_c$ is to pre-specify authorized locations to establish new feedback interconnections in the network.

The network synthesis problem (6.17) is inherently combinatorial and it is known that a simpler version of this problem with $\rho(L) = \lambda_2^{-1}$ is in fact NP-hard [53]. There have been some prior attempts to tackle problem (6.17) for some specific choices of performance measures, such as total effective resistance and the inverse of algebraic connectivity, based on convex relaxation methods [54, 55] and greedy methods [59]. In Sections 6.8 and 6.9, we propose approximation algorithms to compute sub-optimal solutions for (6.17) with respect to the broad class of systemic performance measures. We propose an exact solution for (6.17) when $k = 1$ and two tractable and efficient approximation methods when $k > 1$ with computable performance bounds. Besides, in Section 6.9, we demonstrate that a subclass of systemic performance measures has a supermodularity property. This provides approximation guarantees for our proposed approximation algorithm.

6.6 Notable Classes of Systemic Performance Measures

In the following, we will revisit several existing and widely-used examples of performance measures in linear consensus networks and prove that they are indeed systemic performance measures according to the definition.

6.6.1 Sum of Convex Spectral Functions

This class of performance measures is generated by forming summation of a given function of non-zero Laplacian eigenvalues.

Theorem 6.6.1. *For a given matrix $L \in \mathfrak{L}_n$, suppose that $\varphi : \mathbb{R}_+ \to \mathbb{R}$ is a decreasing convex function. Then, the following spectral function*

$$\rho(L) \;=\; \sum_{i=2}^{n} \varphi(\lambda_i) \tag{6.18}$$

is a systemic performance measure. Moreover, if φ is also a homogeneous function of order $-\kappa$ with $\kappa > 1$, then the following spectral function

$$\rho(L) \;=\; \left(\sum_{i=2}^{n} \varphi(\lambda_i) \right)^{\frac{1}{\kappa}} \tag{6.19}$$

is also a systemic performance measure.

Proof. First we show that measure (6.18) is monotone with respect to the positive definite cone. If we assume that $L_2 \preceq L_1$, then based on Theorem A.1 in [66, Sec. 20], it follows that

$$\lambda_i(L_2) \;\leq\; \lambda_i(L_1), \;\; \text{for} \;\; i = 1, 2, \cdots, n. \tag{6.20}$$

Thus, using (6.20) and the fact that $\varphi(.)$ is decreasing, we get the monotonicity property of measure (6.18). Also, it is not difficult to show that measure (6.18) satisfies Property 2. To do so, let L_1 and L_2 be two Laplacian matrices in $\mathfrak{L}_n$. Recall that $\Lambda(L_i)$, $i = 1, 2$ is the vector of eigenvalues of L_i in ascending order. According to Theorem G.1 in [66, Sec. 9], we know that

$$\Lambda(\alpha L_1 + (1-\alpha)L_2) \;\trianglelefteq\; \alpha\Lambda(L_1) + (1-\alpha)\Lambda(L_2), \tag{6.21}$$

for every $0 \leq \alpha \leq 1$, and $\trianglelefteq$ denotes the majorization preorder [66]. Besides, we note that based on Proposition. C.1 in [66, Sec.3], measure (6.18) is a Schur-convex function. Consequently, using this property and (6.21), we have

$$\begin{aligned}\rho(\alpha L_1 + (1-\alpha)L_2) \;&=\; \sum_{i=2}^{n} \varphi\left(\lambda_i(\alpha L_1 + (1-\alpha)L_2)\right) \\ &\leq\; \sum_{i=2}^{n} \varphi\big(\alpha\lambda_i(L_1) + (1-\alpha)\lambda_i(L_2)\big). \end{aligned} \tag{6.22}$$

From (6.22) and the desired convexity property of $\varphi(.)$, we get the convexity property as follows

$$\begin{aligned}\rho(\alpha L_1 + (1-\alpha)L_2) \;&\leq\; \sum_{i=2}^{n} \varphi\left(\alpha\lambda_i(L_1) + (1-\alpha)\lambda_i(L_2)\right) \\ &\leq\; \alpha \sum_{i=2}^{n} \varphi\left(\lambda_i(L_1)\right) + (1-\alpha) \sum_{i=2}^{n} \varphi\left(\lambda_i(L_2)\right) \\ &=\; \alpha\rho(L_1) + (1-\alpha)\rho(L_2),\end{aligned}$$

for every $0 \leq \alpha \leq 1$. Finally, systemic measure (6.18) is orthogonal invariant because it is a spectral function. Hence, measure (6.18) satisfies all properties of Definition 6.4.1. This completes the proof of first part.

Next, we show that measure (6.19) satisfies Properties 1, 2, and 3 given by Definition 6.4.1. Similar to the previous case, it is straightforward to verify that measure (6.19) has Property 1. Now we show that measure (6.19) has Property 2, i.e., it is a convex function over the set of Laplacian matrices. By hypothesis, $\varphi(.)$ is a homogeneous function of order $-\kappa$, therefore, we have

$$\varphi(\lambda_i) = \lambda_i^{-\kappa}\varphi(1). \tag{6.23}$$

Using (6.23) and (6.19), we get

$$\rho(L) = K\left(\sum_{i=2}^{n} \lambda_i^{-\kappa}\right)^{\frac{1}{\kappa}}, \tag{6.24}$$

where $K = \sqrt[\kappa]{\varphi(1)}$. It is well-known function (6.24) is convex for $\lambda_i > 0$ where $i = 2, \ldots, n$ and $\kappa > 1$. Based on the proof of Part (i), measure $\rho^{\kappa}(.)$ is a Schur-convex function. Consequently, we get

$$\begin{aligned} &\rho(\alpha L_1 + (1-\alpha)L_2) \leq \\ &\qquad K\left(\sum_{i=2}^{n} \big(\alpha\lambda_i(L_1) + (1-\alpha)\lambda_i(L_2)\big)^{-\kappa}\right)^{\frac{1}{\kappa}}. \end{aligned} \tag{6.25}$$

Now using (6.26) and the convexity of (6.24) with respect to λ_i's, we have

$$\begin{aligned} &\rho(\alpha L_1 + (1-\alpha)L_2) \\ &\qquad \leq\ K\left(\sum_{i=2}^{n} \big(\alpha\lambda_i(L_1) + (1-\alpha)\lambda_i(L_2)\big)^{-\kappa}\right)^{\frac{1}{\kappa}} \\ &\qquad \leq\ \alpha\rho(L_1) + (1-\alpha)\rho(L_2). \end{aligned}$$

This completes the proof. □

There are several important examples of performance measures that belong to this class.

Spectral Zeta Functions

For a given network (6.6)-(6.7), its corresponding spectral zeta function of order $q \geq 1$ is defined by

$$\zeta_q(L) := \left(\sum_{i=2}^{n} \lambda_i^{-q} \right)^{1/q}, \tag{6.26}$$

where $\lambda_2, \ldots, \lambda_n$ are eigenvalues of L [140]. According to Assumption 6.3.5, all the Laplacian eigenvalues $\lambda_2, \ldots, \lambda_n$ are strictly positive and, as a result, function (6.26) is well-defined. The spectral zeta function of a graph captures all its spectral features. In fact, it is straightforward to show that every two graphs in $\mathfrak{L}_n$ with identical zeta functions for all parameters $q \geq 1$ are isospectral [2].

Since $\varphi(\lambda) = \lambda^{-q}$ for $q \geq 1$ is a decreasing convex function, the spectral function (6.26) is a systemic performance measure according to Theorem 6.6.1. The systemic performance measure $\frac{1}{2}\zeta_1(L)$ is equal to the $\mathcal{H}_2$-norm squared of a first-order consensus network (6.6)-(6.7) and $\frac{1}{\sqrt{2}}\zeta_2(L)$ equal to the $\mathcal{H}_2$-norm of a second-order consensus model of a network of multiple agents (c.f. [5]).

Gamma Entropy

The notion of gamma entropy arises in various applications such as the design of minimum entropy controllers and interior point polynomial-time methods in convex programming with matrix norm constraints [142]. As it is shown in [143], the notion of gamma entropy can be interpreted as a performance measure for linear time-invariant systems with random feedback controllers by relating the gamma entropy to the mean-square value of the closed-loop gain of the system.

[2] This is because for a given graph with n nodes, Laplacian eigenvalues $\lambda_2, \ldots, \lambda_n$ can be uniquely determined by using equation (6.26) and having the value of $\zeta_q(L)$ for $n-1$ distinct values of q. We refer to algebraic geometric tools for existing algorithms to solve this problem [141].

Definition 6.6.2. *The γ-entropy of network* (6.6)-(6.7) *is defined as*

$$I_\gamma(L) := \begin{cases} \frac{-\gamma^2}{2\pi}\int_{-\infty}^{\infty} \log\det\left(I-\gamma^{-2}G(j\omega)G^*(j\omega)\right)d\omega & \text{for } \gamma \geq \|G\|_{\mathcal{H}_\infty} \\ \\ \infty & \text{otherwise} \end{cases}$$

where $G(j\omega)$ is the transfer function of network (6.6)-(6.7) *from ξ to y.*

Theorem 6.6.3. *For a given linear consensus network* (6.6)-(6.7)*, the value of the γ-entropy can be explicitly computed in terms of network's Laplacian eigenvalues as follows*

$$I_\gamma(L) = \begin{cases} \sum_{i=2}^{n} f_\gamma(\lambda_i) & \gamma \geq \lambda_2^{-1} \\ \\ \infty & \text{otherwise} \end{cases} \tag{6.27}$$

where $f_\gamma(\lambda_i) = -\gamma^2\left((\lambda_i^2-\gamma^{-2})^{\frac{1}{2}}-\lambda_i\right)$. Moreover, the γ-entropy $I_\gamma(L)$ is a systemic performance measure.

Proof. First we obtain the transfer function of network (6.6)-(6.7) from ξ to y. In order to do that, let us rewrite the network in its disagreement form (6.37)-(6.38). Then, it follows that

$$\begin{aligned} G(s) &= M_n\left(sI_n + L + \frac{1}{n}J_n\right)^{-1} M_n \\ &= M_n U \,\mathrm{diag}\left[\frac{1}{s+1}, \frac{1}{s+\lambda_2}, \cdots, \frac{1}{s+\lambda_n}\right] U^{\mathrm{T}} M_n \\ &= U \,\mathrm{diag}\left[0, \frac{1}{s+\lambda_2}, \cdots, \frac{1}{s+\lambda_n}\right] U^{\mathrm{T}}, \end{aligned} \tag{6.28}$$

where U is the corresponding orthonormal matrix of eigenvectors of L. Now, we calculate the γ-entropy by substituting the transfer function (6.28) in (6.27) as follows

$$\begin{aligned} I_\gamma(G) &= \frac{-\gamma^2}{2\pi}\int_{-\infty}^{\infty} \log\det\left(I_n - \gamma^{-2}G(j\omega)G^*(j\omega)\right) d\omega \\ &= \frac{-\gamma^2}{2\pi}\int_{-\infty}^{\infty} \log\det\left(I_n - \gamma^{-2}G(j\omega)G^*(j\omega)\right) d\omega. \end{aligned}$$

Then, using the fact that $UU^{\mathrm{T}} = I_n$ and (6.28), one can write:

$$\log\det\left(I_n - \gamma^2 G(j\omega)G^*(j\omega)\right) = \log\prod_{i=2}^{n}\left(1 - \frac{\gamma^{-2}}{\lambda_i^2+\omega^2}\right). \tag{6.29}$$

Moreover, we know that

$$\int_{-\infty}^{\infty}\log\left(1 - \frac{\gamma^{-2}}{\lambda_i^2+\omega^2}\right) d\omega = -\gamma^2\left(\left(\lambda_i^2 - \gamma^{-2}\right)^{\frac{1}{2}} - \lambda_i\right), \tag{6.30}$$

for $\gamma \geq \lambda_i^{-1}$. Therefore, based on this result, (6.27) and (6.30), it follows that

$$\begin{aligned} \sum_{i=2}^{n}\int_{-\infty}^{\infty}\log\det\left(1 - \frac{\gamma^{-2}}{\lambda_i^2+\omega^2}\right) d\omega = \\ \sum_{i=2}^{n}\gamma^2\left(\sqrt{\lambda_i^2 - \gamma^{-2}} - \lambda_i\right), \end{aligned} \tag{6.31}$$

for $\gamma \geq \lambda_2^{-1}$. Note that $f_\gamma(.)$ is a convex decreasing function in $[\gamma^{-1}, \infty)$, therefore, according to Theorem 6.6.1 and (6.31), the γ-entropy $I_\gamma(L)$ is a systemic performance measure. □

The following result presents the connection between the γ-entropy measure and the $\mathcal{H}_2$-norm of the network.

Theorem 6.6.4. *The following equality holds for the γ-entropy measure of network* (6.6)-

(6.7)

$$\lim_{\gamma\to\infty} I_\gamma(L) \;=\; \frac{1}{2}\sum_{i=2}^{n}\lambda_i^{-1} \;=\; \|G\|_{\mathcal{H}_2}^2 \;=\; \lim_{t\to\infty}\mathbb{E}\big\{y^T(t)y(t)\big\},$$

where $G(.)$ is the transfer function of network (6.6)-(6.7)*.*

Proof. We utilize the following limit equation

$$\lim_{\gamma\to\infty}\gamma^2\left(\sqrt{x^2-\gamma^{-2}}-x\right)=x^{-1},$$

for all $x>0$ to prove that $\lim_{\gamma\to\infty} I_\gamma(L)=\frac{1}{2}\sum_{i=2}^{n}\lambda_i^{-1}$. Finally, we use [12, Theorem 1] to show that $\frac{1}{2}\sum_{i=2}^{n}\lambda_i^{-1}=\|G\|_{\mathcal{H}_2}^2=\lim_{t\to\infty}\mathbb{E}\big\{y^{\mathrm{T}}(t)y(t)\big\}$. □

Expected Transient Output Covariance

We consider a transient performance measure at time instant $t>0$ that is defined by

$$\tau_t(L):=\mathbb{E}\big\{y^{\mathrm{T}}(t)y(t)\big\}, \tag{6.32}$$

where it is assumed that each $\xi_i(t)$ for all $t\geq 0$ is a white Gaussian noise with zero mean and unit variance and all ξ_i's are independent of each other.

In the following, we show that this performance measure is a spectral function of Laplacian eigenvalues.

Theorem 6.6.5. *For a given linear consensus network* (6.6)-(6.7)*, the transient measure can be expressed as*

$$\tau_t(L) \;=\; \sum_{i=2}^{n}\frac{1-e^{-\lambda_i t}}{2\lambda_i}. \tag{6.33}$$

Moreover, $\tau_t(L)$ is a systemic performance measure for all $t>0$.

Proof. The covariance matrix of the output vector is governed by the following matrix differential equation

$$\dot{Y}(t) \;=\; -L\,Y(t) - Y(t)\,L + M_n, \tag{6.34}$$

where $Y(t) = \mathrm{cov}(y(t), y(t))$. Using the closed-form solution of (6.34), which is given by

$$Y(t) \;=\; \int_0^t e^{-L\tau} M_n e^{-L\tau} d\tau, \tag{6.35}$$

we get

$$\begin{aligned} \mathbb{E}\big\{y^{\mathrm{T}}(t)y(t)\big\} \;&=\; \mathbf{Tr}(Y(t)) = \mathbf{Tr}\left(\int_0^t e^{-L\tau} M_n e^{-L\tau} d\tau\right) \\ &=\; \sum_{i=2}^{n} \int_0^t e^{-2\lambda_i \tau} d\tau = \sum_{i=2}^{n} \frac{1 - e^{-\lambda_i t}}{2\lambda_i}. \end{aligned} \tag{6.36}$$

Since $f(x) = \frac{1-e^{-xt}}{2x}$ is convex and decreasing with respect to x on $\mathbb{R}_+$, we can conclude that $\tau_t(L)$ is a systemic performance measure according to Theorem 6.6.1. □

We note that when t tends to infinity, the value of the transient performance measure becomes equal to the $\mathcal{H}_2$-norm squared of the network, i.e., $\tau_\infty(L) = \|G\|^2_{\mathcal{H}_2}$.

Hankel Norm

The Hankel norm of a network with (6.6)-(6.7) and transfer function $G(j\omega)$ from ξ to y is defined as the $\mathcal{L}_2$-gain from past inputs to the future outputs, *i.e.*

$$\|G\|^2_H \;:=\; \sup_{\xi \in L_2(-\infty,0]} \frac{\int_0^\infty y^{\mathrm{T}}(t)y(t)dt}{\int_{-\infty}^0 \xi^{\mathrm{T}}(t)\xi(t)dt}.$$

The value of the Hankel norm of network (6.6)-(6.7) can be equivalently computed using the Hankel norm of its disagreement form [20] that is given by

$$\dot{x}_d(t) \;=\; -L_d\, x_d(t) + M_n\, \xi(t), \tag{6.37}$$

$$y(t) \;=\; M_n\, x_d(t), \tag{6.38}$$

where the disagreement vector is defined by

$$x_d(t) \;:=\; M_n\, x(t) \;=\; x(t) - \frac{1}{n} J_n\, x(t). \tag{6.39}$$

The disagreement network (6.37)-(6.38) is stable as every eigenvalue of the state matrix $-L_d \,=\, -(L + \frac{1}{n}J_n)$ has a strictly negative real part. One can verify that the transfer functions from $\xi(t)$ to $y(t)$ in both realizations are identical. Therefore, the Hankel norm of the system from $\xi(t)$ to $y(t)$ in both representations are well-defined and equal, and is given by [144]

$$\eta(L) := \|G\|_H = \sqrt{\lambda_{\max}(PQ)}, \tag{6.40}$$

where the controllability Gramian P is the unique solution of

$$\Big(L + \frac{1}{n}J_n\Big)P + P\Big(L + \frac{1}{n}J_n\Big) - M_n = 0$$

and the observability Gramian Q is the unique solution of

$$Q\Big(L + \frac{1}{n}J_n\Big) + \Big(L + \frac{1}{n}J_n\Big)Q - M_n = 0.$$

Theorem 6.6.6. *The value of the Hankel norm of consensus network* (6.6)-(6.7) *is equal*

to

$$\eta(L) \;=\; \frac{1}{2}\lambda_2^{-1}$$

and it is a systemic performance measure.

Proof. According to the definition (6.40), we get

$$\eta(L) \;=\; \sqrt{\lambda_{\max}(PQ)} \;=\; \sqrt{\lambda_{\max}\left((L^{\dagger})^2\right)} \;=\; \lambda_2^{-1}.$$

Moreover, based on Theorem 6.6.1, we know that the spectral zeta function $\zeta_q(L)$ is a systemic performance measure for all $1 \leq q \leq \infty$. Therefore by setting $q = \infty$, we have

$$\eta(L) = \frac{1}{2}\zeta_\infty(L) = \frac{1}{2}\lim_{q\to\infty}\zeta_q(L) \;=\; \frac{1}{2}\lambda_2^{-1}.$$

As a result, $\eta(L)$ is a systemic performance measure. □

Uncertainty volume

The uncertainty volume of the steady-state output covariance matrix of consensus network (6.6)-(6.7) is defined by

$$|\Sigma| := \det\Big(Y_\infty + \frac{1}{n}J_n\Big), \tag{6.41}$$

where

$$Y_\infty = \lim_{t\to\infty}\mathbb{E}\big\{y(t)y^{\mathrm{T}}(t)\big\}.$$

This quantity is widely used as an indicator of the network performance [19, 145]. Since $y(t)$ is the error vector that represents the distance from consensus, the quantity (6.41) is the volume of the steady-state error ellipsoid.

Theorem 6.6.7. *For a given consensus network* (6.6)-(6.7) *with Laplacian matrix L, the logarithm of the uncertainty volume, i.e.*

$$\upsilon(L) \ := \log|\Sigma| \ = (1-n)\log 2 - \sum_{i=2}^{n} \log \lambda_i \tag{6.42}$$

is a systemic performance measure.

Proof. According to the dynamics of the network (6.6)-(6.7), the time evolution of the mean and the covariance matrix of the state vector are governed by

$$\dot{\bar{y}}(t) \ = \ -\left(L + \frac{1}{n}J_n\right) y(t), \tag{6.43}$$

and

$$\dot{Y}(t) \ = \ -L\,Y(t) - Y(t)\,L + M_n, \tag{6.44}$$

where $\bar{y}(t) = \mathcal{E}(y(t))$ and $Y(t) = \mathrm{cov}(y(t), y(t))$. From (6.43), it follows that

$$\bar{y}(\infty) \ = \ \lim_{t\to\infty} \bar{y}(t) \ = \ 0. \tag{6.45}$$

Consequently, using (6.44) and (6.45) we get

$$Y_\infty \ = \ \lim_{t\to\infty} \mathrm{cov}(y(t), y(t)) \ = \ \frac{1}{2}L^\dagger.$$

Finally, by substituting Y_∞ in (6.41), we get

$$|\Sigma| = \det\left(Y_\infty + \frac{1}{n}J_n\right) = \det\left(\frac{1}{2}L^\dagger + \frac{1}{n}J_n\right) = 2^{-n+1}\prod_{i=2}^{n}\lambda_i^{-1}.$$

From this result and the definition of $\upsilon(L)$, one conclude that

$$\upsilon(L) \;=\; \log 2^{-n+1} \prod_{i=2}^{n} \lambda_i^{-1} \;=\; (n-1)\log 2 - \sum_{i=2}^{n} \log \lambda_i.$$

Because $-\log(.)$ is convex and decreasing in $\mathbb{R}_{++}$, the quantity

$$\upsilon(L) \;-\; (n-1)\log 2 \;=\; -\sum_{i=2}^{n} \log \lambda_i,$$

is a systemic performance measure according to Theorem 6.6.1. Note that $(n-1)\log 2$ is a constant number. Therefore, we conclude that υ is a systemic performance measure. □

6.6.2 Hardy-Schatten Norms of Linear Systems

The p-Hardy-Schatten norm of network (6.6)-(6.7) for $1 < p \leq \infty$ is defined by

$$\|G\|_{\mathcal{H}_p} \;:=\; \left\{ \frac{1}{2\pi} \int_{-\infty}^{\infty} \sum_{k=1}^{n} \sigma_k(G(j\omega))^p \, d\omega \right\}^{\frac{1}{p}}, \tag{6.46}$$

where $G(j\omega)$ is the transfer matrix of the network from ξ to y and $\sigma_k(j\omega)$ for $k = 1, \ldots, n$ are singular values of $G(j\omega)$. It is known that this class of system norms captures several important performance and robustness features of linear time-invariant systems. For example, a direct calculation shows [12] that the $\mathcal{H}_2$-norm of linear consensus network (6.6)-(6.7) can be expressed as

$$\|G\|_{\mathcal{H}_2} \;=\; \Big(\frac{1}{2} \sum_{i=2}^{n} \lambda_i^{-1} \Big)^{\frac{1}{2}}. \tag{6.47}$$

This norm has been also interpreted as a notion of coherence in linear consensus networks [2]. The $\mathcal{H}_\infty$-norm of network (6.6)-(6.7) is an input-output system norm [99] and its

value can be expressed as

$$\|G\|_{\mathcal{H}_\infty} \;=\; \lambda_2^{-1}, \tag{6.48}$$

where λ_2 is the second smallest eigenvalue of L, also known as the algebraic connectivity of the underlying graph of the network. The $\mathcal{H}_\infty$-norm (6.48) can be interpreted as the worst attainable performance against all square-integrable disturbance inputs [99].

Theorem 6.6.8. *The p-Hardy-Schatten norm of a given consensus network* (6.6)-(6.7) *is a systemic performance measure for every exponent $2 \leq p \leq \infty$. Furthermore, the following identity holds*

$$\|G\|_{\mathcal{H}_p} = \alpha_0 \big(\zeta_{p-1}(L)\big)^{1-\frac{1}{p}} \tag{6.49}$$

where $\alpha_0^{-1} = \sqrt[p]{-\beta(\frac{p}{2}, -\frac{1}{2})}$ and $\beta : \mathbb{R} \times \mathbb{R} \to \mathbb{R}$ is the well-known Beta function.

Proof. We utilize the disagreement form of the network that is given by (6.37)-(6.38) and the decomposition (6.28) to compute the $\mathcal{H}_q$-norm of $G(j\omega)$ as follows

$$\begin{aligned}
\|G\|_{\mathcal{H}_p}^p \;&=\; \frac{1}{2\pi} \int_{-\infty}^{\infty} \sum_{k=1}^{n} \sigma_k(G(j\omega))^p \, d\omega \\
&=\; \frac{1}{2\pi} \sum_{i=2}^{n} \int_{-\infty}^{\infty} \left(\frac{1}{\omega^2 + \lambda_i^2} \right)^{\frac{p}{2}} d\omega \\
&=\; \frac{-1}{\beta(\frac{p}{2}, -\frac{1}{2})} \sum_{i=2}^{n} \frac{1}{\lambda_i^{p-1}} \;=\; \frac{-1}{\beta(\frac{p}{2}, -\frac{1}{2})} \zeta_{p-1}(L)^{p-1},
\end{aligned}$$

for all $2 \leq p \leq \infty$. Now we show that measure (6.49) satisfies Properties 1, 2, and 3 in Definition 6.4.1. Similar to the proof of Theorem 6.6.1, it is straightforward to verify that measure (6.49) has Property 1. Next we show that measure (6.49) has Property 2, i.e., it is a convex function over the set of Laplacian matrices. We then show that for all

$2 \leq p \leq \infty$ the following function $f : \mathbb{R}^{n-1}_{++} \to \mathbb{R}$ is concave

$$f(x) \;=\; \left(\sum_{i=1}^{n-1} x_i^{-p+1}\right)^{\frac{1}{-p+1}},$$

where $x \;=\; [x_1, x_2, \cdots, x_{n-1}]^{\mathrm{T}}$. To do so, we need to show $\nabla^2 f(x) \;\preceq\; 0$, where the Hessian of $f(x)$ is given by

$$\frac{\partial^2 f(x)}{\partial x_i^2} \;=\; -\frac{p}{x_i}\left(\frac{f(x)}{x_i}\right)^p \;+\; \frac{p}{f(x)}\left(\frac{f(x)^2}{x_i^2}\right)^p$$

and

$$\frac{\partial^2 f}{\partial x_i \partial x_j} \;=\; \frac{p}{f(x)}\left(\frac{f(x)^2}{x_i x_j}\right)^p.$$

The Hessian matrix can be expressed as

$$\nabla^2 f(x) \;=\; \frac{p}{f(x)}\left(-\operatorname{diag}(z)^{\frac{1+p}{p}} + zz^{\mathrm{T}}\right),$$

where

$$z \;=\; \left[(f(x)/x_1)^p, \cdots, (f(x)/x_n)^p\right]^{\mathrm{T}}.$$

To verify $\nabla^2 f(x) \;\preceq\; 0$, we must show that for all vectors v, $v^{\mathrm{T}} \nabla^2 f(x) v \leq 0$. We know that

$$v^{\mathrm{T}} \nabla^2 f(x) v \;=\; \frac{p}{f(x)}\left(-\sum_{i=1}^{n-1} z_i^{\frac{p-1}{p}} \sum_{i=1}^{n-1} z_i^{\frac{p+1}{p}} v_i^2 + \left(\sum_{i=1}^{n-1} v_i z_i\right)^2\right). \tag{6.50}$$

Using the Cauchy-Schwarz inequality $a^{\mathrm{T}} b \;\leq\; \|a\|_2 \|b\|_2$, where

$$a_i \;=\; \left(\frac{f(x)}{x_i}\right)^{\frac{p-1}{2}} \;=\; z_i^{\frac{p-1}{2p}},$$

and $b_i \;=\; z_i^{\frac{p+1}{2p}} v_i$, it follows that $v^{\mathrm{T}} \nabla^2 f(x) v \;\leq\; 0$ for all $v \;\in\; \mathbb{R}^{n-1}$. Therefore, $f(x)$ is

concave. Let us define $h(x) = x^{\frac{-p+1}{p}}$, where $x \in \mathbb{R}$. Since $f(.)$ is positive and concave, and h is decreasing convex, we conclude that $h(f(.))$ is convex [146]. Hence, we get that $\|G\|_{\mathcal{H}_p}$ is a convex function with respect to the eigenvalues of L. Since this measure is a symmetric closed convex function defined on a convex subset of $\mathbb{R}^{n-1}$, i.e., $n-1$ nonzero eigenvalues, according to [139] we conclude that $\|G\|_{\mathcal{H}_p}$ is a convex of Laplacian matrix L. Finally, measure $\|G\|_{\mathcal{H}_p}$ is orthogonal invariant because it is a spectral function as shown in (6.49). Hence, this measure satisfies all properties of Definition 6.4.1. This completes the proof. □

6.7 Fundamental Limits on the Best Achievable Performance Bounds

In the following, we present theoretical bounds for the best achievable values for the performance measure in (6.17). Let us denote the optimal cost value of the optimization problem (6.17) by $\mathbf{r}_k^*(\varpi)$.

For a given systemic performance measure $\rho : \mathfrak{L}_n \to \mathbb{R}$, we recall that according to Theorem 6.4.2 there exists a spectral function Φ such that

$$\rho(L) \;=\; \Phi\big(\lambda_2, \ldots, \lambda_n\big).$$

Theorem 6.7.1. *Suppose that a consensus network* (6.6)-(6.7) *with an ordered set of Laplacian eigenvalues $\lambda_2 \leq \ldots \leq \lambda_n$, a set of candidate links $\mathcal{E}_c$ endowed with a weight function $\varpi : \mathcal{E}_c \to \mathbb{R}_{++}$, and design parameter $1 \leq k \leq n-1$ are given. Then, the*

following inequality

$$\mathbf{r}_k^*(\varpi) \;>\; \Phi\big(\lambda_{k+2},\ldots,\lambda_n,\underbrace{\infty,\ldots,\infty}_{k\ \text{times}}\big) \tag{6.51}$$

holds for all weight functions ϖ. For $k \geq n$, all lower bounds are equal to $\Phi\big(\infty,\ldots,\infty\big)$.

Proof. For a given weight function $\varpi : \mathcal{E}_c \to \mathbb{R}_{++}$, we show that inequality (6.51) holds for every $\hat{\mathcal{E}} \in \Pi_k(\mathcal{E}_c)$. Assume that $\hat{L}$ is the Laplacian of the graph formed by k added edges. We note that $\mathrm{rank}(\hat{L}) = k' \leq k$. Therefore $\dim(\ker\hat{L}) = n - k' \geq n - k$. Therefore, we can define the nonempty set M_j for $2 \leq j \leq n$, as follows

$$M_j \;=\; \mathrm{span}\{u_1,\ldots,u_{j+k'}\} \cap \mathrm{span}\{v_j,\ldots,v_n\} \cap \ker\hat{L},$$

where u_i's and v_i's are orthonormal eigenvectors of L and $L+\hat{L}$, respectively. We now choose a unit vector $v \in M_j$. It then follows that:

$$\begin{aligned}\lambda_j(L+\hat{L}) \;&\leq\; v^{\mathrm{T}}(L+\hat{L})v \;=\; v^{\mathrm{T}}Lv\\ &\leq\; \lambda_{j+k'}(L) \;\leq\; \lambda_{j+k}(L).\end{aligned} \tag{6.52}$$

Therefore, according to (6.52) and the monotonicity property of the systemic measure ρ, we get

$$\rho(L+\hat{L}) \;>\; \Phi\big(\lambda_{k+2},\cdots,\lambda_n,\underbrace{\infty,\cdots,\infty}_{k\ \text{times}}\big), \tag{6.53}$$

for all $\hat{\mathcal{E}} \in \Pi_k(\mathcal{E}_c)$. Inequality (6.51) now follows from (6.53) and this completes the proof. □

Theorem 6.7.2. *Suppose that in optimization problem* (6.17)*, the set of candidate links form a complete graph, i.e.,* $|\mathcal{E}_c| = \frac{1}{2}n(n-1)$*. Then, there exists a weight function* $\varpi_0 : \mathcal{E}_c \to \mathbb{R}_{++}$ *and a choice of* k *weighted links from* $\mathcal{E}_c$ *with weight function* $\varpi : \mathcal{E}_c \to \mathbb{R}_{++}$ *such that*

$$\mathbf{r}_k^*(\varpi) \;\leq\; \Phi\big(\lambda_2, \ldots, \lambda_{n-k}, \underbrace{\infty, \ldots, \infty}_{k \text{ times}}\big) \tag{6.54}$$

holds for all weight functions ϖ *that satisfies* $\varpi(e) \geq \varpi_0(e)$ *for all* $e \in \mathcal{E}_c$*. Moreover, if the systemic performance measure has the following decomposable form*

$$\rho\,(L) \;=\; \sum_{i=2}^{n} \varphi(\lambda_i), \tag{6.55}$$

where $\varphi : \mathbb{R} \to \mathbb{R}_+$ *is a decreasing convex function and* $\lim_{\lambda\to\infty} \varphi(\lambda) = 0$*, then the best achievable performance measure is characterized by*

$$\mathbf{r}^*(\varpi) \;>\; \sum_{i=k+2}^{n} \varphi(\lambda_i). \tag{6.56}$$

Proof. We will show that there exists $\hat{\mathcal{E}} \in \Pi_k(\mathcal{E}_c)$ for which (6.54) is satisfied. Without loss of generality, we may assume that $k < n-1$. This is because otherwise, by adding $n-1$ links, which forms a spanning tree, and increasing their weights the performance of the resulting network tends to $\Phi(\infty, \cdots, \infty)$ (see Theorem 6.7.3). Let $\hat{\mathcal{E}} \subset \mathcal{E}$ be the set of k links that do not form any cycle with $\varpi_0(e) = \infty$ for all $e \in \hat{\mathcal{E}}$. Then, we know that

$$\Lambda(L + \hat{L}) \;\geq\; \Lambda(L) \tag{6.57}$$

and the k largest eigenvalues of $L + \hat{L}$ are equal to ∞. Using (6.57) and the monotonicity

property of the systemic performance measure, we get

$$\rho(L+\hat{L}) \;\leq\; \Phi\big(\lambda_2,\cdots,\lambda_{n-k},\underbrace{\infty,\cdots,\infty}_{k \text{ times}}\big). \tag{6.58}$$

From $\mathbf{r}^*(\varpi) \leq \rho(L+\hat{L})$ and using (6.58), we obtain (6.54). Note that inequality (6.56) is a direct consequence of (6.54) and $\lim_{\lambda\to\infty}\varphi(\lambda)=0$. □

Examples of systemic performance measures that satisfies conditions of Theorem 6.7.1 include $\zeta_q^q(L)$ for $q \geq 1$, $I_\gamma(L)$, and $\tau_t(L)$.

Theorem 6.7.3. *Let us consider a linear consensus network* (6.6)-(6.7) *that is endowed with systemic performance measure $\rho : \mathfrak{L}_n \to \mathbb{R}$. Then, the network performance can be arbitrarily improved*[3] *by adding only $n-1$ links that form a spanning tree.*

Proof. Let us denote the Laplacian matrix of the spanning tree by $L_{\mathcal{T}}$. In the following, we show that the performance of resulting network can be arbitrarily improved by increasing the weights of the spanning trees. Based on the monotonicity property, we have

$$\rho(L+\kappa L_{\mathcal{T}}) \leq \rho(\kappa L_{\mathcal{T}}), \quad \kappa > 0, \tag{6.59}$$

Also, we know that $\Lambda(\kappa L_{\mathcal{T}}) = \kappa\Lambda(L_{\mathcal{T}})$. Therefore, using the fact that the spanning tree has only one zero eigenvalue, (6.13), we get

$$\lim_{\kappa\to\infty}\rho(\kappa L_{\mathcal{T}}) = \Phi(\infty,\cdots,\infty).$$

Using this limit and (6.59) we get the desired result. □

[3]This implies that the value of the systemic performance measure can be made close enough to $\Phi(\infty,\cdots,\infty)$, the lower bound in inequality (6.51).

The result of Theorem 6.7.1 can be effectively applied to select a suitable value for the design parameter k in optimization problem (6.17). Let us denote the value of the lower bound in (6.51) by ϱ_k. The performance of the original network is then $\varrho_0 = \rho(L)$. The percentage of performance enhancement can be computed by formula $\frac{\varrho_0 - \varrho_k}{\varrho_0} \times 100$ for all values of parameter $1 \leq k \leq n-1$. For a given desired performance level, we can look up these numbers and find the minimum number of required links to be added to the network. This is explained in details in Example 6.10.3 and Figure 6.5 in Section 6.10. In next sections, we propose approximation algorithms to compute near-optimal solutions for the network synthesis problem (6.17).

6.8 A Linearization-Based Approximation Method

Our first approach is based on a linear approximation of the systemic performance measure when weights of the candidate links in $\mathcal{E}_c$ are small enough. In the next result, we calculate Taylor expansion of a systemic performance measure using notions of directional derivative for spectral functions.

Theorem 6.8.1. *Suppose that a linear consensus network* (6.6)-(6.7) *endowed with a differentiable systemic performance measure ρ is given. Let us consider the cost function in optimization problem* (6.17)*. If $\hat{L}$ is the Laplacian matrix of an appended subgraph $\hat{\mathcal{G}} = (\mathcal{V}, \hat{\mathcal{E}}, \varpi)$, then*

$$\rho(L + \epsilon \hat{L}) \;=\; \rho(L) + \epsilon \, \mathbf{Tr}\left(\nabla \rho(L) \hat{L}\right) + \mathcal{O}(\epsilon^2)$$

where the derivative of ρ at L is given by

$$\nabla \rho(L) \;=\; W^T \left(\operatorname{diag} \nabla \phi \left(\Lambda(L)\right)\right) W \tag{6.60}$$

for any matrix W that is defined by (6.15).

Proof. The expression (6.60) can be calculated using the spectral form of a given systemic performance measure described by (6.14) and according to [147, Corollary 5.2.7]. Using the directional derivative of ρ along matrix $\hat{L}$, the Taylor expansion of $\rho(L+\epsilon\hat{L})$ is given by

$$\rho(L+\epsilon\hat{L}) \;=\; \rho(L) + \epsilon\nabla_{\hat{L}}\rho(L) + \mathcal{O}(\epsilon^2), \tag{6.61}$$

where $\nabla_{\hat{L}}\rho(L)$ is the directional derivative of ρ at L along matrix $\hat{L}$

$$\nabla_{\hat{L}}\rho(L) \;=\; \left\langle \nabla\rho(L), \hat{L} \right\rangle \;=\; \mathbf{Tr}\left(\nabla\rho(L)\hat{L}\right), \tag{6.62}$$

where $\langle ., . \rangle$ denotes the inner product operator. Then, substituting (6.62) in (6.61) yields the desired result. □

According to the monotonicity property of systemic performance measures, the inequality

$$\mathbf{Tr}\left(\nabla\rho(L)\hat{L}\right) \;\leq\; 0$$

holds for every Laplacian matrix $\hat{L}$. This implies that when weights of the candidate links are small enough, one can approximate the optimization problem (6.17) by the following optimization problem

$$\underset{\hat{\mathcal{E}}\in\Pi_k(\mathcal{E}_c)}{\text{minimize}} \qquad \mathbf{Tr}\left(\nabla\rho(L)\hat{L}\right), \tag{6.63}$$

where $\hat{L}$ is the Laplacian matrix of an appended candidate subgraph $\hat{\mathcal{G}} = (\mathcal{V}, \hat{\mathcal{E}}, \varpi)$. Therefore, the problem boils down to select the k-largest elements of the following set

$$\Big\{\varpi(e)\big(\nabla\rho(L)_{ii} + \nabla\rho(L)_{jj} - \nabla\rho(L)_{ij} - \nabla\rho(L)_{ji}\big)\Big| e = \{i,j\} \in \mathcal{E}_c\Big\},$$

Table 6.2: Linearization-based algorithm

Algorithm: Adding k links using linearization
Input: L, $\mathcal{E}_c$, ϖ, and k
set $\hat{L} = \mathbf{0}$
for $i = 1$ *to* k
find $e = \{i, j\} \in \mathcal{E}_c$ that returns the maximum value for
$\varpi(e)\big(\nabla\rho(L)_{ii} + \nabla\rho(L)_{jj} - \nabla\rho(L)_{ij} - \nabla\rho(L)_{ji}\big)$
set the solution $e^\star$
update
$\hat{L} = \hat{L} + \varpi(e^\star)L_{e^\star}$, and
$\mathcal{E}_c = \mathcal{E}_c \setminus \{e^\star\}$
end for

where $\varpi(e)$ is weight of link e. Table 6.2 presents our linearization approach as an algorithm. In some special cases, one can obtain an explicit closed-form formula for systemic performance measure of the resulting augmented network.

Theorem 6.8.2. *Suppose that linear consensus network* (6.6)-(6.7) *with Laplacian matrix* L *is endowed with systemic performance measure* (6.6.1) *for* $q = 1$. *Let us consider optimization problem* (6.17)*, where* $\hat{L}$ *is the Laplacian matrix of a candidate subgraph* $\hat{\mathcal{G}} = (\mathcal{V}, \hat{\mathcal{E}}, \varpi)$. *Then,*

$$\zeta_1(L + \epsilon\hat{L}) \;=\; \zeta_1(L) - \epsilon \sum_{e\in\hat{\mathcal{E}}} \varpi(e) r_e(L^2) + \mathcal{O}(\epsilon^2),$$

where $r_e(L^2)$ *is the effective resistance between the two ends of* e *in a graph with node set* $\mathcal{V}$ *and Laplacian matrix* L^2.

Proof. We use the following identity

$$(A + \epsilon X)^{-1} = A^{-1} - \epsilon A^{-1} X A^{-1} + \mathcal{O}(\epsilon^2), \tag{6.64}$$

for given matrices $A, X \in \mathbb{R}^{n\times n}$. Based on [5, Theorem 4], the performance measure

$\zeta_1(.)$ can be calculated by

$$\zeta_1(L+\epsilon\hat{L}) \;=\; \mathbf{Tr}((L+\epsilon\hat{L})^{\dagger}). \tag{6.65}$$

Moreover, according to the definition of the Moore-Penrose generalized matrix inverse, we have

$$\Big(L+\epsilon\hat{L}\Big)^{\dagger} \;=\; \Big(\bar{L}+\epsilon\hat{L}\Big)^{-1} - \frac{1}{n}J_n,$$

where $\bar{L} = L + \frac{1}{n}J_n$. Using (6.64) and (6.65), it follows that

$$\Big(L+\epsilon\hat{L}\Big)^{\dagger} \;=\; \bar{L}^{-1} - \frac{1}{n}J_n - \epsilon\bar{L}^{-1}\hat{L}\bar{L}^{-1} + \mathcal{O}(\epsilon^2). \tag{6.66}$$

Then we show that

$$\mathbf{Tr}(\bar{L}^{-1}\hat{L}\bar{L}^{-1}) \;=\; \mathbf{Tr}(\hat{L}\bar{L}^{-2}) \;=\; \sum_{e\in\hat{\mathcal{E}}} \varpi(e) r_e(L^2). \tag{6.67}$$

Using (6.65), (6.66) and (6.67), we get the desired result. □

According to Theorem 6.8.2, when weights of the candidate links are small, in order to solve problem (6.17), it is enough to find k-largest element of the following set

$$\big\{\varpi(e) r_e(L^2) \;\big|\; e \in \mathcal{E}_c\big\}.$$

Since the weights of the candidate links are given, we only need to calculate the effective resistance $r_e(L^2)$ for all $e \in \mathcal{E}_c$, .

As we discussed earlier, the design problem (6.17) is generally NP-hard. Our proposed approximation algorithm in this section works in polynomial-time. In example 6.10.4, we discuss and compare optimality gap and time complexity of this method with

Table 6.3: Simple greedy algorithm

Algorithm: Adding links Consecutively
Input: L, $\mathcal{E}_c$, ϖ, and k
1: *set* $\tilde{L} = L$
2: *for* $i = 1$ *to* k
3: *find* link $e \in \mathcal{E}_c$ with maximum $\rho(\tilde{L}) - \rho(\tilde{L} + \varpi(e)L_e)$
4: *set* the solution $e^\star$
5: *update*
6: $\tilde{L} = \tilde{L} + \varpi(e^\star)L_{e^\star}$, and
7: $\mathcal{E}_c = \mathcal{E}_c \setminus \{e^\star\}$
8: *end for*

other methods. The computational complexity of the linearization-based algorithm in Table 6.2 is $\mathcal{O}(n^3)$ for a given differentiable systemic performance measure from Table 6.1. This involves computation of $\nabla\rho$ for the original graph, which requires $\mathcal{O}(n^3)$ operations. The rest of the algorithm can be done in $\mathcal{O}(pk)$ for small k and $\mathcal{O}(p \log p)$ operations for large k.

6.9 Greedy Approximation Algorithms

In this section, we propose an optimal algorithm to solve the network growing problem (6.17) when $k = 1$. It is shown that for some commonly used systemic performance measures, one can obtain a closed-form solution for $k = 1$. We exploit our results and propose a simple greedy approximation algorithm for (6.17) with $k > 1$ by adding candidate links one at a time. For some specific subclasses of systemic performance measures, we prove that our proposed greedy approximation algorithm enjoys guaranteed performance bounds with respect to the optimal solution of the combinatorial problem (6.17). Finally, we discuss time complexity of our proposed algorithms.

6.9.1 Simple Greedy by Sequentially Adding Links

The problem of adding only one link can be formulated as follows

$$\underset{e\in\mathcal{E}_c}{\text{minimize}} \quad \rho(L+L_e), \tag{6.68}$$

where L_e is the Laplacian matrix of a candidate subgraph $\hat{\mathcal{G}}_e = (\mathcal{V}, \{e\}, \varpi)$. Let us denote the optimal cost of (6.68) by $\mathrm{r}_1^*(\varpi)$. In order to formulate the optimal cost value of (6.68), we need to define the notion of a companion operator for a given systemic performance measure.

Theorem 6.9.1. *For a given systemic performance measure $\rho : \mathfrak{L}_n \to \mathbb{R}$, there exists a companion operator $\psi : \mathfrak{L}_n \to \mathbb{R}$ such that*

$$\rho(L) = \psi(L^\dagger), \tag{6.69}$$

for all $L \in \mathfrak{L}_n$. Moreover, the companion operator of ρ is characterized by

$$\psi(X) = \Phi(\mu_n^{-1}, \ldots, \mu_2^{-1}), \tag{6.70}$$

for all $X \in \mathfrak{L}_n$ with eigenvalues $\mu_2 \leq \ldots \leq \mu_n$, where operator $\Phi : \mathbb{R}^{n-1} \to \mathbb{R}$ is defined by (6.13)*.*

Proof. According to Theorem 6.4.2, there exists a Schur-convex spectral function $\Phi : \mathbb{R}^{n-1} \to \mathbb{R}$ such that

$$\rho(L) \;=\; \Phi(\lambda_2, \ldots, \lambda_n).$$

In addition, we know that for the Moore-Penrose pseudo-inverse of matrix $L \in \mathfrak{L}_n$, we

have the following

$$\lambda_i(L^\dagger) \;=\; \lambda^{-1}_{n-i+1}(L) \;=\; \lambda^{-1}_{n-i+1},$$

for $i = 2, \dots n$, and $\lambda_1(L) = \lambda_1(L^\dagger) = 0$. Consequently, we can rewrite $\rho(L)$ using its companion operator as

$$\rho(L) = \Phi\left(\lambda_n^{-1}(L^\dagger), \dots, \lambda_2^{-1}(L^\dagger)\right).$$

Therefore, by defining $\psi : \mathfrak{L}_n \to \mathbb{R}$ as (6.70), we get identity (6.69). □

Table 6.4 shows some important examples of systemic performance measure and their corresponding companion operators.

Theorem 6.9.2. *Suppose that a linear consensus network* (6.6)-(6.7) *endowed by a systemic performance measure $\rho : \mathfrak{L}_n \to \mathbb{R}$ is given. The optimal cost value of the optimization problem* (6.68) *is given by*

$$\mathrm{r}_1^*(\varpi) \;=\; \min_{e\in\mathcal{E}_c} \; \psi\left(L^\dagger - \frac{1}{\varpi^{-1}(e) + r_e(L)} U_e\right), \tag{6.71}$$

where ψ is the corresponding companion operator of ρ and U_e for a link $e = \{i, j\}$ is a rank-one matrix defined by

$$U_e \;=\; (L_i^\dagger - L_j^\dagger)(L_i^\dagger - L_j^\dagger)^T, \tag{6.72}$$

in which $L_i^\dagger$ is the i^{th} column of matrix $L^\dagger$.

Proof. We use the following matrix identity

$$(L + L_e)^\dagger \;=\; \left(\bar{L} + E_e \varpi(e) E_e^{\mathrm{T}}\right)^{-1} - \frac{1}{n} J_n,$$

where E_e is the incidence matrix of graph $\hat{\mathcal{G}}_e$ and $\bar{L} = L + \frac{1}{n}J_n$. By utilizing the Woodbury matrix identity, we get

$$(L + L_e)^\dagger \;=\; L^\dagger - \bar{L}^{-1}E_e\left(w_1^{-1}(e) + E_e^{\mathrm{T}}\bar{L}^{-1}E_e\right)^{-1}E_e^{\mathrm{T}}\bar{L}^{-1}. \tag{6.73}$$

From the definition of the effective resistance between nodes i and j, it follows that

$$r_e(L) \;=\; E_e^{\mathrm{T}}\bar{L}^{-1}E_e \;=\; l_{ii}^\dagger + l_{jj}^\dagger - l_{ij}^\dagger - l_{ji}^\dagger.$$

On the other hand, we have

$$\bar{L}^{-1}E_e \;=\; \left(L^\dagger - \frac{1}{n}J_n\right)E_e \;=\; L^\dagger E_e \;=\; L_i^\dagger - L_j^\dagger. \tag{6.74}$$

Therefore, using (6.73) and (6.74), we have

$$\begin{aligned}(L + L_e)^\dagger &= L^\dagger - \frac{1}{\varpi^{-1}(e) + r_e(L)}(L_i^\dagger - L_j^\dagger)(L_i^\dagger - L_j^\dagger)^{\mathrm{T}} \\ &= L^\dagger - \frac{1}{\varpi^{-1}(e) + r_e(L)}U_e.\end{aligned} \tag{6.75}$$

From (6.69) and (6.75), we can conclude the desired equation (6.71). □

In some special cases, the optimal solution (6.71) can be computed very efficiently using a simple separable update rule.

Theorem 6.9.3. *Suppose that linear consensus network* (6.6)-(6.7) *with Laplacian matrix* L*. Then, for every link* $e \in \mathcal{E}_c$ *we have*

$$\zeta_1(L + L_e) = \zeta_1(L) - \tfrac{r_e(L^2)}{\varpi^{-1}(e) + r_e(L)},$$

$$\zeta_2^2(L+L_e) = \zeta_2^2(L) + \left[\frac{r_e(L^2)}{\varpi^{-1}(e)+r_e(L)}\right]^2 - \frac{2r_e(L^3)}{\varpi^{-1}(e)+r_e(L)},$$
$$\upsilon(L+L_e) \;=\; \upsilon(L) \;-\; \log\big(1+r_e(L)\varpi(e)\big),$$

where $r_e(L^m)$ is the effective resistance between the two ends of link e in a graph with node set $\mathcal{V}$ and Laplacian matrix L^m for $m \in \{1,2,3\}$.

Proof. Based on Theorem 6.9.2, it is straightforward to get the desired result for $\zeta_1(.)$ and $\zeta_2(.)$. For the last part, using the definition of $\upsilon(.)$ and (6.42), we get

$$\begin{aligned}\upsilon(L+L_e) &= \log\det\left(\frac{1}{2}(L+L_e)^\dagger + \frac{1}{n}J_n\right)\\ &= \log\det\left(2(L+L_e)+\frac{1}{n}J_n\right)^{-1}.\end{aligned} \tag{6.76}$$

According to the matrix determinant lemma we have

$$\det(A+uv^{\mathrm{T}}) \;=\; (1+v^{\mathrm{T}}A^{-1}u)\,\det(A). \tag{6.77}$$

Now using (6.76) and (6.77), it follows that

$$\begin{aligned}\det\left(2(L+L_e)+\frac{1}{n}J_n\right)^{-1} \;=\; &\\ &\det\left(\left(2L+\frac{1}{n}J_n\right)^{-1} - \frac{1}{2\varpi^{-1}(e)+2r_e(L)}U\right)\\ &= \left(1-\frac{r_e(L)}{\varpi^{-1}(e)+r_e(L)}\right)\det\left(2L+\frac{1}{n}J_n\right)^{-1},\end{aligned}$$

then by taking $\log$ from both sides, we get the desired result. □

In these special cases, the computational complexity of calculating the optimal solution for network design problem (6.68) is relatively low. For $q=1$, the optimal cost value

is equal to $\zeta_1(L + L_{e^*})$, where

$$e^* = \arg\max_{e \in \mathcal{E}_c} \frac{r_e(L^2)}{\varpi^{-1}(e) + r_e(L)}, \tag{6.78}$$

and for $q = 2$, the optimal cost value is equal to $\zeta_2(L + L_{e^*})$, where

$$e^* = \arg\min_{e \in \mathcal{E}_c} \left(\left[\frac{r_e(L^2)}{\varpi^{-1}(e) + r_e(L)} \right]^2 - \frac{2r_e(L^3)}{\varpi^{-1}(e) + r_e(L)} \right)$$

Moreover, for (6.42), the optimal cost value is equal to $\upsilon(L + L_{e^*})$, where

$$e^* = \arg\min_{e \in \mathcal{E}_c} \log\big(1 + r_e(L)\varpi(e)\big).$$

The location of the optimal link is sensitive to its weight. For example when optimizing with respect to ζ_1, maximizers of $r_e(L)$, $r_e(L^2)$ and $r_e(L^2)/r_e(L)$ can be three different links. In Example 6.10.1 and Figure 6.1 of Section 6.10, we illustrate this point by means of a simulation. Furthermore, one can obtain the following useful fundamental limits on the best achievable cost values.

Theorem 6.9.4. *Let us denote the value of performance improvement by adding an edge e with an arbitrary positive weight to linear consensus network* (6.6)-(6.7) *by*

$$\Delta\rho(L) = \rho(L) - \rho(L + L_e).$$

Then, the maximum achievable performance improvement is

$$\Delta\rho(L) \;\leq\; \psi(L^\dagger) - \psi\Big(L^\dagger - r_e(L)^{-1}U_e\Big), \tag{6.79}$$

where U_e is given by (6.72) *and the upper bound can be achieved as w tends to infinity.*

Systemic Performance Measure	Symbol	Spectral Representation	The Corresponding Companion Operator
Spectral zeta function	$\zeta_q(L)$	$\Big(\sum_{i=2}^{n}\lambda_i^{-q}\Big)^{1/q}$	$\Big(\sum_{i=2}^{n}\mu_i^{q}\Big)^{1/q}$ for $q \geq 1$
Gamma entropy	$I_\gamma(L)$	$\gamma^2\sum_{i=2}^{n}\Big(\lambda_i - \big(\lambda_i^2-\gamma^{-2}\big)^{\frac{1}{2}}\Big)$	$\gamma^2\sum_{i=2}^{n}\Big(\mu_i^{-1} - \big(\mu_i^{-2}-\gamma^{-2}\big)^{\frac{1}{2}}\Big)$
Expected transient output covariance	$\tau_t(L)$	$\frac{1}{2}\sum_{i=2}^{n}\lambda_i^{-1}(1-e^{-\lambda_i t})$	$\frac{1}{2}\sum_{i=2}^{n}\mu_i(1-e^{-\frac{t}{\mu_i}})$
System Hankel norm	$\eta(L)$	$\frac{1}{2}\lambda_2^{-1}$	$\frac{1}{2}\mu_n$
Uncertainty volume of the output	$\upsilon(L)$	$(1-n)\log 2 - \sum_{i=2}^{n}\log\lambda_i$	$(1-n)\log 2 + \sum_{i=2}^{n}\log\mu_i$
Hardy-Schatten system norm or $\mathcal{H}_p$-norm	$\theta_p(L)$	$\Big\{\frac{1}{2\pi}\int_{-\infty}^{\infty}\sum_{k=1}^{n}\sigma_k(G(j\omega))^p\,d\omega\Big\}^{1/p}$ $= \alpha_0\Big(\mathbf{Tr}\,(L^\dagger)^{p-1}\Big)^{\frac{1}{p}}$	$\alpha_0\Big(\sum_{i=2}^{n}\mu_i^{p-1}\Big)^{1/p}$ for $2 \leq p \leq \infty$, where $\alpha_0^{-1} = \sqrt[p]{-\beta(\frac{p}{2},-\frac{1}{2})}$.

Table 6.4: Some important examples of spectral systemic performance measures and their corresponding companion operators.

Moreover, we have the following explicit fundamental limits

$$\Delta\zeta_1(L) \;\leq\; \frac{r_e(L^2)}{r_e(L)}, \tag{6.80}$$

$$\Delta\zeta_2^2(L) \;\leq\; \left[\frac{r_e(L^2)}{r_e(L)}\right]^2 - 2\frac{r_e(L^3)}{r_e(L)}. \tag{6.81}$$

Proof. We utilize monotonicity property of companion operator of a systemic performance measure, i.e., If $L_1^\dagger \preceq L_2^\dagger$, then

$$\psi(L_1^\dagger) \;\leq\; \psi(L_2^\dagger),$$

and the inequality

$$L^\dagger - r_e(L)^{-1}U_e \;\preceq\; L^\dagger - \frac{1}{w^{-1}+r_e(L)}U_e$$

to show that

$$\psi\Big(L^\dagger - r_e(L)^{-1}U_e\Big) \;\leq\; \psi\Big(L^\dagger - \frac{1}{w^{-1}+r_e(L)}U_e\Big).$$

From this inequality, we can directly conclude (6.79). For systemic performance measure $\zeta_1(.)$, inequality (6.79) reduces to

$$\begin{aligned}\Delta\zeta_1(L) &\leq \mathbf{Tr}(L^\dagger) - \mathbf{Tr}\left(L^\dagger - r_e(L)^{-1}U_e\right), \\ &= \mathbf{Tr}\left(r_e(L)^{-1}U_e\right) = r_e(L)^{-1}\,\mathbf{Tr}\left(U_e\right). \end{aligned} \tag{6.82}$$

Moreover, based on the definition of U_e, we have

$$\mathbf{Tr}(U_e) = \mathbf{Tr}(L^\dagger E_e^{\mathrm{T}} E_e L^\dagger) = E_e L^{\dagger,2} E_e^{\mathrm{T}} = r_e(L^2).$$

Using this and (6.82), it follows that

$$\Delta\zeta_1(L) \leq \frac{r_e(L^2)}{r_e(L)}.$$

Similarly for $\zeta_2^2(.)$, using (6.79) and the definition of $\zeta_2(.)$, results in

$$\begin{aligned}\Delta\zeta_2^2(L) &\leq \mathbf{Tr}\left(L^{\dagger,2}\right) - \mathbf{Tr}\left(\left(L^\dagger - r_e(L)^{-1}U_e\right)^2\right), \\ &= \frac{1}{r_e^2(L)}\,\mathbf{Tr}\left(U_e^2\right) - 2\,\mathbf{Tr}\left(r_e(L)^{-1}U_e L^\dagger\right) \\ &= \left[\frac{r_e(L^2)}{r_e(L)}\right]^2 - 2\frac{\mathbf{Tr}\left(U_e L^\dagger\right)}{r_e(L)} \\ &= \left[\frac{r_e(L^2)}{r_e(L)}\right]^2 - 2\frac{\mathbf{Tr}\left(L^\dagger E_e^{\mathrm{T}} E_e L^{\dagger,2}\right)}{r_e(L)} \\ &= \left[\frac{r_e(L^2)}{r_e(L)}\right]^2 - 2\frac{r_e(L^3)}{r_e(L)}. \end{aligned} \tag{6.83}$$

This completes proof. □

The result of Theorem 6.9.4 asserts that, in general, performance improvement may not be arbitrarily large by adding only one new link. In some cases, however, performance

improvement can be arbitrarily good. For instance, for the uncertainty volume of the output, we have

$$\lim_{\varpi(e)\to+\infty} \Delta v(L) = +\infty. \tag{6.84}$$

The result of Theorem 6.9.2 can be utilized to devise a greedy approximation method by decomposing (6.17) into k successive tractable problems in the form of (6.68). In each iteration, Laplacian matrix of the network is updated and then optimization problem (6.68) finds the next best candidate link as well as its location. Since the value of systemic performance measure can be calculated explicitly in each step using Theorem 6.9.2, one can explicitly calculate the value of systemic performance measure for the resulting augmented network. This value can be used to determine the effectiveness of this method. Table 6.3 summarizes all steps of our proposed greedy algorithm, where the output of the algorithm is the Laplacian matrix of the resulting augmented network. In Section 6.10, we present several supporting numerical examples.

Remark 6.9.5. *The optimization problem* (6.68) *with performance measure* $\zeta_\infty(L) = \lambda_2^{-1}$ *was previously considered in [55], where a heuristic algorithm was proposed to compute an approximate solution. Later on, another approximate method for this problem was presented in [54]. Also, there is a similar version of this problem that is reported in [56], where the author studies convergence rate of circulant consensus networks by adding some long-range links. Moreover, a non-combinatorial and relaxed version of our problem of interest has some connections to the sparse consensus network design problem [6, 57, 58], where they consider* ℓ_1*-regularized* $\mathcal{H}_2$ *optimal control problems. When the candidate set* $\mathcal{E}_c$ *is the set of all possible links except the network links, i.e.,* $\mathcal{E}_c = \mathcal{V} \times \mathcal{V} \setminus \mathcal{E}$*, and the performance measure is the logarithm of the uncertainty volume, our result reduces to the result reported in [23].*

6.9.2 Supermodularity and Guaranteed Performance Bounds

A systemic performance measure is a continuous function of link weights on the space of Laplacian matrices $\mathfrak{L}_n$. Moreover, we can represent a systemic performance measure equivalently as a set function over the set of weighted links. Let us denote by $\mathcal{G}(\mathcal{V})$ the set of all weighted graphs with a common node set $\mathcal{V}$.

Definition 6.9.6. *For a given systemic performance measure $\rho : \mathfrak{L}_n \to \mathbb{R}$, we associate a set function $\tilde{\rho} : \mathcal{G}(\mathcal{V}) \to \mathbb{R}$ that is defined as*

$$\tilde{\rho}(\mathcal{G}) \;=\; \rho\Big(\sum_{e\in\mathcal{E}} w(e)L_e\Big) \;=\; \rho(L),$$

where L is Laplacian matrix of $\mathcal{G} = (\mathcal{V}, \mathcal{E}, w)$ and L_e is the Laplacian matrix of $(\mathcal{V}, \{e\}, 1)$, which is an unweighted graph formed by a single link e.

Definition 6.9.7. *The union of two weighted graphs $\mathcal{G}_1 = (\mathcal{V}, \mathcal{E}_1, w_1)$ and $\mathcal{G}_2 = (\mathcal{V}, \mathcal{E}_2, w_2)$ is defined as follows*

$$\mathcal{G}_1 \vee \mathcal{G}_2 \;:=\; (\mathcal{V}, \mathcal{E}_1 \cup \mathcal{E}_2, w)$$

in which

$$w(e) := \begin{cases} \max\{w_1(e), w_2(e)\} & \text{if } e \in \mathcal{E}_1 \cup \mathcal{E}_2 \\ 0 & \text{otherwise} \end{cases} . \tag{6.85}$$

Definition 6.9.8. *The intersection of two weighted graphs $\mathcal{G}_1 = (\mathcal{V}, \mathcal{E}_1, w_1)$ and $\mathcal{G}_2 = (\mathcal{V}, \mathcal{E}_2, w_2)$ is defined as follows*

$$\mathcal{G}_1 \wedge \mathcal{G}_2 \;:=\; (\mathcal{V}, \mathcal{E}_1 \cap \mathcal{E}_2, w)$$

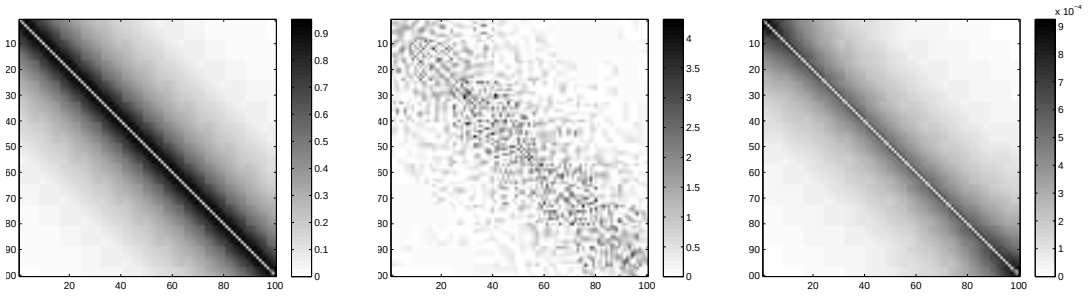

(a) (b) (c)

Figure 6.1: The interconnection topology of all three graphs, except for their highlighted blue links, are identical, which show the coupling graph of the linear consensus network in Example 6.10.1. The coupling graph shown in here is a generic connected graph with 50 nodes and 100 links, which are drawn by black lines. The optimal links are shown by blue line segments.

in which

$$w(e) := \begin{cases} \min\{w_1(e), w_2(e)\} & \textit{if } e \in \mathcal{E}_1 \cap \mathcal{E}_2 \\ 0 & \textit{otherwise} \end{cases} .$$

The following definition is adapted from [148] for our graph theoretic setting.

Definition 6.9.9. *A set function $\tilde{\rho} : \mathcal{G}(\mathcal{V}) \to \mathbb{R}$ is supermodular with respect to the link set if it satisfies*

$$\tilde{\rho}(\mathcal{G}_1 \wedge \mathcal{G}_2) + \tilde{\rho}(\mathcal{G}_1 \vee \mathcal{G}_2) \geq \tilde{\rho}(\mathcal{G}_1) + \tilde{\rho}(\mathcal{G}_2) \tag{6.86}$$

Theorem 6.9.10. *Suppose that systemic performance measure $\rho : \mathfrak{L}_n \to \mathbb{R}$ is differentiable and $\nabla\rho : \mathfrak{L}_n \to \mathbb{R}^{n\times n}$ is monotonically increasing with respect to the cone of positive semidefinite matrices*[4]*. Then, the corresponding set function $\tilde{\rho} : \mathcal{G}(\mathcal{V}) \to \mathbb{R}$, from Definition 6.9.6, is supermodular.*

[4] $L_1 \preceq L_2 \Longrightarrow \nabla\rho(L_1) \preceq \nabla\rho(L_2)$.

Proof. We know that

$$\frac{d}{dt}\rho(L+tX) \;=\; \mathbf{Tr}(\triangledown\rho(L+tX)X). \tag{6.87}$$

where $t \in \mathbb{R}_+$ and $L, X \in \mathfrak{L}_n$. From (6.87), we get

$$\begin{aligned}\frac{d}{dt}\big(\rho(L_1+tX)-\rho(L_2+tX)\big) \;=\;& \\ \mathbf{Tr}\left(\big(\triangledown\rho(L_1+tX)-\triangledown\rho(L_2+tX)\big)X\right),&\end{aligned} \tag{6.88}$$

where $L_1, L_2 \in \mathfrak{L}_n$ and $L_1 \preceq L_2$. From the monotonicity property of $\triangledown\rho$ and (6.88), we get

$$\frac{d}{dt}\big(\rho(L_1+tX)-\rho(L_2+tX)\big) \;\leq\; 0. \tag{6.89}$$

Then, by taking integral from both sides of (6.88), and then using (6.89) we have

$$\int_0^1 \frac{d}{dt}\rho(L_1+tX)dt - \int_0^1 \frac{d}{dt}\rho(L_2+tX)dt \;\leq\; 0,$$

which directly implies that

$$\rho(L_1+X)-\rho(L_1) \;\leq\; \rho(L_2+X)-\rho(L_2). \tag{6.90}$$

On the other hand, the corresponding Laplacian matrices of $\mathcal{G}_1$, $\mathcal{G}_2$, $\mathcal{G}_1 \wedge \mathcal{G}_2$, and $\mathcal{G}_1 \vee \mathcal{G}_2$

are given as follows

$$\begin{cases} L_{\mathcal{G}_1} := \sum_{e\in\mathcal{E}_1} w_1(e)L_e, \\ L_{\mathcal{G}_2} := \sum_{e\in\mathcal{E}_2} w_2(e)L_e, \\ L_{\mathcal{G}_1\wedge\mathcal{G}_2} := \sum_{e\in\mathcal{E}_1\cap\mathcal{E}_2} \min\{w_1(e), w_2(e)\}L_e, \\ L_{\mathcal{G}_1\vee\mathcal{G}_2} := \sum_{e\in\mathcal{E}_1\cup\mathcal{E}_2} \max\{w_1(e), w_2(e)\}L_e. \end{cases} \tag{6.91}$$

Based on these definitions, we have

$$L_{\mathcal{G}_1\wedge\mathcal{G}_2} \preceq L_{\mathcal{G}_1}, L_{\mathcal{G}_2} \preceq L_{\mathcal{G}_1\vee\mathcal{G}_2}. \tag{6.92}$$

By setting $L_1 = L_{\mathcal{G}_1\wedge\mathcal{G}_2}$, $L_2 = L_{\mathcal{G}_1}$, and $X = L_{\mathcal{G}_2} - L_{\mathcal{G}_1\vee\mathcal{G}_2}$ in inequality (6.90), we get

$$\begin{aligned} \rho(L_{\mathcal{G}_1\wedge\mathcal{G}_2} + L_{\mathcal{G}_2} - L_{\mathcal{G}_1\wedge\mathcal{G}_2}) - \rho(L_{\mathcal{G}_1\wedge\mathcal{G}_2}) &= \rho(L_{\mathcal{G}_2}) - \rho(L_{\mathcal{G}_1\wedge\mathcal{G}_2}) \\ &\leq \rho(L_{\mathcal{G}_1\vee\mathcal{G}_2} + L_{\mathcal{G}_2} - L_{\mathcal{G}_1\wedge\mathcal{G}_2}) - \rho(L_{\mathcal{G}_1\vee\mathcal{G}_2}). \end{aligned} \tag{6.93}$$

According to (6.91), we have

$$L_{\mathcal{G}_1\vee\mathcal{G}_2} + L_{\mathcal{G}_1\vee\mathcal{G}_2} = L_{\mathcal{G}_1} + L_{\mathcal{G}_2}. \tag{6.94}$$

Therefore, based on equality (6.94) we can rewrite the right hand side of inequality (6.93), as follows

$$\rho(L_{\mathcal{G}_1\vee\mathcal{G}_2} + L_{\mathcal{G}_2} - L_{\mathcal{G}_1\wedge\mathcal{G}_2}) - \rho(L_{\mathcal{G}_1\vee\mathcal{G}_2}) = \rho(L_{\mathcal{G}_1}) - \rho(L_{\mathcal{G}_1\vee\mathcal{G}_2}). \tag{6.95}$$

Finally, using Definition 6.9.6, (6.93) and (6.95), we can conclude (6.86). □

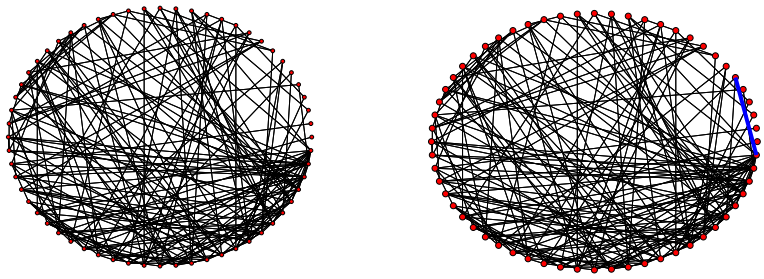

(a) (b)

Figure 6.2: The coupling graph of the network used in Example 6.10.2 is shown in (a) that consists of 60 nodes and 176 links. The location of the optimal link, highlighted by the blue color, is shown in (b).

It should be emphasized that convexity property of a systemic performance measure ρ implies that $\nabla\rho$, if it exists, is a monotone mapping[5]. However, this property is not sufficient for supermodularity of its corresponding set function $\tilde{\rho}$.

Example 6.9.11. *In our first example, we show that the uncertainty volume of the output* (6.42) *satisfies conditions of Theorem 6.9.10. The gradient operator of this systemic performance measure is*

$$\nabla\upsilon(L) = -\Big(L + \frac{1}{n}J_n\Big)^{-1}.$$

It is straightforward to verify that $\nabla\upsilon(L)$ is monotone with respect to the cone of positive semidefinite matrices. Thus, $\upsilon(L)$ is supermodular.

Example 6.9.12. *In our second example, we consider a new class of systemic performance measures that are defined as*

$$\mathfrak{m}_q(L) \;=\; -\sum_{i=2}^{n}\lambda_i^q, \tag{6.96}$$

where $0 \leq q \leq 1$ and $\mathfrak{m}_0(L) = \mathrm{rank}(L) - 1$. According to Theorem 6.6.1, this spectral function is a systemic performance measure as function $-\lambda^q$ for $0 \leq q \leq 1$ is a decreasing

[5] **Tr** $((\nabla\rho(L_1) - \nabla\rho(L_2))(L_1 - L_2)) \geq 0$, where $L_1, L_2 \in \mathfrak{L}_n$.

convex function on $\mathbb{R}_+$. Moreover, its gradient operator, which is given by

$$\nabla \mathfrak{m}_q(L) \;=\; -qL^{q-1},$$

is monotonically increasing for all $0 \leq q \leq 1$. Therefore, according to Theorem 6.9.10, systemic performance measure (6.96) *is supermodular over the set of all weighted graphs with a common node set.*

Remark 6.9.13. *For a given performance measure ρ, there are several different ways to define an extended set function for ρ. These set functions may have different properties. For instance, the extended set function of ζ_1 is supermodular over principle sub-matrices [149], but it is not supermodular over the set of all weighted graphs with a common node set (see Definition 6.9.6).*

For those systemic performance measures that satisfy conditions of Theorem 6.9.10, one can provide guaranteed performance bounds for our proposed greedy algorithm in Subsection 6.9.1. The following result is based a well-known result from [148, Chapter III, Section 3].

Theorem 6.9.14. *Suppose that systemic performance measure $\rho : \mathfrak{L}_n \to \mathbb{R}$ is differentiable and $\nabla\rho : \mathfrak{L}_n \to \mathbb{R}^{n\times n}$ is monotonically increasing with respect to the cone of positive semidefinite matrices. Then, the greedy algorithm in Table 6.3, which starts with $\hat{\mathcal{E}}$ as the empty set and at every step selects an element $e \in \mathcal{E}_c$ that minimizes the marginal cost $\rho(L+L_{\hat{\mathcal{E}}}+L_e)-\rho(L+L_{\hat{\mathcal{E}}})$, provides a set $\hat{\mathcal{E}}$ that achieves a $(1-1/e)$-approximation*[6] *of the optimal solution of the combinatorial network synthesis problem* (6.17).

[6] This means that $\frac{\rho(L+\tilde{L})-\rho(L)}{\rho(L+L^*)-\rho(L)} \;\geq\; 1-\frac{1}{e}$, where L^* is the optimum solution and $\tilde{L}$ is the solution of the greedy algorithm, or equivalently: $\frac{\rho(L+\tilde{L})-\rho(L+L^*)}{\rho(L)-\rho(L+L^*)} \leq \frac{1}{e}$.

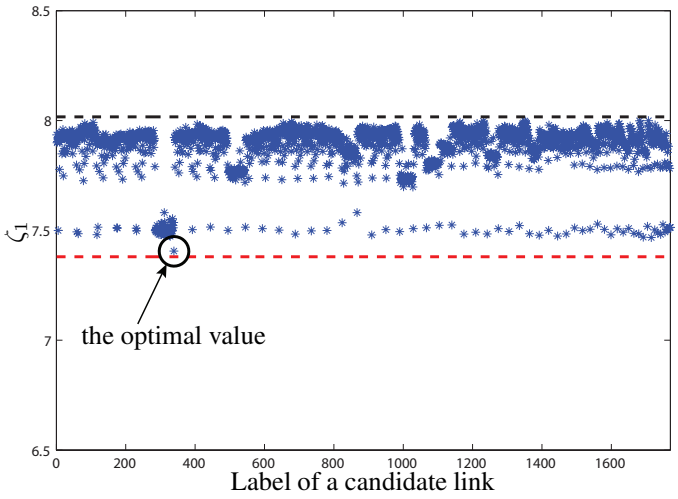

Figure 6.3: This plot is discussed in Example 6.10.2.

Since the class of supermodular systemic performance measures are monotone, the combinatorial network synthesis problem (6.17) is polynomial-time solvable with provable optimality bounds [148]. Supermodularity is not a ubiquitous property for all systemic performance measures. Nevertheless, our simulation results in Section 6.10 assert that the proposed greedy algorithm in Table 6.3 is quite powerful and provides tight and near-optimal solutions for a broad range of systemic performance measures.

6.9.3 Computational Complexity Discussion

As we discussed earlier, the network synthesis problem (6.17) is in general NP-hard. However, this problem is solvable when $k = 1$ and the best link can be found by running an exhaustive search over all possible scenarios, i.e., by calculating the value of a performance measure for all possible p augmented networks, where p is the number of candidate links. The computational complexity of evaluating performance of a given linear consensus network depends on the specific choose of a systemic performance measure. Let us denote computational complexity of a given systemic performance measure $\rho : \mathfrak{L}_n \to \mathbb{R}$

by $\mathcal{O}\left(M_\rho(n)\right)$. In the simple greedy algorithm of Table 6.3, the difference term

$$\rho(\tilde{L}) - \rho\big(\tilde{L} + \varpi(e)L_e\big) \tag{6.97}$$

is calculated and updated for each candidate link at each step, for the total of $k\big(p - \frac{k-1}{2}\big)$ times. Thus, the total computational complexity of our simple greedy algorithm is $\mathcal{O}\left(M_\rho(n)(p - \frac{k-1}{2})k\right)$ operations. This computational complexity is at most $\mathcal{O}\left(M_\rho(n)n^2k\right)$, where $p = \binom{n}{2}$, i.e., when the candidate set contains all possible links. The complexity of the brute-force method is $\mathcal{O}\left(M_\rho(n)\binom{p}{k}\right)$[7]. This can be at most $\mathcal{O}\left(M_\rho(n)2^p/\sqrt{p}\right)$. Moreover, if $k \leq \sqrt{p}$, then the computational complexity will be $\mathcal{O}\left(M_\rho(n)p^k/k!\right)$.

In some occasions, we can take advantage of the rank-one updates in Theorems 6.9.2 and 6.9.3, where it is shown that a rank-one deviation in a matrix results in a rank-one change in its inverse matrix as well. This helps reduce the computational complexity of (6.97) to the order of $\mathcal{O}(n^2)$ instead of $\mathcal{O}(n^3)$ operations. As it is shown in [150], one can apply the rank-one update on the matrix of effective resistances. As a result, we can update the effective resistances of all links in order of $\mathcal{O}(n^2)$. More specifically, the matrix of effective resistances is given by

$$R(L^m) := \mathbb{1}_n \operatorname{diag}\left(L^{\dagger,m}\right) + \operatorname{diag}\left(L^{\dagger,m}\right)\mathbb{1}_n^{\mathrm{T}} - 2L^{\dagger,m} \tag{6.98}$$

for $m \in \{1, 2, 3\}$, where $R(L^m)_{ij} = r_{\{i,j\}}(L^m)$. The update rule (6.98) can be obtained by substituting the rank-one update of $(L + L_e)^\dagger$ from (6.75) in (6.98) and the m-th power of the rank-one update can be calculated in $\mathcal{O}(n^2)$ as it can be cast as only matrix-vector products. Using these facts and the result of Theorem 6.9.3, the computational cost of (6.97) for systemic performance measures ζ_1, ζ_2, and υ can be significantly reduced;

[7] This corresponds to calculating the value of a performance measure for all $\binom{p}{k}$ possible augmented networks.

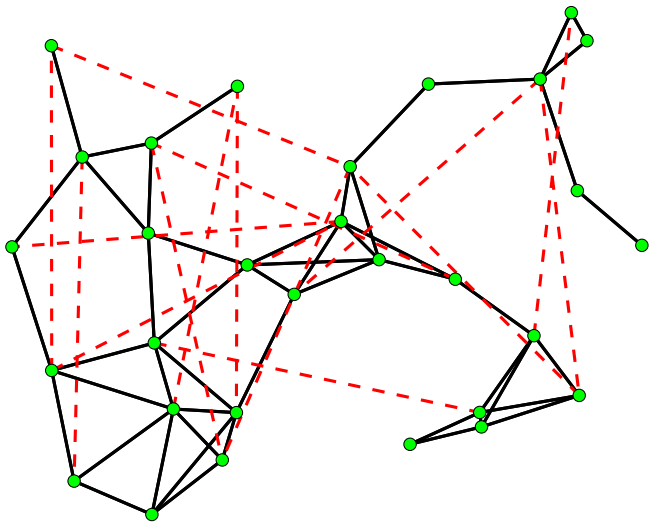

Figure 6.4: This is the coupling graph of the network in Example 6.10.4 with 30 nodes, where the graph has 50 original (black) links and the candidate set includes all 15 dashed red line segments.

more specifically, the computational complexity of our algorithm reduces to

$$\mathcal{O}\left(\underbrace{n^3}_{\text{calculating } L^{\dagger,m}\text{'s at the beginning}} + \underbrace{n^2}_{\text{rank-one update}} \times \underbrace{k}_{\text{number of steps}}\right).$$

For a generic systemic performance measure $\rho : \mathfrak{L}_n \to \mathbb{R}$, according to Theorem 6.4.2, calculating its value requires knowledge of all Laplacian eigenvalues of the coupling graph. It is known that the eigenvalue problem for symmetric matrices requires $\mathcal{O}(n^{2.376}\log n)$ operations [151]. Suppose that calculating the value of spectral function $\Phi : \mathbb{R}^{n-1} \to \mathbb{R}$ in Theorem 6.4.2 needs $\mathcal{O}\left(M_\Phi(n)\right)$ operations. Thus, the value of systemic performance measure $\rho(L)$ in equation (6.13), and similarly (6.97), can be calculated in $\mathcal{O}(n^{2.376}\log n + M_\Phi(n))$. Based on this analysis, we conclude that the complexity of the greedy algorithm in Table 6.3 is at most

$$\mathcal{O}\left(\left(n^{2.376}\log n + M_\Phi(n)\right)\left(p - \frac{k-1}{2}\right)k\right).$$

6.10 Numerical Simulations

In this section, we support our theoretical findings by means of some numerical examples.

Example 6.10.1. *This example investigates sensitivity of location of an optimal link as a function of its weight. Let us consider a linear consensus network* (6.6)-(6.7)*, whose coupling graph is shown in Figure 6.1, endowed by systemic performance measure* (6.26) *with* $q = 1$*. The graph shown in Figure 6.1 is a generic unweighted connected graph with* $n = 50$ *nodes and* 100 *links. We solve the network synthesis problem* (6.68) *for the candidate set with* $|\mathcal{E}_c| = \frac{1}{2}n(n-1)$ *that covers all possible locations in the graph. It is assumed that all candidate links have an identical weight* ϖ_0*. We use our rank-one update method in Theorem 6.9.3 to study the effect of* ϖ_0 *on location of the optimal link. In Figure 6.1(c), we observe that by increasing* ϖ_0*, the optimal location changes. When* $\varpi_0 = 1$*, our calculations reveal that the optimal link in Figure 6.1(a), shown by a blue line segment, maximizes* $r_e(L^2)$ *among all possible candidate links in set* $\mathcal{E}_c$*. By increasing the value of our design parameter to* $\varpi_0 = 1.2$ *in Figure 6.1(b), we observe that the location of the optimal link moves. In our last scenario in Figure 6.1(c), by setting* $\varpi_0 = 1.6$*, the optimal link moves to a new location that maximizes quantity* $r_e(L^2)/r_e(L)$ *among all possible candidate links.*

Example 6.10.2. *The usefulness of our theoretical fundamental hard limits in Theorem 6.7.1 in conjunction with our results in Theorem 6.9.3 is illustrated in Figure 6.3. Suppose that a linear consensus network* (6.6)-(6.7) *with a generic coupling graph with* $n = 60$*, as shown in Figure 6.2(a), is given. Let us consider the network design problem* (6.68) *with systemic performance measure* (6.26) *for* $q = 1$*. The set of candidate links is the set of all possible links in the coupling graph, i.e.,* $|\mathcal{E}_c| = \frac{1}{2}n(n-1)$*, where it is assumed that all*

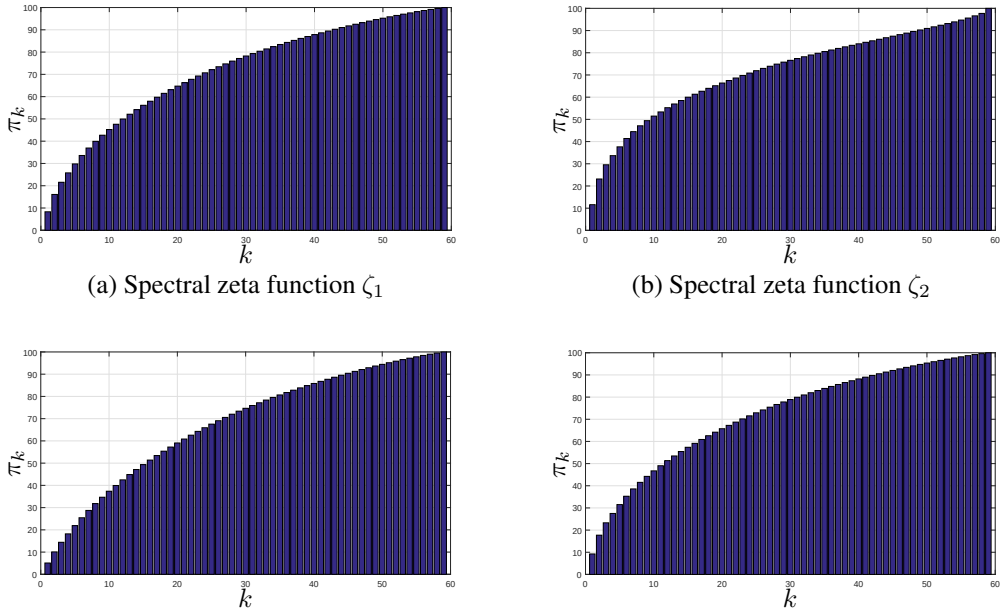

(a) Spectral zeta function ζ_1

(b) Spectral zeta function ζ_2

(c) Expected transient output covariance τ_t, where $t = 1$

(d) γ-entropy $I_\gamma(.)$, where $\gamma = 2$

Figure 6.5: These plots are discussed in Example 6.10.3.

candidate links have an identical weight $\varpi_0 = 20$. *Our goal is to compare optimality of our low-complexity update rule against brute-force search over all* $|\mathcal{E}_c| = 1770$ *possible augmented graphs. The value of the systemic performance measure for each candidate graph is marked by blue star in Figure 6.3. In this plot, the black circle highlights the value of performance measure for the network resulting from the rank-one search* (6.78). *The red dashed line in Figure 6.3 shows the best achievable value for* ζ_1 *according to Theorem 6.7.1. The value of this hard limit can be calculated merely using Laplacian eigenvalues of the original graph shown in Figure 6.2(a). The location of the optimal link is shown in Figure 6.2(b). One observes from Figure 6.3 that our theoretical fundamental limit justifies near-optimality of our rank-one update strategy* (6.78) *for networks with generic graph topologies.*

Example 6.10.3. *This example follows up on our discussion at the end of Section 6.7,*

where it is explained that the result of Theorem 6.7.1 can be utilized to choose reasonable values for design parameter k in the network design problem (6.17)*. We explain the procedure by considering a linear consensus network* (6.6)-(6.7) *with a given coupling graph by Figure 6.2(a). The value of the lower bound (i.e., hard limit) in* (6.51) *is used to form the following quantity*

$$\pi_k := \frac{\varrho_0 - \varrho_k}{\varrho_0} \times 100$$

that represents the percentage of performance enhancement for all values of parameter $1 \leq k \leq n-1$*. Figure 6.5 illustrates the value of π_k with respect to four systemic performance measures: ζ_1, ζ_2, τ_t and I_γ. Depending on the desired level of performance, one can compute a sensible value for design parameter k merely by looking up at the corresponding plots. For instance, in order to achieve* 50% *performance improvement, one should add at least* 13, 10, 16, *and* 12 *weighted links with respect to ζ_1, ζ_2, τ_t and I_γ, respectively. We verified tightness of this estimate by running our greedy algorithm in Table 6.3, where the candidate set is equal to the set of all possible links with identical weight* 10*. Our simulation results reveal that by adding* 13, 10, 16, *and* 12 *links from the candidate set, the network performance improves by* 40.60%, 45.10%, 37.76%, *and* 40.61% *with respect to ζ_1, ζ_2, τ_t, and I_γ, respectively. Our theoretical bounds predict that network performance can be further improved by increasing weights of the candidate links. In our example, if we increase the weight from* 10 *to* 500*, the network performance boosts by more than* 46% *for all mentioned systemic performance measures.*

Example 6.10.4. *We compare optimality gaps of our proposed greedy (see Table 6.3) and linearization-based (see Table 6.2) methods versus brute-force and simple-random-sampling methods. The brute-force method runs an exhaustive search to find the global optimal solution of problem* (6.17)*; however, it cannot be used for medium to large size*

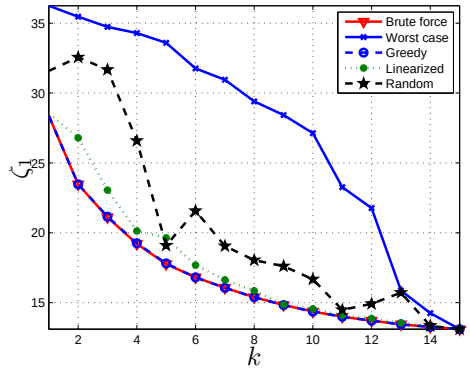

(a) Spectral zeta function ζ_1

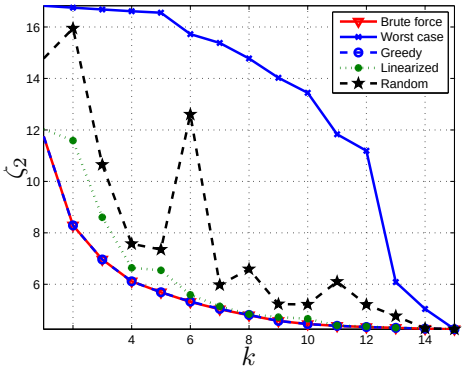

(b) Spectral zeta function ζ_2

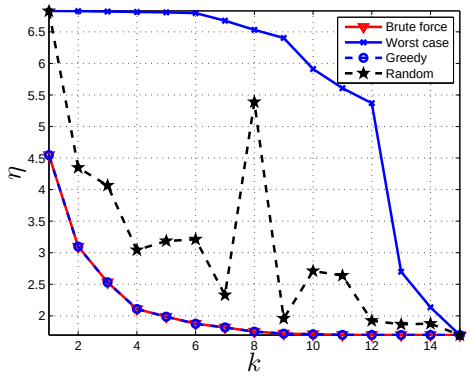

(c) Hankel norm η

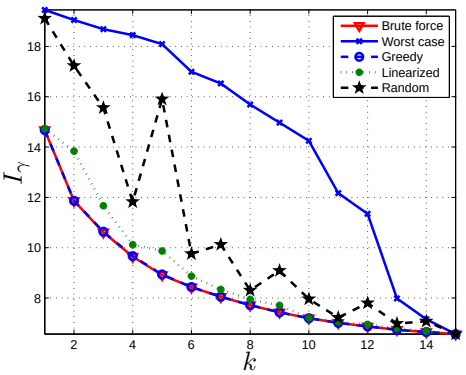

(d) γ-entropy I_γ where $\gamma = 20$

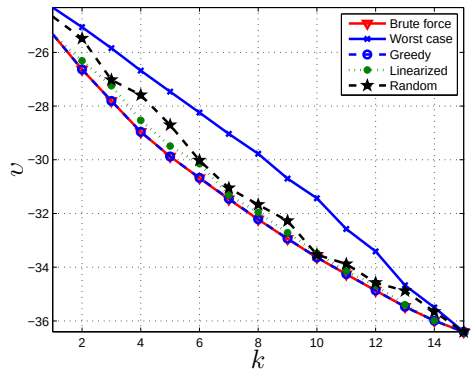

(e) Uncertainty Volume v

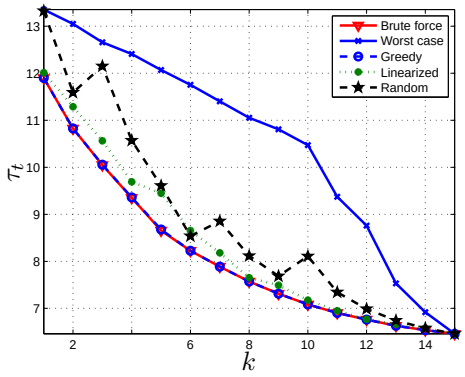

(f) Expected output covariance τ_t where $t = 10$

Figure 6.6: These plots compare optimality gaps of five different methods towards solving the network synthesis problem (6.17) and the details are discussed in Example 6.10.4.

networks. In order to make our comparison possible, we consider a linear consensus network (6.6)-(6.7) *with* $n = 30$ *nodes over the graph shown in Figure 6.4. Weights of all links, both in the coupling graph and the candidate set, are equal to* 1*. Our control objective is to solve the network synthesis problem* (6.17)*, where the candidate set consists of* 15 *links that are shown by red-dashed lines in Figure 6.4. The outcome of our simulation results are explicated in Figure 6.6, where we run our algorithms and compute the corresponding values for systemic performance measures for all* $k = 1, \ldots, 15$*. One observes that our greedy algorithm performs nearly as optimal as the brute-force method. This is mainly due to convexity and monotonicity properties of the class of systemic performance measures that enable the greedy algorithm to produce near-optimal solutions with respect to this class of measures. As one expects, our greedy algorithm outperforms our linearization-based method. It is noteworthy that the time complexity of the linearization method is comparably less than the greedy algorithm. The usefulness of the linearization-based method accentuates itself when weight of candidate links are small and/or* k *is large.*

6.11 Discussion and Conclusion

In the following, we provide explanations for some of the outstanding and remaining problems related to this chapter.

Convex Relaxation: The constraints of the combinatorial problem (6.17) can be relaxed by allowing the link weights to vary continuously. The relaxed problem will be a spectral convex optimization problem [152]. In some special cases, such as when the cost function is ζ_1 or ζ_2, the relaxed problem can be equivalently cast as a semidefinite programming problem [18, 19]. However, for a generic systemic performance measure, we

need to develop some low-complexity specialized optimization techniques to solve the corresponding spectral optimization problem, which is beyond the scope of this chapter.

Higher-Order Approximations: In Subsection 6.8, we employed the first-order approximation of a systemic performance measure. One can easily extend our algorithm by considering second-order approximations of a systemic performance measure in order to gain better optimality gaps.

Non-spectral Systemic Performance Measures: The class of spectral systemic performance measures can be extended to include non-spectral measures as well. This can done by relaxing and replacing the orthogonal invariance property by permutation invariance property. The local deviation error is an example of a non-spectral systemic performance measure [18, 43]. Our ongoing research involves a comprehensive treatment of this class of measures.

Chapter 7

Analysis and Optimal Design of Distributed System Throttlers

7.1 Abstract

In this chapter, we investigate the performance analysis and synthesis of distributed system throttlers (DST). A throttler is a mechanism that limits the flow rate of incoming metrics, *e.g.*, byte per second, network bandwidth usage, capacity, traffic, *etc*. This can be used to protect a service's backend/clients from getting overloaded, or to reduce the effects of uncertainties in demand for shared services. We study performance deterioration of DSTs subject to demand uncertainty. We then consider network synthesis problems that aim to improve the performance of noisy DSTs via communication link modifications as well as server update cycle modifications.

7.2 Introduction

System throttling (also known as rate-limiting) aims to limit the total number of requests from all clients to a shared service and provide a harmonized and fair quota allocation among them (where the definition of fairness is application-specific). Examples of systems in need of throttling protection include cloud-based services and traffic management services. A number of works on rate-limiting systems and congestion control have been published in the recent literature [153–160].

System throttlers can be classified into centralized and distributed types. In a centralized system throttler (CST), there is a single decision maker that sets the per-client limits according to aggregated metrics it receives from multiple servers, which in turn aggregate them from metrics reported by the clients. CSTs are designed based on a globally aggregated view of usage metrics. On the other hand, a distributed system throttler (DST) does not have a centralized mechanism for setting per-client limits: it consists of multiple servers, each of which makes autonomous decisions and updates its own limit based on measurements it takes as well as local information.

While the centralized approach has benefits, including consistency and ease of implementation and analysis, it also has drawbacks relative to a decentralized version: (i) Less local adaptability: in a centralized version, each server needs to send information to the decision-making server and wait for its command, which means a delayed response time. (ii) Limited communication: there is no inter-server communication except to the decision-making server. However, we want to facilitate information propagation to improve the performance and make the network more flexible and fast when handling uncertainty in demand.

There are some related works in the literature that study performance and robustness issues in noisy linear distributed systems; for example, see [2,5,12,17,18,36,42,161,162]

and the references therein. In [2], the authors investigate the deviation from the mean of states of a continuous-time consensus network on tori with additive noise inputs. A rather comprehensive performance analysis of noisy linear consensus networks with arbitrary graph topologies has been recently reported in [12]. In [12], several fundamental trade-offs between a $\mathcal{H}_2$-based performance measure and sparsity measures of a continuous-time linear consensus network are studied. Moreover, [61] studies a $\mathcal{H}_2$-based performance measure of continuous-time linear consensus system in the presence of a time-delay and additive noise inputs. Most of these papers treat continuous-time systems only; in discrete-time networks, however, the time-step size along with the topology of the network plays an important role on the network performance.

We should mention that papers [159, 160] investigate the notion of Distributed Rate-Limiting as a mechanism that controls the aggregate service used by a client of a cloud-based service. The main idea is to improve a set of cloud servers with the ability to exchange information with them towards the common purpose: control of the aggregate usage that a cloud-based service uses. However, a comprehensive performance analysis and synthesis are yet to be done for these networks with an arbitrary underlying graph.

In this chapter, our goal is to develop a unified framework for analysis and design of discrete-time distributed rate-limiting systems with a local aggregated view of usage metrics. We investigate performance deterioration (*e.g.*, over-throttling, mismatch, convergence rate) of DSTs with respect to external uncertainties and the update cycle of servers. We develop a graph-theoretic framework to relate the underlying structure of the system to its overall performance measure. We then compare the performance/robustness of DSTs with different topologies. In this work, in addition to the overall performance measure for a network, each node has its own performance measure, which is one of the main differentiators between this work and some other related work [2, 12, 42, 61].

The rest of this chapter is organized as follows. In Section 7.3, we present some basic mathematical concepts and notations employed in this chapter. In Section 7.4, we define and study a distributed system throttler (DST). In Section 7.5, we evaluate the overall performance of a DST with a given nodal performance measure. In Section 7.6, we focus on throttling algorithms which are used by servers. In Section 7.7, we study the impact of the server update cycle on performance. In Section 7.8, two synthesis problems are studied. In Section 7.9, some numerical results are demonstrated. In Section 7.10, we conclude our work and suggest directions for future research.

7.3 Mathematical Notation

Throughout the chapter, the discrete time index is denoted by k. The sets of real (integer), positive real (integer), and strictly positive real (integer) numbers are represented by $\mathbb{R}$ ($\mathbb{Z}$), $\mathbb{R}_+$ ($\mathbb{Z}_+$) and $\mathbb{R}_{++}$ ($\mathbb{Z}_{++}$), respectively. Capital letters, such as A or B, stand for real-valued matrices. We use $\mathrm{diag}(x_1, x_2, \ldots, x_n)$ to denote n-by-n diagonal square matrix with x_1 to x_n on its diagonal. For a square matrix X, $\mathbf{Tr}(X)$ refers to the summation of on-diagonal elements of X. We represent the n-by-1 vector of ones by $\mathbb{1}$. The n-by-n identity matrix is denoted by I. The Moore-Penrose pseudoinverse of matrix A is denoted by $A^\dagger$, *i.e.*, $A^\dagger = \left(A + \frac{1}{n}\mathbb{1}\mathbb{1}^T\right)^{-1} - \frac{1}{n}\mathbb{1}\mathbb{1}^T$. We assume that all graphs are connected, undirected, simple graphs. We represent graph $\mathcal{G}$ by (V, E, w), where V is the node set, E is the edge set, and $w : E \to \mathbb{R}_+$ is the link weight function. We denote by L the Laplacian matrix of the coupling graph $\mathcal{G}$ with the following eigenvalues

$$\lambda_1 = 0 \leq \lambda_2 \leq \cdots \leq \lambda_n. \tag{7.1}$$

In this work, we assume that all graphs are connected, which means $\lambda_2 > 0$.

The *effective resistance* between nodes i and j is defined by:

$$r_{ij} := l^{\dagger}_{ii} + l^{\dagger}_{jj} - l^{\dagger}_{ji} - l^{\dagger}_{ij} \tag{7.2}$$

where $l^{\dagger}_{ji}$ is the (i, j)th entry in $L^{\dagger}$. The white Gaussian noise with zero mean and variance σ^2 is represented by $v \sim N(0, \sigma^2)$.

7.4 A Distributed System Throttler

A distributed system throttler (DST) is a graph $\mathcal{G}$ with n nodes. Each node in the graph is a server with assigned clients that can send it requests. Links in the graph represent communication channels between servers. The global goal of a DST is to keep the aggregate number of accepted requests from all clients for a shared service at or below a prescribed level. The DST does not have a centralized mechanism for setting per-client limits. Instead it consists of multiple servers, each of which makes its own decisions and updates its own limit based on its own measurements and local information from its neighbors (on graph $\mathcal{G}$). Figure 7.1 depicts an example of a distributed throttler with six nodes (servers).

Let's denote by $r_i(k)$ the total number of client requests received by server i at time k. Each node has a total limit on the number of requests that it is allowed to service at time k represented by $x_i(k)$. It is also associated with a performance measure $p_i(k)$ which represents how well that node is working at time k. Examples of typical performance measures are: over-throttling at time k, the ratio of the total allowed usage to total requested usage, or any function of $r_i(k)$, $x_i(k)$, and time. We will talk about functional properties of the performance measure later on in this chapter (see Table I).

In this setup, we assume that each node updates its state $x_i(k)$ based on its neighbors' states and performance measures (*i.e.*, a local aggregated view of usage metrics). The

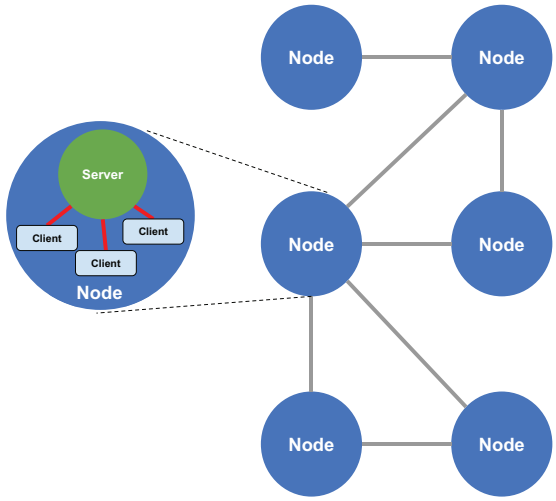

Figure 7.1: An example of a distributed system throttler (DST) with 6 servers. Nodes show servers and links present communication links between servers.

Table 7.1: Examples of nodal performance measures.

Case I	Amount of throttled traffic	$p_i(k) := r_i(k) - x_i(k)$
Case II	Throttled-to-requested traffic ratio	$p_i(k) := \big(r_i(k) - x_i(k)\big)/r_i(k)$
Case III	Logarithm of requested-to-allowed traffic ratio	$p_i(k) := \log\big(r_i(k)/x_i(k)\big)$
Case IV	Amount of allowed traffic	$p_i(k) := x_i(k)$

update law is given by the following difference equation:

$$x_i(k+1) \;=\; x_i(k) \;+\; \gamma \sum_{i \sim j} w_{ij}\big(p_i(k) - p_j(k)\big), \;\; k \in \mathbb{Z}_+, \tag{7.3}$$

where $i \sim j$ denotes that nodes i and j are connected by a link in the underlying graph, $w_{ij} \;=\; w(\{i,j\})$ is the weight of link $\{i,j\}$ in graph $\mathcal{G}$, and parameter γ is a positive number which depends on the size of the time step (*i.e.*, $x(k) := x(k\Delta t)$ where $\Delta t = \gamma$).

The dynamics of the entire network can be written in the following compact form

$$x(k+1) \;=\; x(k) \;+\; \gamma\, L\, p(k), \;\; k \in \mathbb{Z}_+, \tag{7.4}$$

where $x(k)$ is an n-by-1 vector of node limits at time k, $p(k)$ is an n-by-1 vector of

nodal performance measures at time, and L is the Laplacian matrix of the coupling graph $\mathcal{G}$. Then, the accepted number of requests at server i at time k is given by $a_i(k) := \min\{x_i(k), r_i(k)\}$. The total number of requests, the total limit, and the total accepted request for the entire network are defined by

$$r_{\text{total}}(k) := \sum_{i=1}^{n} r_i(k), \tag{7.5}$$

$$l_{\text{total}} := \sum_{i=1}^{n} x_i(0), \tag{7.6}$$

and

$$a_{\text{total}}(k) := \sum_{i=1}^{n} \min\{x_i(k), r_i(k)\}. \tag{7.7}$$

respectively. The ideal curve for total accepted request is given by

$$a_{\text{ideal}}(k) := \min\{l_{\text{total}}, r_{\text{total}}(k)\}. \tag{7.8}$$

The following lemma shows that the total nodal limit is fixed over time.

Lemma 7.4.1. *The total summation of nodal limits is fixed over time, which means*

$$\sum_{i=1}^{n} x_i(k) = \sum_{i=1}^{n} x_i(0), \quad \textit{for all } k \in \mathbb{Z}_{++}, \tag{7.9}$$

and we denote this quantity by l_{total}.

Proof. We multiply both sides of (7.4) by $\mathbb{1}^T$ on the left and get

$$\sum_{i=1}^{n} x_i(k+1) = \sum_{i=1}^{n} x_i(k) + \gamma\, \mathbb{1}^T L\, p(t). \tag{7.10}$$

Assume that $p_i(k)$'s are bounded. Since L is the Laplacian matrix of an undirected graph,

its row and column sums are zero which, completes the proof. □

Based on this result, the total sum of nodal limits is constant and it depends only on initial values, *i.e.*,

$$l_{\text{total}} \;:=\; \sum_{i=1}^{n} x_i(0).$$

Remark 7.4.2. *A similar result is reported in [160], which guarantees the capacity constraint for a generalize distributed rate-limiting system. The condition* (7.10) *holds for any linear consensus network even for those over directed graphs.* ⋄

In the next section, we study the overall performance of DST networks based on their nodal performance measure and the behavior of incoming network traffic/request.

7.5 Properties of Typical Nodal Performance Measures

Each node i is associated with a performance measure $p_i(k)$, which shows the performance of server i at time k. Some examples of performance measures are presented in Table 7.1.

Let us define $p_i(k)$ to be the numbers of throttled request at node i at time k

$$p_i(k) \;:=\; r_i(k) - x_i(k). \tag{7.11}$$

Then, (7.3) can be rewritten as

$$p(k+1) \;=\; (I - \gamma\, L)\, p(k) \;+\; \big(r(k+1) - r(k)\big), \;\; k \in \mathbb{Z}_+. \tag{7.12}$$

Based on the behavior of incoming network traffic/requests, two cases are considered.

Steady loads

Let us assume that the number of client requests incoming at node i is constant across time:

$$r_i(k+1) - r_i(k) \;=\; 0, \;\; k \in \mathbb{Z}_+. \tag{7.13}$$

Equation (7.12) can then be simplified as below

$$p(k+1) \;=\; (I - \gamma\, L)\, p(k), \;\; k \in \mathbb{Z}_+. \tag{7.14}$$

Lemma 7.5.1. *[114] For any $i, j \in \{1, 2, \cdots, n\}$, we have*

$$\lim_{k\to\infty} |p_i(k) - p_j(k)| \;=\; 0,$$

if and only if $\max\{1 - \gamma\lambda_2, \gamma\lambda_n - 1\} < 1$.

Proof. It is straightforward. □

Based on this result, as long as graph $\mathcal{G}$ is connected we can find a positive γ, which guarantees reaching a consensus state (for a small enough positive number γ).

We can now cover the convergence rate based on properties of the underlying graph and the design parameter γ.

Let us define the following performance measure which shows the convergence rate of the DST

$$\Phi_{\rm cr} \;=\; \max_{i\geq 2} |1 - \gamma\lambda_i|, \tag{7.15}$$

smaller $\Phi_{\rm cr}$ meaning faster asymptotic convergence.

Remark 7.5.2 (Role of Topologies for Small γ)**.** *Networks with n servers can be ranked based on their convergence rates; consequently, the path graph topology has the worst*

convergence rate and the complete graph has the best convergence rate (for small enough γ). Also, it can be shown that among tree graphs, star graphs have the best one and path graphs have the worst one. $\diamond$

Non-Steady Loads

Assumption (7.13) is strong and can be relaxed. Let us assume that

$$v_i(k+1) \;:=\; r_i(k+1) - r_i(k) \tag{7.16}$$

where $v(k) \in \mathbb{R}^n$ is a zero mean random vector such as

$$\begin{aligned} \mathbb{E}\left[v(k)\right] \;&=\; 0, \\ \mathbb{E}\left[v(k)v^T(k)\right] \;&=\; \mathrm{Cov}(v), \\ \mathbb{E}\left[v(k)v^T(s)\right] \;&=\; 0, \;\; k \neq s. \end{aligned} \tag{7.17}$$

Then, (7.12) can then be simplified as below

$$p(k+1) \;=\; (-\gamma L + I)\, p(k) \;+\; v(k+1), \;\; k \in \mathbb{Z}_+. \tag{7.18}$$

We can now define the following overall performance measure for the network

$$\Phi_{\mathrm{ss}} \;=\; \lim_{t\to\infty} \mathbb{E}\left[\frac{1}{2n}\sum_{i,j}\left(p_i(k) - p_j(k)\right)^2\right], \tag{7.19}$$

The quantity (7.19) shows the steady-state dispersion of p_i's from their average [2,12,42].

The following theorem presents a closed-form formula for the overall performance of DST (7.18), based on the Laplacian matrix of the underlying graph and the covariance

matrix of the input vector v.

Theorem 7.5.3. *For a given DST* (7.18)*, the overal performance measure* (7.19) *can be quantified as*

$$\Phi_{ss} = \frac{1}{2\gamma}\mathrm{Trace}\left[\left(L - \frac{\gamma}{2}L^2\right)^{\dagger}\mathrm{Cov}(v)\right], \tag{7.20}$$

where $\mathrm{Cov}(v)$ *is the covariance matrix of random vector* $v(k)$*.*

Proof. The overall performance measure is the same as the squared $\mathcal{H}_2$-norm of a discrete linear time invariant system (7.18). Therefore, the measure can be quantified as follows:

$$\Phi_{\mathrm{ss}} \;=\; \mathrm{Trace}\left[P\,\mathrm{Cov}(v)\right], \tag{7.21}$$

where $P \succeq 0$ is the solution of the following discrete Lyapunov equation

$$(I - \gamma L)P(I - \gamma L)^T \;-\; P \;+\; I \;=\; 0.$$

By doing some calculation it follows that

$$P \;=\; (2L - \gamma L^2)^{\dagger}. \tag{7.22}$$

Using (7.21) and (7.22) we get the desired result. □

Remark 7.5.4 (Independent v_i's)**.** *In the case where* v_i*'s are independent then* $\mathrm{Cov}(v)$ *is a diagonal matrix* $\gamma\,\mathrm{diag}(\sigma_1^2, \ldots, \sigma_n^2)$ *where* σ_i *depends on the property of signal* r_i*. We get*

$$\Phi_{ss} \;=\; \frac{1}{2}\sum_{i=1}^{n} c_{ii}^{\dagger}\sigma_i^2, \tag{7.23}$$

where $(L-\frac{\gamma}{2}L^2)^\dagger = [c_{ij}^\dagger]$. *Based on* (7.23)*, we can obtain a centrality measure for servers. Indeed,* $c_{ii}^\dagger$ *shows the impact of server* i *on the overall performance. See [42] for more details on centrality measures with respect to* $\mathcal{H}_2$*-norm of the system (the focus of [42] is on the class of continuous-time linear consensus networks however).* $\diamond$

Remark 7.5.5 (Independent and identically-distributed v_i's)**.** *Based on Theorem 7.5.3, the overall performance measure of the network can be calculated based on spectral eigenvalues of the coupling graph and the variance of changing demands (i.e.,* $r_i(k+1) - r_i(k) \sim N(0, \gamma\,\sigma^2)$*) as follows*

$$\Phi_{\rm ss} \;=\; \begin{cases} \sum_{i=2}^{n} \frac{\sigma^2}{\lambda_i(2-\gamma\,\lambda_i)},\; 0<\lambda_i<2/\gamma \;\; \textit{for } i=2,\cdots,n \\ \infty, \qquad\qquad \textit{otherwise} \end{cases} \tag{7.24}$$

We note that $0 < \lambda_i < 2/\gamma$ *for* $i = 2, \cdots, n$ *is the same as the condition that the system without noise converges (cf., Lemma 7.4.1).* $\diamond$

The quantity (7.24) has a close connection with the "total effective resistance" of an electric network as follows

$$\lim_{\gamma\to 0} \Phi_{\rm ss} \;=\; \frac{\sigma^2}{2n} \sum_{i>j} r_{ij}, \tag{7.25}$$

where r_{ij} is the effective resistance between node i and j, *i.e.*,

$$r_{ij} \;:=\; l_{ii}^\dagger \;+\; l_{jj}^\dagger \;-\; l_{ij}^\dagger \;-\; l_{ji}^\dagger, \;\; L^\dagger = [l_{ij}^\dagger].$$

For more details see [163].

Remark 7.5.6 (Another interpretation of the overall measure)**.** *Let us assume that* $r_i(0)$*'s are given with the normal distribution, and* r_i*'s remain constant. Then the expected total*

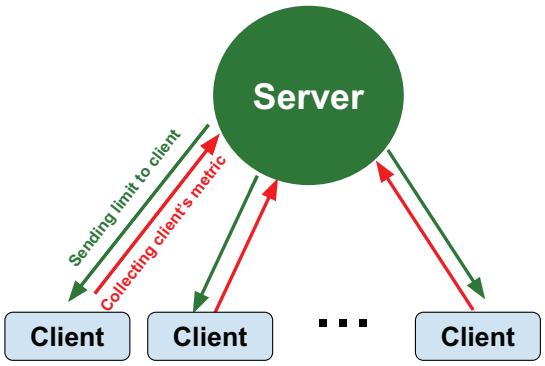

Figure 7.2: A server with its clients.

mismatch loss can be obtained based on

$$\mathbb{E}\left[\frac{1}{n}\sum_{k=0}^{\infty}\sum_{i>j}\left(p_i(k)-p_j(k)\right)^2\Delta t\right] = \frac{1}{2\gamma}\text{Trace}\left[\left(L-\frac{\gamma}{2}L^2\right)^{\dagger}\text{Cov}(v)\right] = \Phi_{ss}. \tag{7.26}$$

◇

Due to space limitations, other nodal performance measures defined in Table 7.1 are briefly analyzed in the appendix.

7.6 Throttling Algorithms at Node Level

In this part, we focus on the structure of each node. Each node consists of a server with its clients (see, for example, Figure 7.2). Each node can have its own algorithm to handle its clients. To do so, each server collects all metrics (*i.e.*, number of requests) from its clients, then aggregates all metrics and then pushes new limits to its clients based

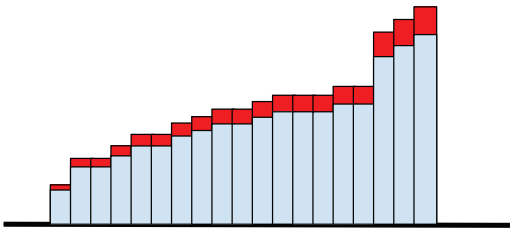

Figure 7.3: Requested quota and throttled quota for each user based on an algorithm which keeps the throttled ratios uniform over all tasks.

on the aggregated information (all in one update cycle). For example, viable throttling algorithms can be considered to throttle same amount, ratio, or the logarithm of ratio from all tasks until the total limit is reached (please see performance measures in Table I).

Figure 7.3 depicts requested quota (*i.e.*, number of requests) and throttled quota for each client based on an algorithm which keeps the throttled ratios uniform over all tasks. Each bar shows the number of requests per client. Blue bars show clients' requests. The red area shows the throttled request traffic. The clients are sorted by ascending order of requests. Similarly, Figure 7.4 demonstrates a simple load balancing algorithm[1] which distributes incoming requests across all tasks as uniformly as possible. The blue dashed line shows the allowed limit on each task.

We should note that the total number of request, $r_i(k)$, at this server (server i) is the area of all bars and the total allowed request is the area of all blue bars, *i.e.*, $a_i(k)$.

[1]Distributing incoming network traffic/request across all tasks as uniform as possible.

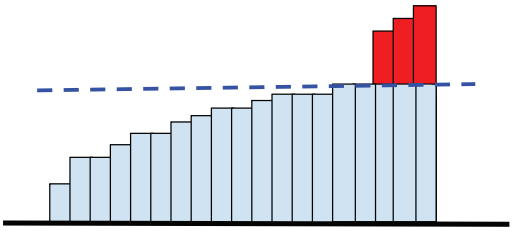

Figure 7.4: Requested quota and throttled quota for each user based on a simple load balancing algorithm.

7.7 Impact of the Server Update Cycle

In this section, we study the effect of the server update cycle on our analysis. As shown in Section 7.5, the overall performance measure of a DST depends on its Laplacian eigenvalues and the server update cycle. To enhance the overall performance of the network, one can obtain the optimal update cycle for all servers.

The following theorem presents the optimal update cycle for a DST in the case of steady loads (*i.e.*, when the number of client requests is constant across time).

Theorem 7.7.1. *For a given DST* (7.14) *with a graph $\mathcal{G}$, the optimal update cycle is given by*

$$\gamma_{\text{optimal}} = \frac{2}{\lambda_2 + \lambda_n}. \tag{7.27}$$

Proof. We need to solve the following convex optimization

$$\underset{\gamma>0}{\text{minimize}} \quad \max_{i\geq 2} |1 - \gamma\lambda_i| \tag{7.28}$$

It is not difficult to see that $2(\lambda_2 + \lambda_n)^{-1}$ minimizes the cost function. We have

$$0 < \lambda_2 \leq \cdots \leq \lambda_n,$$

and, accordingly, we can rewrite the cost function as follows

$$\max_{i \geq 2} |1 - \gamma\lambda_i| = \max\left\{1 - \gamma\lambda_2, \gamma\lambda_n - 1\right\}. \tag{7.29}$$

To minimize (7.29), we need

$$1 - \gamma\lambda_2 \;=\; \gamma\lambda_n - 1, \tag{7.30}$$

since if $1-\gamma\lambda_2 \neq \gamma\lambda_n - 1$, one can decrease the cost function by increasing or decreasing γ . Therefore, the optimal γ is the solution of (7.30). This completes the proof. □

In the case of non-steady loads, having a closed-form formula for the optimal update time based on the Laplacian eigenvalues seems difficult. However, one can obtain the solution by solving the following convex optimization problem:

$$\underset{\gamma>0}{\text{minimize}} \;\; \frac{1}{2\gamma}\text{Trace}\left[\left(L - \frac{\gamma}{2}L^2\right)^{\dagger}\right] \tag{7.31}$$

In this case, the optimal update time can be bounded from above and below by $1/\lambda_n$ and $1/\lambda_2$, respectively.

7.8 DST Synthesis Problems

In this section, we present our main results on the design of optimal distributed rate-limiting system. We formulate our problems as convex optimization problems. Questions

we are trying to answer in this section are

- What are the optimal link weights for the *fastest* DST network?

- What are the optimal link weights for the *most robust* DST network?

Depending on which nodal and overall performance measures are chosen, one can come up with different optimal topologies.

7.8.1 The Fastest DST Process

Here we briefly describe the problem of finding the fastest DST on a given underlying topology. The optimal weights can be found by solving the following optimization problem

$$\begin{aligned} &\underset{w(e)}{\text{minimize}} \;\; \max_{i\geq 2} |1-\gamma\lambda_i| \\ &\text{subject to} \;\; w(e) \;\geq\; 0, \;\; \text{for all} \;\; e \in E \end{aligned} \tag{7.32}$$

This problem was studied before in [139]. Problem (7.32) can be cast as a semidefinite programming (SDP) problem as follows

$$\begin{aligned} &\underset{w(e),\theta}{\text{minimize}} \;\; \theta \\ &\text{subject to} \;\; -\theta I \preceq I - \gamma \sum_{e\in E} w(e) L_e - \frac{1}{n}\mathbb{1}\mathbb{1}^T \preceq \theta I \\ &\qquad\qquad w(e) \geq 0, \;\; e \in E \end{aligned} \tag{7.33}$$

where L_e is the unweighted Laplacian matrix of link e.

7.8.2 The Most Robust DST Process

Here we briefly describe the problem of finding the most robust DST on a given underlying topology. The optimal weights can be found by solving the following problem

$$\begin{aligned} \underset{w(e)}{\text{minimize}} \;\; & \frac{1}{2\gamma}\text{Trace}\left[\left(L-\frac{\gamma}{2}L^2\right)^{\dagger}\right] \\ \text{subject to} \;\; & w(e) \;\geq\; 0, \;\; \text{for all} \;\; e\in E \\ & L \;=\; \sum_{e\in E} w(e)L_e \\ & \max_{i\geq 2}|1-\gamma\lambda_i| \;\leq\; 1 \end{aligned} \tag{7.34}$$

We note that $\Phi_{\text{ss}} = \frac{1}{2\gamma}\text{Trace}\left(\left(L-\frac{\gamma}{2}L^2\right)^{\dagger}\right)$ is a convex function of the link weights. To find the solution of (7.34) one can use a variety of standard methods for convex optimization (*e.g.*, interior-point methods and subgradient-based methods).

Theorem 7.8.1. *Problem* (7.34) *can be formulated as a SDP problem as follows*

$$\begin{aligned} \underset{w(e),Y}{\text{minimize}} \;\; & \frac{1}{2\gamma}\text{Trace}\,[Y]-\frac{1}{2\gamma^2} \\ \text{subject to} \;\; & w(e) \;\geq\; 0, \;\; \text{for all} \;\; e\in E \\ & L \;=\; \sum_{e\in E} w(e)L_e \\ & 0 \;\preceq\; I-\frac{1}{2}\left(\gamma L+(1/n)\mathbb{1}\mathbb{1}^T\right) \;\preceq\; I \\ & \begin{bmatrix} L+\frac{1}{\gamma n}\mathbb{1}\mathbb{1}^T & L & I \\ L & \frac{2}{\gamma}I & 0 \\ I & 0 & Y \end{bmatrix} \;\succeq\; 0 \end{aligned} \tag{7.35}$$

Proof. We need the following condition to hold in order to guarantee that the network is

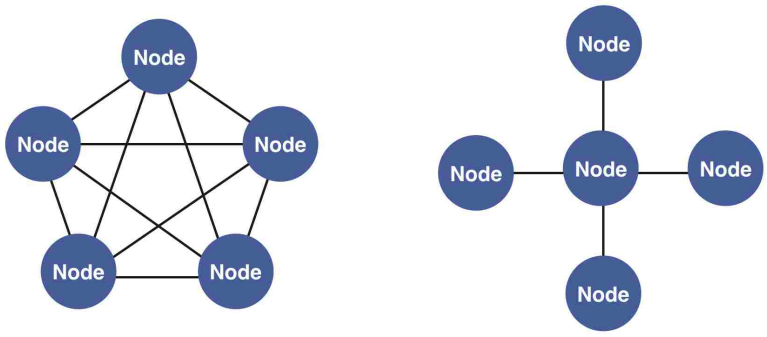

Figure 7.5: Two DST networks with 5 servers over a complete graph and a star graph.

marginally stable:

$$0 \preceq I - \frac{1}{2}\left(\gamma L + (1/n)\mathbb{1}\mathbb{1}^T\right) \preceq I. \tag{7.36}$$

Then, according to (7.36) and the Schur complement condition for positive semidefiniteness it follows that

$$\begin{bmatrix} L + \frac{1}{\gamma n}\mathbb{1}\mathbb{1}^T & L \\ L & \frac{2}{\gamma}I \end{bmatrix} \succeq 0. \tag{7.37}$$

Again, using the Schur complement condition for positive semidefiniteness, (7.35) and (7.37), we get the following equivalent condition

$$Y - \frac{1}{\gamma n}\mathbb{1}\mathbb{1}^T \succeq \left(L - \frac{\gamma}{2}L^2\right)^{\dagger}, \tag{7.38}$$

which completes the proof. □

7.9 Illustrative Numerical Simulations

In this section, we support our theoretical developments with illustrative examples that provide better insight into the role of the underlying graph topology in the DST network.

Example 7.9.1. *Consider two DST networks with five servers over complete graph $\mathcal{K}_5$ and star graph $\mathcal{S}_5$ as depicted in Figure 7.5. Let us assume that the update cycle is given and fixed (without loss of generality $\gamma = 1$). Based on the results presented in Theorem 7.7.1, one can obtain the optimal weight links for both networks to get the fastest DST (See Table II).*

Table 7.2: Optimal link weights.

	Complete Graph $\mathcal{K}_5$	Star Graph $\mathcal{S}_5$
Optimal Weight	$w(e) = 1/5$	$w(e) = 1/3$

For each network the weights are uniform since their underlying graphs are edge-transitive.

Example 7.9.2. *Consider two DST networks with 10 servers over graphs depicted in Figures 7.6 and 7.7. Let us assume that in both graphs all links have a weight of one. Based on the results presented in Theorem 7.7.1, one can obtain the optimal update cycle for both networks to get the fastest DST (see Table III).*

Table 7.3: Optimal update cycles.

	Graph $\#1$	Graph $\#2$
Optimal update cycle	$\Delta t = 0.4226$	$\Delta t = 0.2222$

Moreover, let us consider $1,000$ clients that are randomly assigned to 10 servers such that each server has 100 clients. Figure 7.8 shows the simulation results that are obtained for each of these two DST networks given a randomly generated usage curve over $1,000$ cycles. As expected, the overall performance of the DST over graph $\#2$ is better (i.e., over-throttling is less severe) than the performance of the DST over graph $\#1$ (for small time step $\gamma = 0.02$).

Table 7.4: Overall network performance measures.

	Graph #1	Graph #2
$\Phi_{\mathbf{cr}}$	0.9969	0.9727
$\Phi_{\mathbf{ss}}$	334.7965	69.3075
Over-throttling %	6.2%	2.8%

In Figure 7.8, the blue curve shows the total number of requests versus time, i.e.,

$$r_{total}(k) \;=\; \sum_{i=1}^{10} r_i(k),$$

the black dashed line presents the total limit for the entire network, i.e.,

$$l_{total} \;=\; \sum_{i=1}^{10} x_i(0),$$

and the red and green curves show the total accepted requests for graph #1 *and graph* #2 *respectively, i.e.,*

$$a_{total}(k) \;=\; \sum_{i=1}^{10} \min\left\{x_i(k), r_i(k)\right\}.$$

We should note that, the ideal curve for total accepted request is given by (7.8)*. Therefore, the percentage of over-throttling can be defined as follows*

$$\textit{Over-throttling \%} := \frac{\sum_{k=0}^{N}\left(a_{ideal}(k) - a_{total}(k)\right)}{\sum_{k=0}^{N} a_{ideal}(k)} \times 100,$$

where N *is the number of cycles (in this example* $N = 1,000$*).*

7.10 Conclusion

In this chapter, we investigate performance deterioration (*e.g.*, over-throttling) of distributed system throttlers with respect to external uncertainties and server time cycles.

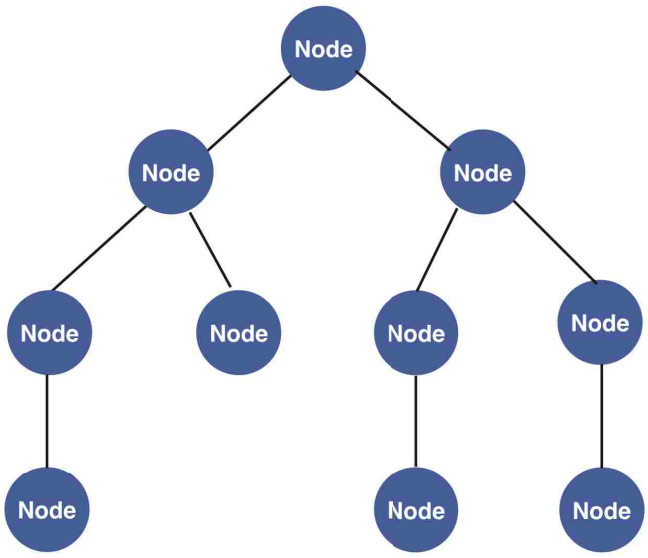

Figure 7.6: A DST network with 10 servers over a tree graph (graph #1).

We develop a graph-theoretic framework to relate the underlying structure of the system to its overall performance measure. We then compare the performance/robustness of the proposed distributed system throttlers with different underlying graphs. A promising research direction is to investigate the overall performance measure of DST networks with respect to the other nodal performance measures.

Appendix: Other Nodal Performance Measures

In this part, we present the dynamics of the DST for other nodal performance measure defined in Table I (*Case I* is studied in Section 7.5).

Case II:

Assume that the performance measure at server i is given by

$$p_i(k) \;=\; \frac{r_i(k) - x_i(k)}{r_i(k)}, \tag{7.39}$$

and $r_i(k) > 0$. Then, we can rewrite (7.3) in the following form

$$\begin{aligned} x(k+1) = \gamma\, L\ \mathrm{diag}\left[r_1(k)^{-1}, \cdots, r_n(k)^{-1}\right](r(k) - x(k)) \\ +\ x(k),\ \ k \in \mathbb{Z}_+. \end{aligned} \tag{7.40}$$

Let assume that $r_i(k) = \mathfrak{r}$ for all $k \in \mathbb{Z}_+$ and $i \in \{1, 2, \cdots, n\}$. So, we have

$$x_i(k) \;=\; -\,\mathfrak{r}\,(p_i(k) - 1)\,. \tag{7.41}$$

Then, it follows that

$$p(k+1) \;=\; \left(I - \frac{\gamma}{\mathfrak{r}} L\right) p(k). \tag{7.42}$$

In this case, in addition to the coupling graph and the update cycle, the values of $\mathfrak{r}$ plays a role in the convergence rate of the network (same for other overall performance measures).

Case III:

Next, we assume that the performance measure at server i is given by

$$p_i(k) \;=\; \log r_i(k) - \log x_i(k). \tag{7.43}$$

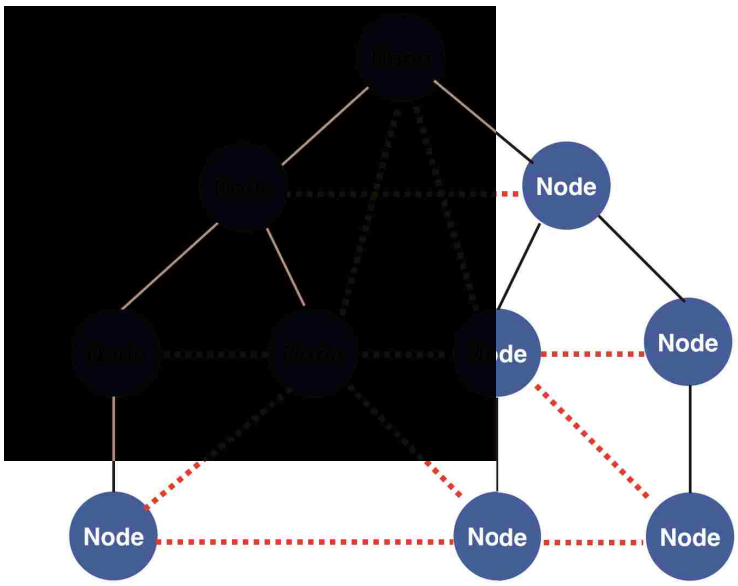

Figure 7.7: A DST network with 10 servers over a tree graph with some additional links, red dotted links (graph $\#2$).

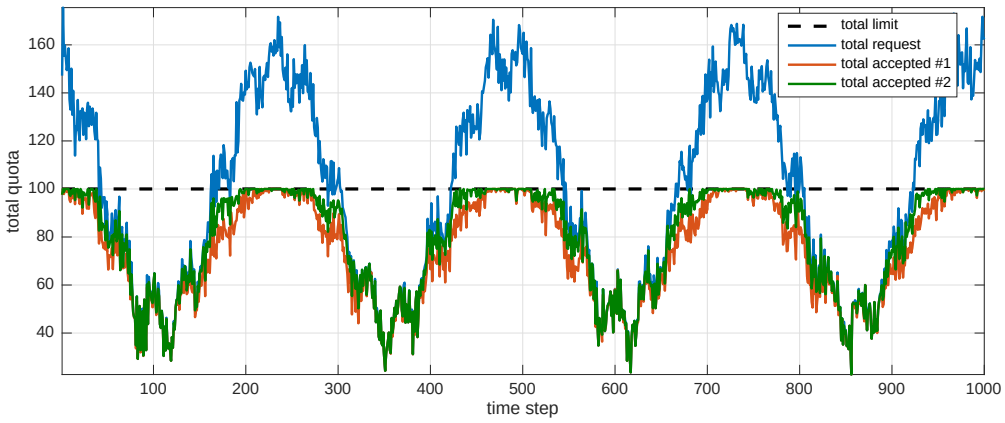

Figure 7.8: The simulation results for two DST networks with $\gamma = 0.02$ over graphs $\#1$ and $\#2$ with 10 nodes.

Assume that $r_i(k) = \mathfrak{r}$, for all $k \in \mathbb{Z}_+$ and $i \in \{1, 2, \cdots, n\}$. Therefore, we get

$$x_i(k) \;=\; \mathfrak{r}\, e^{-p_i(k)}. \tag{7.44}$$

Then, it follows that

$$\exp\left(-p(k+1)\right) \;=\; \exp\left(-p(k)\right) + \frac{\gamma}{\mathfrak{r}}\, L\, p(k), \;\; k \in \mathbb{Z}_+, \tag{7.45}$$

where $\exp p(k) := \left[e^{p_1(k)}, \cdots, e^{p_n(k)}\right]^T$. Let us define

$$\bar{p}(k) := \exp\left(-p(k)\right), \tag{7.46}$$

using (7.45) and (7.46), it follows that

$$\bar{p}(k+1) \;=\; \bar{p}(k) - \frac{\gamma}{\mathfrak{r}}\, L\, \ln \bar{p}(k), \;\; k \in \mathbb{Z}_+, \tag{7.47}$$

where

$$\ln \bar{p}(k) \;:=\; \left[\ln \bar{p}_1(k), \cdots, \ln \bar{p}_n(k)\right]^T.$$

Case IV:

Finally, let us assume that

$$p_i(k) \;=\; x_i(k),$$

for $i = 1, \cdots, n$. Then, dynamics (7.3) can be rewritten in the following form

$$p(k+1) \;=\; (I + \gamma L)\, p(k). \tag{7.48}$$

In this case, based on Lemma 7.5.1 the system is unstable, which means the state trajectories are unbounded. Therefore we consider additional constraints to make them bounded as follows: the state of node i at time $k+1$ is not updated (*i.e.*, $x_i(k+1) = x_i(k)$) and its information at time k is not used for updating the states of neighboring nodes at time $k+1$ when

- $x_i(k) = r_i(k)$ and $x_i(k+1) - x_i(k) > 0$,

- $x_i(k) = 0$ and $x_i(k+1) - x_i(k) < 0$.

We should note that also in this case the following equality holds

$$\sum_{i=1}^{n} x_i(k) = \sum_{i=1}^{n} x_i(0).$$

In a steady-state, each state x_i reaches its boundaries (i.e., 0 and r_i) or a value between them.

Chapter 8

Network Sparsification with Guaranteed Systemic Performance Measures

8.1 Abstract

A sparse consensus network is one whose number of coupling links is proportional to its number of subsystems. Optimal design problems for sparse consensus networks are more amenable to efficient optimization algorithms. More importantly, maintaining such networks are usually more cost effective due to their reduced communication requirements. Therefore, approximating a given dense consensus network by a suitable sparse network is an important analysis and synthesis problem. In this chapter, we develop a framework to produce a sparse approximation of a given large-scale network with guaranteed performance bounds using a nearly-linear time algorithm. First, the existence of a sparse approximation of a given network is proven. Then, we present an efficient and fast algo-

rithm for finding a near-optimal sparse approximation of a given network. Finally, several examples are provided to support our theoretical developments.

8.2 Introduction

Performance improvement in interconnected networks of coupled dynamical systems as well as reducing their design complexity by sparsifying their underlying coupling structures are two of the important design issues, which have been subject of active research in past few years [4, 6, 18–23].

In [18], we introduce a class of operators, so called systemic performance measure, for linear consensus networks that provides a unified framework to evaluate network-wide performance of a network. Several existing and popular performance measures in the literature, such as $\mathcal{H}_2$ and $\mathcal{H}_\infty$ norms of a consensus network from its disturbance input to its output, are examples of systemic performance measures. This class of operators captures the quintessence of a viable performance measure for consensus networks: homogeneity, monotonicity, convexity, and orthogonal/permutation invariance. An important contribution of this reference paper is that it enables us to optimize performance of a consensus network solely based on its intrinsic features. The authors formulate several optimal design problems, such as weight adjustment as well as rewiring of coupling links, with respect to this general class of systemic performance measures and propose efficient algorithms to solve them.

In [5,12], we quantify several fundamental tradeoffs between a $\mathcal{H}_2$-based performance measure and sparsity measures of a linear consensus network. The problem of sparse consensus network design has been considered before in [6, 57, 58], where they formulate an ℓ_0-regularized $\mathcal{H}_2$ optimal control problem. There are also some less related papers to the subject of this chapter that we are not able to discuss them here due to space limitations.

The main shortcoming of all these works is that they are heavily relied on computational tools with no analytical performance guarantees for the obtained solution. More importantly, the proposed methods in these papers suffer from computational complexity as the network size grows.

In this chapter, we specifically address the following network design problem: given a linear consensus network with an undirected connected underlying graph, the *network sparsification* problem seeks to replace the coupling graph of the original network with a reasonably sparser subgraph so that the behavior of the original and the sparsified networks is similar in an appropriately defined sense. Such situations arise frequently when real-world large-scale dynamical networks need to be simulated, controlled or redesigned using efficient computational tools that are specifically tailored for optimization problems with sparse structures. We develop a general methodology that computes sparsifiers of a given consensus network using a nearly-linear time $\tilde{\mathcal{O}}(m)$[1] algorithm with guaranteed systemic performance bounds, where m is the number of links. Unlike other existing work on this topic in the literature, our proposed framework: (i) works for a broad class of systemic performance measures including $\mathcal{H}_2$-based performance measures, (ii) does not involve any sort of relaxations such as ℓ_0 to ℓ_1, (iii) provides guarantees for the existence of a sparse solution, (iv) can partially sparsify predetermined portions of a given network; and most importantly, (v) gives guaranteed systemic performance certificates.

While our approach is relied on several existing works in algebraic graph theory [63, 64], our control theoretic contributions are threefold. First, we show that every given linear consensus network has a sparsifier network such that the two networks yield comparable performances with respect to any systemic performance measure. Second, we develop a framework to find a sparse approximation of large-scale consensus networks

[1] We use $\tilde{\mathcal{O}}(.)$ to hide poly $\log\log$ terms from the asymptotic bounds. Thus, $f(n) \in \tilde{\mathcal{O}}\left(g(n)\right)$ means that there exists $k > 0$ such that $f(n) \in \mathcal{O}\left(g(n)\log^k g(n)\right)$.

using a fast randomized algorithm. We note that while the coupling graph of the sparsified network is a subset of the coupling graph of the original network, the weights of links (the strength of each coupling) in the sparsified network are adjusted accordingly to reach predetermined levels of systemic performance. Third, we prove that our development can also be applied for partial sparsification of large-scale networks, which means that we can sparsify a prespecified subgraph of the original network to find an approximation of the network with fewer links. This is practically plausible as our algorithm can be spatially localized, if necessary, and it does not require to receive information of the entire coupling graph of the network.

8.3 Notation and Preliminaries

The set of real, positive real, and strictly positive real numbers are represented by $\mathbb{R}$, $\mathbb{R}_+$ and $\mathbb{R}_{++}$, respectively. A matrix is generally represented by an upper case letter, say $X = [x_{ij}]$, where x_{ij} is the $(i,j)^{\text{th}}$ element of matrix X and X^{T} indicates the transposition of matrix X. We assume that $\mathbb{1}_n$ and I_n denote the $n \times 1$ vector of all ones and the $n \times n$ identity matrix, respectively. J_n denotes the $n \times n$ matrix of all ones, and $M_n = I_n - 1/n J_n$ defines the centering matrix. All graphs that we deal with in this chapter are assume to be finite, simple, undirected, and connected. The graphs herein are generally represented by $\mathcal{G} = (\mathcal{V}, \mathcal{E}, w)$, where $\mathcal{V}$ is the set of nodes, $\mathcal{E} \subset \mathcal{V} \times \mathcal{V}$ is the set of links, and $w : \mathcal{V} \times \mathcal{V} \to \mathbb{R}_+$ is the weight function. The value of the weight function is zero for $e \in \mathcal{V} \times \mathcal{V} \setminus \mathcal{E}$ and non-zero for $e \in \mathcal{E}$. The degree of each node $i \in \mathcal{V}$ is defined by:

$$d_i := \sum_{e=\{i,j\} \in \mathcal{E}} w(e). \tag{8.1}$$

The adjacency matrix $A = [a_{ij}]$ of graph $\mathcal{G}$ is defined in such a way that $a_{ij} = w(e)$ if $e = \{i, j\} \in \mathcal{E}$, and $a_{ij} = 0$ otherwise. The Laplacian matrix of graph $\mathcal{G}$ with n nodes is defined by $L := \Delta - A$, where $\Delta = \mathrm{diag}[d_1, \ldots, d_n]$. Since graph $\mathcal{G}$ is both undirected and connected, matrix L has $n - 1$ positive eigenvalues and one zero eigenvalue. We denote the set of Laplacian matrices of all connected weighted graphs with n nodes by $\mathfrak{L}_n$. The eigenvalues of a Laplacian matrix are indexed in ascending order $0 = \lambda_1 \leq \lambda_2 \leq \cdots \leq \lambda_n$. The Moore-Penrose pseudo-inverse of L is denoted by $L^\dagger = [l^\dagger_{ji}]$ which is a square, symmetric, doubly-centered and positive semi-definite matrix. For a given Laplacian matrix L, the corresponding resistance matrix $R = [r_{ij}]$ is defined using the Moore-Penrose pseudo-inverse of L by setting

$$r_{ij} \;=\; l^\dagger_{ii} + l^\dagger_{jj} - 2l^\dagger_{ij}.$$

The quantity r_{ij} is called the effective resistance between nodes i and j. Moreover, we denote the effective resistance of link $e = \{i, j\}$ by $r(e) = r_{ij} = r_{ji}$.

The spectral zeta function of order $q \geq 1$ is defined by

$$\rho_{\mathrm{zeta,q}}(L) \;:=\; \left(\sum_{i=2}^{n} \lambda_i^{-q} \right)^{1/q}, \tag{8.2}$$

where $\lambda_2, \ldots, \lambda_n$ are eigenvalues of Laplacian matrix L [140].

8.4 Problem Formulation

Network model: We consider a class of consensus networks, where each node corresponds to a subsystem with scalar state variables x_i and control inputs u_i whose dynamics evolve

in time according to

$$\dot{x}_i(t) \;=\; u_i(t) + \xi_i(t) \tag{8.3}$$

$$y_i(t) \;=\; x_i(t) - \bar{x}(t) \tag{8.4}$$

for all $i = 1, \ldots, n$, where $x_i(0) = 0$ is the initial condition and

$$\bar{x}(t) = \frac{1}{n}\big(x_1(t) + \ldots + x_n(t)\big)$$

is the average of all states at time instant t. The impact of the uncertain environment on each agent's dynamics is modeled by the exogenous noise/disturbance input $\xi_i(t)$. By applying the following feedback control law to the agents of this network

$$u_i(t) \;=\; \sum_{j=1}^{n} k_{ij}\big(x_j(t) - x_i(t)\big). \tag{8.5}$$

The closed-loop dynamics of network (8.3-8.5) can be written in the following compact form

$$\mathcal{N}(L): \begin{cases} \dot{x}(t) \;=\; -Lx(t) + \xi(t), \;\; x(0) \;=\; x_0 \\ y(t) \;=\; \big(I_n - \frac{1}{n}\mathbb{1}_n\mathbb{1}_n^{\mathrm{T}}\big)\, x(t) \end{cases} \tag{8.6}$$

where x, ξ and y denote the state vector of the entire network, the exogenous disturbance input and the output vector of the network, respectively. Matrix $L = [l_{ij}]$ is a Laplacian matrix which is defined by

$$l_{ij} := \begin{cases} -k_{ij} & \text{if} \quad i \neq j \\ \\ k_{i1} + \ldots + k_{in} & \text{if} \quad i = j \end{cases} \tag{8.7}$$

The underlying coupling graph of the consensus network (8.6) is a graph $\mathcal{G} = (\mathcal{V}, \mathcal{E}, w)$ with node set $\mathcal{V} = \{1, \ldots, n\}$, link set

$$\mathcal{E} = \Big\{ \{i, j\} \;\big|\; \forall\, i, j \in \mathcal{V},\ k_{ij} \neq 0 \Big\}, \tag{8.8}$$

and weight function

$$w(e) = k_{ij}, \tag{8.9}$$

for all $e = \{i, j\} \in \mathcal{E}$, and $w(e) = 0$ if $e \notin \mathcal{E}$. The Laplacian matrix of graph $\mathcal{G}$ is equal to L.

Assumption 8.4.1. *All feedback gains (weights) satisfy the following properties for all* $i, j \in \mathcal{V}$*:*

(a) non-negativity: $k_{ij} \geq 0$*,*

(b) symmetry: $k_{ij} = k_{ji}$*,*

(c) simpleness: $k_{ii} = 0$*.*

Property (b) implies that feedback gains are symmetric and (c) means that there is no self-feedback loop in the network.

Assumption 8.4.2. *The coupling graph* $\mathcal{G}$ *of the consensus network* (8.6) *is connected and time-invariant.*

Based on Assumption 8.4.2, one can verify that the only mode of the state matrix of the network which is not stable has the corresponding eigenvector $\mathbb{1}_n$. This mode is unobservable from the performance output as the output matrix of the network satisfies $\left(I_n - \frac{1}{n}\mathbb{1}_n\mathbb{1}_n^{\mathsf{T}}\right)\mathbb{1}_n = 0$.

The problem: The focus of this chapter is to develop a framework to find a sparse approximation of a given consensus network. A sparse consensus network is one whose

number of feedback gains (*i.e.* non-zero k_{ij}'s) is proportional to the number of its subsystems, which means that in average its subsystems connected to a few subsystems and its number is independent of the network size. Sparse consensus networks are often easier to build, maintain or simulate than dense networks. But in many cases, we deal with dense networks. Therefore, by approximating a dense network of interest by a suitable sparse network, one can save time and cost. Our goal is to present a nearly-linear time $\mathcal{O}(m \log^c m)$ algorithm (for some constant c) to compute a sparse approximation of a given linear consensus network, such that the two networks yield comparable performances with respect to any systemic performance measure.

8.5 Systemic Performance Measures

A systemic measure in this chapter refers to a real-valued operator over the set of all consensus networks with dynamics (8.6), with the purpose of quantifying the performance of a network. Since every network with dynamics (8.6) is uniquely determined by its Laplacian matrix, it is reasonable to define a systemic performance measure as an operator on set $\mathfrak{L}_n$.

Definition 8.5.1. *An operator $\rho : \mathfrak{L}_n \to \mathbb{R}_+$ is said to be a Schur-convex systemic measure, or for short SCSM, if it satisfies the following properties for all matrices in $\mathfrak{L}_n$:*

1. Homogeneity: For some $\alpha > 0$,

$$\rho(\kappa L) \;=\; \kappa^{-\alpha}\rho(L),\; \forall \kappa > 1.$$

2. Monotonicity: If $L_2 \preceq L_1$, then

$$\rho(L_1) \;\leq\; \rho(L_2).$$

3. Convexity: For all $0 \leq c \leq 1$*,*

$$\rho(cL_1 + (1-c)L_2) \ \leq \ c\rho(L_1) + (1-c)\rho(L_2).$$

4. Orthogonal invariance: For any orthogonal matrix U*,*

$$\rho(L) \ = \ \rho(ULU^T).$$

We adopt an axiomatic approach to introduce and categorize a general class of performance measures that captures the quintessence of a meaningful measure of performance in large-scale dynamical networks [164]. Property 1 implies that intensifying the coupling weights by ratio $\kappa > 1$ results in κ^α times better performance. Property 2 guarantees that strengthening couplings in a consensus network never worsens the network performance with respect to a given SCSM. The monotonicity property induces a partial ordering on all linear consensus networks with dynamics (8.6). This property imposes emergence of fundamental tradeoffs between performance of a network and sparsity of its coupling graph. In essence, adding new coupling links or strengthening the existing couplings would result in a better network performance. Property 3 is defined for the pure purpose of having favorable (convex) design optimization problems. Property 4 clearly indicates that a SCSM depends only on the eigenvalues of the Laplacian matrix. Property 4 has two important implications. First, it reveals that two linear consensus networks with isospectral coupling graphs[2] shall yield the same performance with respect to a given SCSM. Second, it implies that a SCSM depends on the entire topology of the underlying graph of network, which explains the terminology why this class of performance measures are referred to as systemic measures. We now try to generalize this class of measures by

[2]Two graphs are called isospectral if and only if their Laplacian matrices have the same multisets of eigenvalues.

$\rho(.)$	SCSM	CSM
$\rho_{\mathcal{H}_\infty} = {\lambda_2}^{-1}$	✓	✓
$\rho_{\mathcal{H}_2} = \left(\frac{1}{2}\sum_{i=2}^{n} {\lambda_i}^{-1}\right)^{\frac{1}{2}}$	✓	✓
$\rho_{\text{zeta},p} = \left(\sum_{i=2}^{n} \lambda_i^{-p}\right)^{\frac{1}{p}}$	✓	✓
$\rho_{\text{local}} = \frac{1}{2}\sum_{i=1}^{n} {d_i}^{-1}$		✓

Table 8.1: Examples of convex systemic measures and Schur-convex systemic measures.

relaxing Property 4.

Definition 8.5.2. *An operator $\rho : \mathfrak{L}_n \to \mathbb{R}_+$ is said to be a convex systemic measure, or for short CSM, if it satisfies Properties 1, 2, 3 and*

4. permutation invariance: For every permutation matrix P,*

$$\rho(L) \;=\; \rho(PLP^T),$$

for all matrices in $\mathfrak{L}_n$.

Notice that since the condition of Property 4* is weaker than that of Property 4, any SCSM is also a CSM. We now present some existing and widely-used systemic performance measures for linear consensus networks (see Table 8.1).

$\mathcal{H}_p$ system norms: For linear consensus network with dynamics (8.6), we define $\mathcal{H}_p$ norm of the system for $2 \leq p \leq \infty$ by

$$\|G\|_{\mathcal{H}_p} \;:=\; \left(\frac{1}{2\pi}\int_{-\infty}^{\infty}\sum_{k=1}^{n}\sigma_k(G(j\omega))^p\,d\omega\right)^{\frac{1}{p}}, \tag{8.10}$$

where G is the transfer matrix of the network with dynamics (8.6) from $\xi(t)$ to $y(t)$ and $\sigma_k(j\omega)$ for $k = 1, \ldots, n$ are singular values of $G(j\omega)$. In order to guarantee that performance measure (8.10) is well-defined, marginally stable and unstable modes of

consensus network should be unobservable from the performance output $y(t)$. Thus this performance measure is well-defined as long as the coupling graph $\mathcal{G}$ is connected. This class of system norms captures several important performance and robustness features of large-scale dynamical networks. For instance, a direct calculation shows that the $\mathcal{H}_2$-norm of a linear consensus network with dynamics (8.6) is given by

$$\|G\|_{\mathcal{H}_2} \;=\; \Big(\frac{1}{2}\sum_{i=2}^{n}\lambda_i^{-1}\Big)^{\frac{1}{2}}. \tag{8.11}$$

This system norm quantifies to what degree the effect of exogenous stochastic disturbance inputs propagate throughout the network [12]. The $\mathcal{H}_\infty$-norm of a network is indeed an input-output system norm and its value for a linear consensus network with dynamics (8.6) is given by

$$\|G\|_{\mathcal{H}_\infty} \;=\; \lambda_2^{-1}, \tag{8.12}$$

where λ_2 is the second smallest eigenvalue of L, also known as the algebraic connectivity of the under graph of network [20]. The value of $\mathcal{H}_\infty$-norm of a network with dynamics (8.6) can be interpreted as the worst attainable performance for all square integrable disturbance inputs.

Theorem 8.5.3. *For a given network $\mathcal{N}(L)$, the following performance measure*

$$\rho_{\mathcal{H}_p}(L) \;:=\; \|G\|_{\mathcal{H}_p} = \alpha_0\big(\zeta_{p-1}(L)\big)^{1-\frac{1}{p}}, \tag{8.13}$$

where $\alpha_0^{-1} \;=\; \sqrt[p]{-\beta(\frac{p}{2},-\frac{1}{2})}$ and $\beta \;:\; \mathbb{R}\times\mathbb{R} \;\to\; \mathbb{R}$ is the well-known Beta function. Moreover, this measure is a SCSM for all $2 \leq p \leq \infty$.

Proof. We utilize the disagreement form of the network that is given by

$$\dot{x}_d(t) \;=\; -L_d\, x_d(t) + \left(I_n - \frac{1}{n}\mathbb{1}_n\mathbb{1}_n^{\mathrm{T}}\right)\, \xi(t), \tag{8.14}$$

$$y(t) \;=\; \left(I_n - \frac{1}{n}\mathbb{1}_n\mathbb{1}_n^{\mathrm{T}}\right)\, x_d(t), \tag{8.15}$$

where the disagreement vector is defined by

$$x_d(t) \;:=\; \left(I_n - \frac{1}{n}\mathbb{1}_n\mathbb{1}_n^{\mathrm{T}}\right)\, x(t) \;=\; x(t) - \frac{1}{n}J_n\, x(t). \tag{8.16}$$

The disagreement network (8.14)-(8.15) is stable as every eigenvalue of the state matrix $-L_d = -(L + \frac{1}{n}J_n)$ has strictly negative real part. One can verify that the transfer functions from $\xi(t)$ to $y(t)$ in both realizations are identical. We use the following decomposition

$$\begin{aligned} G(s) \;&=\; M_n\left(sI_n + L + \frac{1}{n}J_n\right)^{-1} M_n \\ &=\; M_n\Big(U\,\mathrm{diag}\left[s+1, s+\lambda_2, \cdots, s+\lambda_n\right]U^{\mathrm{T}}\Big)^{-1} M_n \\ &=\; M_n U\,\mathrm{diag}\left[\frac{1}{s+1}, \frac{1}{s+\lambda_2}, \cdots, \frac{1}{s+\lambda_n}\right] U^{\mathrm{T}} M_n \\ &=\; U\,\mathrm{diag}\left[0, \frac{1}{s+\lambda_2}, \cdots, \frac{1}{s+\lambda_n}\right] U^{\mathrm{T}}, \end{aligned} \tag{8.17}$$

to compute the $\mathcal{H}_q$-norm of $G(j\omega)$ as follows

$$\begin{aligned} \|G\|_{\mathcal{H}_p}^p \;&=\; \frac{1}{2\pi}\int_{-\infty}^{\infty}\sum_{k=1}^{n}\sigma_k(G(j\omega))^p\, d\omega \\ &=\; \frac{1}{2\pi}\sum_{i=2}^{n}\int_{-\infty}^{\infty}\left(\frac{1}{\omega^2+\lambda_i^2}\right)^{\frac{p}{2}} d\omega \\ &=\; \frac{-1}{\beta(\frac{p}{2},-\frac{1}{2})}\sum_{i=2}^{n}\lambda_i^{1-p} \;=\; \frac{-1}{\beta(\frac{p}{2},-\frac{1}{2})}\zeta_{p-1}(L)^{p-1}, \end{aligned}$$

for all $2 \leq p \leq \infty$. Now we show that measure (8.13) satisfies Properties 1, 2, 3, and 4 in Definition 8.5.1. It is straightforward to verify that measure (8.13) has Properties 1 and 2. Next we show that measure (8.13) has Property 2, i.e., it is a convex function over the set of Laplacian matrices. We then show that for all $2 \leq p \leq \infty$ the following function $f : \mathbb{R}^{n-1}_{++} \rightarrow \mathbb{R}$ is concave

$$f(x) \;=\; \left(\sum_{i=1}^{n-1} x_i^{-p+1} \right)^{\frac{1}{1-p}},$$

where $x \;=\; [x_1, x_2, \cdots, x_{n-1}]^{\mathrm{T}}$. To do so, we need to show $\nabla^2 f(x) \preceq 0$, where the Hessian of $f(x)$ is given by

$$\frac{\partial^2 f(x)}{\partial x_i^2} \;=\; -\frac{p}{x_i} \left(\frac{f(x)}{x_i} \right)^p \;+\; \frac{p}{f(x)} \left(\frac{f(x)^2}{x_i^2} \right)^p$$

and

$$\frac{\partial^2 f}{\partial x_i \partial x_j} \;=\; \frac{p}{f(x)} \left(\frac{f(x)^2}{x_i x_j} \right)^p.$$

The Hessian matrix can be expressed as

$$\nabla^2 f(x) \;=\; \frac{p}{f(x)} \left(-\operatorname{diag}(z)^{\frac{1+p}{p}} + z z^{\mathrm{T}} \right),$$

where

$$z \;=\; \left[(f(x)/x_1)^p, \cdots, (f(x)/x_n)^p \right]^{\mathrm{T}}.$$

To verify $\nabla^2 f(x) \preceq 0$, we must show that for all vectors v, $v^{\mathrm{T}} \nabla^2 f(x) v \leq 0$. We know that

$$\nabla^2 f(x) v =$$

(a) (b)

Figure 8.1: Two isospectral graphs with six nodes [1].

$$\frac{p}{f(x)}\left(-\sum_{i=1}^{n-1} z_i^{\frac{p-1}{p}} \sum_{i=1}^{n-1} z_i^{\frac{p+1}{p}} v_i^2 + \left(\sum_{i=1}^{n-1} v_i z_i\right)^2\right). \tag{8.18}$$

Using the Cauchy-Schwarz inequality $a^{\mathrm{T}}b \leq \|a\|_2\|b\|_2$, where

$$a_i = \left(\frac{f(x)}{x_i}\right)^{\frac{p-1}{2}} = z_i^{\frac{p-1}{2p}},$$

and $b_i = z_i^{\frac{p+1}{2p}} v_i$, it follows that $v^{\mathrm{T}}\nabla^2 f(x)v \leq 0$ for all $v \in \mathbb{R}^{n-1}$. Therefore, $f(x)$ is concave. Let us define $h(x) = x^{\frac{-p+1}{p}}$, where $x \in \mathbb{R}$. Since $f(.)$ is positive and concave, and h is decreasing convex, we conclude that $h(f(.))$ is convex [146]. Hence, we get that $\|G\|_{\mathcal{H}_p}$ is a convex function with respect to the eigenvalues of L. Since this measure is a symmetric closed convex function defined on a convex subset of $\mathbb{R}^{n-1}$, i.e., $n-1$ nonzero eigenvalues, according to [139] we conclude that $\|G\|_{\mathcal{H}_p}$ is a convex of Laplacian matrix L. Finally, measure $\|G\|_{\mathcal{H}_p}$ is orthogonal invariant because it is a spectral function as shown in (8.13). Hence, this measure satisfies all properties of Definition 8.5.1. This completes the proof. □

Local deviation error: The local deviation error of subsystem i is equal to the deviation of the state of subsystem i from the weighted average of states of its neighbors, which

can be formally defined as

$$\varepsilon_i(t) \;:=\; x_i(t) - \frac{1}{d_i} \sum_{e=\{i,j\}\in\mathcal{E}} w(e)\, x_j(t). \tag{8.19}$$

The expected cumulative local deviation is then given by

$$\rho_{\text{local}}(L) \;=\; \lim_{t\to\infty} \mathbb{E}\left[\sum_{i=1}^{n} \varepsilon_i(t)^2\right], \tag{8.20}$$

where input ξ of network (8.6) is a white noise process with identity covariance.

Theorem 8.5.4. *The operator $\rho : \mathfrak{L}_n \to \mathbb{R}_+$ defined by (8.20) is a CSM. Moreover, it can also be expressed as:*

$$\rho_{local}(L) = \frac{1}{2} \sum_{i=1}^{n} {d_i}^{-1}, \tag{8.21}$$

where d_i is the degree of node $i \in \mathcal{V}$.

Proof. Let us define the total local deviation error at time t by

$$\varepsilon_{\text{total}}(t) \;:=\; \sum_{i\in\mathcal{V}} \varepsilon_i(t)^2. \tag{8.22}$$

We reformulate (8.19) as

$$\begin{aligned} \varepsilon_i(t) \;&=\; d_i^{-1} \left(d_i x_i(t) - \sum_{e=\{i,j\}\in\mathcal{E}} w(e)\, x_j(t) \right) \\ &=\; d_i^{-1} \sum_{e=\{i,j\}\in\mathcal{E}} w(e)\, (x_i(t) - x_j(t)) \end{aligned} \tag{8.23}$$

Therefore, we get

$$\varepsilon(t) = \operatorname{diag}\left[d_1^{-1}, \cdots, d_n^{-1}\right] L\, x(t).$$

where $\varepsilon(t)$ is a vector of $\varepsilon_i(t)$'s. Also, we can rewrite (8.22) as follows

$$\begin{aligned} \varepsilon_{\text{total}}(t) &= \varepsilon^{\mathrm{T}}(t)\varepsilon(t) \\ &= x^{\mathrm{T}}(t)Qx(t), \end{aligned} \tag{8.24}$$

where Q is given by

$$Q \;=\; L \;\text{diag}\left[d_1^{-2}, \cdots, d_n^{-2}\right]\; L.$$

Therefore, based on [12, Thm. 5] the steady-state deviation of $\varepsilon_{\text{total}}$, as a performance measure, is given by

$$\begin{aligned} \rho_{\text{local}}(L) &= \lim_{t\to\infty} \mathbb{E}\left[\varepsilon_{\text{total}}(t)\right] = \frac{1}{2}\,\mathbf{Tr}\left(L^{\dagger}Q\right), \\ &= \frac{1}{2}\sum_{i\in\mathcal{V}} {d_i}^{-1}. \end{aligned} \tag{8.25}$$

Now we show this measure is a convex systemic measure. We first show that (8.25) has property 1, which means

$$\rho_{\text{local}}(\kappa L) \;=\; \frac{1}{2}\sum_{i\in\mathcal{V}} (\kappa d_i)^{-1} \;=\; \kappa^{-1}\rho_{\text{local}}(L).$$

Also, it is monotone, because if $L_1 \preceq L_2$ then we have

$$e_i^{\mathrm{T}} L_1 e_i \;\leq\; e_i^{\mathrm{T}} L_2 e_i,$$

where e_i is the vector with a 1 in the i-th coordinate and 0's elsewhere. Therefore, we have $L_1(i,i) \leq L_2(i,i)$, which guarantees the monotonicity of $\rho_{\text{local}}(.)$. Moreover, its convexity follows from convexity of $1/x$ where $x \in \mathbb{R}_+$. Because, consider two Laplacian matrices L_1 and L_2 with node degree $d_i^{(1)}$'s and $d_i^{(2)}$, respectively. Then, for all $0 \leq c \leq 1$

we get

$$\begin{aligned}
\rho_{\text{local}}(cL_1 + (1-c)L_2) &= \sum_{i\in\mathcal{V}} \frac{1}{c\, d_i^{(1)} + (1-c)\, d_i^{(2)}} \\
&\leq \sum_{i\in\mathcal{V}} \left(\frac{c}{d_i^{(1)}} + \frac{1-c}{d_i^{(2)}} \right) \\
&= \sum_{i\in\mathcal{V}} \frac{c}{d_i^{(1)}} + \sum_{i\in\mathcal{V}} \frac{1-c}{d_i^{(2)}} \\
&= c\rho_{\text{local}}(L_1) + (1-c)\rho_{\text{local}}(L_2).
\end{aligned}$$

Finally, $\rho_{\text{local}}(.)$ is permutation invariance, because the multiset of node degrees does not change by relabeling of nodes. This completes the proof. □

We remark that for first-order consensus network (8.6) defined over d-regular underlying graph, the corresponding microscopic measure (8.25) scales linearly with network size; this result reduces to the result given in [2] for regular lattices.

Figure 8.1 shows an example of pair of graphs which are isospectral but not isometric[3]. Note that these isospectral networks have many quantities in common such as all SCSMs, however, their local deviation error values $\rho_{\text{local}}(.)$ are different.

8.6 Network Sparsifications

Our main contributions in this chapter are presented in this section. We develop a sparsification framework for the class of linear consensus networks governed by (8.6) that provides performance guarantees with respect to a general class of systemic measures. Since SCSM is a subclass of CSM, we state our results for the most general case with respect to CSM. First, we introduce a notion of approximation for the class of consensus

[3]Which means their adjacency matrices are not permutation-similar.

networks.

Definition 8.6.1. *For a fixed constant $\epsilon \in [0,1]$, a consensus network $\mathcal{N}(L_s)$ is ϵ-approximation of $\mathcal{N}(L)$ if and only if*

$$(1-\epsilon)^{\alpha} \;\leq\; \frac{\rho\,(L)}{\rho\,(L_s)} \;\leq\; (1+\epsilon)^{\alpha}, \tag{8.26}$$

for every homogenous convex systemic measure $\rho : \mathfrak{L}_n \to \mathbb{R}_+$ of order $\alpha > 0$.

Lemma 8.6.2. *$\mathcal{N}(L_s)$ is an ϵ-approximation of $\mathcal{N}(L)$ if and only if the following inequalities hold*

$$(1-\epsilon)L \;\preceq\; L_s \;\preceq\; (1+\epsilon)L. \tag{8.27}$$

Proof. According to the monotonicity and homogeneity properties of convex system measures, it follows that if (8.27) satisfies then we have

$$(1+\epsilon)^{-\alpha}\rho(L) \;\leq\; \rho(L_s) \;\leq\; (1-\epsilon)^{-\alpha}\rho(L). \tag{8.28}$$

Therefore, according to (8.28) and Definition 8.6.1, $\mathcal{N}(L_s)$ is an ϵ-approximation of $\mathcal{N}(L)$. Now let us consider the following measures

$$\rho_v(L) \;=\; v^{\mathrm{T}} L^{\dagger} v, \tag{8.29}$$

for any given $v \in \mathbb{R}^n$, this measure is a homogenous convex systemic measure of order $\alpha = 1$. Now, using measure $\rho_v(.)$ and Definition 8.6.1, for any $v \in \mathbb{R}^n$ and $v \notin \text{Span}\{\mathbb{1}\}$, we get

$$(1-\epsilon) \;\leq\; \frac{\rho_v(L)}{\rho_v(L_s)} \;\leq\; (1+\epsilon),$$

which means

$$(1+\epsilon)^{-1} \;\leq\; \frac{v^{\mathrm{T}} L_s^{\dagger} v}{v^{\mathrm{T}} L^{\dagger} v} \;\leq\; (1-\epsilon)^{-1}, \tag{8.30}$$

since $v^{\mathrm{T}} L^{\dagger} v > 0$, (8.30) can be rewrite as follows

$$(1+\epsilon)^{-1} v^{\mathrm{T}} L^{\dagger} v \;\leq\; v^{\mathrm{T}} L_2^{\dagger} v \;\leq\; (1-\epsilon)^{-1} v^{\mathrm{T}} L^{\dagger} v. \tag{8.31}$$

We know that L and L_s are Laplacian matrices and (8.31) holds for all $v \notin \text{Span}\{\mathbb{1}\}$. Therefore, we get

$$(1+\epsilon)^{-1} L^{\dagger} \;\leq\; L_s^{\dagger} \;\leq\; (1-\epsilon)^{-1} L^{\dagger},$$

using this, we finally get the desired result:

$$(1-\epsilon) L \;\leq\; L_s \;\leq\; (1+\epsilon) L.$$

□

This result is fundamental as it enables us to take advantage of monotonicity property of systemic measures in our approximations.

8.6.1 Existence of ϵ-Approximations

Among all ϵ-approximation of a given consensus network with a dense coupling graph, we are interested in its sparsifiers, i.e., those networks with sparse coupling graphs.

Definition 8.6.3. *$\mathcal{N}(L_s)$ is a (ϵ, d)-sparsifier of a given network $\mathcal{N}(L)$ with n nodes if the following conditions hold:*
1. $\mathcal{N}(L_s)$ is an ϵ-approximation of network $\mathcal{N}(L)$; and
2. the coupling graph of $\mathcal{N}(L_s)$ has at most $dn/2$ links (i.e. feedback gains).

The second condition implies that the average number of connected links to nodes in the sparsifier is at most d. In the following theorem, we show existence of sparsifiers for

every given consensus network.

Theorem 8.6.4. *Suppose that a consensus network $\mathcal{N}(L)$ with coupling graph $\mathcal{G} = (\mathcal{V}, \mathcal{E}, w)$ and $d > 1$ are given. Then, there exists a consensus network $\mathcal{N}(L_s)$ with coupling graph $\mathcal{G}_s = (\mathcal{V}, \mathcal{E}_s, w_s)$ such that $\mathcal{N}(L_s)$ is a $(\frac{2\sqrt{d}}{d+1}, 2d)$-sparsifier of $\mathcal{N}(L)$ and $\mathcal{E}_s \subset \mathcal{E}$.*

Proof. According to [64, Th. 1.1], coupling graph $\mathcal{G} = (\mathcal{V}, \mathcal{E}, w)$ has a weighted subgraph $\hat{\mathcal{G}} = (\mathcal{V}, \hat{\mathcal{E}}, \hat{w})$ with $|\hat{\mathcal{E}}| = \lceil d(n-1) \rceil$ that satisfies

$$L \preceq L_{\mathcal{H}} \preceq \left(\frac{1+\sqrt{d}}{1-\sqrt{d}}\right)^2 L \tag{8.32}$$

where $L_{\mathcal{H}}$ is the Laplacian matrix of graph $\mathcal{H}$. We define $\mathcal{G}_s = (\mathcal{V}, \mathcal{E}_s, w_s)$ by its Laplacian matrix L_s where

$$L_s := \frac{d+1-2\sqrt{d}}{d+1} L_{\mathcal{H}}. \tag{8.33}$$

Therefore, according to (8.32) and (8.33), it follows that

$$\left(1 - \frac{2\sqrt{d}}{d+1}\right) L \preceq L_s \preceq \left(1 + \frac{2\sqrt{d}}{d+1}\right) L. \tag{8.34}$$

Using (8.34) and Lemma 8.6.2, it yields that $\mathcal{N}(L_s)$ is a $(\frac{2\sqrt{d}}{d+1}, 2d)$-sparsifier of $\mathcal{N}(L)$ and this completes the proof.

□

Our result is based on a graph-theoretic result by [64]. Specifically, Theorem 8.6.4 shows that every given linear consensus network with dynamics (8.6) has a sparse consensus network such that the two networks yield comparable performances with respect to any systemic performance measure $\rho : \mathfrak{L}_n \to \mathbb{R}_+$.

In our next result, we show that every consensus network has a sparse consensus network such that: (i) it yields a better systemic performance than the original network, and (ii) the total weight sum of the coupling graph of the sparsifier is controlled, i.e., it is less than a constant multiplier of that of the original network. For a given coupling graph with Laplacian matrix L and the set of links $\mathcal{E}$, we denote the total weight sum of the coupling graph by

$$w_{\text{total}}(L) \;:=\; \sum_{e\in\mathcal{E}} w(e). \tag{8.35}$$

Corollary 8.6.5. *For a given consensus network $\mathcal{N}(L)$ with coupling graph $\mathcal{G}=(\mathcal{V},\mathcal{E},w)$ and every $d>1$, there exists a consensus network $\mathcal{N}(L_s)$ with coupling graph $\mathcal{G}_s=(\mathcal{V},\mathcal{E}_s,w_s)$ that has at most dn links and $\mathcal{E}_s\subset\mathcal{E}$. Moreover, we have*

$$w_{total}(L_s) \;\leq\; \left(\frac{\sqrt{d}+1}{\sqrt{d}-1}\right)^2 w_{total}(L) \tag{8.36}$$

and

$$\rho\left(L_s\right) \;\leq\; \rho\left(L\right),$$

for every convex systemic measure $\rho:\mathfrak{L}_n\to\mathbb{R}_+$.

Proof. According to Theorem 8.6.4, $\mathcal{N}(L)$ has a $(\frac{2\sqrt{d}}{d+1},2d)$-sparsifier, $\mathcal{N}(L_{\hat{s}})$, with $\mathcal{E}_{\hat{s}}\subset\mathcal{E}$, which means that we have

$$\left(1-\frac{2\sqrt{d}}{d+1}\right)^{\alpha} \;\leq\; \frac{\rho\left(L\right)}{\rho\left(L_{\hat{s}}\right)} \;\leq\; \left(1+\frac{2\sqrt{d}}{d+1}\right)^{\alpha}, \tag{8.37}$$

for every homogenous convex systemic measure $\rho:\mathfrak{L}_n\to\mathbb{R}_+$ of order $\alpha>0$. We now define $L_s=\frac{d+1-2\sqrt{d}}{d+1}L_{\hat{s}}$, then it follows that

$$\rho(L_{\hat{s}}) \;=\; \left(\frac{d+1}{d+1-2\sqrt{d}}\right)^{\alpha}\rho(L_s) \tag{8.38}$$

Finally by substituting $\rho(L_{\hat{s}})$ from (8.38) in the left hand side inequality of (8.37), we have

$$\rho\left(L_s\right) \ \leq \ \rho\left(L\right),$$

Note that $\rho(L) = 1/w_{\text{total}}(L)$ is a convex systemic measure with $\alpha = 1$, therefore from the left hand side inequality in (8.37), we get (8.36).

□

According to Definitions 8.5.1 and 8.5.2, we note that linear consensus networks with smaller systemic performance measure are more desirable and they exhibit better network-wide performance.

8.6.2 Computing Sparsifiers via Random Sampling

In this part, we employ a randomized algorithm to compute a (ϵ, d)-sparsifier of a given network. A randomized algorithm employs a degree of randomness as part of its logic. Randomization allows us to design provably accurate algorithms for problems that are massive and computationally expensive or NP-hard. For this aim based on [63], we sample low-connectivity coupling links with high probability and high-connectivity coupling links with low probability. For a given consensus network $\mathcal{N}(L)$ with n nodes, we sample links of the coupling graph of this network M times in order to produce a $(\epsilon, 2M/n)$-sparsifier of it. Let us denote probability of selecting a link $e \in \mathcal{E}$ by $\pi(e)$ that is proportional to $w(e)r(e)$, where $w(e)$ and $r(e)$ are the weight and the effective resistance of link e, respectively. In each step of sampling, we add the selected link e to the sparsifier network with weight $w(e)/(M\pi(e))$. All details of this algorithm is explained below:

Fortunately, the following theorem, which is a modified version of a theorem in [63], provides us with a proof certificate that the above randomized algorithm is capable of

Table 8.2: Network Sparsification Algorithm

Algorithm:
Input: $\mathcal{G} = (\mathcal{V}, \mathcal{E}, w)$
1: *set* $\mathcal{G}_s$ to be the empty graph on $\mathcal{V}$
2: *for* $i = 1$ *to* M
3: *sample* link $e \in \mathcal{E}$ with probability $\pi(e)$
add it to $\mathcal{G}_s$ with link weight $w(e)/(M\pi(e))$
4: *end for*

generating a sparse approximation of a given consensus network.

Theorem 8.6.6. *For a given consensus network $\mathcal{N}(L)$, a fixed constant $\epsilon \in (1/\sqrt{n}, 1]$ and an integer number $M = \mathcal{O}(n \log n/\epsilon^2)$, Network Sparsification Algorithm produces a $(\epsilon, 2M/n)$-sparsifier of network $\mathcal{N}(L)$ with high probability*[4].

Proof. We give only a sketch of the proof here, for more details please see [63]. We consider the following projection matrix

$$\Pi \;=\; W^{1/2} E L^{\dagger} E^{\mathrm{T}} W^{1/2}, \tag{8.39}$$

where E is m-by-n incidence matrix, and W is a diagonal matrix with link weights on its diagonal, (we know that $L = E^{\mathrm{T}} W E$). Matrix Π is m-by-m matrix with eigenvalues zero and one and multiplicity of $m - n + 1$ and $n - 1$, respectively [63, Lemma 3]. Now, we show that the sampling of links in Network Sparsification Algorithm corresponds to picking $M = \mathcal{O}(n \log n)$ columns at random from matrix Π. Then by using [165, Thm. 3.1] we can get the desired result.

□

Network Sparsification Algorithm produces a sparsifier with with $\mathcal{O}(n \log n/\epsilon^2)$ links

[4] An event holds with high probability if it holds with probability $1 - \mathcal{O}(n^{-a})$ for some $a > 0$ independent of n.

(*i.e.* feedback gains) in expectation and runs in approximately linear time $\tilde{\mathcal{O}}(m)$, where m is the number of links [166]. To do so, good approximations of all effective resistances are needed, and Spielman and Srivastava prove that $\mathcal{O}(\log n)$ calls to a solver for symmetric diagonally dominant (SDD) linear systems can provide sufficiently good approximations to all effective resistances. Moreover, in [64] the authors show that a spectral sparsifier with $\mathcal{O}(n/\epsilon^2)$ links can be computed in $\mathcal{O}(n^3 m/\epsilon^2)$ time with a slower deterministic algorithm to select links. The best known classical algorithm for calculating effective resistances relies on solving a Laplacian linear system and takes $\tilde{\mathcal{O}}(m)$ time [64, 167].

8.6.3 Partial/Localized Network Sparsification

Our methodology can be extended further to explore several interesting network design problems, such as partial or localized sparsification of a given large-scale consensus network. In this subsection, we only look at one of such design problems. Let us consider a slightly modified version of (8.6) by involving a predesigned state feedback controller

$$\mathcal{N}(L_0+L_1):\begin{cases}\dot{x}(t) \;=\; -L_0x(t) \;+\; u(t) \;+\; \xi(t)\\ u(t) \;=\; -L_1x(t)\\ y(t) \;=\; \left(I_n-\frac{1}{n}\mathbb{1}_n\mathbb{1}_n^{\mathrm{T}}\right)x(t)\end{cases} \tag{8.40}$$

with initial condition $x(0)=x_0$, where L_0 is the Laplacian matrix of the open-loop network and the Laplacian matrix L_1 is the predesigned state feedback gain. It is assumed that the control input u is designed in an optimal fashion. Thus, the corresponding coupling subgraph to L_1, which is denoted by $\mathcal{G}_1$, is possibly dense. Now, our design objective is to find a state feedback sparsifier for the closed-loop network $\mathcal{N}(L_0+L_1)$ that partially (or locally) sparsifies $\mathcal{G}_1$. Let us represent such a sparsifier by $\hat{\mathcal{G}}_1$ with Laplacian matrix

$\hat{L}_1$.

Theorem 8.6.7. *Suppose that a linear consensus network in the form of (8.40), a homogenous convex systemic measure $\rho : \mathfrak{L}_n \to \mathbb{R}_+$ of order α, and a number $d > 1$ are given. For $\epsilon = \frac{2\sqrt{d}}{d+1}$, there exists a subgraph sparsifier $\hat{\mathcal{G}}_1 = (\mathcal{V}, \hat{\mathcal{E}}, \hat{w})$ for $\mathcal{G}_1 = (\mathcal{V}, \mathcal{E}, w)$ with at most dn links that satisfies $\hat{\mathcal{E}} \subset \mathcal{E}$ and*

$$(1-\epsilon)^\alpha \;\leq\; \frac{\rho(L_0 + L_1)}{\rho(L_0 + \hat{L}_1)} \;\leq\; (1+\epsilon)^\alpha. \tag{8.41}$$

Furthermore, it follows that

$$w_{\textit{total}}(\hat{L}_1) \;\leq\; (1+\epsilon)\, w_{\textit{total}}(L_1).$$

Proof. According to [64, Th. 1.1], coupling graph $\mathcal{G}_1 = (\mathcal{V}, \mathcal{E}, w)$ has a weighted subgraph $\mathcal{H} = (\mathcal{V}, \hat{\mathcal{E}}, \hat{w})$ with $|\hat{\mathcal{E}}| = \lceil d(n-1) \rceil$ that satisfies

$$L_1 \;\preceq\; L_{\mathcal{H}} \;\preceq\; \frac{d+1+2\sqrt{d}}{d+1-2\sqrt{d}} L_1 \tag{8.42}$$

where $L_{\mathcal{H}}$ is the Laplacian matrix of graph $\mathcal{H}$. We define $\hat{\mathcal{G}}_1 = (\mathcal{V}, \hat{\mathcal{E}}, \hat{w})$ by its Laplacian matrix $\hat{L}_1$, where

$$\hat{L}_1 \;:=\; \frac{\sqrt{d}-1}{\sqrt{d}+1} L_{\mathcal{H}}. \tag{8.43}$$

Therefore, according to (8.42) and (8.43), it follows that

$$\frac{\sqrt{d}-1}{\sqrt{d}+1} L_1 \;\preceq\; \hat{L}_1 \;\preceq\; \frac{\sqrt{d}+1}{\sqrt{d}-1} L_1. \tag{8.44}$$

Moreover, we know that

$$\frac{\sqrt{d}-1}{\sqrt{d}+1}L_0 \preceq L_0 \preceq \frac{\sqrt{d}+1}{\sqrt{d}-1}L_0. \tag{8.45}$$

From (8.44) and (8.45), we have

$$\frac{\sqrt{d}-1}{\sqrt{d}+1}(L_0+L_1) \preceq (L_0+\hat{L}_1) \preceq \frac{\sqrt{d}+1}{\sqrt{d}-1}(L_0+L_1). \tag{8.46}$$

Then, using (8.46) and Lemma 8.6.2, it yields that $\mathcal{N}(L_0+\hat{L}_1)$ is a $(\frac{2\sqrt{d}}{d+1}, 2d)$-sparsifier of $\mathcal{N}(L_0+L_1)$, and this completes the proof.

□

This result is particularly useful is large-scale consensus networks where our objective is to sparsify only a small portion of network without drastically affecting the global performance measures.

8.6.4 A Parallel Network Sparsification Algorithm

As we shown in Subsection 8.6.3, our proposed sparsification method can also be applied for partial sparsification of large-scale networks. Therefore, based on this fact, we can introduce a distributed/parallel version of this algorithm. Hence, this distributed method can be used at a time on many different processing devices. Each processing device only uses the information of an assigned subgraph.

Definition 8.6.8. *We define a backbone/base subgragh of the network as a subgraph which is formed by links that we want to keep in the sparsifier network without changing their weights and we denote its Laplacian matrix by L_0 and the subgraph by $\mathcal{G}_0$.*

We can assume that the original coupling graph is the union on the base graph and p

link-disjoint subgraphs, *i.e.*

$$L = L_0 + \sum_{i=1}^{p} L_i. \tag{8.47}$$

Assumption 8.6.9. *The subgraphs are link-disjoint and dense subgraphs.*

without loss of generality, we can assume that the node set of all subgraphs is $\mathcal{V}$, same as the node set of the original graph. Therefore, their corresponding Laplacian matrices are n-by-n matrices.

Theorem 8.6.10. *Suppose that a linear consensus network in the form of (8.40), a homogenous convex systemic measure $\rho : \mathfrak{L}_n \to \mathbb{R}_+$ of order α, and a number $d > 1$ are given. Assume that the coupling graph $\mathcal{G}$ is the union of the base graph $\mathcal{G}_0$ and p link-disjoint dense subraphs $\mathcal{G}_i$ where $i = 1, 2, \cdots, p$. Then, for $\epsilon = \frac{2\sqrt{d}}{d+1}$, there exists a set of subgraph sparsifier $\{\hat{\mathcal{G}}_i\}_{i=1}^p$ for $\{\mathcal{G}_i\}_{i=1}^p$ where each sparsifier subgraphs has average degrees of at most d that satisfies*

$$(1-\epsilon)^\alpha \;\le\; \frac{\rho(L_0 + \sum_{i=1}^p L_i)}{\rho(L_0 + \sum_{i=1}^p \hat{L}_i)} \;\le\; (1+\epsilon)^\alpha. \tag{8.48}$$

Furthermore, it follows that

$$w_{\textit{total}}(\hat{L}_i) \;\le\; (1+\epsilon)\, w_{\textit{total}}(L_i),$$

for $i = 1, 2, \cdots, p$.

Proof. According to [64, Th. 1.1], for $i = 1, \cdots, p$, coupling graph $\mathcal{G}_i = (\mathcal{V}, \mathcal{E}_i, w_i)$ has a weighted subgraph $\mathcal{H}_i = (\mathcal{V}, \hat{\mathcal{E}}_i, \hat{w}_i)$ with $|\hat{\mathcal{E}}_i| = \lceil d(n-1) \rceil$ that satisfies

$$L_i \;\preceq\; L_{\mathcal{H}_i} \;\preceq\; \frac{d+1+2\sqrt{d}}{d+1-2\sqrt{d}} L_i \tag{8.49}$$

where $L_{\mathcal{H}_i}$ is the Laplacian matrix of graph $\mathcal{H}_i$. We define $\hat{\mathcal{G}}_i = (\mathcal{V}, \hat{\mathcal{E}}_i, \hat{w}_i)$ by its Laplacian matrix $\hat{L}_i$, where

$$\hat{L}_i \ := \ \frac{\sqrt{d}-1}{\sqrt{d}+1} L_{\mathcal{H}_i}. \tag{8.50}$$

Therefore, according to (8.49) and (8.50), it follows that

$$\frac{\sqrt{d}-1}{\sqrt{d}+1} L_i \ \preceq \ \hat{L}_i \ \preceq \ \frac{\sqrt{d}+1}{\sqrt{d}-1} L_i. \tag{8.51}$$

Moreover, we know that

$$\frac{\sqrt{d}-1}{\sqrt{d}+1} L_0 \ \preceq \ L_0 \ \preceq \ \frac{\sqrt{d}+1}{\sqrt{d}-1} L_0. \tag{8.52}$$

From (8.51) and (8.52), we have

$$\frac{\sqrt{d}-1}{\sqrt{d}+1}(L_0 + \sum_{i=1}^{p} L_i) \preceq L_0 + \sum_{i=1}^{p} \hat{L}_i \preceq \frac{\sqrt{d}+1}{\sqrt{d}-1}(L_0 + \sum_{i=1}^{p} L_i). \tag{8.53}$$

Then, using (8.53) and Lemma 8.6.2, it yields that $\mathcal{N}(L_0 + \sum_{i=1}^{p} \hat{L}_i)$ is a $(\frac{2\sqrt{d}}{d+1}, 2d)$-sparsifier of $\mathcal{N}(L_0 + \sum_{i=1}^{p} L_i)$, and this completes the proof.

□

Assume that the coupling graph $\mathcal{G}$ is the union of the base graph $\mathcal{G}_0$ and p link-disjoint dense subgraphs $\mathcal{G}_i$ where $i = 1, \cdots, p$. Now for each subgraph we employ Network Sparsification Algorithm to find its sparsifier. Since these computations can be carried out simultaneously based on Theorem 8.6.10, we can get a sparsifier for the entire network much faster by parallelizing the algorithm across multiple processors in parallel computing environments.

8.7 $\mathcal{H}_2$-Norm Bounds for ϵ-Approximation

In this section, we show that our proposed framework generates sparsifiers that approximately preserve frequency characteristics of the original (dense) consensus network. Our sparsification method shares some common roots with the classical model reduction techniques, where the objective is to find a reduced order models that yield small $\mathcal{H}_2$-norm error (c.f., [168]). In network sparsification, it is also desirable to reduce the total number of links in a network in order to obtain a less complex network with a small $\mathcal{H}_2$-norm error. In our following results, we explicitly obtain $\mathcal{H}_2$-norm error bounds for network sparisifiers. First, we state a general result that yields a tight upper bound on the $\mathcal{H}_2$-norm error of two consensus networks in terms of their Laplacian matrices.

Lemma 8.7.1. *Suppose that $\mathcal{N}(L)$ and $\mathcal{N}(\hat{L})$ are two given consensus networks governed by dynamics* (8.6)*. Then,*

$$\frac{\|G-\hat{G}\|_{\mathcal{H}_2}^2}{\|G\|_{\mathcal{H}_2}^2} \;\leq\; \frac{\mathbf{Tr}\left(\hat{L}^\dagger + L^\dagger - 4(L+\hat{L})^\dagger\right)}{\mathbf{Tr}\,(L^\dagger)}, \tag{8.54}$$

where $G(s)$ and $\hat{G}(s)$ are transfer functions from input ξ to output y of $\mathcal{N}(L)$ and $\mathcal{N}(\hat{L})$, respectively.

Proof. In the first step, we define dynamical network $\mathcal{N}^*$ based on two given networks L and $L_{\mathcal{H}}$

$$\begin{cases} \dot{x}(t) \;=\; -\begin{bmatrix} L+\frac{1}{n}J_n & 0 \\ 0 & L_s+\frac{1}{n}J_n \end{bmatrix} x(t) + \begin{bmatrix} M_n \\ M_n \end{bmatrix} \xi(t) \\ \\ y(t) \;=\; \begin{bmatrix} M_n & -M_n \end{bmatrix} x(t) \end{cases} \tag{8.55}$$

where $x \in \mathbb{R}^{2n}$, $\xi \in \mathbb{R}^n$, $y \in \mathbb{R}^n$ and G^* denotes its transfer function from ξ to y.

$$\|G^*\|_{\mathcal{H}_2} \;=\; \|G - G_s\|_{\mathcal{H}_2}. \tag{8.56}$$

Calculating the $\mathcal{H}_2$ norm of the network reduces to solving an Algebraic Lyapunov Equation (ALE) [99]. Using the state matrices of (8.55) and the ALE we get

$$\mathfrak{A}X \;+\; X\mathfrak{A} \;=\; \begin{bmatrix} M_n & -M_n \\ -M_n & M_n \end{bmatrix} \tag{8.57}$$

where

$$\mathfrak{A} \;=\; -\begin{bmatrix} L + \frac{1}{n}J_n & 0_{n\times n} \\ 0_{n\times n} & L_s + \frac{1}{n}J_n \end{bmatrix}$$

and

$$X \;=\; \begin{bmatrix} X_1 & X_2 \\ X_2^{\mathrm{T}} & X_3 \end{bmatrix}.$$

We now decompose equation (8.57) to three Sylvester equations: The first equation is

$$\left(L + \frac{1}{n}J_n\right) X_1 \;+\; X_1 \left(L + \frac{1}{n}J_n\right) \;=\; M_n,$$

and its solution is

$$X_1 \;=\; \frac{1}{2}L^{\dagger}. \tag{8.58}$$

The second equation is

$$\left(L_s + \frac{1}{n}J_n\right) X_3 \;+\; X_3 \left(L_s + \frac{1}{n}J_n\right) \;=\; M_n,$$

and its unique solution is given by

$$X_3 \;=\; \frac{1}{2}L_s^{\dagger}. \tag{8.59}$$

Finally, the third one is

$$\left(L+\frac{1}{n}J_n\right)X_2 \;+\; X_2\left(L_s+\frac{1}{n}J_n\right) \;=\; -M_n, \tag{8.60}$$

has an unique solution

$$X_2 \;=\; -\int_0^{\infty} e^{-(L+\frac{1}{n}J_n)t}M_n e^{-(L_s+\frac{1}{n}J_n)t}dt,$$

the integrand can be reformulated as

$$\begin{aligned} e^{-(L+\frac{1}{n}J_n)t}M_n e^{-(L_s+\frac{1}{n}J_n)t} \;&=\; e^{-(L+\frac{1}{n}J_n)t}e^{-(L_s+\frac{1}{n}J_n)t} \\ &+\frac{1}{n}e^{-(L+\frac{1}{n}J_n)t}J_n e^{-(L_s+\frac{1}{n}J_n)t} \\ &=\; e^{-(L+\frac{1}{n}J_n)t}e^{-(L_s+\frac{1}{n}J_n)t}+\frac{e^{-2t}}{n}J_n. \end{aligned} \tag{8.61}$$

Based on the Golden-Thompson inequality for Hermitian matrices, we have

$$\begin{aligned} &\mathbf{Tr}\left(e^{-(L+\frac{1}{n}J_n)t}M_n e^{-(L_s+\frac{1}{n}J_n)t}\right) \\ &=\; \mathbf{Tr}\left(e^{-(L+\frac{1}{n}J_n)t}e^{-(L_s+\frac{1}{n}J_n)t}+\frac{e^{-2t}}{n}J_n\right) \\ &\geq\; \mathbf{Tr}\left(e^{-(L+L_s+\frac{2}{n}J_n)t}+\frac{e^{-2t}}{n}J_n\right) \end{aligned} \tag{8.62}$$

Therefore, the trace of X_2 can be bounded by

$$\begin{aligned}
\mathbf{Tr}(X_2) &= -\mathbf{Tr}\left(\int_0^\infty e^{-(L+\frac{1}{n}J_n)t} M_n e^{-(L_s+\frac{1}{n}J_n)t} dt\right) \\
&= -\int_0^\infty \mathbf{Tr}\left(e^{-(L+\frac{1}{n}J_n)t} M_n e^{-(L_s+\frac{1}{n}J_n)t}\right) dt \\
&\leq -\int_0^\infty \mathbf{Tr}\left(M_n e^{-(L_s+L+\frac{2}{n}J_n)t}\right) dt \\
&= -\mathbf{Tr}\left((L+L_s)^\dagger\right). \qquad (8.63)
\end{aligned}$$

Calculating the $\mathcal{H}_2$ norm of the network reduces to

$$\begin{aligned}
\|G^*\|_{\mathcal{H}_2}^2 &= \mathbf{Tr}\left(\begin{bmatrix} M_n & M_n \end{bmatrix} \begin{bmatrix} X_1 & X_2 \\ X_2 & X_3 \end{bmatrix} \begin{bmatrix} M_n \\ M_n \end{bmatrix}\right) \\
&= \mathbf{Tr}\left(\begin{bmatrix} X_1 & X_2 \\ X_2 & X_3 \end{bmatrix} \begin{bmatrix} M_n & M_n \\ M_n & M_n \end{bmatrix}\right) \qquad (8.64)
\end{aligned}$$

From (8.58), (8.59) and (8.64), it follows that

$$\begin{aligned}
\|G^*\|_{\mathcal{H}_2}^2 &= \frac{1}{2}\mathbf{Tr}(L^\dagger + L_s^\dagger) - \mathbf{Tr}((X_2 + X_2^{\mathrm{T}})M_n) \\
&\leq \frac{1}{2}\mathbf{Tr}(L^\dagger + L_s^\dagger) - 2\,\mathbf{Tr}\left((L+L_s)^\dagger\right),
\end{aligned}$$

where in the last inequality we use (8.63). Finally, from this and (8.56), we have

$$\|G - G_s\|_{\mathcal{H}_2}^2 \leq \frac{1}{2}\mathbf{Tr}\left(\hat{L}^\dagger + L^\dagger - 4(L+\hat{L})^\dagger\right),$$

which completes the proof.

□

We note that the right hand side of inequality (8.54) is always non-negative, *i.e.*

$$0 \;\leq\; \mathbf{Tr}\left(\hat{L}^\dagger + L^\dagger - 4(L+\hat{L})^\dagger\right),$$

because, $\mathbf{Tr}(L^\dagger)$ is convex on $\mathfrak{L}_n$, and we have

$$\mathbf{Tr}\left(\frac{1}{2}L + \frac{1}{2}\hat{L}\right)^\dagger \;\leq\; \frac{1}{2}\,\mathbf{Tr}\left(L^\dagger\right) + \frac{1}{2}\,\mathbf{Tr}\left(\hat{L}^\dagger\right).$$

The inequality (8.27) implies proximity of ϵ-approximations on the cone of positive semidefinite matrices. In the following result, it is proven that the frequency specifications of two ϵ-approximations are indeed very similar in $\mathcal{H}_2$ sense.

Theorem 8.7.2. *If $\mathcal{N}(L_s)$ is an ϵ-approximation sparsifier of $\mathcal{N}(L)$ for some $0 \leq \epsilon < 1$, then*

$$\frac{\|G - G_s\|_{\mathcal{H}_2}}{\|G\|_{\mathcal{H}_2}} \;\leq\; \sqrt{\frac{\epsilon(4-\epsilon)}{(1-\epsilon)(2+\epsilon)}},$$

where $G(s)$ and $G_s(s)$ represent the transfer functions from input ξ to output y of $\mathcal{N}(L)$ and $\mathcal{N}(L_s)$, respectively.

Proof. Based on the definition of ϵ-approximation, we get

$$\mathbf{Tr}(L_s^\dagger) \;\leq\; \frac{1}{1-\epsilon}\,\mathbf{Tr}(L^\dagger), \tag{8.65}$$

because $\mathbf{Tr}(L^\dagger)$ is a homogenous convex systemic measure of order $\alpha = 1$. Moreover, according to Lemma 8.6.2, we have

$$(2+\epsilon)^{-1}(L)^\dagger \;\leq\; (L+L_s)^\dagger. \tag{8.66}$$

By taking trace from both sides of (8.66), we get

$$\mathbf{Tr}\left((L+L_s)^\dagger\right) \;\geq\; \frac{1}{2+\epsilon}\,\mathbf{Tr}\left(L^\dagger\right). \tag{8.67}$$

Using Lemma 8.7.1, we get

$$\begin{aligned}\frac{\|G-G_s\|_{\mathcal{H}_2}^2}{\|G\|_{\mathcal{H}_2}^2} &\leq \frac{\mathbf{Tr}\left(\hat{L}^\dagger + L^\dagger - 4(L+\hat{L})^\dagger\right)}{\mathbf{Tr}(L^\dagger)} \\ &= \frac{\mathbf{Tr}\left({L_s}^\dagger\right) + \mathbf{Tr}\left(L^\dagger\right) - 4\,\mathbf{Tr}\left((L+L_s)^\dagger\right)}{\mathbf{Tr}(L^\dagger)} \\ &\leq \frac{\epsilon(4-\epsilon)}{(1-\epsilon)(2+\epsilon)},\end{aligned} \tag{8.68}$$

the last inequality is obtained by using inequalities (8.65) and (8.67). This completes the proof.

□

Remark 8.7.3. *This result is important as it asserts that for tight ϵ-approximations, i.e., for small enough value of ϵ, the frequency characteristics of the sparsifier are very similar to that of the original network in $\mathcal{H}_2$ sense. Figure 8.2 demonstrates the proposed lower bound based on Lemma 8.7.1 on the $\mathcal{H}_2$-norm error of a consensus networks and its ϵ-approximation network.*

8.8 Illustrative Examples

In this section, we present several numerical examples to illustrate our theoretical developments.

Example 8.8.1. *We first consider a consensus network with 40 agents defined over an unweighted graph with two dense components which are connected by a link ("cut edge").*

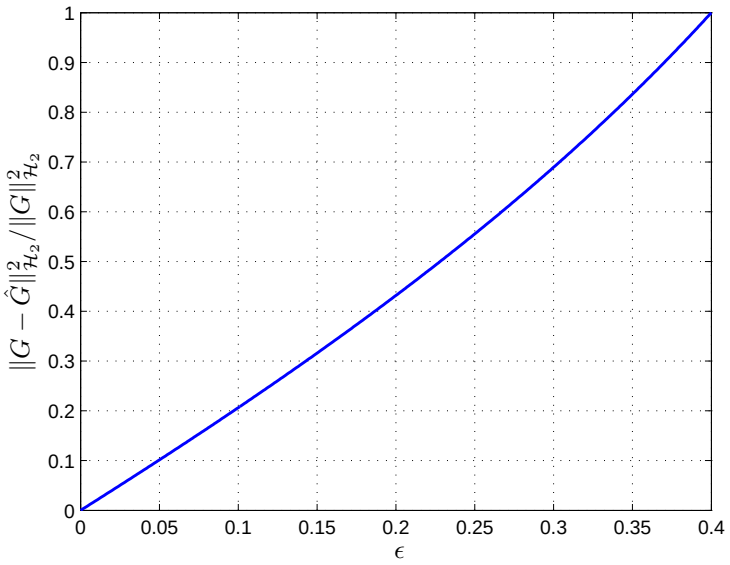

Figure 8.2: This plot presents the lower bound given by Lemma 8.7.1 on the $\mathcal{H}_2$-norm error of a consensus networks and its ϵ-approximation network.

Each of the components are obtained by adding 100 *randomly selected links to an empty graph with* 20 *nodes (see Figure 8.3. (a)). The probability of selecting a link of original coupling graph is depicted in Figure 8.4. As you can see in Figure 8.4, the probability of selecting the "cut edge" is much higher from the probability of other links. The Figure 8.3. (b) illustrates one example of a sparsifier of this network based on Network Sparsification Algorithm. This network has* 61 *links and all CSM's and SCSM's are close to their values of original network* $\mathcal{N}$*.The sparsity pattern of the obtained sparsifier network based on Network Sparsification Algorithm is shown in Figure 8.5. Table 8.3 clearly illustrates that the proposed method guarantees that systemic performances of both networks remain close to each other.*

Example 8.8.2. *Let us consider a consensus network with 100 agents and exponentially decaying coupling given by*

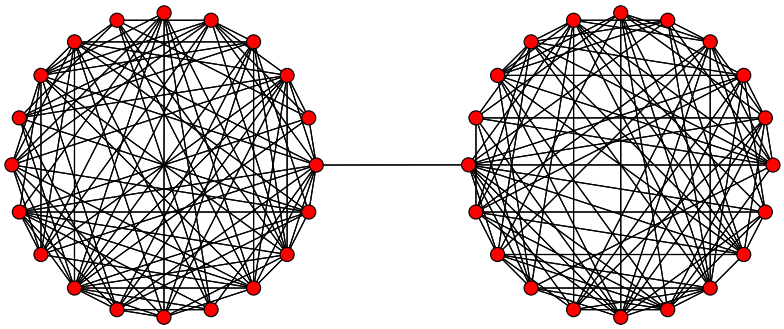

(a)

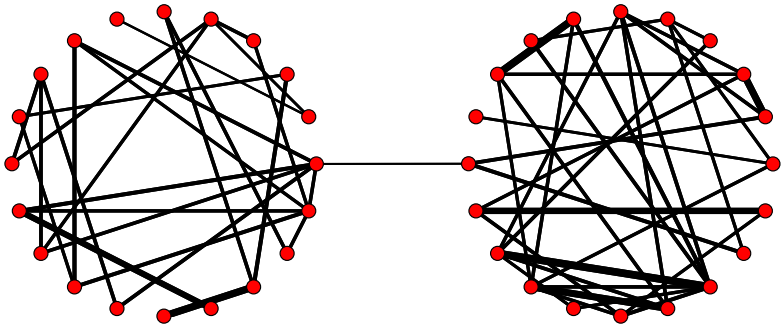

(b)

Figure 8.3: (a) An unweighted graph with 40 nodes, 201 links and $\rho_{\mathcal{H}_2}(L) = 2.7837$ and $w_{\text{total}}(L) = 201$. (b) A sparse approximation weighted graph with 40 nodes, 61 links and $\rho_{\mathcal{H}_2}(L_s) = 3.0805$ and $w_{\text{total}}(L_s) = 199.88$.

$$w(\{i,j\}) = \begin{cases} c\exp(-\gamma|i-j|) & \text{if } i \neq j \\ 0 & \text{if } i = j \end{cases} \tag{8.69}$$

where c and γ are positive numbers and $i, j \in \mathcal{V}$. This class of networks arises in various applications, where there is a notion of spatial distance between the subsystems, c.f., [169]. According to Theorem 8.6.4, this network has a $(0.5, 27.85)$-sparsifier. Fig-

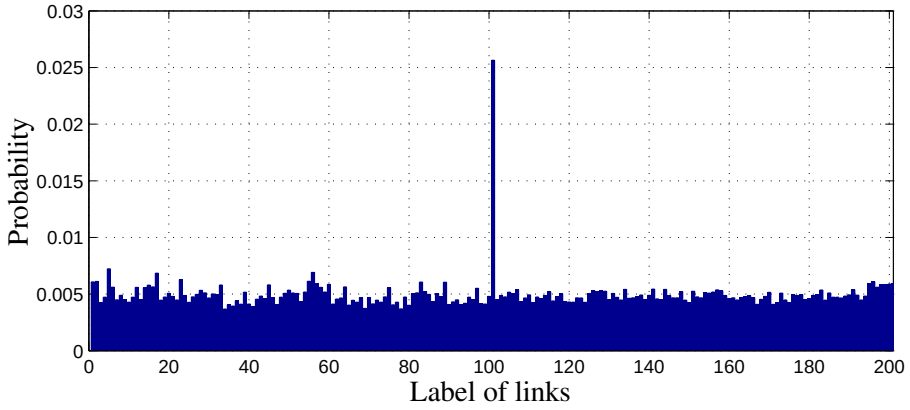

Figure 8.4: The probability of selecting a link based on Network Sparsification Algorithm for a given network in Figure 8.3. (a). The probability of selecting the "cut edge" is much higher from the probability of other links

Systemic measure: ρ	$\frac{\lvert\rho(L_s)-\rho(L)\rvert}{\rho(L)} \times 100$
$\rho_{\mathcal{H}_\infty} = {\lambda_2}^{-1}$	16.42 %
$\rho_{\mathcal{H}_2} = \left(\frac{1}{2}\sum_{i=2}^{n} {\lambda_i}^{-1}\right)^{\frac{1}{2}}$	10.66 %
$\rho_{\text{zeta},2} = \left(\sum_{i=2}^{n} {\lambda_i}^{-2}\right)^{\frac{1}{2}}$	13.24 %
$\rho_{\text{local}} = \frac{1}{2}\sum_{i\in\mathcal{V}} {d_i}^{-1}$	30.14 %

Table 8.3: Degradation ratio of systemic performance measures of the network and its sparse approximation with 70 % fewer links.

ure 8.6. a shows the Adjacency matrix of the coupling graph of consensus network with coupling weight function (8.69); and Figure 8.6. b illustrates one example of $(0.5, 22.28)$*-sparsifiers which is obtained based on Network Sparsification Algorithm. This sparse network has fewer coupling links (*1114 *links) compare to its original network with* $4,950$ *links. However, all CSM's are within a factor of* $(1 \pm 0.5)^{\alpha}$ *of their values of the original network (see Definition 8.6.1).*

Figure 8.7 depicts the probability distribution of sampling links (see Network Sparsification Algorithm). For instance, the probability of selecting link $e = \{i, j\}$ *in the network sparsification algorithm is the* $(i, j)^{th}$ *element of the matrix presented in Figure*

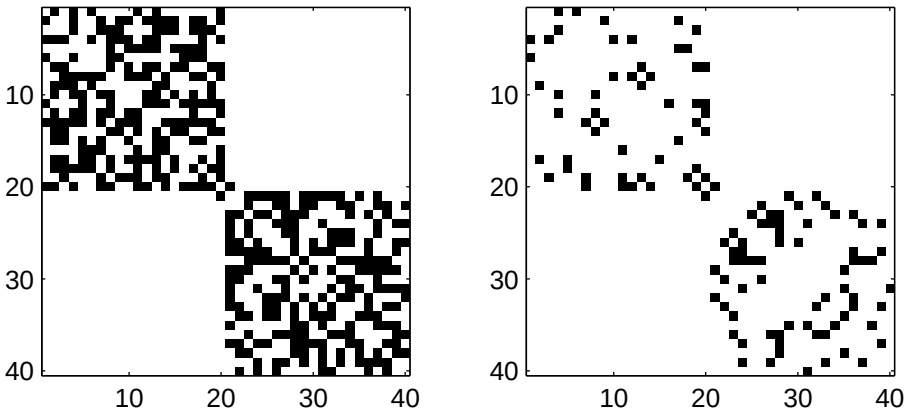

Figure 8.5: Sparsity patterns (Adjacency matrices) of the graphs depicted in Figure 8.3.

8.7. Therefore, based on this figure, low-connectivity coupling links are sampled with high probability and high-connectivity coupling links are sampled with low probability.

Table 8.4 clearly shows that systemic performances of both networks remain close to each other. Moreover, their total weight sums of coupling graphs are very close to each other, i.e., $w_{total}(L_s)/w_{total}(L) = 1.0028$.

Systemic measure: ρ	$\frac{\lvert\rho(L_s)-\rho(L)\rvert}{\rho(L)} \times 100$
$\rho_{\mathcal{H}_\infty} = \lambda_2^{-1}$	12.01%
$\rho_{\mathcal{H}_2} = \left(\frac{1}{2}\sum_{i=2}^{n} {\lambda_i}^{-1}\right)^{\frac{1}{2}}$	3.38 %
$\rho_{\text{zeta},2} = \left(\sum_{i=2}^{n} \lambda_i^{-2}\right)^{\frac{1}{2}}$	10.73 %
$\rho_{\text{local}} = \frac{1}{2}\sum_{i\in\mathcal{V}} d_i^{-1}$	3.16 %

Table 8.4: Degradation errors of some systemic performance measures of the given network $\mathcal{N}(L)$ in Example 8.8.2 and its sparsifier $\mathcal{N}(L_s)$ with 77.49 % fewer links.

Example 8.8.3. *In this example, we consider a consensus network with* 100 *agents defined over a proximity graph of points that are distributed randomly in a* 30×30 *square. Every agent is connected to all of its spatial neighbors within a closed ball of radius* $r = 10$*. Figure 8.8. a shows the coupling graph of this consensus network with* 100 *nodes and*

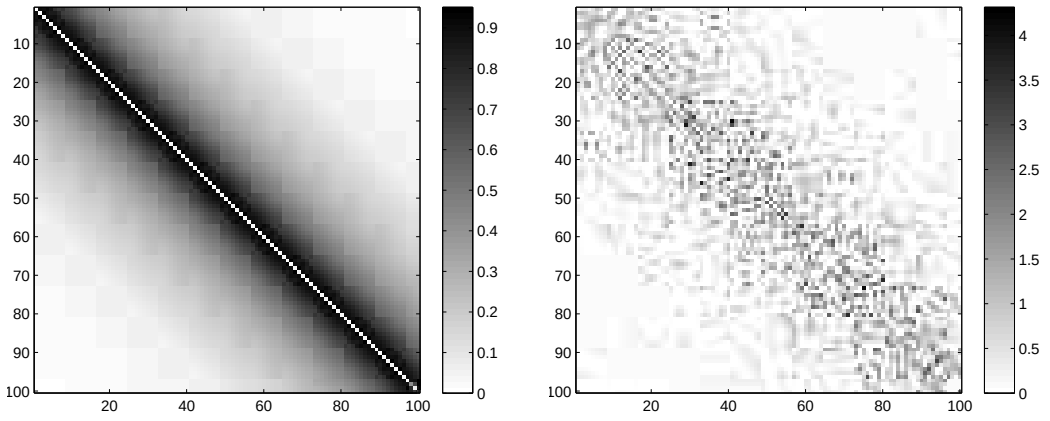

(a) (b)

Figure 8.6: (a) This plot demonstrates the sparsity pattern of the given consensus network in Example 8.8.2 with parameters $c = 1$ and $\gamma = 0.05$. This network has 100 agents and $4,950$ links. (b) This plot presents the sparsity pattern of its sparsifier with 1114 links. For these networks we have $w_{\text{total}}(L_s)/w_{\text{total}}(L) = 1.0028$ and $\|G - G_s\|_{\mathcal{H}_2}/\|G\|_{\mathcal{H}_2} = 0.18$.

1291 *links; and Figure 8.8. b illustrates one example of (0.5, 16.62)-sparsifiers of this network which is obtained based on Network Sparsification Algorithm. This network has fewer coupling links (*831 *links) compare to its original network. Moreover, based on Definitions 8.6.1 and 8.6.3 all CSM's are within a factor of* $(1 \pm 0.5)^{\alpha}$ *of their values of the original network (see Definition 8.6.1). Table 8.5 clearly illustrates that systemic performances of both networks remain close to each other. Moreover, their total weight sums of coupling graphs are very close to each other, i.e.,* $w_{total}(L_s)/w_{total}(L) = 1.0018$. *Note that the systemic measures presented in Table 8.5 are CSM's with homogeneity of order* $\alpha = 1$.

Example 8.8.4. *Let us consider an abstract model of the formation control problem for a*

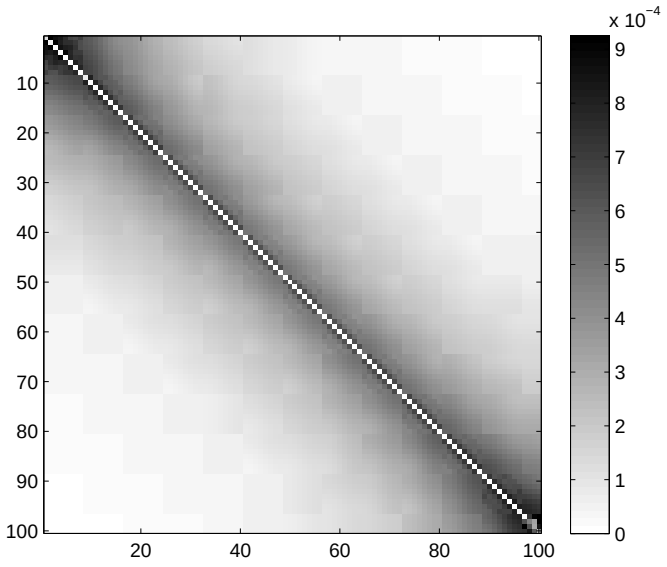

Figure 8.7: This plot presents the probability distribution of sampling links for the given consensus network in Example 8.8.2. The probability of selecting link $e = \{i, j\}$ is the $(i, j)^{\text{th}}$ element of this matrix.

group of autonomous vehicles, which is given by

$$\begin{cases} \begin{bmatrix} \dot{x}(t) \\ \dot{v}(t) \end{bmatrix} = \begin{bmatrix} 0 & I \\ -L & -\beta L \end{bmatrix} \begin{bmatrix} x(t) \\ v(t) \end{bmatrix} + \begin{bmatrix} 0 \\ I \end{bmatrix} \xi(t) \\ \quad y(t) \;=\; \left(I_n - \frac{1}{n}\mathbb{1}_n\mathbb{1}_n^{\mathrm{T}}\right) v(t) \end{cases} \tag{8.70}$$

where $\beta > 0$ is a design parameter. Each vehicle has a position and a velocity variable and the state variable of the entire network is denoted by $[\ x(t) \quad v(t)\ ]^T$ and is measured relative to a pre-specified desired trajectory $x_d(t)$ and velocity $v_d(t)$. Without loss of generality, we assume that the position and velocity of each vehicle are scalar variables. The reason is that one can decouple higher d-dimensional models into d decoupled (8.70) *models. The overall objective is for the network to reach a desired formation pattern, where each autonomous vehicle travels at the constant desired velocity v_d while preserv-*

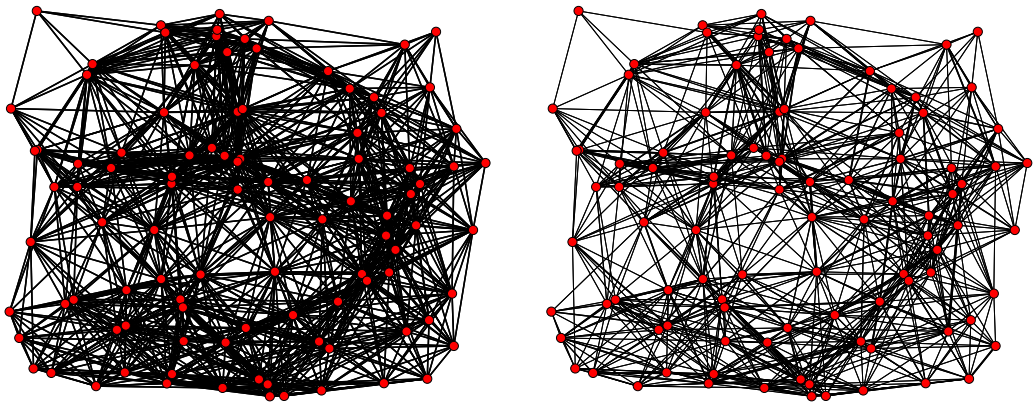

(a) (b)

Figure 8.8: (a) An unweighted coupling (proximity) graph of a consensus network $\mathcal{N}(L)$ with 100 agents is presnted. Every agent is connected to all of its spatial neighbors within a closed ball of radius $r = 10$. This graph has 1291 links and $w_{\text{total}}(L) = 1291$. (b) This graph shows a (0.5, 16.62)-sparsifier with 100 agents, which is obtained based on Network Sparsification Algorithm. The coupling graph of this sparsifier is a weighted graph with 831 links (35.63% fewer than the original graph) and $w_{\text{total}}(L_s) = 1293.4$. The $\mathcal{H}_2$ error of these two networks is $\|G - G_s\|_{\mathcal{H}_2}/\|G\|_{\mathcal{H}_2} = 0.17$.

ing a pre-specified distance between itself and each of its neighbors. In this model, the state feedback controller uses both position and velocity measurements and L is in fact the corresponding feedback gain, which represents the coupling topology in the controller array, and constant β is a design parameter [2, 35]. We consider the steady state variance of the performance output of this network as the performance measure. This quantity is indeed equivalent to the square of the $\mathcal{H}_2$-norm of the system from the exogenous disturbance input to the performance output [2, 11, 35, 36, 38, 170]. We quantify the square of the $\mathcal{H}_2$-norm of (8.70) *in [5] based on the Laplacian eigenvalues of the coupling graph as follows*

$$\lim_{t\to\infty} \mathbb{E}\left[y^T(t)y(t)\right] \;=\; \frac{1}{2\beta}\sum_{i=2}^{n} \lambda_i^{-2} \;=\; \frac{1}{2\beta}\,\rho^2_{\textit{zeta},2}(L). \tag{8.71}$$

This is a SCSM, therefore we can use our proposed method to find a sparsifier that approximates (8.71).

Systemic measure: ρ	$\frac{\lvert\rho(L_s)-\rho(L)\rvert}{\rho(L)} \times 100$
$\rho_{\mathcal{H}_\infty} = {\lambda_2}^{-1}$	10.62%
$\rho_{\mathcal{H}_2} = \left(\frac{1}{2}\sum_{i=2}^{n} {\lambda_i}^{-1}\right)^{\frac{1}{2}}$	3.37%
$\rho_{\text{zeta,2}} = \left(\sum_{i=2}^{n} \lambda_i^{-2}\right)^{\frac{1}{2}}$	10.15%
$\rho_{\text{local}} = \frac{1}{2}\sum_{i\in\mathcal{V}} d_i^{-1}$	3.18%

Table 8.5: Degradation errors of some systemic performance measures of the given network $\mathcal{N}(L)$ in Example 8.8.3 and its sparsifier $\mathcal{N}(L_s)$ with 35.63% fewer links.

Let us consider the coupling graph of network (8.70) *is given by Figure 8.8. a. Then, as we mentioned in Example 8.8.3, Figure 8.8. b illustrates one example of (0.5, 16.62)-sparsifiers of this network which is obtained based on Network Sparsification Algorithm. As shown in Example 8.8.3, this network has fewer coupling links (*831 *links) compare to its original network. Table 8.6 shows that systemic performances of both networks remain close to each other. Moreover, their total weight sums of coupling graphs are very close to each other, i.e.,* $w_{total}(L_s)/w_{total}(L) = 1.0018$*. Note that the systemic measure presented in the following table is a SCSM with homogeneity of order* $\alpha = 2$*.*

Systemic measure: ρ	$\frac{\lvert\rho(L_s)-\rho(L)\rvert}{\rho(L)} \times 100$
$\frac{1}{2\beta}\sum_{i=2}^{n} \lambda_i^{-2}$	8.15%

Table 8.6: Degradation errors of the systemic performance measures (8.71) of the given network (8.70) in Example 8.8.4 and its sparsifier with 35.63% fewer links.

8.9 Discussion and Conclusion

In this work, we focus on one notion of graph sparsification, and we show how this notion (spectral sparsification) can be used in performance and complexity analysis of interconnected networks of coupled dynamical systems. However, several notions of graph sparsifications have been considered in theoretical computer science. While the other notions

are interesting from a combinatorial standpoint, their connections to performance analysis of dynamical networks are not clear yet. For a given graph, there are several sparse subgraphs as follows: *Distance sparsifiers* that approximate all pairwise distances up to a multiplicative and/or additive error (see [171] and subsequent research on spanners), *Cut sparsifiers* that approximate every cut to an arbitrarily small multiplicative error [172], *Spectral sparsifiers or sparsifier* that approximate every eigenvalue to an arbitrarily small multiplicative error [166], and many more. It is shown that sparsifiers can be constructed by sampling links according to their strength, effective resistance [63], edge connectivity [167], or by sampling random spanning trees [173]. Benczúr and Karger propose a randomized algorithm to construct a cut sparsifier in $\mathcal{O}(m \log^2 n)$ time for unweighted graphs and $\mathcal{O}(m \log^3 n)$ time for weighted graphs [167, 172]. The notion of spectral sparsifier is stronger then cut sparsifier, which means spectral sparsifiers are also cut sparsifiers.

In this chapter, we introduce the notion of a sparsifier of a large-scale consensus network. The sparsifier of a consensus network is also a consensus network with identical subsystems, but with a sparse subgraph of the original network, such that these two networks are similar in some meaningful ways. First, we show that each consensus network has a sparsifier network. Second, a framework to produce a high-quality sparse approximation of a given consensus network with a nearly-linear time algorithm is developed. Unlike previous works on this topic, our methodology: (i) works for a broad class of systemic performance measures including $\mathcal{H}_2$-based performance measures, (ii) does not involve any sort of relaxations such as ℓ_0 to ℓ_1; (iii) provides guarantees for the existence of a sparse solution, (iv) can partially sparsify predetermined portions of a given network; and most importantly, (v) gives guaranteed systemic performance certificates. Finally, several supporting examples are provided to illustrate our theoretical findings. Future re-

search includes extensions our results to the case of nonlinear consensus networks and consensus algorithms with high-order agent dynamics.

Chapter 9

Conclusions and Future Directions

In what follows, the contributions made in each part of this dissertation are first summarized, and possible future directions are then outlined.

In the first part, we develop some basic principles to investigate performance deterioration of dynamical networks subject to external disturbances. We first discover some of the inherent fundamental tradeoffs between notions of sparsity and performance in linear consensus networks. Also, for this class of linear consensus networks, we introduce new insights into the network centrality based not only on the network graph but also on a more structured model of network uncertainties. Our results assert that agents or links can be ranked according to this centrality index and their rank can drastically change from the lowest to the highest, or vice versa, depending on the noise structure. This fact hints at the emergence of fundamental tradeoffs on network centrality in the presence of multiple concurrent network uncertainties with different structures. Then, for the class of generic linear networks, we show that the $\mathcal{H}_2$-norm, as a performance measure, can be tightly bounded from below and above by some spectral functions of state and output matrices of the system. We have shown that the spectral lower bound in Theorem 4.5.1 is tighter than all existing lower bounds reported in Table 4.1. Finally, we study nonlinear autocatalytic

networks and exploit their structural properties to characterize their existing hard limits and essential tradeoffs.

In the second part of this dissertation, we consider problems of network synthesis for performance enhancement. Performance improvement in interconnected networks of coupled dynamical systems as well as reducing their design complexity by sparsifying their underlying coupling structures are two of the critical design issues. First, we propose an axiomatic approach for the design and performance analysis of noisy linear consensus networks by introducing a notion of systemic performance measure. We build upon this new notion and investigate a general form of combinatorial problem of growing a linear consensus network via minimizing a given systemic performance measure. Two efficient polynomial-time approximation algorithms are devised to tackle this network synthesis problem. Furthermore, several theoretical fundamental limits on the best achievable performance for the combinatorial problem is derived that assist us to evaluate optimality gaps of our proposed algorithms. Then, in Chapter 7, we investigate the optimal design of distributed system throttlers. A throttler is a mechanism that limits the flow rate of incoming metrics, *e.g.*, byte per second, network bandwidth usage, capacity, traffic, *etc*. This can be used to protect a service's backend/clients from getting overloaded, or to reduce the effects of uncertainties in demand for shared services. We develop a graph-theoretic framework to relate the underlying structure of the system to its overall performance measure. We then compare the performance/robustness of the proposed distributed system throttlers with different underlying graphs. Finally, in the last chapter, we develop a framework to produce a sparse approximation of a given large-scale network with guaranteed performance bounds using a nearly-linear time algorithm. Our methodology is drastically different from the classical methods in this area: (i) works for a broad class of systemic performance measures including $\mathcal{H}_2$-based performance measures, (ii) does not

involve any sort of relaxations such as ℓ_0 to ℓ_1; (iii) provides guarantees for the existence of a sparse solution, (iv) can partially sparsify predetermined portions of a given network; and most importantly, (v) gives guaranteed systemic performance certificates. Finally, several supporting examples are provided to illustrate our theoretical findings. Future research includes extensions our results to the case of nonlinear consensus networks and consensus algorithms with high-order agent dynamics.

9.1 Future Directions

We conclude this thesis with a few future works and open problems.

- In this thesis, we focus on first-order consensus networks. However, it is straightforward to generalize the results for higher-order consensus networks, which have applications in synchronous power networks and formation control (see [5, 174]).

- Another interesting generalization of this work will be to investigate performance and robustness of noisy linear consensus networks with time-delay. For a linear consensus network with uniform time-delay, the closed form formula for the $\mathcal{H}_2$-norm is derived in [61]. Thus, an interesting research direction is to generalize the results of Chapters 2, 3, 6, and 8 for this class of networks.

- The work presented in this dissertation was focused on dynamical networks over time-invariant coupling graphs. However, this study could be extended to include a more general coupling graph, *e.g.*, time-varying graph, switching graph, periodically time-varying graph, *etc*.

- In Chapter 7, we focus on DST networks with the amount of throttled traffic as its nodal performance. A promising research direction is to investigate the overall

performance measure of DST networks with respect to the other nodal performance measures presented in Table 7.1.

- In Chapter 8, we consider the Problem of Network Sparsifications. It is interesting to study the effect of a different link sampling function on the quality of the resulting graph of Network Sparsification Algorithm in Table 8.2. Moreover, it is interesting to discuss advantages and disadvantages of sampling by effective resistances. In the first step, one can use the link centrality measures in Table 3.2 to obtain the corresponding link sampling function.

Bibliography

[1] M. Newman, *The Laplacian Spectrum of Graphs*. University of Manitoba, 2001.

[2] B. Bamieh, M. Jovanović, P. Mitra, and S. Patterson, "Coherence in large-scale networks: Dimension-dependent limitations of local feedback," *IEEE Transactions on Automatic Control*, vol. 57, no. 9, pp. 2235–2249, sept. 2012.

[3] H. Hao and P. Barooah, "Stability and robustness of large platoons of vehicles with double-integrator models and nearest neighbor interaction," *International Journal of Robust and Nonlinear Control*, vol. 23, no. 18, pp. 2097–2122, 2013.

[4] M. Siami and N. Motee, "Robustness and performance analysis of cyclic interconnected dynamical networks," in *The 2013 SIAM Conference on Control and Its Application*, Jan. 2013, pp. 137–143.

[5] ——, "Fundamental limits on robustness measures in networks of interconnected systems," in *52nd IEEE Conference on Decision and Control*, Dec. 2013, pp. 67–72.

[6] M. Fardad, F. Lin, and M. R. Jovanović, "Design of optimal sparse interconnection graphs for synchronization of oscillator networks," *IEEE Transactions on Automatic Control*, vol. 59, no. 9, pp. 2457–2462, 2014.

[7] A. Chapman and M. Mesbahi, "System theoretic aspects of influenced consensus: Single input case," *IEEE Transactions on Automatic Control*, vol. 57, no. 6, pp. 1505–1511, 2012.

[8] F. Dörfler, M. R. Jovanović, M. Chertkov, and F. Bullo, "Sparsity-promoting optimal wide-area control of power networks," *IEEE Trans. Power Syst.*, vol. 29, no. 5, pp. 2281–2291, 2014.

[9] D. Zelazo, S. Schuler, and F. Allgöwer, "Performance and design of cycles in consensus networks," *Systems & Control Letters*, vol. 62, no. 1, pp. 85–96, 2013.

[10] N. Elia, J. Wang, and X. Ma, "Mean square limitations of spatially invariant networked systems," in *Control of Cyber-Physical Systems*, ser. Lecture Notes in Control and Information Sciences, D. C. Tarraf, Ed. Springer International Publishing, 2013, vol. 449, pp. 357–378.

[11] G. F. Young, L. Scardovi, and N. E. Leonard, "Robustness of noisy consensus dynamics with directed communication," in *American Control Conference (ACC), 2010*, July 2010, pp. 6312–6317.

[12] M. Siami and N. Motee, "Fundamental limits and tradeoffs on disturbance propagation in linear dynamical networks," *IEEE Transactions on Automatic Control*, vol. 61, no. 12, pp. 4055–4062, Dec 2016.

[13] R. Carli, F. Fagnani, P. Frasca, T. Taylor, and S. Zampieri, "Average consensus on networks with transmission noise or quantization," in *2007 European Control Conference*, 2007, pp. 1852–1857.

[14] A. Sahai and S. Mitter, "The necessity and sufficiency of anytime capacity for stabilization of a linear system over a noisy communication link," *IEEE Transactions on Information Theory*, vol. 52, no. 8, pp. 3369–3395, Aug 2006.

[15] F. Fagnani and S. Zampieri, "Average consensus with packet drop communication," *SIAM Journal on Control and Optimization*, vol. 48, no. 1, pp. 102–133, 2009.

[16] M. Huang and J. H. Manton, "Coordination and consensus of networked agents with noisy measurements: Stochastic algorithms and asymptotic behavior," *SIAM Journal on Control and Optimization*, vol. 48, no. 1, pp. 134–161, 2009.

[17] D. Zelazo and M. Mesbahi, "Edge agreement: Graph-theoretic performance bounds and passivity analysis," *IEEE Transactions on Automatic Control*, vol. 56, no. 3, pp. 544–555, 2011.

[18] M. Siami and N. Motee, "Systemic measures for performance and robustness of large–scale interconnected dynamical networks," in *Proceedings of the 53rd IEEE Conference on Decision and Control*, Dec. 2014, pp. 5119–5124.

[19] ——, "Schur–convex robustness measures in dynamical networks," in *Proceedings of the 2014 American Control Conference*, 2014, pp. 5198–5203.

[20] R. Olfati-Saber and R. Murray, "Consensus problems in networks of agents with switching topology and time-delays," *IEEE Transactions on Automatic Control*, vol. 49, no. 9, pp. 1520–1533, Sept 2004.

[21] M.-A. Belabbas, "Algorithms for sparse stable systems," in *Proceedings of the 52nd IEEE Conference on Decision and Control*, 2013, pp. 3457–2462.

[22] ——, "Sparse stable systems," *Systems & Control Letters*, vol. 62, no. 10, pp. 981–987, 2013.

[23] T. H. Summers, F. L. Cortesi, and J. Lygeros, "On submodularity and controllability in complex dynamical networks," *IEEE Transactions on Control of Network Systems*, vol. 3, no. 1, pp. 91–101, March 2016.

[24] A. Goldbete, *Biochemical Oscillations and Cellular Rhythms*. Cambridge University Press, Cambridge, 1996.

[25] M. R. Jovanović and B. Bamieh, "On the ill-posedness of certain vehicular platoon control problems," *IEEE Transactions on Automatic Control*, vol. 50, no. 9, pp. 1307–1321, 2005.

[26] M. Jovanovic, J. Fowler, B. Bamieh, and R. D'Andrea, "On the peaking phenomenon in the control of vehicular platoons," *Systems and Control Letters*, vol. 57, no. 7, pp. 528–537, 2008.

[27] H. Raza and P. Ioannou, "Vehicle following control design for automated highway systems," *IEEE Control Syst. Mag.*, vol. 16, no. 6, pp. 43–60, 1996.

[28] P. Seiler, A. Pant, and K. Hedrick, "Disturbance propagation in vehicle strings," *IEEE Trans. Automat. Control*, vol. 49, no. 10, pp. 1835–1842, 2004.

[29] D. Swaroop and J. Hedrick, "Constant spacing strategies for platooning in automated highway systems," *Journal of dynamic systems, measurement, and control*, vol. 121, no. 3, pp. 462–470, 1999.

[30] D. Neilson, "Mems subsystems for optical networking," in *8th Micro optics Conference (MOC 01)*, Osaka, Japan, 2001.

[31] M. Napoli, B. Bamieh, and M. Dahleh, "Optimal control of arrays of microcantilevers," in *Proceedings of the 37th IEEE Conference Decision and Control*, 1998, pp. 2077–2082.

[32] R. H. Middleton and J. H. Braslavsky, "String instability in classes of linear time invariant formation control with limited communication range," *IEEE Trans. Automat. Control*, vol. 55, no. 7, pp. 1519–1530, 2010.

[33] K. Vinay, "Fundamental limitation on achievable decentralized performance," *Automatica*, vol. 43, no. 10, pp. 1849–1854, 2007.

[34] P. Padmasola and N. Elia, "Bode integral limitations of spatially invariant multiagent systems," in *Proceedings of the 45th IEEE Conference on Decision and Control*, Dec 2006, pp. 4327–4332.

[35] S. Patterson and B. Bamieh, "Network coherence in fractal graphs," in *50th IEEE Conference on Decision and Control and European Control Conference (CDC-ECC)*, Dec. 2011, pp. 6445–6450.

[36] E. Lovisari, F. Garin, and S. Zampieri, "Resistance-based performance analysis of the consensus algorithm over geometric graphs," *SIAM Journal on Control and Optimization*, vol. 51, no. 5, pp. 3918–3945, 2013.

[37] F. Lin, M. Fardad, and M. R. Jovanović, "Algorithms for leader selection in stochastically forced consensus networks," *IEEE Transactions on Automatic Control*, vol. 59, no. 7, pp. 1789–1802, 2014.

[38] A. Jadbabaie and A. Olshevsky., "Combinatorial bounds and scaling laws for noise amplification in networks," in *European Control Conference (ECC)*, July 2013, pp. 596–601.

[39] D. E. Knuth, "Big omicron and big omega and big theta," *BCM Sigact News*, vol. 8, no. 2, pp. 18–24, 1976.

[40] K. Fitch and N. Leonard, "Information centrality and optimal leader selection in noisy networks," in *Proceedings of the 52nd IEEE Conference on Decision and Control*, 2013, pp. 7510–7515.

[41] L. F. Bertuccelli, H. Choi, P. Cho, and J. P. How, "Real-time multi-uav task assignment in dynamic and uncertain environments," in *Proceedings of AIAA Guidance, Navigation, and Control Conference*, 2009.

[42] M. Siami, S. Bolouki, B. Bamieh, and N. Motee, "Centrality measures in linear consensus networks with structured uncertainties," *IEEE Transaction on Control of Network Systems*, 2016, accepted.

[43] M. Siami and N. Motee, "Network sparsification with guaranteed systemic performance measures," *IFAC-PapersOnLine*, vol. 48, no. 22, pp. 246 – 251, 2015.

[44] B. N. Kholodenko, "Negative feedback and ultrasensitivity can bring about oscillations in the mitogen-activated protein kinase cascades," *European Journal of Biochemistry*, vol. 267, pp. 1583 – 1588, 2000.

[45] W. H. Kwon, Y. S. Moon, and S. C. Ahn, "Bounds in algebraic riccati and lyapunov equations: a survey and some new results," *International Journal of Control*, vol. 64, no. 3, pp. 377–389, 1996.

[46] Y. Fang, K. Loparo, and X. Feng, "New estimates for solutions of lyapunov equations," *IEEE Transactions on Automatic Control*, vol. 42, no. 3, pp. 408–411, Mar 1997.

[47] C. H. Lee, "New results for the bounds of the solution for the continuous riccati and lyapunov equations," *IEEE Transactions on Automatic Control*, vol. 42, no. 1, pp. 118–123, Jan 1997.

[48] M. Siami and N. Motee, "New spectral bounds on h_2-norm of linear dynamical networks," *Automatica*, 2016, accepted.

[49] N. Motee, F. Chandra, B. Bamieh, M. Khammash, and J. Doyle, "Performance limitations in autocatalytic networks in biology," in *Proceedings of the 49th IEEE Conference Decision and Control*, Atlanta, 2010, pp. 4715–4720.

[50] M. Siami and N. Motee, "On existence of hard limits in autocatalytic networks and their fundamental tradeoffs," in *3rd IFAC Workshop on Distributed Estimation and Control in Networked Systems*, September 2012, pp. 294–298.

[51] M. Siami, B. Bamieh, G. Buzi, M. Khammash, J. Doyle, and N. Motee, "Performance limitations in autocatalytic pathways," *Submitted*, 2016.

[52] G. F. Young, L. Scardovi, and N. E. Leonard, "Rearranging trees for robust consensus," in *50th IEEE Conference on Decision and Control and European Control Conference (CDC-ECC)*, 2011, pp. 1000–1005.

[53] D. Mosk-Aoyama, "Maximum algebraic connectivity augmentation is NP-hard," *Operations Research Letters*, vol. 36, no. 6, pp. 677–679, Nov. 2008.

[54] A. Kolla, Y. Makarychev, A. Saberi, and S. Teng, "Subgraph sparsification and nearly optimal ultrasparsifiers," in *Proc. 42nd Sympos. Theory Computing*, 2010.

[55] A. Ghosh and S. Boyd, "Growing well-connected graphs," in *Proceedings of the 45th IEEE Conference Decision and Control*, 2006.

[56] M. Fardad, "On the optimality of sparse long-range links in circulant consensus networks," in *Proceedings of the 2015 American Control Conference*, July 2015, pp. 2075–2080.

[57] S. Hassan-Moghaddam and M. R. Jovanović, "An interior point method for growing connected resistive networks," in *Proceedings of the 2015 American Control Conference*, Chicago, IL, 2015, pp. 1223–1228.

[58] X. Wu and M. R. Jovanović, "Sparsity-promoting optimal control of consensus and synchronization networks," in *Proceedings of the 2014 American Control Conference*, 2014, pp. 2948–2953.

[59] T. Summers, I. Shames, J. Lygeros, and F. Dörfler, "Topology design for optimal network coherence," in *Proceedings of European Control Conferance*, July 2015, pp. 575–580.

[60] M. Siami and N. Motee, "Growing linear consensus networks via systemic performance measures," *Submitted*, 2016.

[61] Y. Ghaedsharaf, M. Siami, C. Somarakis, and N. Motee, "Interplay between performance and communication delay in noisy linear dynamical networks," in *Proceedings of The 15th European Control Conference*, June 2016.

[62] M. Siami and J. Skaf, "Structural analysis and optimal design of distributed system throttlers," *Submitted*, 2016.

[63] D. A. Spielman and N. Srivastava, "Graph sparsification by effective resistances," in *Proceedings of the 14th Annual ACM Symposium on Theory of Computing*, ser. STOC '08. New York, NY, USA: ACM, 2008, pp. 563–568.

[64] J. Batson, D. Spielman, and N. Srivastava, "Twice-ramanujan sparsifiers," *SIAM Review*, vol. 56, no. 2, pp. 315–334, 2014.

[65] M. Siami and N. Motee, "Almost linear-time sparsification of consensus networks with guaranteed systemic performance measures," *Submitted*, 2016.

[66] A. W. Marshall, I. Olkin, and B. C. Arnold, *Inequalities: Theory of Majorization and Its Applications*. Springer Science+Business Media, LLC, 2011.

[67] J. A. Bondy, *Graph Theory With Applications*. Elsevier Science Ltd, 1976.

[68] W. J. Rugh, *Linear System Theory*. Upper Saddle River, NJ, USA: Prentice-Hall, Inc., 1996.

[69] P. Barooah and J. Hespanha, "Graph effective resistance and distributed control: Spectral properties and applications," in *Proceedings of the 45th IEEE Conference on Decision and Control*, Dec. 2006, pp. 3479–3485.

[70] I. Gutman and L. Pavlovi, "On the coefficients of the laplacian characteristic polynomial of trees." *Bulletin: Classe des Sciences Mathématiques et Naturelles. Sciences Mathématiques*, vol. 127, no. 28, pp. 31–40, 2003.

[71] A. Dobrynin, R. Entringer, and I. Gutman, "Wiener index of trees: Theory and applications," *Acta Applicandae Mathematica*, vol. 66, no. 3, pp. 211–249, 2001.

[72] Y. Yang and X. Jiang, "Unicyclic graphs with extremal kirchhoff index," *MATCH Commun. Math. Comput. Chem*, vol. 60, no. 1, pp. 107–120, 2008.

[73] D. Easley and J. Kleinberg, *Networks, Crowds, and Markets: Reasoning About a Highly Connected World*. Cambridge, UK: Cambridge University Press, 2010.

[74] M. Kraning, E. Chu, J. Lavaei, and S. Boyd, "Dynamic network energy management via proximal message passing," *Foundations and Trends in Optimization*, vol. 1, no. 2, pp. 73–126, 2014.

[75] Y. Yang, "Bounds for the kirchhoff index of bipartite graphs," *Journal of Applied Mathematics*, vol. 2012, 2012.

[76] R. B. Rapat, "Resistance matrix of a weighted graph," *MATCH Communications in Mathematical and in Computer Chemistry*, vol. 50, pp. 73–82, 2004.

[77] H. Deng, "On the minimum kirchhoff index of graphs with given number of cut-edges," *MATCH Commun. Math. Comput. Chem.*, vol. 63, no. 1, pp. 171–180, 2009.

[78] B. Zhou, "On sum of powers of laplacian eigenvalues and laplacian estrada index of graphs," 2011, arXiv/1102.1144.

[79] N. Motee and Q. Sun, "Sparsity measures for spatially decaying systems," in *roceedings of the 2014 American Control Conference*, June 2014, pp. 5459–5464.

[80] O. Rojo, R. Soto, and H. Rojo, "An always nontrivial upper bound for laplacian graph eigenvalues," *Linear Algebra and its Appl.*, vol. 312, no. 1–3, pp. 155–159, 2000.

[81] M. Newman, *Networks: an introduction*. Oxford University Press, 2010.

[82] M. Benzi and C. Klymko, "On the limiting behavior of parameter-dependent network centrality measures," *SIAM Journal on Matrix Analysis and Applications*, vol. 36, no. 2, pp. 686–706, 2015.

[83] P. Bonacich, "Power and centrality: A family of measures," *American journal of sociology*, pp. 1170–1182, 1987.

[84] L. Katz, "A new status index derived from sociometric analysis," *Psychometrika*, vol. 18, no. 1, pp. 39–43, 1953.

[85] D. J. Watts and S. H. Strogatz, "Collective dynamics of "small-world" networks," *nature*, vol. 393, no. 6684, pp. 440–442, 1998.

[86] S. Brin and L. Page, "Reprint of: The anatomy of a large-scale hypertextual web search engine," *Computer networks*, vol. 56, no. 18, pp. 3825–3833, 2012.

[87] J. M. Anthonisse, "The rush in a directed graph," *Stichting Mathematisch Centrum. Mathematische Besliskunde*, no. BN 9/71, pp. 1–10, 1971.

[88] L. C. Freeman, "A set of measures of centrality based on betweenness," *Sociometry*, pp. 35–41, 1977.

[89] H. Tanner, "On the controllability of nearest neighbor interconnections," in *43rd IEEE Conference on Decision and Control*, vol. 3, 2004, pp. 2467–2472.

[90] M. R. Faghani and U. T. Nguyen, "A study of xss worm propagation and detection mechanisms in online social networks," *IEEE Transactions on Information Forensics and Security*, vol. 8, no. 11, pp. 1815–1826, 2013.

[91] L. C. Freeman, "Centrality in social networks conceptual clarification," *Social networks*, vol. 1, no. 3, pp. 215–239, 1972.

[92] P. Bonacich, "Factoring and weighting approaches to status scores and clique identification," *Journal of Mathematical Sociology*, vol. 2, no. 1, pp. 113–120, 1972.

[93] M. Piraveenan, M. Prokopenko, and L. Hossain, "Percolation centrality: Quantifying graph-theoretic impact of nodes during percolation in networks," *PLoS ONE*, vol. 8, no. 1, pp. 1789–1802, 2013.

[94] M. G. Everett and S. P. Borgatti, "Analyzing clique overlap," *Connections*, vol. 21, no. 1, pp. 49–61, 1998.

[95] G. Ranjan and Z.-L. Zhang, "Geometry of complex networks and topological centrality," *Physica A: Statistical Mechanics and its Applications*, vol. 392, no. 17, pp. 3833–3845, 2013.

[96] I. Gutman and W. Xiao, "Generalized inverse of the laplacian matrix and some applications," *Bulletin: Classe des Sciences Mathématiques et Naturelles. Sciences Mathématiques*, vol. 129, no. 29, pp. 15–23, 2004.

[97] W. Ren, R. W. Beard, and T. W. McLain, "Coordination variables and consensus building in multiple vehicle systems," in *Cooperative Control*. Springer, 2005, pp. 171–188.

[98] Z. Lin, B. Francis, and M. Maggiore, "Necessary and sufficient graphical conditions for formation control of unicycles," *IEEE Transactions on Automatic Control*, vol. 50, no. 1, pp. 121–127, 2005.

[99] J. Doyle, K. Glover, P. Khargonekar, and B. Francis, "State-space solutions to standard $\mathcal{H}_2$ and $\mathcal{H}_\infty$ control problems," *IEEE Transactions on Automatic Control*, vol. 34, no. 8, pp. 831–847, Aug 1989.

[100] D. Boley, G. Ranjan, and Z.-L. Zhang, "Commute times for a directed graph using an asymmetric laplacian," *Linear Algebra and its Applications*, vol. 435, no. 2, pp. 224 – 242, 2011.

[101] D. F. Gleich, "Pagerank beyond the web," *SIAM Review*, vol. 57, no. 3, pp. 321–363, 2015.

[102] M. Siami and N. Motee, "Performance analysis of linear consensus networks with structured stochastic disturbance inputs," in *American Control Conference (ACC)*, 2015, pp. 4080–4085.

[103] F. A. Chandra, G. Buzi, and J. C. Doyle, "Glycolytic Oscillations and Limits on Robust Efficiency," *Science*, vol. 8, pp. 187–192, 2011.

[104] B. Bamieh and M. Dahleh, "Exact computation of traces and $\mathcal{H}_2$ norms for a class of infinite-dimensional problems," *IEEE Transactions on Automatic Control*, vol. 48, no. 4, pp. 646–649, April 2003.

[105] P. Benner, J. R. Li, and T. Penzl, "Numerical solution of large-scale lyapunov equations, riccati equations, and linear-quadratic optimal control problems," *Numerical Linear Algebra with Applications*, vol. 15, no. 9, pp. 755–777, 2008. [Online]. Available: http://dx.doi.org/10.1002/nla.622

[106] N. Komaroff, "Simultaneous eigenvalue lower bounds for the lyapunov matrix equation," *IEEE Transactions on Automatic Control*, vol. 33, no. 1, pp. 126–128, Jan. 1988.

[107] S. D. Wang, T. S. Kuo, and C. F. Hsu, "Trace bounds on the solution of the algebraic matrix riccati and lyapunov equation," *IEEE Transactions on Automatic Control*, vol. 31, no. 7, pp. 654–656, Jul. 1986.

[108] B. Kwon, M. Youn, and Z. Bien, "On bounds of the riccati and lyapunov matrix equations," *IEEE Transactions on Automatic Control*, vol. 30, no. 11, pp. 1134–1135, Nov. 1985.

[109] T. Mori, N. Fukuma, and M. Kuwahara, "Bounds in the lyapunov matrix differential equation," *Automatic Control, IEEE Transactions on*, vol. 32, no. 1, pp. 55–57, Jan 1987.

[110] R. Horn and C. Johnson, *Matrix Analysis*. Cambridge University Press, 1990.

[111] D. S. Bernstein, "Inequalities for the trace of matrix exponentials," *SIAM Journal on Matrix Analysis and Applications*, vol. 9, no. 2, pp. 156–158, 1988.

[112] J. Lasserre, "A trace inequality for matrix product," *IEEE Transactions on Automatic Control*, vol. 40, no. 8, pp. 1500–1501, 1995.

[113] N. Komaroff, "Upper summation and product bounds for solution eigenvalues of the lyapunov matrix equation," *IEEE Transactions on Automatic Control*, vol. 37, no. 7, pp. 1040–1042, Jul 1992.

[114] R. Olfati-Saber, J. A. Fax, and R. M. Murray, "Consensus and cooperation in networked multi-agent systems," *Proceedings of the IEEE*, vol. 95, no. 1, pp. 215–233, Jan 2007.

[115] J. Bang-Jensen and G. Z. Gutin, *Digraphs: Theory, Algorithms and Applications*. Springer Publishing Company, Incorporated, 2008.

[116] B. Norman, *Algebraic Graph Theory*. Cambridge University Press, Cambridge, 1973.

[117] M. Siami, N. Motee, and G. Buzi, "Characterization of hard limits on performance of autocatalytic pathways," in *American Control Conference (ACC)*, 2013, pp. 2313–2318.

[118] M. Arcak and E. Sontag, "A passivity-based stability criterion for a class of interconnected systems and applications to biochemical reaction networks," in *Proceedings of the 46th IEEE Conference Decision and Control*, Dec. 2007, pp. 4477–4482.

[119] J. Tyson and H. Othmer, "The Dynamics of Feedback Control Circuits in Biochemical Pathways," *Prog. Theor. Biol.*, vol. 5, pp. 1–62, 1978.

[120] V. Y. Pan and Z. Q. Chen, "The complexity of the matrix eigenproblem," in *the 31st annual ACM symposium on Theory of computing*, 1999, pp. 507–516.

[121] L. Ljung, *Signal Analysis and Prediction*. Boston, MA: Birkhäuser Boston, 1998, ch. System Identification, pp. 163–173.

[122] G. Buzi and J. Doyle, "Topological tradeoffs in autocatalytic metabolic pathways," in *Proceedings of the 49th IEEE Conference on Decision and Control*, Dec 2010, pp. 4697–4702.

[123] R. Middleton, K. Lau, and J. Braslavsky, "Conjectures and counterexamples on optimal l 2 disturbance attenuation in nonlinear systems," in *Proceedings of the 42nd IEEE Conference Decision and Control*, vol. 3, 2003, pp. 2561–2566.

[124] B. Schwartz, A. Isidori, and T. Tarn, "l_2 disturbance attenuation and performance bounds for linear non-minimum phase square invertible systems," in *Proceedings of the 35th IEEE Conference Decision and Control*, vol. 1. IEEE, 1996, pp. 227–228.

[125] A. J. van der Schaft, "l_2-gain analysis of nonlinear systems and nonlinear state-feedback h_∞ control," *IEEE Trans. Automat. Control*, vol. 37, no. 6, pp. 770–784, 1992.

[126] M. Seron, J. Braslavsky, P. V. Kokotovic, and D. Q. Mayne, "Feedback limitations in nonlinear systems: From bode integrals to cheap control," *IEEE Trans. Automat. Control*, vol. 44, no. 4, pp. 829–833, 1999.

[127] E. E. Sel'kov, "Stabilization of energy charge, generation of oscillations and multiple steady states in energy metabolism as a result of purely stoichiometric regulation," *European Journal of Biochemistry*, vol. 59, pp. 151–157, 1975.

[128] F. Hynne, S. Danø, and P. G. Sørensen, "Full-scale model of glycolysis in saccharomyces cerevisiae," *Biophysical chemistry*, vol. 94, no. 1, pp. 121–163, 2001.

[129] A. Betz and B. Chance, "Phase relationship of glycolytic intermediates in yeast cells with oscillatory metabolic control," *Archives of biochemistry and biophysics*, vol. 109, pp. 585–594, 1965.

[130] R. Sepulchre, M. Jankovic, and P. Kokotovic, *Constructive Nonlinear Control*. "Springer-Verlag, 1997.

[131] A. J. van der Schaft, *L_2 Gain and Passivity Techniques in Nonlinear Control*. Springer, Berlin, Germany, 2000.

[132] C. Scherer, "h_∞-control by state-feedback for plants with zeros on the imaginary axis," *SIAM Journal Control and Optimization control and optimization*, vol. 30, no. 1, pp. 123–142, 1992.

[133] E. G. Al'Brekht, "On the optimal stabilization of nonlinear systems," *Journal of Applied Mathematics and Mechanics*, vol. 25, no. 5, pp. 1254–1266, 1961.

[134] D. L. Lukes, "Optimal regulation of nonlinear dynamical systems," *SIAM Journal Control*, vol. 7, no. 1, pp. 75–100, 1969.

[135] H. Kwakernaak and R. Sivan, "The maximally achievable accuracy of linear optimal regulators and linear optimal filters," *IEEE Trans. Automat. Control*, vol. 17, no. 1, pp. 79–86, 1972.

[136] W. Abbas and M. Egerstedt, "Robust graph topologies for networked systems," in *3rd IFAC Workshop on Distributed Estimation and Control in Networked Systems*, September 2012, pp. 85–90.

[137] F. Lin, M. Fardad, and M. R. Jovanović, "Optimal control of vehicular formations with nearest neighbor interactions," *IEEE Transactions on Automatic Control*, vol. 57, no. 9, pp. 2203–2218, 2012.

[138] A. Jadbabaie, J. Lin, and A. S. Morse, "Coordination of groups of mobile autonomous agents using nearest neighbor rules," *IEEE Transactions on Automatic Control*, vol. 48, no. 6, pp. 988–1001, June 2003.

[139] S. Boyd., "Convex optimization of graph laplacian eigenvalues," in *International Congress of Mathematicians*, 2006, pp. 1311–1319.

[140] S. Hawking, "Zeta function regularization of path integrals in curved space-time," *Communications in Mathematical Physics*, vol. 133, no. 55, 1977.

[141] B. Sturmfels, "Solving systems of polynomial equations," in *American Mathematical Society, CBMS Regional Conferences Series, No 97*, 2002.

[142] V. D. Blondel, E. D. Sontag, M. Vidyasagar, and J. C. Willems, *Open Problems in Mathematical Systems and Control Theory*. Springer Verlag, 1999.

[143] E. F. S. Boyd, L. El Ghaoui and V. Balakrishnan, *Linear Matrix Inequalities in System and Control Theory*. Society for Industrial Mathematics, 1997.

[144] K. Glover, "All optimal hankel-norm approximations of linear multivariable systems and their l_∞-error bounds," *International Journal of Control*, vol. 39, no. 6, pp. 1115–1193, 1984.

[145] M. H. de Badyn, A. Chapman, and M. Mesbahi, "Network entropy: A system-theoretic perspective," in *Proceedings of 54th IEEE Conference Decision and Control*, Dec 2015, pp. 5512–5517.

[146] S. Boyd and L. Vandenberghe, *Convex optimization*. Cambridge University Press, 2004.

[147] J. Borwein and A. Lewis, *Convex analysis and nonlinear optimization*. Springer, 2006.

[148] L. A. Wolsey and G. L. Nemhauser, *Integer and Combinatorial Optimization*. Wiley, 1988.

[149] S. Friedland and S. Gaubert, "Submodular spectral functions of principal submatrices of a hermitian matrix, extensions and applications," *Linear Algebra and its Applications*, vol. 438, no. 10, pp. 3872 – 3884, 2013.

[150] Y. Ghaedsharaf and N. Motee, "Complexities and performance limitations in growing time-delay noisy linear consensus networks," in *Proc. 6th IFAC Workshop on Distributed Estimation and Control in Networked Systems*, 2016.

[151] S.-T. Yau and Y. Y. Lu, "Reducing the symmetric matrix eigenvalue problem to matrix multiplications," *The SIAM Journal on Scientific Computing*, vol. 14, no. 1, pp. 121–136, 1993.

[152] A. S. Lewis, "The mathematics of eigenvalue optimization," *Mathematical Programming*, vol. 97, no. 1-2, pp. 155–176, 07 2003.

[153] Y. Xia, L. Subramanian, I. Stoica, and S. Kalyanaraman, "One more bit is enough," *ACM SIGCOMM Computer Communication Review*, vol. 35, no. 4, pp. 37–48, 2005.

[154] K. Tan, F. Jiang, Q. Zhang, and X. Shen, "Congestion control in multihop wireless networks," *IEEE Transactions on Vehicular Technology*, vol. 56, no. 2, pp. 863–873, March 2007.

[155] Y. Zhang, S. R. Kang, and D. Loguinov, "Delay-independent stability and performance of distributed congestion control," *IEEE/ACM Transactions on Networking*, vol. 15, no. 4, pp. 838–851, Aug 2007.

[156] R. Johari and D. K. H. Tan, "End-to-end congestion control for the internet: Delays and stability," *IEEE/ACM Transactions on Networking*, vol. 9, no. 6, pp. 818–832, Dec. 2001. [Online]. Available: http://dx.doi.org/10.1109/90.974534

[157] R. Gibbens and F. Kelly, "Resource pricing and the evolution of congestion control," *Automatica*, vol. 35, no. 12, pp. 1969 – 1985, 1999.

[158] F. P. Kelly, A. K. Maulloo, and D. K. H. Tan, "Rate control for communication networks: Shadow prices, proportional fairness and stability," *The Journal of the Operational Research Society*, vol. 49, no. 3, pp. 237–52, 1998.

[159] B. Raghavan, K. Vishwanath, S. Ramabhadran, K. Yocum, and A. C. Snoeren, "Cloud control with distributed rate limiting," in *Proc. 2007 Conference on Applications, Technologies, Architectures, and Protocols for Computer Communications*, ser. SIGCOMM '07. New York, NY, USA: ACM, 2007, pp. 337–348.

[160] R. Stanojevic and R. Shorten, "Generalized distributed rate limiting," in *Proc. 17th International Workshop on Quality of Service*, 2009, pp. 1–9.

[161] F. Lin, M. Fardad, and M. R. Jovanović, "Design of optimal sparse feedback gains via the alternating direction method of multipliers," *IEEE Transactions on Automatic Control*, vol. 58, no. 9, pp. 2426–2431, Sept 2013.

[162] A. Jadbabaie and A. Olshevsky, "On performance of consensus protocols subject to noise: Role of hitting times and network structure," *arXiv preprint arXiv:1508.00036*, 2015.

[163] A. Ghosh, S. Boyd, and A. Saberi, "Minimizing effective resistance of a graph," *SIAM Rev.*, vol. 50, no. 1, pp. 37–66, 2008.

[164] C. Chen, G. Iyengar, and C. C. Moallemi, "An axiomatic approach to systemic risk," *Management Science*, vol. 59, no. 6, pp. 1373–1388, 2013.

[165] M. Rudelson and R. Vershynin, "Sampling from large matrices: An approach through geometric functional analysis," *Journal of the ACM*, vol. 54, no. 4, Jul. 2007. [Online]. Available: http://doi.acm.org/10.1145/1255443.1255449

[166] D. A. Spielman and S.-H. Teng, "Nearly-linear time algorithms for graph partitioning, graph sparsification, and solving linear systems," in *Proceedings of the Thirty-sixth Annual ACM Symposium on Theory of Computing*, ser. STOC '04. New York, NY, USA: ACM, 2004, pp. 81–90. [Online]. Available: http://doi.acm.org/10.1145/1007352.1007372

[167] W. S. Fung, R. Hariharan, N. J. Harvey, and D. Panigrahi, "A general framework for graph sparsification," in *Proceedings of the Forty-third Annual ACM Symposium on Theory of Computing*, ser. STOC '11. New York, NY, USA: ACM, 2011, pp. 71–80. [Online]. Available: http://doi.acm.org/10.1145/1993636.1993647

[168] S. Gugercin, A. C. Antoulas, and C. Beattie, "h_2 model reduction for large-scale linear dynamical systems," *SIAM Journal on Matrix Analysis and Applications*, vol. 30, no. 2, pp. 609–638, 2008.

[169] N. Motee and Q. Sun, "Sparsity and spatial localization measures for spatially distributed systems," *SIAM Jounal on Control and Optimization*, 2016, to be published.

[170] B. Bamieh and D. Gayme, "The price of synchrony: Resistive losses due to phase synchronization in power networks," in *American Control Conference (ACC)*, September 2012, pp. 5815–5820.

[171] D. Peleg and A. A. Schäffer, "Graph spanners," *Journal of Graph Theory*, vol. 13, no. 1, pp. 609–638, 1989.

[172] A. A. Benczúr and D. R. Karger, "Approximating s-t minimum cuts in Õ(n2) time," in *Proceedings of the Twenty-eighth Annual ACM Symposium on Theory of Computing*, ser. STOC '96. New York, NY, USA: ACM, 1996, pp. 47–55. [Online]. Available: http://doi.acm.org/10.1145/237814.237827

[173] N. Goyal, L. Rademacher, and S. Vempala, "Expanders via random spanning trees," in *Proceedings of the Twentieth Annual ACM-SIAM Symposium on Discrete Algorithms*, ser. SODA '09. Philadelphia, PA, USA: Society for Industrial and Applied Mathematics, 2009, pp. 576–585. [Online]. Available: http://dl.acm.org/citation.cfm?id=1496770.1496834

[174] M. Siami, "Disturbance propagation in interconnected linear dynamical networks," Master's thesis, Lehigh University, April 2014.

Biography

Milad Siami received the B.Sc. degrees in electrical engineering and pure mathematics both from Sharif University of Technology (SUT) in 2009, M.Sc. degrees in electrical engineering and mechanical engineering from SUT and Lehigh University, Bethlehem, PA, in 2011 and 2014, and Ph.D. degree in mechanical engineering from Lehigh University in January 2017. He was a research student with the Department of Mechanical and Environmental Informatics, Tokyo Institute of Technology, Japan, from 2009 to 2010, and also a long-term visiting researcher at Institute for Mathematics and Its Applications (IMA), University of Minnesota, Fall 2015. Moreover, he was a Research Intern at Google NYC, Summer 2016. He received a Gold Medal of National Mathematics Olympiad, Iran (2003) and the Best Student Paper Award at the 5th IFAC Workshop on Distributed Estimation and Control in Networked Systems (2015). Furthermore, he was awarded RCEAS Fellowship (2012), Byllesby Fellowship (2013), Rossin College Doctoral Fellowship (2015), and Graduate Student Merit Award (2016) at Lehigh University.